

**SEDIMENTOLOGY AND DIAGENESIS OF
UPPER DEVONIAN CARBONATES,
CANNING BASIN,
WESTERN AUSTRALIA**

written by
Malcolm W. Wallace (BSc. Hon.)

Submitted in partial fulfilment of the requirements
for the degree of
Doctor of Philosophy
(Geology)
University of Tasmania
(December, 1987)

*graduating
1988*

This thesis contains no material which has been accepted for the award of any other higher degree or graduate diploma in any tertiary institution and to the best of the author's knowledge and belief, the thesis contains no material previously published or written by another person, except when due reference is made in the text of the thesis.

Malcolm Wallace
Malcolm Wallace

Abstract

Two Upper Devonian carbonate sequences in the Canning Basin were investigated: a) an outcropping sequence in the Geikie Gorge region on the Lennard Shelf; and b) a subsurface sequence on the Barbwire Terrace.

The outcropping Frasnian-Famennian carbonates of the Geikie Gorge region form part of the Devonian "Great Barrier Reef" of the Canning Basin and consist of a series of platforms and atolls which fringe the basin margin. The platforms have steep, reef-fringed margins and the framework lithologies consist predominantly of cyanobacterial framestones. A widespread deeper water stromatolite unit straddles the Frasnian-Famennian boundary and appears to represent a major halt in reef growth. Stromatolite structures are most common in the reefal-slope subfacies and appear to have formed by soft-body collapse in combination with later internal erosion and sedimentation.

The carbonates of the Geikie Gorge region have suffered a long and complex diagenetic history which began in Devonian sea water with extensive marine cementation of platform-margin lithologies. Devonian - Lower Carboniferous burial diagenesis was the most important episode of diagenesis as almost all primary porosity was occluded by calcite cementation (non-luminescent to bright-luminescent to dull-luminescent) during this interval. Dolomitization and consequent secondary porosity development also occurred during this interval. Some karstification and calcite cementation took place during Late Carboniferous subaerial exposure. Minor calcite cementation occurred during Permian - Cenozoic burial. Karstification, dedolomitization and calcite recrystallization took place during Cenozoic meteoric diagenesis. Recrystallized sparry calcites commonly display cathodoluminescent crystal growth zonations which mimic cementation fabrics.

The Barbwire Terrace carbonates consist predominantly of low-energy peritidal and shallow-subtidal lithologies in which most of the clay-free lithologies have been thoroughly dolomitized. The peritidal lithologies resemble those found in the modern arid tidal flats of the Persian Gulf. Cyclic sequences are not well developed in the peritidal lithologies. No true reef-framework lithologies were recognized in the sequence.

The dominant synsedimentary diagenetic process was supratidal dolomitization and associated anhydrite precipitation. The $\delta^{18}\text{O}$ value for Devonian marine dolomite $\{\delta^{18}\text{O} = -2 \text{ ‰ (PDB)}\}$ was estimated by assuming that the lowest $\delta^{18}\text{O}$ values for the supratidal dolomite represent replacement in marine waters. The most important diagenetic process affecting the carbonates was regional dolomitization and this occurred during Devonian - Lower Carboniferous burial diagenesis. Regional dolomitization was not restricted to the peritidal lithologies and thick sequences (up to 600 m) of dolomite with no primary calcite are common. The regional dolomites have lower $\delta^{18}\text{O}$ values than the supratidal synsedimentary dolomite and saddle dolomite cements are common, suggesting elevated temperatures of precipitation. Karstification and calcite cementation took place in the dolomites during Late Carboniferous subaerial exposure. Poikilitic calcite cements were precipitated during Permian - Cenozoic burial diagenesis.

Acknowledgements

Prasada Rao provided valuable advice on many aspects of the project and provided financial support for the analytical work. Clive Burrett and Max Banks have also given useful advice throughout the project. A number of technical staff at the University of Tasmania helped with various aspects of the project and I would like to thank Julie Beattie, Peter Cornish, Penny Green, Wieslaw Jablonski, Vagn Jensen, Barbara Lewis, June Pongrantz, Mike Power, Phil Robinson and Simon Stevens.

I am greatly indebted to Phillip Playford of the Geological Survey of W.A., who initially suggested the Geikie Gorge study area and has contributed greatly to the project throughout the course of research. Charles Kerans also provided valuable advice and assistance. Bill Meyers and Bruce Ward gave helpful advice in the field and their assistance was appreciated. Neil Hurley kindly supplied a copy of his dissertation on the reef complexes of the Oscar Range. Vicki Pedone also provided information on her study of dolomites in the Emanuel Range. I would also like to thank my wife, Margaret for her assistance in the field.

I would like to thank Western Mining Corporation, Australian Hydrocarbons and Poseidon Oil for their generous financial and logistic support and for access to the core material. It would not have been possible to carry out the project without this support. The following people employed by Western Mining also provided assistance during the course of project: Simon Ashton, Clinton Foster, Roy France, Wayne Harris, Geoff O'Brien, Graham Pitt, Joe Scibiorski, and Robert Weeden. Alan Eddie provided invaluable assistance and advice regarding fieldwork in the bush. Steve Slater and John Ashton of Challenger Geological Services also helped out in many ways.

The Geological Survey of Western Australia kindly supplied air photos and drafted the final version of the map. BHP Minerals supplied 1: 25 000 topographic and their help was much appreciated. Amoco Minerals also provided composite air photo mosaics. Neville McTaggart provided assistance during the course of research and participated in helpful discussions on Lennard Shelf geology. The Western Australian National Parks Service kindly allowed the author to carry out mapping in the Geikie Gorge National Park. I would also like to thank the owners of Brooking Springs and Fossil Downs for permitting mapping to be carried out on their properties.

The following people reviewed various portions of this manuscript and their editing was much appreciated: Max Banks, Clive Burrett, Steve Carey, Roy France, Peter Homewood, Charles Kerans, Hans-G Machel, Catherine Pierre, Phillip Playford, Prasada Rao and Robert Weeden.

The project was carried out while the author was receiving a Commonwealth Post-Graduate Scholarship.

Contents

LIST OF FIGURES.....	vii
-----------------------------	------------

CHAPTER

1 INTRODUCTION.....	1
Aims and Scope of Project.....	1
Regional Geology and Geography.....	1
Previous Investigations.....	3
Methods of Analysis.....	5
2 GEOLOGY OF THE GEIKIE GORGE REGION.....	7
Major Geological Features of the Map Sheet.....	7
Precambrian.....	8
Devonian.....	8
Devonian-Carboniferous.....	8
Carboniferous-Permian.....	8
Quaternary.....	8
Devonian Reef Complexes.....	9
3 SEDIMENTOLOGY OF THE DEVONIAN REEF COMPLEXES IN THE GEIKIE GORGE REGION.....	14
Platform Facies- Pillara Limestone.....	14
Marginal-slope Facies.....	25
Environmental Synthesis.....	36
4 STROMATACTIS AND ASSOCIATED STRUCTURES IN THE DEVONIAN REEF COMPLEXES.....	37
Introduction.....	37
Stromatactis Cavities.....	39
Zebra Limestone.....	42
Wackestones and Bindstones with Abundant Stromatactis and Shelter Cavities.....	45
Cavity-Filling Materials.....	45
Marine Origin of Cavity Systems.....	45
The Stromatactis, Shelter and Sheet Cavity Association.....	48
The Roof of Stromatactis and Sheet Cavities.....	48
Internal Sediment-Host Rock Relationships.....	49
A Soft-Body Decay Model for Stromatactis and Associated Structures.....	49
Significance and Conclusions.....	51

5	MARINE DIAGENESIS IN THE DEVONIAN REEF COMPLEXES OF THE GEIKIE GORGE REGION.....	54
	Introduction.....	54
	Internal Sediments.....	54
	Micritic Encrustations.....	57
	Microlenticular Encrustations.....	57
	Dendritic Encrustations.....	58
	Microcrystalline Cement.....	61
	Fibrous Cements.....	61
	Scalenohedral Cements.....	65
	Aragonite Dissolution.....	66
	Neptunian Dykes and Sills.....	66
	Discussion.....	67
	Synthesis of Marine Diagenesis.....	68
6	POST-MARINE DIAGENESIS IN THE DEVONIAN REEF COMPLEXES OF THE GEIKIE GORGE REGION.....	70
	Introduction.....	70
	Clear Equant Calcite Cements.....	70
	Dolomitization and Dolomite Cementation.....	78
	Compaction.....	85
	Cenozoic Cave Precipitates.....	86
	Karstification.....	87
	Dedolomitization and Associated Calcite Recrystallization.....	90
	Synthesis of Post-Marine Diagenesis.....	96
7	SEDIMENTOLOGY OF THE DEVONIAN CARBONATES ON THE BARBWIRE TERRACE.....	99
	Introduction.....	99
	Supratidal Facies.....	101
	Intertidal Facies.....	107
	Subtidal Facies.....	107
	Discussion.....	116
	Environmental Synthesis.....	119
8	DIAGENESIS IN THE DEVONIAN CARBONATES OF THE BARBWIRE TERRACE.....	120
	Introduction.....	120
	Devonian Syndepositional Diagenesis.....	120
	Discussion of Syndepositional Diagenesis.....	122
	Limestone Cementation.....	124
	Discussion of Limestone Cementation.....	129
	Regional Dolomitization.....	129
	Origin of Regional Dolomitization.....	135

Dolomite Diagenesis.....	140
Discussion of Dolomite Diagenesis.....	142
Compaction.....	143
Porosity Development and Occlusion.....	145
Synthesis of Diagenesis.....	146
9 CONCLUSIONS.....	148
Sedimentology.....	148
Diagenesis.....	149
Suggestions for Further Research.....	152
REFERENCES.....	154
APPENDICES.....	173
A. Sample Catalogue.....	173
B. Analytical Data.....	176
C. Stratigraphic Sections, Stromatoporoid unit of the Pillara Limestone..	181
GEOLOGICAL MAP OF THE GEIKIE GORGE REGION....	Enclosure

List of Figures

FIGURE

1.	Location map of the northern Canning Basin.....	2
2.	Location and geology of the Geikie Gorge region.....	7
3.	Facies nomenclature of the Devonian reef complexes.....	9
4.	Evolution and stratigraphic nomenclature of the Devonian reef complexes.....	10
5.	Stratigraphic nomenclature used for the Devonian carbonates in the Geikie Gorge region.....	11
6.	Lithologies of the stromatoporoid unit, Pillara Limestone.....	15-16
7.	Lithologies of the Pillara Limestone and Napier Formation.....	19-20
8.	Lithologies of the reef-margin subfacies, Pillara Limestone.....	22-23
9.	Lithologies of the Frasnian and Famennian Napier Formation units.....	27-28
10.	Lithologies of the deeper water stromatolite unit.....	30-31
11.	Interpreted structure of the deeper water stromatolite-encrusted platform margins.....	33
12.	Geopetal measurements in the deeper water stromatolite unit.....	34
13.	Distribution of stromatactis and associated structures in the Devonian reef complexes.....	39
14.	Sponge associated stromatactis cavities of the reefal-slope subfacies....	40-41
15.	Stromatactis cavities and zebra limestones.....	43-44
16.	Zebra limestones, stromatactis and shelter cavities.....	46-47
17.	Interpreted origin for stromatactis, shelter and sheet cavities.....	50
18.	Marine diagenetic phases in the reef complexes of the Geikie Gorge region.....	55-56
19.	Marine diagenetic phases in the reef complexes of the Geikie Gorge region.....	59-60
20.	Neptunian dykes of the platform margins.....	62-63
21.	Carbon and oxygen isotope values for marine fibrous cements in the Geikie Gorge region.....	65
22.	Interpreted paragenetic sequence for the marine diagenetic phases.....	67
23.	Clear equant cements in plane light and cathodoluminescence.....	72-73
24.	Carbon and oxygen isotope values for equant calcite cements and replacement dolomite from the Geikie Gorge region.....	74
25.	Distribution of dolomite in the northern Geikie Gorge region.....	78
26.	Dolomitization and dedolomitization fabrics.....	80

27.	Iron, manganese, sodium and strontium contents of dolomites from the Geikie Gorge region.....	82
28.	Model of dolomitization in the Geikie Gorge region.....	84
29.	Cenozoic diagenetic fabrics.....	88-89
30.	Carbon and oxygen isotope values for dedolomite, recrystallized calcite, speleothem calcite and dendritic cave crusts.....	90
31.	Recrystallization of radiaxial fibrous calcite.....	92-93
32.	Interpreted paragenesis for the major diagenetic phases in the Geikie Gorge region.....	98
33.	Well location map for the Barbwire Terrace.....	99
34.	Stratigraphy on the Barbwire Terrace.....	100
35.	Summary of lithotope characteristics.....	101
36.	Distribution of lithotopes in the Devonian carbonates, Barbwire Terrace.	102
37.	Supratidal and intertidal lithologies of the Devonian carbonates, Barbwire Terrace.....	103-104
38.	Subtidal lithologies of the Devonian carbonates, Barbwire Terrace.....	108-109
39.	Clayey lime mudstones and marls from the Devonian carbonates.....	113-114
40.	Lithotope sequences in the Devonian carbonates of the Barbwire Terrac.	115
41.	Relationships between the peritidal lithotopes.....	116
42.	Idealized lithotope sequence for the peritidal lithotopes.....	117
43.	Carbon and oxygen isotope values for synsedimentary supratidal dolomite together with an estimate of the Devonian marine dolomite composition.....	121
44.	Strontium and sodium values for the Devonian dolomite types of the Barbwire Terrace.....	122
45.	Iron and manganese values for the Devonian dolomites of the Barbwire Terrace.....	123
46.	Diagenetic fabrics in the Devonian carbonates of the Barbwire Terrace...	125-126
47.	Textures illustrating the timing of regional dolomitization.....	127-128
48.	Fabrics of the regional dolomite type.....	130-131
49.	Paragenesis of the regional dolomites in Boab #1.....	134
50.	Carbon and oxygen isotope values for the regional dolomites of the Barbwire Terrace.....	135
51.	Dissolution of iron-rich zones in the limpid dolomite cement.....	141
52.	Carbon and oxygen isotope values for calcite cements within the regional dolomites.....	142
53.	Interpreted porosity paragenesis in the regionally dolomitized lithologies	146
54.	Interpreted paragenesis of the major diagenetic phases in the Devonian carbonates of the Barbwire Terrace.....	147
55.	Interpreted carbonate mineral stability zones in the Devonian ocean.....	150
56.	Generalized carbon and oxygen isotope compositional fields for the Devonian carbonates of the Barbwire Terrace and the Lennard Shelf...	151

1. INTRODUCTION

Aims and Scope of Project

This project evolved from a detailed investigation of two Devonian carbonate sequences in the Northern Canning Basin, Western Australia. The Geikie Gorge area forms part of the spectacularly well preserved limestone reef complexes which fringe the northern margin of the Canning Basin (Fig. 1). In contrast, the Devonian carbonates of the Barbwire Terrace are entirely concealed and are strongly dolomitized (Fig. 1). The major objectives of the project were to:

- a) produce a detailed geological map of the Geikie Gorge region.
- b) investigate particular aspects of the sedimentology of the reef complexes (e.g. the origin of stromatactis structures) and to refine further the facies scheme developed by Playford (1980).
- c) investigate the diagenetic history of the reef complexes.
- d) determine the major environments of deposition for the Devonian carbonates of the Barbwire Terrace.
- e) investigate the diagenetic history of the Devonian carbonates of the Barbwire Terrace.

Regional Geology and Geography

Physiography and Climate

The large (430, 000 km²) intracratonic Canning Basin lies largely within the Great Sandy Desert of north-western Australia and was, for many years, known as the "Desert Basin" (Jutson, 1934). The present name of the basin is taken from the Canning Stock Route (after the pioneer surveyor A.W. Canning) established across the Great Sandy Desert in 1906 (Purcell, 1984). Much of the basin is covered by a longitudinal dune field consisting of red aeolian sand. This makes access difficult and as there is very little surface water, the desert has remained unsettled. The longitudinal dunes trend WNW-ESE (aligned with the prevailing easterly winds) and are part of a continent-wide dune system which is believed to have developed during an arid period in the Quaternary.

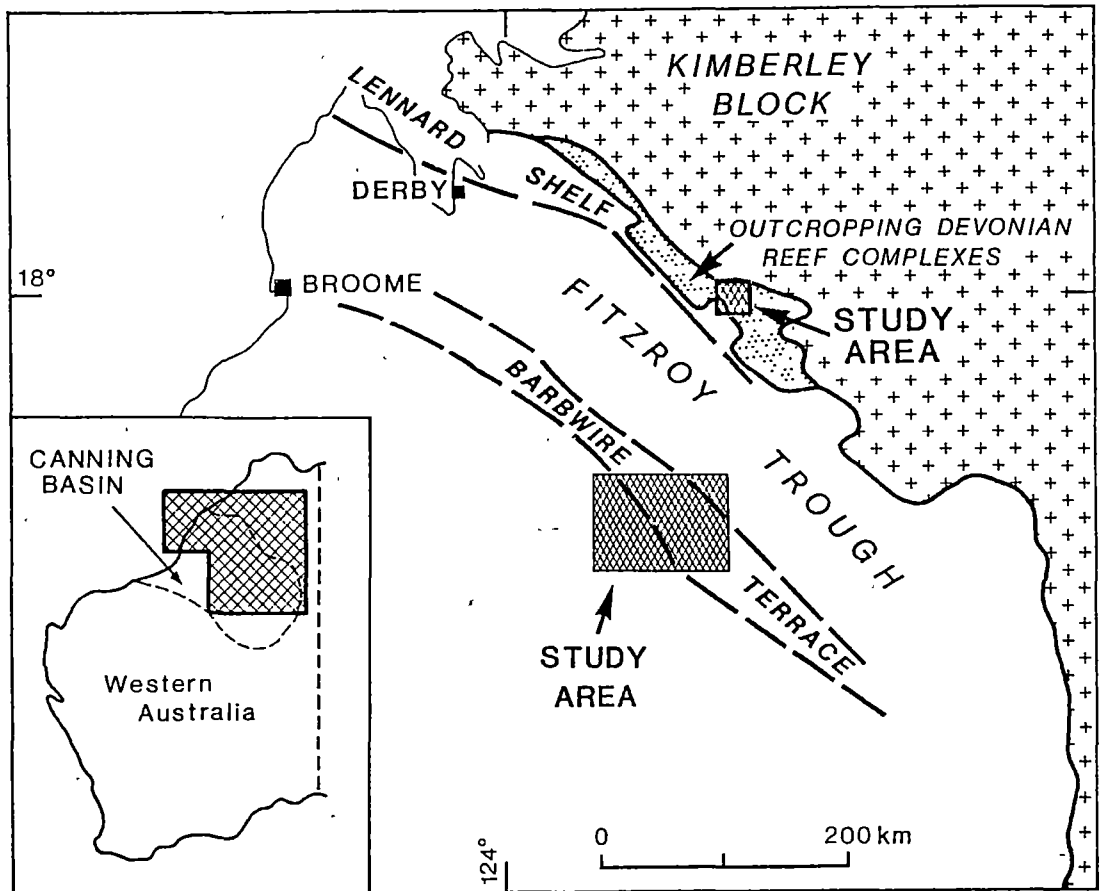


Figure 1. Map of the northern Canning Basin showing the location of the study areas.

In the northern part of the basin, the topography is more varied, with the Devonian reef complexes forming a series of rugged limestone ranges which fringe the basin margin. Between the limestone ranges and the Great Sandy Desert lies the Fitzroy Valley, which is a relatively flat plain of recent alluvium and includes the valleys of the Fitzroy, Lennard, Barker and Margaret rivers (Purcell, 1984).

The climate is characterized by a warm dry season (April to November) and a hot wet season (December to March). Generally all of the rainfall occurs during the wet months (causing extensive flooding) and little or no rain falls in the dry season. The climate is classified as true desert-tropical (semi desert-tropical in the northern parts of the basin) (Beard and Webb, 1974).

The vegetation in the region is dominated by spinifex (*Triodia*) grasslands and savanna; a vegetation type unique to arid Australian environments. Trees and shrubs in the region include *Acacia*, *Eucalyptus*, *Adansonia* (boab), *Owenia* (desert walnuts), *Bauhinia*, *Cassia*, and *Eremophila*.

Regional Geology of the Northern Canning Basin

The Canning Basin was initiated during the early Ordovician and contains at least 10 km of Palaeozoic sediments. The basin geology has been documented in detail in many recent publications (Forman and Wales, 1981; Towner and Gibson, 1983; numerous papers in Purcell, 1984). The major structural element in the northern Canning Basin is

the Fitzroy Trough which is bordered to the north by the Lennard Shelf and to the south by the Barbwire Terrace (Fig. 1).

The Fitzroy Trough underwent rapid subsidence during the Palaeozoic, and thick deposits of clastic sediments accumulated within it. Thick sequences of carbonates accumulated on the flanking terraces and shelves adjacent to the Fitzroy Trough in the Late Devonian to Early Carboniferous. On the Lennard Shelf, the Devonian-Carboniferous carbonates include reef complexes and shallow shelf carbonates, and outcrop in a belt approximately 350 km long. On the Barbwire Terrace, subsurface Devonian-Carboniferous carbonates are over 1000 m thick (Ashton, 1984).

The Devonian-Carboniferous carbonates are also prospective targets for petroleum reservoirs and Mississippi Valley type lead-zinc deposits.

Previous Investigations on the Upper Devonian Carbonates of the Lennard Shelf and Barbwire Terrace

The outcropping limestones of the Lennard Shelf were first discussed in 1883 by E. T. Hardman but he did not recognize them as reef complexes (Playford and Lowry, 1966). Wade, in 1924, was the first to recognize their reefal origin (Playford and Lowry, 1966). Teichert published a number of important papers on the palaeontology and stratigraphy of the Devonian carbonates (Teichert, 1939, 1941, 1943, 1947, 1949) which established the biostratigraphy of the reef complexes.

Guppy *et al.*, (1958) refined the stratigraphy of the reef complexes and most importantly, recognized that the strong dip on marginal slope beds was largely depositional. Guppy *et al.*, (1958) believed that the contact between platform and marginal slope facies was an unconformity. Rattigan and Veevers (1961) further refined the stratigraphy of the reef complexes.

Playford and Lowry (1966) were the first to present relatively large scale (1: 100 000 scale) maps of the reef complexes and were the first to examine the petrology of the reef complexes in detail. Building on the work of West Australian Petroleum Pty. Ltd. (Wapet) geologists, Playford and Lowry (1966) presented a depositional model for the reef complexes in which the platform and marginal-slope facies were suggested to be lateral facies equivalents. Playford (1969) then compared the Devonian reef complexes of Canada with those of the Lennard Shelf. Read (1973a, b) studied vertical lithological cycles in the platform facies from various localities on the Lennard Shelf (including one from the Geikie Range) but did not consider lateral facies transitions or the platform-margin and marginal-slope lithologies.

The Playford and Lowry (1966) bulletin and subsequent publications (Playford, 1976) were accessible to a large number of researchers worldwide and the significance of these spectacularly exposed ancient reef complexes soon became well known. However, after an intensive petrologic and field study, Logan and Semeniuk (1976) suggested that the carbonates were largely of metamorphic origin and not reef complexes at all. Logan and Semeniuk proposed that the abutment zone (platform margin of Playford and Lowry, 1966) was a zone of intense deformation and pressure solution and thrusting which bordered the unmetamorphosed Pillara Limestone. Logan and Semeniuk (1976) further proposed many complex nomenclatural systems covering what they interpreted as pressure solution structures, tectonically induced cavity systems and calcite precipitates.

Playford (1980) then published an updated interpretation of the reef complexes which included much new work on the stratigraphy, platform margin types, faunal distribution, and structural evolution of the reef complexes. Playford (1980) also refuted the metamorphic hypothesis of Logan and Semeniuk (1976) and strengthened the reef model by presenting detailed work on the depositional dips of the marginal slope beds (from geopetal structures) and by giving quantitative estimates of the amount of stylolitization that had taken place. Detailed maps and cross sections were published in an excursion guide for the Fifth Australian Geological Convention (Playford, 1981).

The Canning Basin Symposium volume (Purcell, 1984) contains 45 papers and eight papers dealt with the Devonian reef complexes. Detailed geological investigations of the Pillara Range carbonates were published by Hall (1984), Benn (1984) and Cooper *et al.* (1984). Playford (1984) documented the platform-margin relationships in the reef complexes and outlined some of the major diagenetic processes. Logan (1984) presented a version of the structural-metamorphic hypothesis for the origin of carbonates on the Lennard Shelf but failed to address previous criticisms (Playford, 1980) of the hypothesis. Etminan *et al.* (1984) gave a review of geochemical studies on the reef complexes.

Playford *et al.*, (1984) reported high iridium concentrations in cyanobacterial (*Frutexites*) carbonates at the Frasnian-Famennian boundary within the reef complexes. Iridium contents were higher in the cyanobacterial colonies than in the surrounding sediments and Playford *et al.*, (1984) suggested that the iridium may have been biologically concentrated or that it may be comparable with other meteoroid-impact-related iridium anomalies at the Cretaceous-Tertiary mass extinction boundary (Alvarez *et al.*, 1980).

Kerans (1985) carried out a major regional investigation on the petrography and diagenesis of the reef complexes in which he described all of the major lithologies and diagenetic components. Kerans *et al.*, (1986) gave a review of the marine diagenesis of the carbonates and Kendall (1985) made a detailed crystallographic study of marine radiaxial fibrous calcites. This work laid the foundation for more detailed studies on individual aspects of the reef complexes (Hurley, 1986; Ward, *in prep*; Pedone, *in prep*). Hurley (1986) made a detailed study of the sedimentology and diagenesis of the Oscar Range reef complex as well as investigating the palaeomagnetism of the reef complexes (Hurley and Van der Voo, 1987). This work established a palaeolatitude of 15°S for the reef complexes.

Palaeontologically, the reef complexes have been very thoroughly investigated. Cephalopods were studied by Teichert (1941, 1943, 1949), Glenister (1958) and Petersen (1975). Numerous studies of conodonts (reviewed in Nicoll, 1984) have been carried out on the reef complexes. Corals have been studied by Hill and Jell (1970); bryozoans by Ross (1961); brachiopods by Coleman (1951), Veevers (1959) and Grey (1978); algae by Wray (1967); stromatolites by Playford and Cockbain (1969), and Playford *et al.* (1976); plant microfossils by Balme and Hassell (1962), and Playford, G. (1976); radiolarians by Nazarov *et al.*, (1982); fish by Long (1987) and numerous others (Dennis-Bryan and Miles, 1983; Dennis and Miles, 1979); crustaceans by Briggs and Rolfe (1983), and Rolfe (1966); stromatoporoids by Cockbain (1984); and sponges by Rigby (1986).

The Upper Devonian carbonates of the Barbwire Terrace do not outcrop and were first intersected in the subsurface in the wells Crossland Nos. 1 and 3, and

Barbwire No. 1 (WAPET, 1971, 1972). In the 1980's, Western Mining Corporation embarked on a program of slim-hole diamond drilling in the region. Numerous stratigraphic wells were drilled and many intersected the Devonian carbonates (Ashton, 1984). The present study of the Barbwire Terrace carbonates is based on the continuously cored sections which resulted from this drilling program.

Methods of Analysis

Field mapping was done on mylar overlays over 1: 25 000 colour aerial photographs. The western portion of the Geikie Gorge region was mapped using aerial photographs produced by Kevron Aerial Surveys (Fitzroy Crossing, Runs 7-11, 1981) while the eastern portion was mapped using Aerial Surveys Australia photographs (Baramundi, Runs 7-9, 1981). The photographs were supplied by the Geological Survey of Western Australia. Data were plotted on 1: 25 000 topographic maps supplied by BHP Minerals.

The petrographic classification used throughout this report is Embry and Klovan's (1971) modification of Dunham's (1962) carbonate classification scheme. Choquette and Pray's (1970) porosity classification is used throughout this report. Petrographic analysis was carried out on stained (alizarin red-S and potassium ferricyanide, Dickson, 1966) and unstained polished thin sections. Polished, unstained thin sections were examined under cathodoluminescence using a Nuclide ELM-2B Luminoscope. Operating conditions for cathodoluminescence petrography were 8 kV beam energy and approximately 0.6 milliamps beam current. Electron micrographs were taken on a Philips 505 SEM. Microprobe analyses (one probe traverse across a dolomite crystal) were performed on a JEOL JXA50A electron microprobe using an energy dispersive system with silicate standards and ZAF corrections. An analytical precision of 0.2 wt% is expected using this system.

Isotope and Trace Element Geochemistry

Individual diagenetic phases (calcite and dolomite cements etc.) were separated and sampled using a dental drill. Stable isotope analyses were performed on 1 to 30 mg samples using phosphoric acid at 25°C and run on a Micromass VG 602D ratio mass spectrometer. All analyses were converted to PDB values and corrected for ^{17}O as described by Craig (1957) and Mook and Grootes (1973). Precision was determined by daily analysis of the calcite standards TKL-1 (Te Kuiti Limestone No. 1) and MLT (University of Tasmania internal standard) and through duplication of approximately 5% of samples ($1\sigma = 0.08$ ‰ for $\delta^{13}\text{C}$ and 0.11 ‰ for $\delta^{18}\text{O}$). With regard to accuracy, daily analyses of the TKL - 1 standard differed by an average of 0.08 ‰ for $\delta^{13}\text{C}$ and 0.14 ‰ for $\delta^{18}\text{O}$ from those values listed by Blattner and Hulston (1978) {Mean values for daily TKL-1 analyses were $\delta^{18}\text{O} = -4.38$ ‰ (PDB) and $\delta^{13}\text{C} = -1.73$ ‰ (PDB)}. Dolomite $\delta^{18}\text{O}$ values are approximately 0.8 ‰ too positive because they have not been corrected for the dolomite-calcite phosphoric acid fractionation factor (Sharma and Clayton, 1965). This is because the precise value of the phosphoric acid fractionation factor for dolomite has not yet been precisely determined and Land (1980) has recommended that dolomite analyses should not be corrected.

Trace and major element analyses were performed on a Varian AA6 atomic absorption spectrometer using 50 mg samples. A method similar to that used by Robinson (1980) was employed, where samples are placed in 1M HCL for two hours. The GFS 400 dolomite standard was used to monitor the precision. Minor contamination from the non-carbonate fraction can be expected for the iron results (Robinson, 1980).

2. GENERAL GEOLOGY OF THE GEIKIE GORGE REGION

Major Geological Features of the Map Sheet

The Devonian carbonates of the Geikie Gorge map sheet (see map enclosure and Fig. 2) consist of a series of reef-rimmed platforms and shallow basins, bordered to the north-east by Precambrian basement. The carbonates have a gentle structural dip to the south-west so that the oldest carbonates outcrop in the north-east portion of the map. However, the age distribution within the reef complexes is also strongly controlled by the primary depositional structure of the carbonates. Frasnian lithologies are largely restricted to the platforms and Famennian carbonates are entirely restricted to the basins. This is because the Famennian platform carbonates were removed during Late Carboniferous erosion.

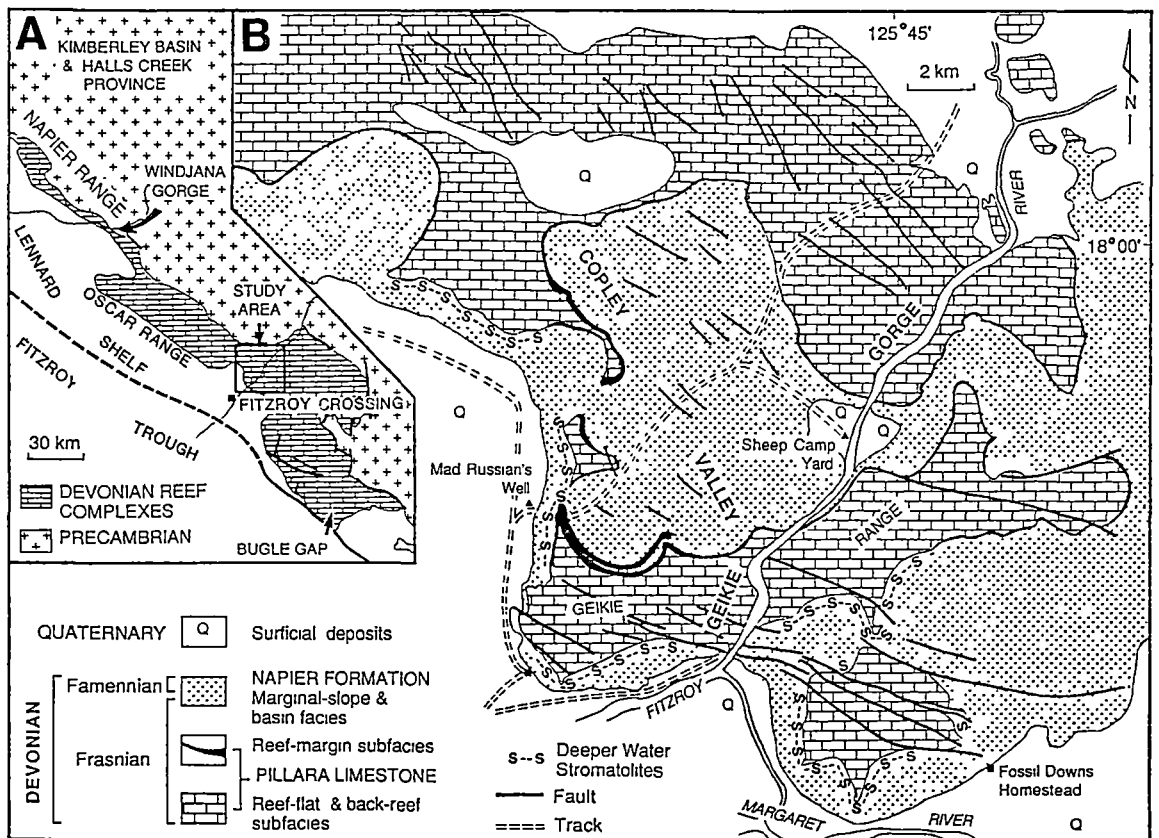


Figure 2. A) Location of Geikie Gorge region within the outcropping Devonian reef complexes. B) Geological map of the Geikie Gorge region.

Numerous NW-SE trending faults are present within the carbonates and displacement on these is generally small. Intense syn-sedimentary fracturing is commonly associated with these faults, suggesting that some of the faults were active during the Late Devonian.

Precambrian

The Lower Proterozoic Lennard Granite and McSherrys Granodiorite (Gellatly *et al.*, 1968; Derrick and Playford, 1973) of the Lamboo Complex are very poorly exposed in the map area but are well exposed to the north. The Lennard Granite, exposed in the north of the sheet, is a coarse-grained porphyritic biotite granite which forms small plugs, lenticular stocks and small batholiths (Derrick and Playford, 1973). In the Oscar Range to the west, the younger Oscar Range Succession underlies the Devonian carbonates and these rocks may extend under the Devonian carbonates of the Geikie Gorge region.

Devonian

Devonian carbonates in the sheet area range in age from Frasnian to Famennian. The carbonates are directly underlain by Precambrian rocks and are overlain conformably by the Devonian-Carboniferous Fairfield Group or unconformably by the Upper Carboniferous-Lower Permian Grant Group. The Devonian carbonates are discussed more fully in later sections of this report.

Devonian-Carboniferous

The Upper Devonian-Lower Carboniferous Fairfield Group (Thomas, 1957; Druce and Radke, 1979) does not crop out in the sheet area but was intersected in the subsurface (from the spoil of Mad Russian's Well). It consists of limestones, dolomites, shales and siliciclastics and is interpreted to be of dominantly shallow-marine origin (Druce and Radke, 1979).

Carboniferous-Permian

The Upper Carboniferous-Lower Permian Grant Group unconformably overlies all older rocks and consists of sandstones, siltstones, conglomerates and some pebbly mudstones. It is generally considered to be of glacial marine and non-marine origin. In the sheet area, Grant Group sandstones with poikilitic calcite cements occur in karst depressions (a few acres in area) within the Upper Devonian carbonates. Hurley (1986) noted that sandstones of the Grant Group fill cavities within the Devonian carbonates to depths of 210 m in the southeast Oscar Range. The top of the Devonian limestone ranges on the Lennard Shelf have a remarkably uniform elevation and a relatively planar morphology and this is thought to be the exhumed pre-Grant unconformity surface, which has undergone little tectonic deformation since then.

Quaternary

Deposits mapped as Quaternary in age include black soils, alluvium and sandy soils. Black soils are very widespread around the limestone ranges and commonly display gilgai features (patterned ground, Playford and Lowry, 1966). The clay is thought to

be the residual clay which was left after the dissolution of limestones in the meteoric environment (Playford and Lowry, 1966). Sandy soils are commonly developed on the small areas of Grant Group exposure.

Quaternary travertine deposits are commonly developed along springs and creeks in the carbonates. Travertine dams and pools occur along creeks in the Geikie Gorge region and these may be precipitated by partly biochemical processes (Julia, 1983).

Devonian Reef Complexes

Depositional Model

The Devonian reef complexes of the Lennard Shelf consist largely of reef-fringed platforms (developed close to sea level) flanked by dipping marginal-slope deposits which descend into deeper (tens to hundreds of meters) basinal environments. The platforms range in size from several hundred square kilometres to small platform atolls and pinnacle reefs. Some platforms were not reef rimmed and lacked the steep marginal slope deposits. Detailed lithological mapping and microfacies analysis carried out in this study have confirmed the validity of Playford's (1980) facies subdivisions (Fig. 3). The stratigraphic nomenclature used reflects the major facies subdivisions and is illustrated in Figure 4 (from Playford, 1980).

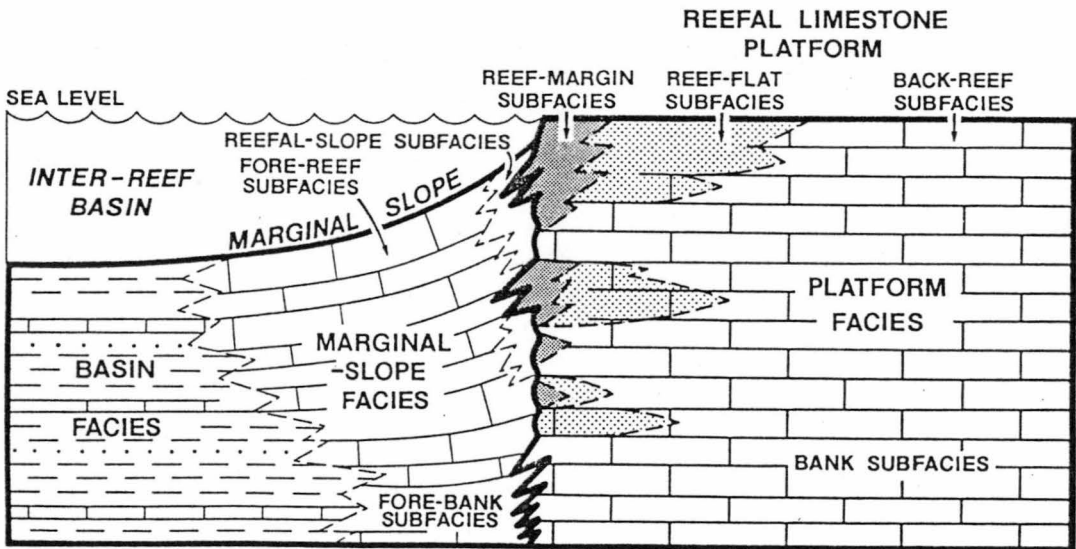


Figure 3. Facies nomenclature of the Devonian reef complexes (after Playford, 1984)

In the Geikie Gorge region, platforms invariably have steep margins. The back-reef subfacies consists of well-bedded limestones (with minor dolomites) that range from high-energy peritidal peloid-oid-oncoid grainstones (commonly with fenestral fabrics) to low energy lime mudstones and skeletal wackestones. The reef-flat subfacies is developed in a narrow zone (generally around 250 m wide) around the platform margins and consists of thickly bedded fenestral peloidal (or ooid) grainstones in which fenestral stromatolites are commonly developed. The reef-margin subfacies is developed in a very narrow zone (generally 5-10 m wide) which rims the

platform margins and consists of massive cyanobacterial-stromatoporoid framestones with abundant marine cements and internal sediments.

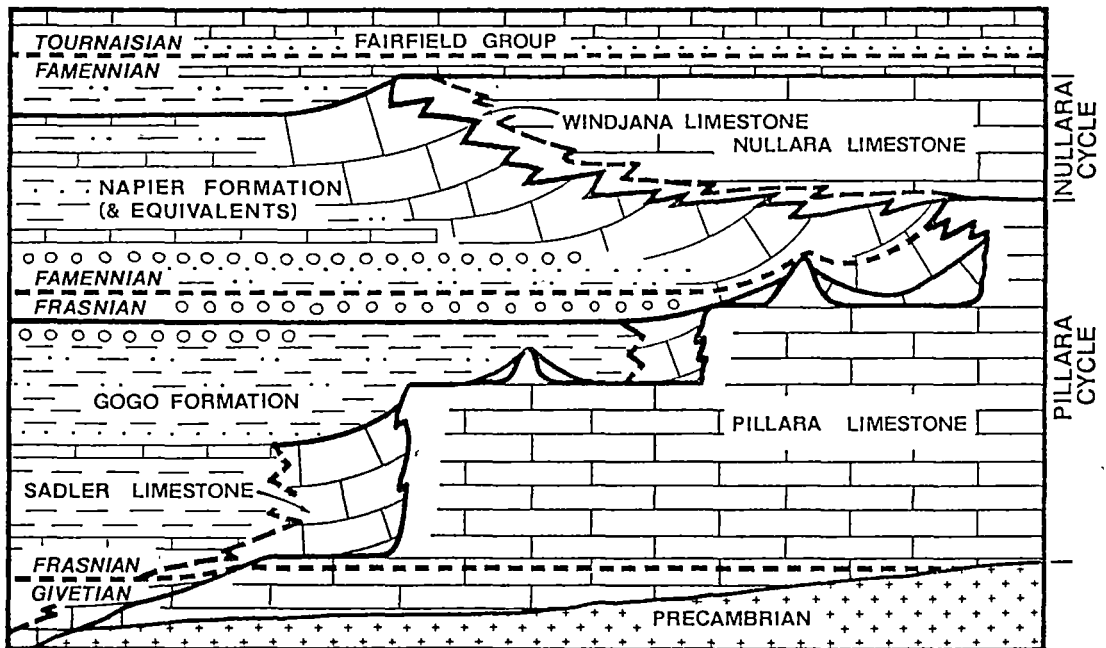


Figure 4. Diagrammatic section illustrating development of reef complexes through time and relationship of stratigraphic units (after Playford, 1984).

The reefal-slope subfacies (of the upper marginal slope) is a narrow zone of poorly bedded (dipping) limestones which range from skeletal-peloid grainstones and packstones to skeletal wackestones. The reefal-slope subfacies commonly has a high proportion *in-situ* skeletal components (particularly sponges) and an abundance of stromatactis structures. Dips in the reefal-slope subfacies can be almost vertical and are largely of depositional origin (geopetal evidence, Playford, 1980 and discussed later). Down-dip, the reefal-slope subfacies grades into the well-bedded fore-reef subfacies which consists of peloidal grainstones and many breccia types. Dips in the fore-reef subfacies range up to 35° .

The basin facies does not outcrop in the Geikie Gorge area because of its high clay content. Elsewhere on the Lennard Shelf, the basin facies consists of laminated and nodular impure limestones, marls and calcareous shales.

Virtually all of the subfacies have gradational boundaries with laterally adjacent subfacies.

Mappable Units

The Devonian reef complexes were subdivided and mapped using a stratigraphy based on that of Playford and Lowry (1966). However, in this report, Frasnian and Famennian carbonates were differentiated (Playford and Lowry did not differentiate Frasnian and Famennian deposits). Hence the Napier Formation is here subdivided into a Frasnian and a Famennian unit. In addition, the Pillara Limestone has been

subdivided into a number of units. Figure 5 illustrates the stratigraphic relationships between the mappable units.

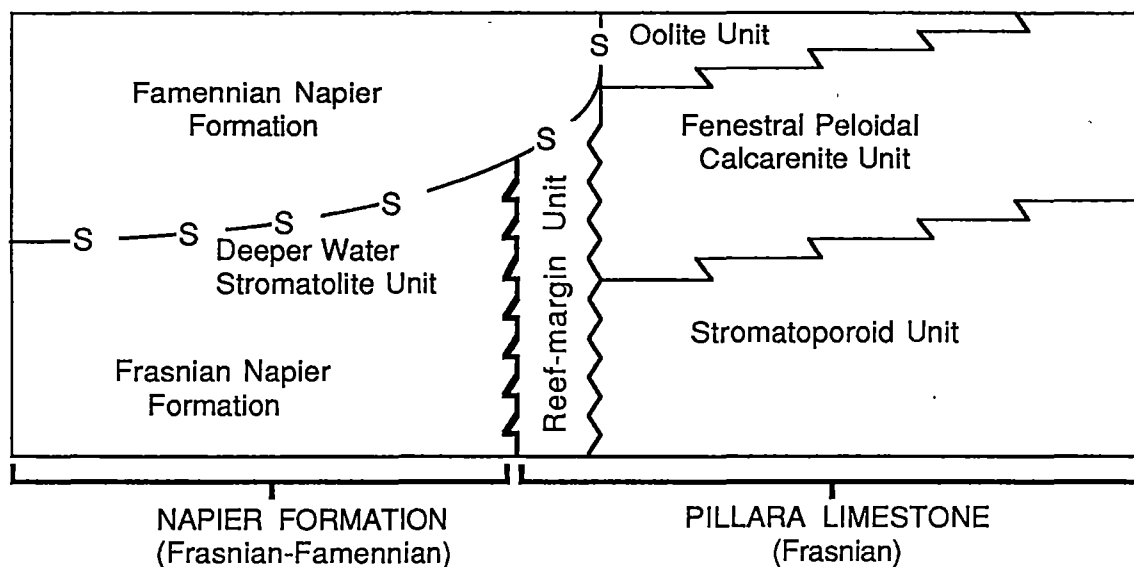


Figure 5. Stratigraphic nomenclature used for the Devonian carbonates of the Geikie Gorge area.

Three previous geological maps of the Geikie Gorge area have been published (Guppy *et al.*, 1958; Rattigan and Veevers, 1961; Playford and Lowry, 1966). Guppy *et al.* (1958) together with Rattigan and Veevers (1961) subdivided the marginal-slope deposits into numerous different formations at different localities (e.g. Copley Formation, Oscar Formation, Brooking Formation and Geikie Formation). These subdivisions have been abandoned in this study because they could not be differentiated in the field.

Platform Facies; The platform carbonates in the Geikie Gorge area are all of Frasnian age and therefore belong to the Pillara Limestone (Playford and Lowry, 1966). Only the reef-margin subfacies was mapped as a distinct unit. The reef-flat and back-reef subfacies were not separated. The platform carbonates were subdivided into four informal units:

- 1) The *Pillara Limestone stromatoporoid unit (Dps)* includes back-reef and reef-flat lithologies and is the oldest unit in the Geikie Gorge area. It was distinguished in the field by its bedding characteristics (thickly bedded in reef-flat and well bedded in back-reef subfacies, lacks depositional dips) and by the abundance of stromatoporoids (bulbous *Actinostroma* and branching *Amphipora*). Fenestral grainstones are common in the reef-flat subfacies of this unit.
- 2) The *Pillara Limestone fenestral peloidal calcarenite unit (Dpp)* includes back-reef and reef-flat lithologies. It was distinguished by its bedding characteristics (as above) and by the abundance of fenestral fabrics.
- 3) The *Pillara Limestone oolite unit (Dpo)* includes reef-flat and back-reef lithologies and is the youngest platform unit in the Geikie Gorge region. It has bedding

characteristics similar to those described above and is characterized by an abundance of ooids.

4) The *Pillara Limestone reef-margin unit (Dpr)* was mapped as a separate unit which occurs as a discontinuous unit fringing the platform facies. It was distinguished in the field by its massive unbedded fabric, by its light colour, and by the abundance of *Renalcis* and other cyanobacteria. The reef-margin subfacies generally has transitional boundaries with the reefal-slope and reef-flat subfacies.

Read (1973b) subdivided the Pillara Limestone into three units: The Menyous Member, Red Bull Member and Big Spring Member. However, this classification has not been generally adopted by recent workers because Read (1973a,b) considered the members as lateral facies equivalents on a broad shelf (e.g. Fig. 24, Read, 1973a). Read (1973a,b) did not recognize the presence of discrete platforms and believed that most formation contacts were faults.

Hurley (1986) subdivided the Pillara Limestone in the south-eastern Oscar Range into several units. Hurley's (1986) reef-margin unit is equivalent to the reef-margin unit recognized in this report. Hurley's (1986) *Amphipora* unit may be partially equivalent to the stromatoporoid unit of this report. Hurley's fenestral oolite unit may be partially equivalent the fenestral peloidal and oolite units of this report. In both the south-eastern Oscar Range and Geikie Gorge regions, there is a gradation from older stromatoporoid carbonates to younger fenestral and ooid dominated carbonates. However, this generalization is likely to be complicated by lateral facies changes and individual platform effects. Hurley's calcarenite member was not recognized in the Geikie Gorge region.

Marginal-slope facies; The reefal-slope and fore-reef subfacies were not mapped as separate units. Marginal-slope carbonates were subdivided informally into three units:

1) The *Napier Formation, Frasnian unit (Dnr)* includes reefal-slope and fore-reef lithologies and was distinguished in the field by its bedding characteristics (well-bedded in fore-reef subfacies, thickly bedded in reefal-slope, strong depositional dips) and by the abundance of various breccia types. The Frasnian age of the unit was interpreted from the macrofossil content and because the unit underlies the deep water stromatolite unit (discussed below).

2) The *deeper-water stromatolite unit* consists of a narrow discontinuous zone of non-fenestral stromatolites which generally fringes the platform carbonates of the Pillara limestone and less commonly occurs as a series of horizons in the fore-reef subfacies. It was recognized in the field by its massive appearance, generally impure composition, red or olive-drab colour, and commonly by striking stromatolitic textures. Because of its relatively impure composition, it commonly occurs as a low-relief area between the platform facies and the Famennian Napier Formation.

Deeper-water stromatolites have been recorded from many localities in Devonian reef complexes (Playford and Cockbain, 1969; Playford *et al.*, 1976). Dating by detailed conodont studies (Druce, 1976) demonstrates the stromatolites to be of latest Frasnian-earliest Famennian age. Hurley (1986) has also documented a major deep-water stromatolite unit of a similar age, thus demonstrating the shelf-wide extent of the unit. The deep-water stromatolite unit is therefore a useful datum which lies approximately between Frasnian and Famennian marginal-slope deposits (more fully discussed later).

3) The *Napier Formation, Famennian unit (Dna)* has similar lithological characteristics to the Frasnian unit of the Napier Formation. The Famennian age of the unit is indicated by the macrofossil content and because the unit is underlain by the deep-water stromatolite unit.

3. SEDIMENTOLOGY OF THE DEVONIAN REEF COMPLEXES IN THE GEIKIE GORGE AREA

Platform Facies - Pillara Limestone

Four informal units are identified in the Pillara Limestone: 1) the stromatoporoid unit; 2) the fenestral peloidal grainstone unit; 3) the oolite unit; and 4) the reef-margin unit. The major lithologies from each of these units is described below.

Stromatoporoid Unit

The stromatoporoid unit was so named because of the abundance of *Amphipora* (a delicately branching stromatoporoid) and other bulbous stromatoporoids (*Actinostroma*) in the back-reef subfacies of this unit. The unit is commonly completely dolomitized (the distribution of dolomite is discussed later). This unit includes both back-reef and reef-flat subfacies and outcrops in the north-eastern portion of the Geikie Gorge area.

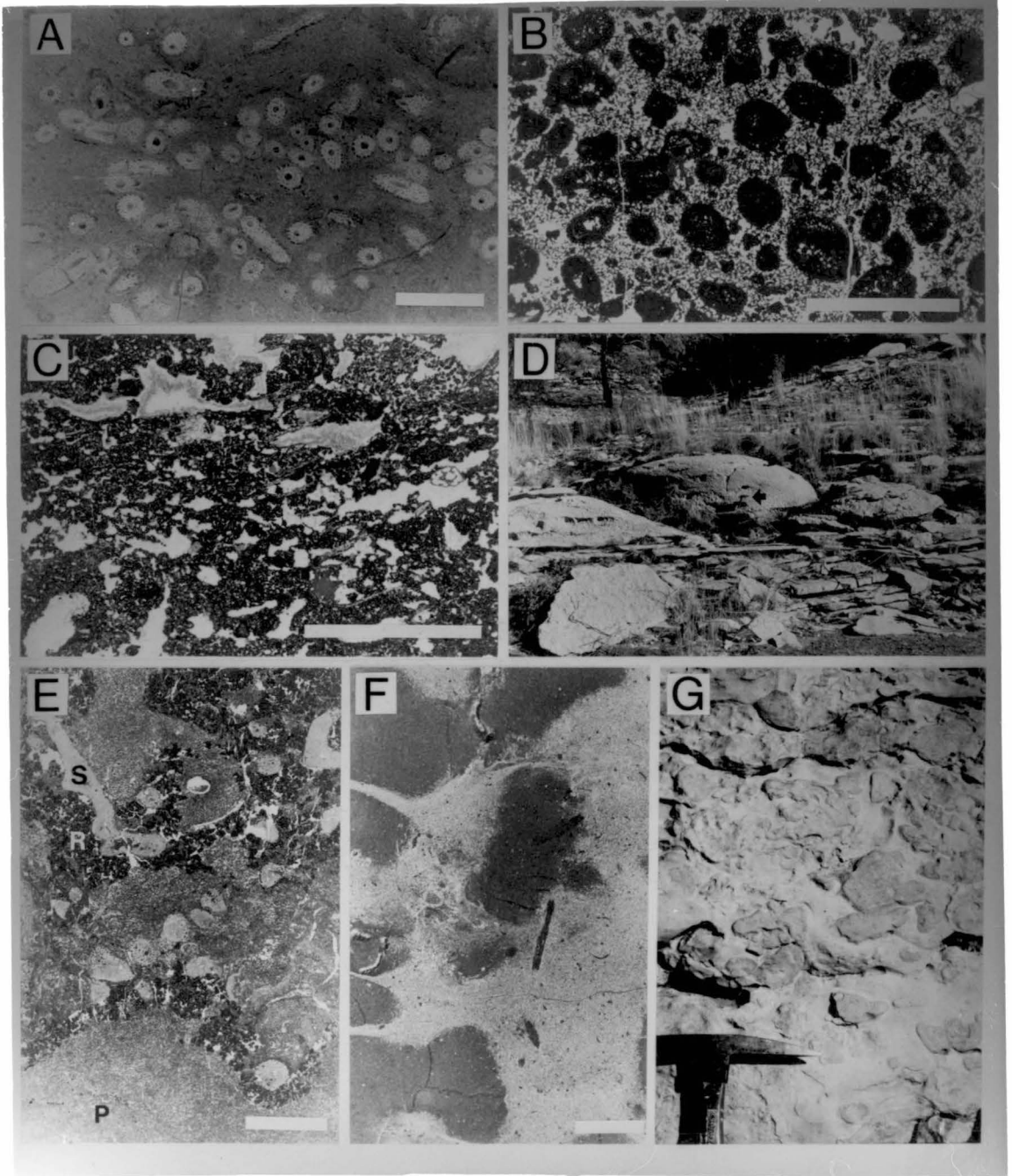
Back-reef subfacies; The dominant lithologies are *Amphipora* floatstones and rudstones, peloidal-skeletal grainstones, bulbous stromatoporoid floatstones and rudstones, oncoid floatstones and rudstones, and clayey nodular lime mudstones (Fig. 6). The matrices of floatstones and rudstones are either lime mud or peloidal-skeletal grainstones. Minor lithologies include fenestral peloidal grainstones and packstones, fenestral *Amphipora* rudstones, and intraclast grainstones and rudstones. Fenestral fabrics present include tubular, laminoid and irregular morphologies. When traced laterally, beds commonly show strong lithological changes over relatively short distances.

Weakly developed lithological cycles are occasionally developed within the back-reef subfacies of the unit and these consist of, in descending order:

- Peloidal-skeletal grainstones,
- Amphipora* floatstones,
- Amphipora* rudstones,
- Clayey bulbous stromatoporoid rudstones.

Figure 6. Lithologies of the stromatoporoid unit of the Pillara Limestone.

- A) Polished slab of an *Amphipora* floatstone with a fine peloidal-skeletal grainstone matrix. Back-reef subfacies, Pillara Limestone, northern Geikie Gorge. Scale bar = 1 cm. UTGD sample no. 70272
- B) Thin-section photomicrograph of an oncoid rudstone with a peloidal grainstone matrix. Back-reef subfacies, Pillara Limestone, northern Geikie Gorge. Scale bar = 1 cm. UTGD sample no. 70271
- C) Thin-section photomicrograph of a fenestral peloidal grainstone from the reef-flat subfacies. Note the fibrous cements which line many of the cavities. Pillara Limestone, northern Geikie Gorge. Scale bar = 1 cm. UTGD sample no. 70297
- D) Stromatoporoid-*Renalcis* mound within well-bedded lithologies of the stromatoporoid unit. Back-reef subfacies, Pillara Limestone, northern Geikie Gorge. Hammer for scale (arrow).
- E) Thin-section photomicrograph of a Stromatoporoid-*Renalcis* framestone from the upper portion of a mound within the stromatoporoid unit. Stachyodiform stromatoporoids (S) are encrusted by *Renalcis* (R). The interstices in the framework are filled with peloidal grainstones (P). Back-reef subfacies, Pillara Limestone, northern Geikie Gorge. Scale bar = 1 cm. UTGD sample no. 70270
- F) Stained (alizarin red-S) polished slab of clayey nodular lime mudstone from the back-reef subfacies of the stromatoporoid unit. The dark nodules consist of clayey lime mudstone and the light interstitial material is dolomitized calcareous shale. Pillara Limestone, northern Geikie Gorge. Scale bar = 1 cm. UTGD sample no. 70284
- G) Vertical exposure of bulbous stromatoporoid rudstones and floatstones from the back-reef subfacies of the stromatoporoid unit. Pillara Limestone, northern Geikie Gorge. Hammer for scale.



Small stromatoporoid *-Renalcis* mounds (1-4 m high and 1-5 m wide) were observed at two localities (Appendix C, sections 1 and 2) in the back-reef subfacies of the stromatoporoid unit. The mounds have a massive fabric and an ellipsoidal or domal outline in section (Fig. 6B). They consist predominantly of stromatoporoid rudstones but also contain crinoidal debris, brachiopods, solitary rugose corals, thamnoporids and bryozoans. The stromatoporoids generally have a bulbous morphology and are commonly in position of growth. The matrix in the mounds consists of fine peloidal-skeletal grainstones and packstones.

In the upper parts of the larger mounds, thick coatings (up to 2 cm thick) of *Renalcis* line the stromatoporoids (bulbous *Actinostroma* and branching *Stachyodes*) and the lithology would be classified as a **stromatoporoid-*Renalcis* framestone** (Fig. 6E). *Sphaerocodium* is also present in the framestones. Several generations of internal sediment commonly fill large cavities in the framestones. No fibrous marine cements were observed within the cavities but, as is usually the case, microcrystalline cement surrounds the *Renalcis* colonies.

At both localities, the mounds were restricted to a single horizon and it may be that the two occurrences belong to a single horizon. Hurley (1986) described a similar horizon within his *Amphipora* unit (informal subdivision of the Pillara Limestone) of the north-western Oscar Range and was able to trace the bed for several kilometres. It is possible that the stromatoporoid-*Renalcis* mound horizon at Geikie Gorge correlates with that observed in the Oscar Range. However, this cannot be confirmed without more accurate dates on the horizons.

Reef-flat subfacies; The reef-flat subfacies of the stromatoporoid unit consists predominantly of **fenestral peloidal-skeletal grainstones** (Fig. 6C) which grade into **columnar fenestral stromatolitic framestones** closer to the reef margin. Columnar stromatolites directly adjacent to the reef-margin subfacies are commonly coated by *Renalcis*. Fenestrae most commonly have an irregular morphology but laminoid fenestrae are also present. Other lithologies in the reef-flat subfacies include ***Amphipora* rudstones and floatstones and peloidal-skeletal grainstones**. The lithologies of the reef-flat subfacies of the stromatoporoid unit closely resemble the back-reef lithologies of the fenestral peloidal grainstone unit.

Interpretation; The back-reef subfacies of the stromatoporoid unit is interpreted as being deposited in a relatively quiet water, restricted, lagoonal environment. This is based on the generally fine-grained nature of the lithologies, the low diversity but high abundance of fauna and the paucity of exposure indicators. *Amphipora* is characteristic of Devonian restricted lagoonal settings (Wilson, 1975; Burchette, 1981).

The lateral impersistence of many of the lithologies in the back-reef subfacies of the stromatoporoid unit suggests an irregular bottom topography with frequent lateral facies transitions. The minor tubular and laminoid fenestral grainstone lithologies in the unit may represent small intertidal-supratidal islands (Pratt and James, 1986).

The reef-flat deposits of the stromatoporoid unit probably developed in a relatively high-energy shallow-water environment similar to that in Holocene reef flats today (Mullins and Neumann, 1979; Longman, 1981). The abundance of irregular fenestral fabrics in the reef-flat lithologies suggests that many of the lithologies were cyanobacterially bound. The similarity between the internal fabrics of the columnar fenestral stromatolites (discussed below) and that in the bedded fenestral grainstones of

the reef-flat subfacies supports this interpretation. The columnar fenestral stromatolites of the reef-flat subfacies are commonly coated by *Renalcis* and this suggests the stromatolites may have developed in subtidal conditions.

Fenestral fabrics are commonly considered reliable indicators of intertidal-supratidal deposition (Shinn, 1968a, 1983a). However, Shinn (1983a) has suggested that they may also develop in subtidal conditions. Playford *et al.* (1976) also noted that Holocene subtidal stromatolites at Shark Bay have fenestral fabrics which are very similar to those in the Devonian columnar fenestral stromatolites of the Lennard Shelf.

Fenestral Peloidal Calcarenite Unit

The fenestral peloidal calcarenite unit crops out in the southern platforms of the Geikie Gorge area and is well exposed the southern reaches of Geikie Gorge (see map, enclosure). The unit is slightly younger than the stromatoporoid unit.

Back-reef subfacies; The back-reef subfacies of the unit consists of well-bedded **fenestral and non-fenestral peloidal grainstones and packstones**. Minor lithologies include *Amphipora* rudstones and floatstones, fenestral and non-fenestral ooid and pisoid grainstones (Fig. 7A, B) and intraclast grainstones. Fenestral pores generally have an irregular morphology, but laminoid and more rarely tubular fenestrae are also present.

Ooids and pisoids are commonly fragmentary and often have radial fractures (Fig. 7B). Adeleye (1975) has suggested that these textures are a result of desiccation of the ooids and this may indicate that the lithologies were subject to periodic subaerial exposure. The red or buff colour of many lithologies may also suggest periodic subaerial exposure. Occasionally, pisoids have a vertical colour gradient from pink at the top to red at the base and this suggests vadose leaching. Vadose meniscus cements are also present in this unit.

Reef-flat subfacies; The reef-flat subfacies of this unit is characterized by **columnar fenestral stromatolitic framestones** (Fig. 7C). Individual fenestral stromatolite columns are generally around 1 to 5 cm in width and may be up to 40 cm high. The columns commonly branch or coalesce upwards and generally become wider. Internally, the stromatolites consist of fenestral peloidal grainstones and have a poorly laminated to unlaminated fabric (Fig. 7C). Fenestrae generally have an irregular to laminoid morphology. The crude lamination is defined by a combination of grain size changes, the presence or absence of micrite and the abundance of fenestrae. The outer walls (and some laminae within the columns) of the stromatolites generally have a light colour in hand-specimen and this is due to the presence of intergranular micrite in the walls of stromatolites (Fig. 7C). The micrite is not an internal sediment and may have been precipitated at the growing surface of the stromatolites. Fenestral and non-fenestral peloidal-skeletal grainstones generally fill the interstices between the stromatolite columns. The fabric of the stromatolites is similar to those from the Holocene of Shark Bay (Playford *et al.*, 1976).

Fenestral peloidal-skeletal grainstones and megalodont floatstones (Fig. 7D) are also present within the reef-flat subfacies of the fenestral peloidal calcarenite unit.

Figure 7

A) Thin-section photomicrograph of fenestral ooid grainstone from the back-reef subfacies of the oolite unit. Laminoid, irregular and bubble fenestrae are present. Pillara Limestone, western Copley Valley. Scale bar = 1 cm. UTGD sample no. 70301

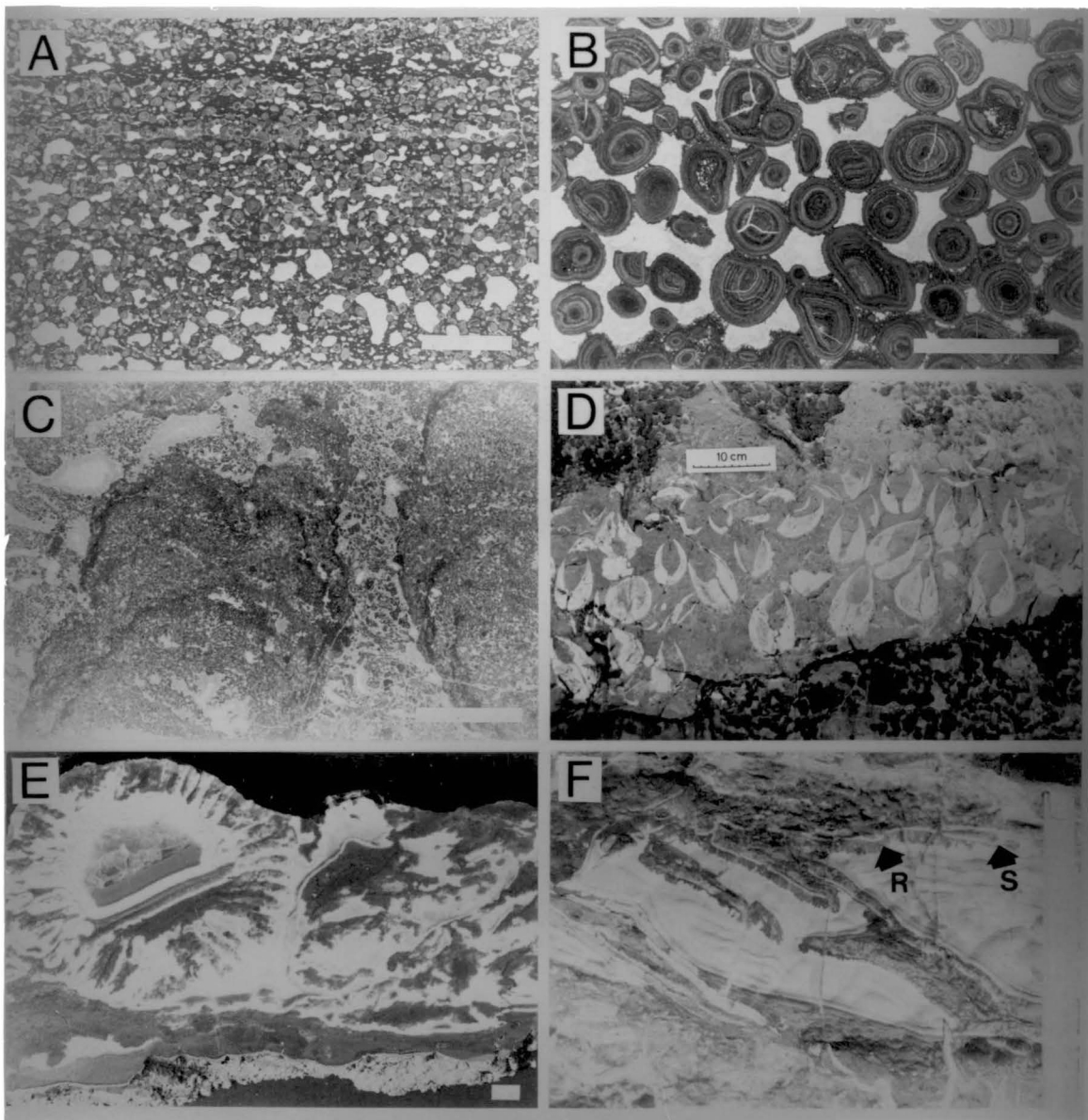
B) Thin-section photomicrograph of pisoid rudstone from the back-reef subfacies of the fenestral peloidal calcarenite unit. Note the radial fractures in many of the pisoids and the presence of many fragmentary pisoids. Pillara Limestone, southern Copley Valley. Scale bar = 1 cm. UTGD sample no. 70300

C) Thin-section photomicrograph of fenestral columnar stromatolite framestone from the reef-flat subfacies of the peloidal fenestral calcarenite unit. The matrix consists of fenestral peloidal-skeletal grainstones. Pillara Limestone, western Copley Valley. Scale bar = 1 cm. UTGD sample no. 70249

D) Vertical exposure of megalodont bivalve rudstone from the reef-flat subfacies of the peloidal fenestral calcarenite unit. Most of the bivalves are in position of growth. Pillara Limestone, western Copley Valley.

E) Polished slab of sponge floatstone from the reefal-slope subfacies of the Frasnian Napier Formation. The matrix consists of lime mudstones with abundant cement-filled stromatactis cavities. The light material is fibrous marine cement and the dark material is lime mud. Western Copley Valley. Scale bar = 1 cm. UTGD sample no. 70317

F) Vertical exposure of laminar stromatoporoid-*Renalcis* bindstone from the reefal-slope subfacies of the Frasnian Napier Formation. Laminar stromatoporoids (S) support large fibrous marine cement-filled shelter cavities. The undersides of the laminar stromatoporoids are encrusted by *Renalcis* (R). Northern Geikie Gorge. Ruler on right is in centimetres.



Interpretation; The fenestral peloidal calcarenite unit lacks the well-developed lagoonal facies of the stromatoporoid unit. The unit apparently developed at a time when the back-reef deposits were subject to relatively high-energy shallow-water conditions. The columnar fenestral stromatolite reef-flat deposits presumably indicate still higher energy conditions. Cyanobacterial binding of the back-reef sediments was very common and some of this may have occurred under shallow subtidal, rather than intertidal, conditions. However, the presence of subaerial exposure features suggests many lithologies developed in intertidal or supratidal conditions.

Oolite Unit

The oolite unit only outcrops over a small area in the southern part of the map sheet near Brooking Springs homestead (see map, enclosure). It is characterized by an abundance of **fenestral and non-fenestral ooid-pisoid grainstones and packstones**. Fenestrae may have an irregular or laminoid fabric. Ooids and pisoids range in size from <1 mm up to 5 mm in diameter.

The reef-flat subfacies of the oolite unit consists of predominantly of **fenestral ooid grainstones**.

Interpretation; The oolite unit differs from the fenestral peloidal calcarenite unit by having ooids as the dominant clastic constituents. Otherwise, the two units have similar lithologies and presumably the oolite unit developed in similarly high-energy shallow-water conditions.

Reef-Margin Unit

The reef-margin unit corresponds to the reef-margin subfacies defined by Playford (1980) and outcrops discontinuously as a narrow zone on the basinward side of the reef-flat subfacies. The reef-margin unit is unbedded and may be up to 250 m wide but it is more commonly less than 50 m wide. Marine-cement-filled cavities of various types are common in the reef-margin unit. Neptunian dykes are abundant and are filled by internal sediments, cyanobacterial encrustations and marine cements.

Contacts with the adjacent reef-flat and reefal-slope subfacies are commonly gradational, particularly in the older Frasnian margins in the north-east of the map sheet. However, many reef-margin - reefal-slope contacts are very sharp (e.g. Fig. 8F). These types of margins most commonly occur in the south-west of the map sheet in the latest Frasnian margins. Occasionally there is evidence of reef-margin erosion prior to marginal-slope deposition. At one locality north of Brooking Springs Homestead, the reef-margin subfacies is particularly wide and is split into two by a narrow strip consisting of well-bedded marginal-slope lithologies. This geometry suggests the reef-margin was advancing over the marginal-slope deposits. Hurley (1986) also found evidence for advancing latest Frasnian reef margins in the Oscar Range.

Reef-flat - reef-margin contacts are commonly quite sharp, and are in many cases, delineated by neptunian dykes. Kerans (1985) described the reef-margin lithologies of the reef complexes in some detail.

Figure 8.

A) Thin-section photomicrograph of cyanobacterial framestone from the reef-margin unit. Masses of *Renalcis* (R) form a framework and are surrounded by peloidal grainstones. Note the neptunian fracture to the left. Pillara Limestone, Geikie Gorge. Scale bar = 1 cm. UTGD sample no. 70294

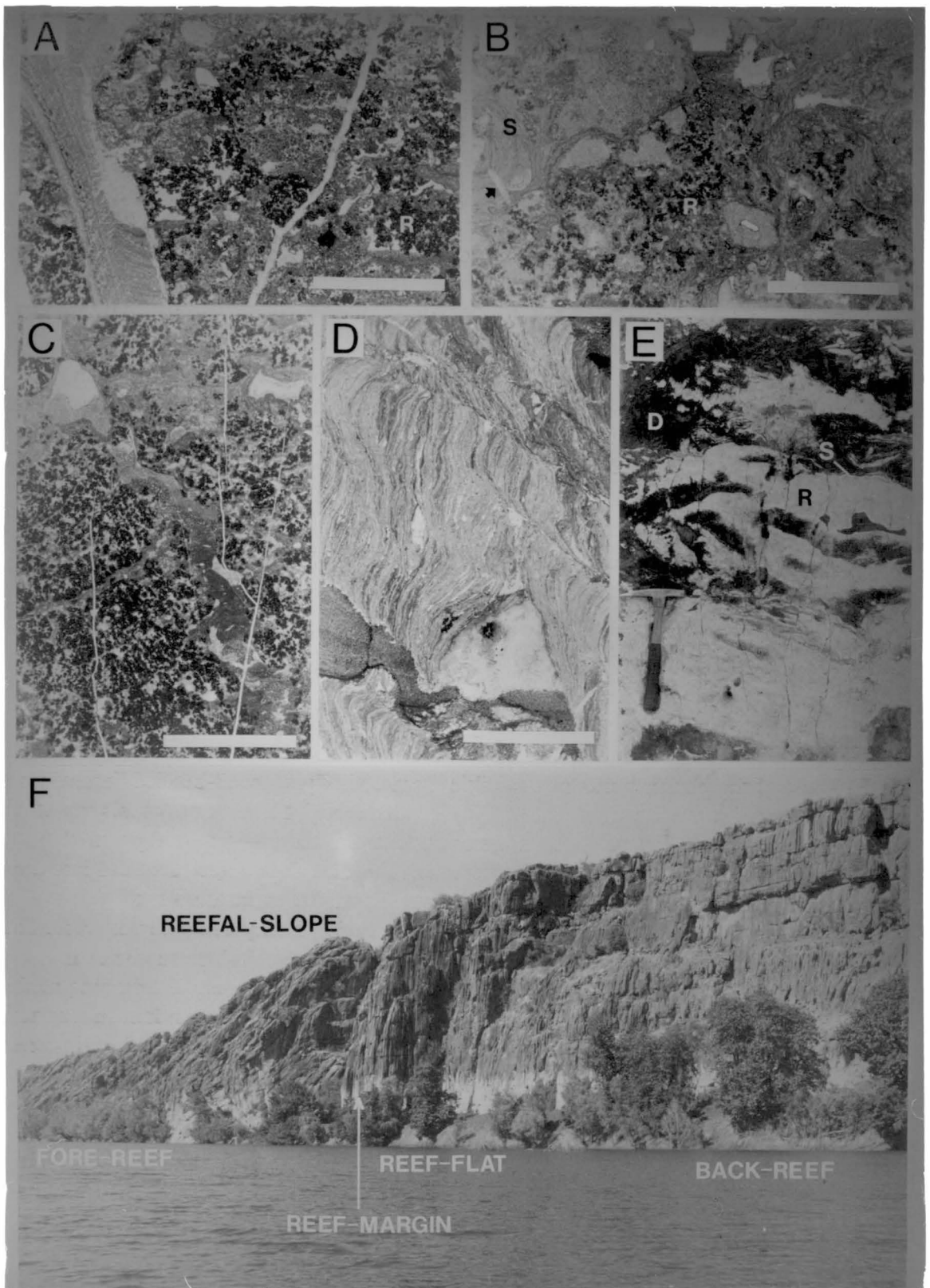
B) Thin-section photomicrograph of *Sphaerocodium-Renalcis* framestone from the reef-margin unit. *Sphaerocodium* (S) and *Renalcis* (R) make up the bulk of the framework. The framework growth direction is towards the right. Cavities in the framework are filled by internal sediments, fibrous marine cements and equant cements. Pillara Limestone, western Copley Valley. Scale bar = 1 cm. UTGD sample no. 70252

C) Thin-section photomicrograph of *Renalcis* framestone from the reef-margin unit. Growth direction is towards the bottom right. Note the syn-sedimentary fracture filled by internal sediment. Pillara Limestone, northern Geikie Gorge. Scale bar = 1 cm. UTGD sample no. 70292

D) Thin-section photomicrograph of *Sphaerocodium* framestone. Growth direction is towards the left. The cavity at the base is filled by dolomitized internal sediment and clear equant cement. Pillara Limestone, Geikie Gorge. Scale bar = 1 cm. UTGD sample no. 70291

E) Vertical exposure of laminar stromatoporoid-*Renalcis* bindstone from the reef-margin facies. Laminar stromatoporoids (S) are overlain by dolomitized grainstones (D). The undersurfaces of the laminar stromatoporoids are encrusted with thick coatings of *Renalcis* (R). Pillara Limestone, northern Geikie Gorge. Hammer for scale.

F) View of the platform margin at Geikie Gorge. Flat-lying, well-bedded limestones of the back-reef subfacies grade into thickly bedded reef-flat limestones consisting of columnar fenestral stromatolite framestones, fenestral and non-fenestral peloidal grainstones, and stromatoporoid wackestones. The reef-flat subfacies grades into the massive reef-margin subfacies which consists of peloidal grainstones and cyanobacterial framestones. The reef-margin subfacies is only a few metres wide. The sharp boundary between reef-margin subfacies and the reefal-slope subfacies is delineated by a neptunian dyke which is filled by ooid grainstones. The dipping reefal-slope subfacies consists of hexactinellid sponge floatstones with abundant stromatactis cavities, peloidal grainstones, lithoclast breccias and minor cyanobacterial grainstones. The reefal-slope subfacies grades into the well-bedded fore-reef subfacies which consists of peloidal grainstones and lithoclast breccias. South of Sheep Camp Yard, Geikie Gorge.



Playford (1984), Kerans (1985) and Hurley (1986) have documented large changes in reef-margin lithologies with time and the style of the margin (advancing, retreating, etc). Givetian and Frasnian reef-margin subfacies generally consist of stromatoporoid-cyanobacterial framestones, whereas Frasnian reef-margin subfacies consist almost exclusively of cyanobacterial framestones. In the Geikie Gorge region, the reef-margin unit is Frasnian in age but older margins in the north-west of the map sheet (laterally equivalent to the stromatoporoid unit) are of the stromatoporoid-cyanobacterial type and younger (probable latest Frasnian) margins (laterally equivalent to the fenestral peloidal calcarenite unit) are of the purely cyanobacterial type.

In the latest Frasnian reef-margin subfacies, **cyanobacterial framestones** (Fig. 8B) are the dominant rock types. **Peloidal-skeletal grainstones and packstones** also constitute a large proportion of the reef-margin unit, and are interstitial to the framestones.

The cyanobacterial framestones consist of a complex framework of intergrown *Renalcis*, *Sphaerocodium*, and many other undescribed cyanobacterial fabrics (e.g. dendritic and microlenticular encrustations, discussed later). Shelter and growth cavities form a substantial part of the lithology and are filled by geopetal sediments, marine cements and cyanobacterial encrustations (Fig. 8).

Cyanobacterial-tabular stromatoporoid framestones (Fig. 8E) constitute a large proportion of the older Frasnian reef margins in the north-east of the map sheet. In these lithologies, large isolated tabular stromatoporoids are commonly underlain by thick (30-40 cm) masses of *Renalcis*, *Sphaerocodium*, and other cyanobacterial fabrics. There are also large volumes of peloidal-skeletal grainstones between the framestones.

Interpretation; The reef-margin subfacies consists predominantly of a true organic framework in which the principal frame-builders are cyanobacteria. The proportion of organic framework appears to be quite high relative to modern reefs. Many Holocene reef framework facies appear to suffer destructive biological and physical processes, notably boring (James and Ginsburg, 1979; Land and Moore, 1980) leaving an average of only 30% framework (Longman, 1981). In contrast, the reef-margin deposits of the Lennard Shelf show remarkably little boring (Fig. 8B). Modern reef-margin facies (reef framework facies of Longman, 1981) are subject to very high energy conditions and it appears likely that this was the case with reef margins in the Geikie Gorge region.

Because of the lack of structure in the reef-margin subfacies, its growth style and palaeotopography are difficult to ascertain. Kerans (1985) documented framework fabrics from Windjana Gorge which suggest lateral accretion of the reef-margin facies by encrustation of a near-vertical reef wall. Sharp contacts between reef-margin and marginal-slope facies are also consistent with the presence of a steep reef wall (Fig. 8F). Lateral accretion of the framework has also been suggested as a mechanism for reef growth in Holocene reefs (James and Ginsburg, 1979).

However, at many localities, reef-margin contacts are gradational. The northernmost reef margin exposed within Geikie Gorge has this characteristic. Here, reefal-slope lithologies grade into the reef-margin facies by a gradual increase in framework lithologies.

Cyanobacteria form the bulk of the framework in virtually all of the reef-margin deposits in the Geikie Gorge region. A major problem in this regard is the palaeoecology of frame-builders like *Renalcis*. When *Renalcis* is observed outside the reef-margin subfacies (in reefal-slope, back-reef stromatoporoid mounds, neptunian fractures etc.), it is always a cavity dweller. Indeed, when large exposures of reef-margin subfacies are studied carefully, *Renalcis* crusts generally appear to fill large growth cavities. Many of the other cyanobacterial fabrics also have a cavity-filling form. This raises the question of how the cyanobacterial framework was constructed.

Hubbard *et al.* (1986) observed several mechanisms for Holocene reef-margin accretion at St Croix in the Virgin Islands. These included 1) overgrowth by platy corals; 2) alternating sedimentation and framework growth; 3) pinnacle growth; 4) slumping of framework blocks; and 5) welding of pinnacles and other structures to the main framework. These processes produced a framework with much cavernous porosity. This style of reef accretion may be applicable to the Devonian reef margins. It may be that a very open type of framework is first produced and this acted as "scaffolding" for the cavity-filling cyanobacteria.

One possible model for reef-margin growth is as follows:

1) Development of a cavity-rich reefal-slope grainstone lithology by soft-bodied binders like sponges.

2) Growth of cyanobacteria in shelter and stromatactis cavities, with continued internal erosion and sedimentation (discussed later).

3) Cyanobacterial growth continued in cavities and unbound sediments were gradually removed. The lithology eventually consists of masses of cyanobacteria with remnants of the original detrital material and internal sediments.

However, when the complexities of Holocene reef margins are considered, it is clear that a huge variety of physical and chemical processes contribute to framework growth. Marine cementation has clearly played a major role in platform-margin development in the Devonian reef complexes and many researchers suggest that submarine cementation is largely responsible for steep platform-margin development (Mullins and Lynt, 1977; Mullins and Neumann, 1979).

Marginal-Slope Facies - Napier Formation

Frasnian and Famennian Napier Formation units

Although Frasnian and Famennian Napier Formation units were distinguished and mapped in the field, they are collectively described here. This is because the Frasnian and Famennian units have a slightly different fauna, but in general, the lithologies in both units are very similar.

Reefal-slope subfacies: The reefal-slope subfacies is that part of the marginal-slope which is adjacent to the reef-margin subfacies. It generally has transitional relationships with the reef-margin subfacies and the fore-reef subfacies. Generally the reefal-slope deposits are poorly bedded and have dips of up to 90 degrees (from geopetal studies, these are largely of depositional origin). In general, reefal-slope deposits developed in a zone not more than 50 m wide.

The reefal-slope subfacies has a diverse range of lithologies which includes peloid-skeletal grainstones and packstones, ooid-skeletal grainstones

and packstones, hexactinellid sponge floatstones, "head-dress" (Kerans, 1985) sponge bindstones, and stromatactis lime mudstones (Fig. 7E). Laminar stromatoporoid-*Renalcis* bindstones (Fig. 7F) are restricted to the older Frasnian reefal-slope deposits. One of the most characteristic features of the reefal-slope subfacies is the abundance of stromatactis and shelter cavities (discussed later). Commonly, lithologies of the fore-reef subfacies are interbedded in the lower part of the reefal-slope subfacies.

Fore-reef subfacies; The fore-reef subfacies consists predominantly of positionally dipping (5 to 35° dips) well-bedded peloid-skeletal grainstones and packstones, and ooid-skeletal grainstones and packstones (Fig. 9A,B,F) Lithoclast rudstones and floatstones (Fig. 9C,D) are also common in the fore-reef subfacies. A great variety of lithoclast breccias are present in the fore-reef deposits. Clast size is enormously variable and can be up to several metres. The clasts are invariably angular and consist of platform, reef-margin and marginal-slope lithologies. The lithoclast breccias are dominantly clast-supported but matrix-supported breccias are also present. Grading of various types is also common. Playford (1984) and Kerans (1985) have described the fore-reef lithologies in more detail and have documented several distinctive breccia types. These include scheck and adnet breccias. Adnet breccias are lithoclastic breccias with a muddy matrix and scheck breccias are virtually matrix-free lithoclastic breccias (Fig. 9D) The names are taken from the Adnet Limestone of the Austrian Jurassic (Garrison and Fischer, 1969).

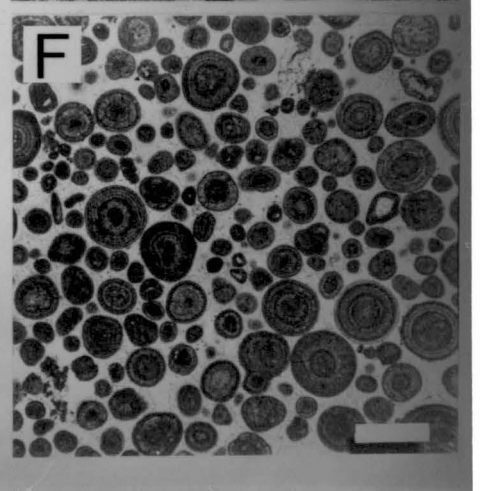
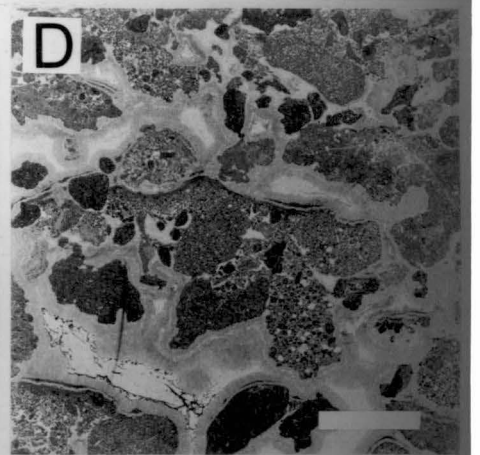
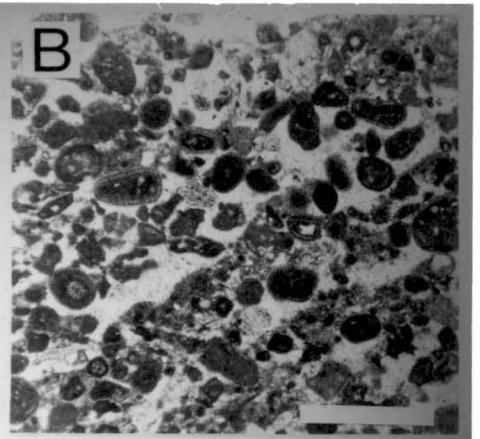
Large isolated blocks are also common in the fore-reef subfacies (Fig. 9A) and may be up to 70 m in diameter. Large blocks tend to be more common in some horizons and their distribution is not random. Megabreccias and large blocks are particularly common in the latest Frasnian marginal-slope deposits directly underlying the deeper water stromatolite unit and these may be related to a major period of erosion of the platforms in latest Frasnian time.

In the Copley Valley and the embayment north of Fossil Downs Homestead (Fig. 2), the fore-reef deposits have lower dips, are finer-grained, have a reddish colouration and have a greater proportion of terrigenous material than typical marginal-slope deposits. Mixed terrigenous-peloidal-ooid grainstones and packstones are the dominant lithologies (Fig. 9E). Normal grading is very common. The fine-grained lithologies commonly have a large proportion of clay and nodular structures are commonly developed within them (Fig. 9E). At some localities, cyclic sequences are developed. Individual cycles have a basal coarse graded fabric which is overlain by a laminated graded lithology. These lithologies may correspond to bouma divisions A-graded and B planar laminated.

Interpretation; The reefal-slope subfacies typically has very steep depositional dips (often beyond the angle of repose for sandy lithologies) and it is clear that many of the lithologies were organically bound at deposition. However, the dominant lithologies are stromatactis peloidal grainstones which lack direct evidence of organic binding. This problem is discussed in detail later and it is concluded that soft-bodied organism(s) probably played a major role in stabilizing the reefal-slope deposits. Kerans (1985) and Hurley (1986) suggested that sponges were the major binders in the reefal-slope deposits and classified many of the stromatactis peloidal grainstones as "sponge bindstones".

Figure 9. Lithologies of the Frasnian and Famennian Napier Formation units.

- A) Dipping well-bedded peloidal grainstones of the fore-reef subfacies from the Famennian Napier Formation. Note the large allochthonous block (partly obscured by tree). Western Copley Valley. Allochthonous block is approximately 3 m high.
- B) Thin-section photomicrograph of peloidal-oid-skeletal grainstone from the fore-reef subfacies of the Famennian Napier Formation. Western Copley Valley. Scale bar = 1 mm. UTGD sample no. 70247
- C) Vertical exposure of a lithoclast breccia ("scheck breccia") bed in the fore-reef subfacies of the Famennian Napier Formation. The breccia coarsens upward. Western Copley Valley. Scale bar = 10 cm.
- D) Thin-section photomicrograph of a lithoclast breccia ("scheck breccia") from the fore-reef subfacies of the Famennian Napier Formation. The lithoclasts largely consist of marginal-slope peloidal grainstones. The lithology is extensively cemented by marine fibrous calcite. Western Copley Valley. Scale bar = 1 cm. UTGD sample no. 70308
- E) Vertical exposure of clayey peloidal grainstones with fining upward cycles. Each cycle has a basal pure peloidal grainstone bed (light coloured) and this becomes finer and more impure upwards. The more impure, finer peloidal grainstones have a distinctive nodular texture which is due to an irregular network of pressure solution seams. Deep fore-reef subfacies of the Frasnian Napier Formation, Geikie Gorge. Hammer for scale.
- F) Thin-section photomicrograph of ooid grainstone from the fore-reef subfacies of the Frasnian Napier Formation. Scale bar = 1 mm. UTGD sample no. 70263



Modern reefal-slope deposits are generally at a water depth of a few tens of metres and have dips beyond the angle of repose (Longman, 1981). Because of the low light intensities, corals commonly have a platy morphology in Holocene reefal-slope deposits (Longman, 1981). The common laminar stromatoporoids of older Frasnian reefal-slope deposits may be the Devonian analogues for platy corals (Fig. 7F).

The majority of sediments in the fore-reef deposits were formed on the platform and were transported to the marginal slope by gravity induced processes. Marginal-slope deposits which face into deep basinal environments consist predominantly of steeply-dipping grainstone lithologies and these are probably grainflow deposits. In the Copley Valley and other shallow basins, the dominant marginal-slope lithologies are shallow-dipping, fine-grained, graded grainstones and packstones and these probably represent proximal turbidite deposits. In general, on margins facing deep basins, only the steeply dipping upper fore-reef grainflow deposits are exposed. Whereas, in the shallow basins (like the Copley Valley), the shallow-dipping lower marginal-slope turbidite deposits are exposed.

However, there are many other types of gravity-flow deposits in the marginal-slope facies including true talus and debris flows. The large isolated blocks within marginal-slope deposits are allochthonous blocks which have broken away from the platform and upper marginal slope.

Deeper-Water Stromatolite Unit

This unit is characterized by an abundance of **non-fenestral stromatolitic framestones** (Fig. 10). The stromatolites are believed to be of normal-marine subtidal origin (rather than intertidal) for several reasons. Firstly, the stromatolites are associated, and intergrown, with normal-marine subtidal faunas like crinoids (in-place holdfasts), ammonoids, rugose corals, serpulids, gastropods, brachiopods and sponges (Fig. 10E). In addition, the stromatolites occur in positionally dipping marginal-slope beds (geopetal evidence, e.g. Playford *et al.*, 1976 at McWhae Ridge). Calculations on the elevation differences on a single stromatolite bed at McWhae Ridge (allowing for post-depositional tilting) indicate a minimum depth of water of 45 m (Playford *et al.*, 1976). However, palaeotopographic cross sections constructed by Playford *et al.*, (1976) suggest the actual water depth probably exceeded 100 m.

The deeper water stromatolite unit has been traced for a distance of approximately 20 km in the Geikie Gorge region and the same unit has been traced for 60 km in the Oscar Range (Playford *et al.*, 1976; Hurley, 1986). A similar unit was recognized in the Bugle Gap region (Playford *et al.*, 1976) and detailed conodont work (Druce, 1976) indicates a latest Frasnian-early Famennian age for the unit at this locality. Hurley (1986, based on unpublished conodont work by R.S. Nicoll), also suggested the stromatolite unit was of latest Frasnian-early Famennian age. Thus, it appears likely that the stromatolite unit is of shelf-wide extent. This makes the unit stratigraphically very important as a marker for the Frasnian-Famennian boundary. The remarkable continuity of the unit and its latest Frasnian-Early Famennian age also makes it of great sedimentological interest.

Figure 10. Lithologies of the deeper-water stromatolite unit

A) Vertical exposure of the non-fenestral stromatolite unit encrusting the platform facies. On the far left (in the background) the platform facies (Pillara Limestone) is exposed. The exposure consists of steeply-dipping scalloped non-fenestral stromatolite horizons and intercalated peloidal grainstones with abundant stromatactis structures. On the right side of the exposure, stromatactis peloidal grainstones and non-fenestral stromatolites grade into steeply dipping fore-reef subfacies of the Famennian Napier Formation. Western Copley Valley. Person for scale.

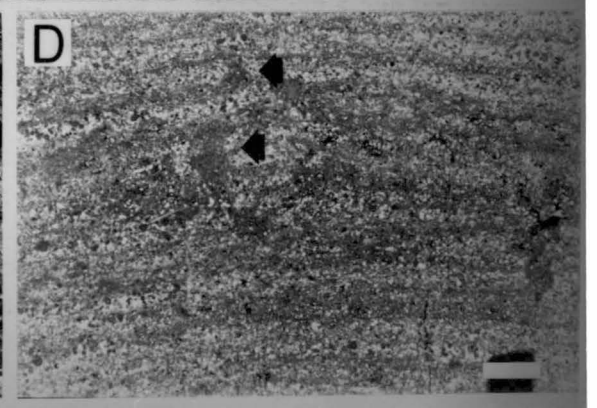
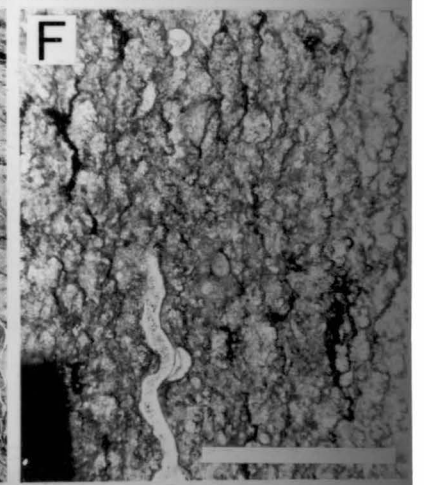
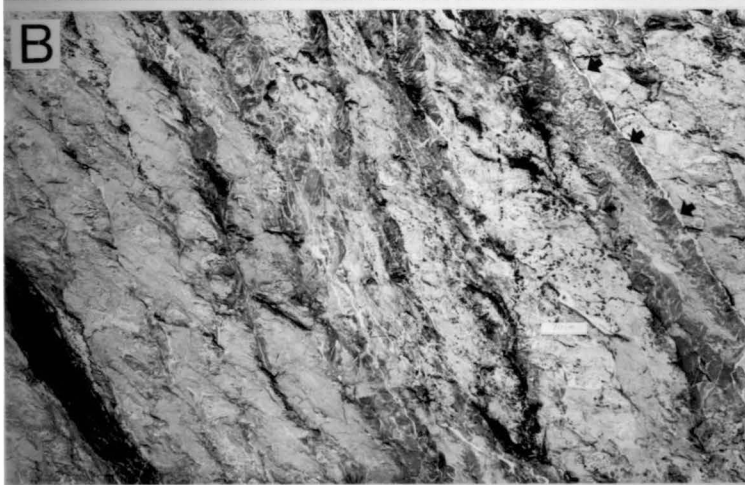
B) Enlargement of figure 10A. Steeply dipping stromatolite and peloidal grainstone horizons are visible. The scalloped stromatolites (arrows) consist of non-fenestral stromatolite columns separated by thin microspar films (light material). Deeper-water stromatolite unit of the Frasnian-Famennian Napier Formation, western Copley Valley. Scale bar = 20 cm.

C) Horizontal exposure of longitudinal non-fenestral stromatolites encrusting reef-flat limestones of the Pillara Limestone. The contact between the two lithologies is near-vertical. The longitudinal stromatolite ridges are aligned with the direction of the near-vertical dip. At many localities the non-fenestral stromatolites encrust broken neptunian fractures within the Pillara Limestone. Western Copley Valley. Scale bar = 10 cm.

D) Thin-section photomicrograph of non-fenestral stromatolite. The stromatolite consists of interlaminated quartz-rich and micrite-rich horizons. Micrite columns (arrows) are also present. Deeper-water stromatolite unit of the Frasnian-Famennian Napier Formation, western Copley Valley. Scale bar = 1 mm. UTGD sample no. 70250

E) Thin-section photomicrograph of non-fenestral stromatolite with less detrital material and a well-developed microlenticular fabric. Serpulids, crinoid holdfasts and rugose corals are preserved in position of growth within the stromatolite. Deeper-water stromatolite unit of the Frasnian-Famennian Napier Formation, western Copley Valley. Scale bar = 1 cm. UTGD sample no. 70248

F) Thin-section photomicrograph of microlenticular structure within a non-fenestral stromatolite. Each lensoid accretionary unit consists of microspar and is capped by a thin layer of dense micrite or iron oxide. A vague radial structure is occasionally present within the lensoid accretionary units. Deeper-water stromatolite unit of the Frasnian-Famennian Napier Formation, western Copley Valley. Scale bar = 1 mm. UTGD sample no. 70248



In the Geikie Gorge region, the stromatolites generally encrust near vertical platform margins and form a discontinuous unit seldom more than five metres wide (Fig. 10C). At a few localities (in the western part of the map sheet), the stromatolites occur in the fore-reef subfacies as a series of thin stromatolite horizons separated by beds of fore-reef lithologies (peloidal grainstones, lithoclast rudstones and floatstones).

In the majority of cases, the stromatolites encrust near-vertical escarpments generally consisting of reef-flat (and more rarely reef-margin) lithologies (Fig. 11). There is commonly evidence of erosion of the platform lithologies prior to stromatolite growth. The contact between the stromatolites and the platform carbonates of the Pillara Limestone is commonly irregular over the scale of metres again suggesting erosion. In addition the common absence of the reef-margin subfacies from stromatolite encrusted platform margins suggests it was removed by erosion prior to stromatolite growth. Where stromatolites do not encrust the platform margin, the reef-margin subfacies is almost always present to some degree.

In general, where the stromatolites develop on near-vertical platform margins (90 to 70 degrees), the first stromatolites to colonize the margins have a longitudinal morphology (Playford *et al.*, 1976). The longitudinal stromatolites form elongate ridges directed down the dip direction of the near-vertical platform scarps. The ridges range in width from 1 cm up to 15 cm. In horizontal exposure surfaces (i.e. a cross-section across the ridges) the longitudinal stromatolites appear to have a columnar appearance (Fig. 10C).

In the outer portions of the stromatolite encrustations, the longitudinal stromatolites generally give way to scalloped stromatolites (Playford *et al.*, 1976). Scalloped stromatolites occur on substrates having dips ranging from 60 to 30 degrees. On vertical exposure surfaces, the stromatolites consist of numerous stepped columns (Fig. 10B). However, in horizontal exposure surfaces, the stromatolites have a scalloped appearance. Individual columns are clearly visible in outcrop because the columns are separated by thin (5 mm) light coloured microspar films (Fig. 10B). The columns range in size from <1 cm up to 5 cm wide.

The form of the stromatolites (i.e. longitudinal or scalloped) appears to be controlled by the substrate inclination. Substrates with dips greater than 70 degrees generally have longitudinal stromatolites and substrates having dips less than 70 degrees have scalloped stromatolites.

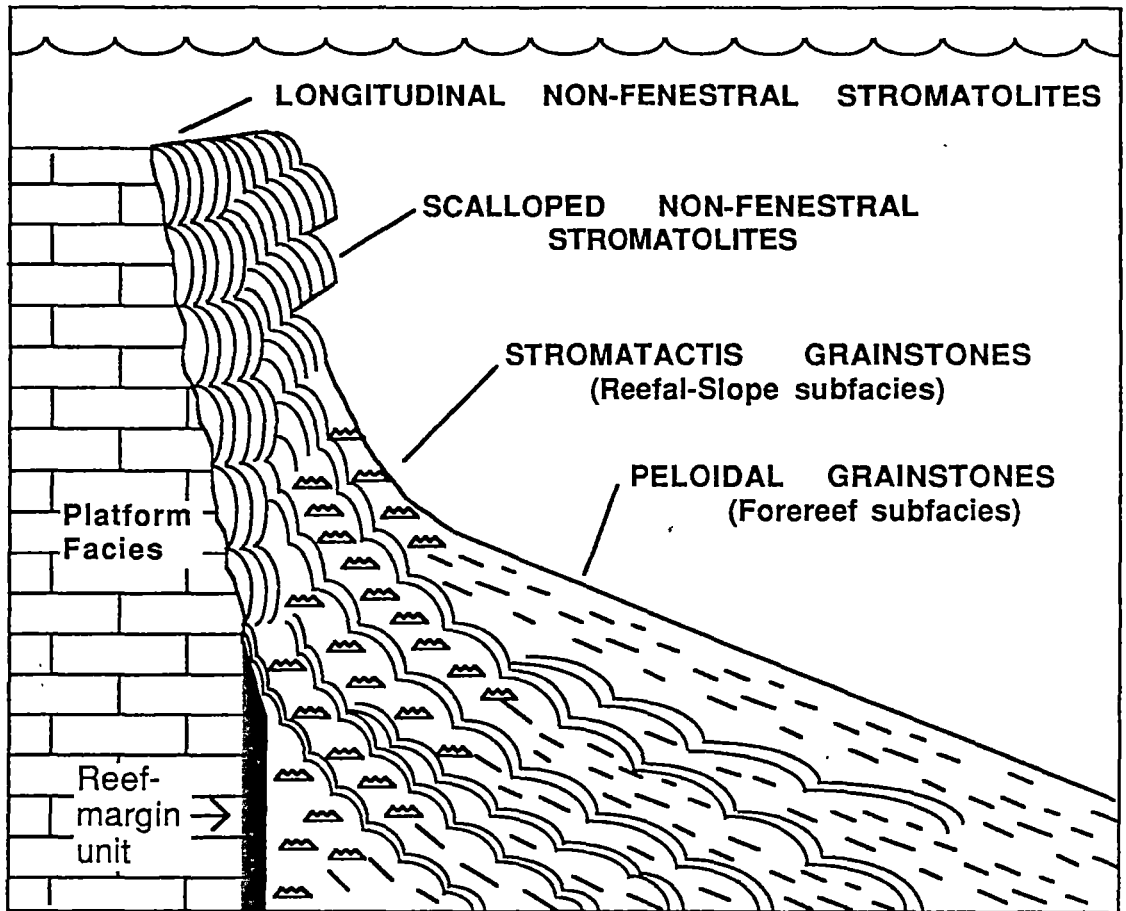


Figure 11. Interpreted structure of platform margins encrusted by non-fenestral stromatolites. The variation in the structure of the stromatolite encrusted margins is explained by exposure at different levels. Where the upper parts of stromatolite margins are exposed, scalloped and longitudinal stromatolites encrust steep eroded scarps (upper part of diagram). Where the lower levels of stromatolite margins are exposed, steeply dipping scalloped stromatolite horizons are separated by stromatactis lithologies (e.g. Fig. 10A). Where most of the stromatolite margin has been removed by erosion and only the lower portions of the margin are exposed, multiple scalloped stromatolite horizons occur within the peloidal grainstones of the fore-reef subfacies.

Stromatolite encrusted margins have gradational contacts with the younger detrital marginal-slope deposits (Fig. 11). Moving away from the encrusted platform margin, scalloped stromatolites generally become interlaminated with **stromatactis peloidal grainstones** (Fig. 7E) typical of the reefal-slope subfacies. The peloidal grainstone lithologies interlaminated with the stromatolite horizons also have dips of around 60 degrees. The dips in the stromatolite and stromatactis grainstone horizons are gradually reduced away from the platform margin and the proportion of stromatolite horizons decreases (Fig.). The stromatolites are finally replaced by peloidal grainstones of Famennian fore-reef lithologies (Fig. 11).

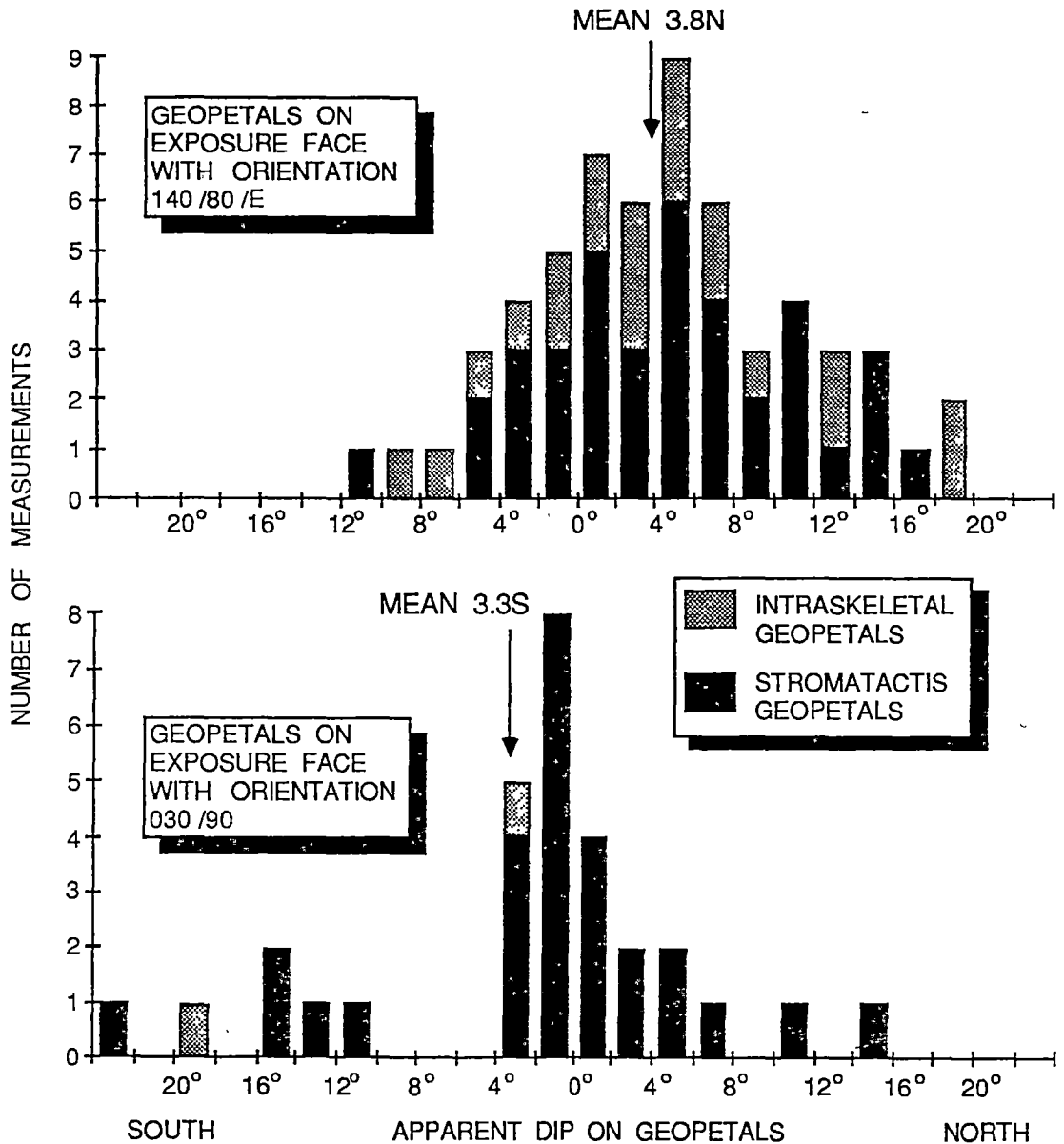


Figure 12. Histograms illustrating geopetal measurements on two different faces within the deeper-water stromatolite unit. This indicates that the lithology has been subject to minor post-depositional tilting of approximately 5 degrees to the west.

It is notable that the stromatactis peloidal grainstone horizons also have dips of up to 60 degrees. Measurement of geopetal structures at one locality indicates post-depositional tilting of around 6 degrees (Fig. 12). However, post-depositional tilting was not in the direction of dip, and the 60 degree dips are almost wholly depositional. This is around 25 degrees beyond the angle of repose for sand-size material and indicates the stromatactis peloidal grainstones were bound at deposition. This is suggestive of a link between stromatactis cavities and organic binding.

Deeper water stromatolites are not restricted to this one unit and often cap large allochthonous blocks in the marginal slope. Non-fenestral stromatolites also occur within neptunian fractures and within some reef-margin lithologies (discussed later).

The microstructure of the deeper water stromatolites is illustrated in figures 10E and 10F. Individual stromatolite columns most commonly consist of finely interlaminated peloidal grainstones and clayey micrites (Fig. 10D). Quartz silt is commonly a major constituent in the stromatolites. Small (<1 mm wide) micritic columns are commonly dispersed throughout the stromatolites (Fig. 10D). Other stromatolites have less detrital material and have a microlenticular fabric (microlenticular cyanobacterial fabric of Kerans, 1985). This fabric consists of a series of stacked micro-accretionary units ranging in size from 50 to 500 μm thick. Each accretionary unit consists of a microspar core and a thin outer margin of micrite. The outer micritic margin commonly has a yellow-red colouration which is presumably due to fine iron oxides (Fig. 10F). Occasionally, micro-stromatolitic columns resembling *Frutexitis* occur on the tops of the micritic laminae.

In well preserved examples, the microspar films between the scalloped stromatolite columns have a microlenticular fabric and generally have virtually no detrital material. The growth direction within the microspar is generally perpendicular to the column walls. The microspar films appear to have grown on the sides of the scalloped stromatolite columns.

It appears likely that the microspars, micrites and iron oxides within the stromatolites are organically induced precipitates. In the largely detrital stromatolites, these precipitates may have bound the sediment.

Interpretation

Conodont dating indicates that deeper water stromatolites are associated with strongly condensed sequences at McWhae Ridge and elsewhere (Playford *et al.*, 1976). Playford *et al.*, (1976) suggested that growth rates for the stromatolites may have been as low as 2 μm per year and that large stromatolite masses may have taken a few million years to grow.

Encrustation of the platform margins and upper marginal-slope beds by extremely slow growing non-fenestral stromatolites suggests that carbonate production on the platforms and reef growth must have been drastically reduced or stopped completely during latest Frasnian - early Famennian time. This hypothesis is also consistent with evidence for erosion of the platforms prior to the stromatolite growth. It is significant that this apparent cessation in reef growth occurred at a major mass extinction boundary. Several explanations may account for this cessation in carbonate production and reef growth:

- a) Sea level fluctuation which either drowned or subaerially exposed the reef complexes (Johnson *et al.*, 1985)
- b) Climatic change (Caputo and Crowell, 1985; Caputo, 1985; Copper, 1986).
- c) A meteoroid impact related event (Alvarez *et al.*, 1980).

An iridium anomaly was found at the Frasnian-Famennian boundary within a deep water stromatolite unit (in a *Frutexitis* -rich horizon at McWhae Ridge, Playford *et al.*, 1984). It may be that this anomaly is comparable to other proposed meteoroid impact-related iridium anomalies at mass extinction boundaries (e.g. Alvarez *et al.*, 1980). However, Playford *et al.* (1984) demonstrated that the iridium content of the *Frutexitis* filaments was higher than that in the surrounding detrital material, suggesting a biological concentration mechanism (Playford *et al.*, *in press*). Playford

et al., (*in press*) suggested that the widespread occurrence of deep water stromatolites may have resulted from the abrupt decline in metazoan species that fed on cyanobacteria.

In the north-western Oscar Range, the Frasnian-Famennian boundary is marked by a disconformity in the platform carbonates (Hurley, 1986) suggesting a period of subaerial exposure. The latest Frasnian advancing platform margins (Hurley, 1986; Playford *et al.*, *in press*) also suggest a regressive phase. Johnson *et al.* (1985) suggest a short-lived drop in sea level occurred at the Frasnian-Famennian boundary. A drop in sea level would stop carbonate production on the platforms and might explain platform margin and marginal-slope colonization by deeper water stromatolites. However, it is difficult to envisage why reef-margin growth was halted completely for such an extended period in this situation.

Other evidence from the reef complexes suggest a major drowning event at the Frasnian-Famennian boundary. At McWhae Ridge and in the north-west Oscar Range (Elimberrie bioherms) drowned Frasnian reefs are overlain by Late Frasnian-Early Famennian deeper water stromatolite masses (Playford *et al.*, 1976). In the Elimberrie no. 1 bioherm, Frasnian reef-margin limestones again show evidence of erosion prior to stromatolite growth. This erosion could equally well be explained by submarine as subaerial erosion; erosion of steep platform margins would be expected in either case.

Environmental Synthesis

Two major types of platform carbonates are present in the Geikie Gorge region. In the older Frasnian platforms (in the north-east portion of the map sheet), the back-reef subfacies is dominated by relatively low-energy lagoonal carbonates of the stromatoporoid unit and the platform margins are of the upright-scarp type. In the latest Frasnian margins, the back-reef subfacies consists of relatively high-energy sands (fenestral peloidal calcarenite and oolite units) and there is some evidence for advancing platform margins. This change from older Frasnian to latest Frasnian sedimentation may reflect a decreasing rate of subsidence or eustatic sea-level rise. The development of lagoonal facies and upright-scarp margins in response to rapid sea level rise or strong subsidence was also suggested by Longman (1981).

The latest Frasnian-early Famennian deeper water stromatolite unit marks an important halt in reef growth. It is possible that this cessation in reef growth was also controlled by sea level fluctuation. The widespread extent of the stromatolite unit on the Lennard Shelf suggests a eustatic rather than a tectonic control on sea level.

Famennian platform carbonates do not outcrop in the Geikie Gorge region. Elsewhere on the Lennard Shelf, Famennian platform margins have a strongly advancing morphology, suggesting low rates of subsidence and relatively static sea levels (Playford, 1980; Hurley, 1986).

4. STROMATACTIS AND ASSOCIATED STRUCTURES IN THE DEVONIAN REEF COMPLEXES OF THE CANNING BASIN

Introduction

Masses of carbonate spar known as stromatactis are important and visually striking constituents of many Palaeozoic buildups. In fact stromatactis has been suggested as a major framebuilder by many researchers. Despite their abundance, there is no general consensus on the origin of these structures and stromatactis remains a problem in carbonate geology. To add to this problem, the origin of the lime mud mounds in which stromatactis commonly occurs is equally obscure as there is a distinct lack of framebuilders in many mounds (Lees *et al.*, 1985). Many researchers have suggested that stromatactis structures are somehow related to the unknown accumulation mechanism for lime mud mounds.

Stromatactis was originally described as a stromatoporoid (Dupont, 1881). The idea that stromatactis spar was a replacement of either an organism or lime mud was popular among early researchers (Lecompte, 1937; Black, 1952; Belliere, 1953; Lowenstam, 1950) and several recent authors have favoured a replacement origin (Ross *et al.*, 1975; Tsien, 1985).

However, Bathurst (1959, 1977) cited convincing fabric criteria indicating that stromatactis spar is a cavity filling precipitate. This was widely accepted and numerous origins have been proposed for cement-filled stromatactis cavities. These include decay of soft-bodied organisms (Bathurst, 1959; Lees, 1964), decay of sponges (Bourque and Gignac, 1983; Playford, 1984; Kerans, 1985), dissolution of bryozoan skeletons (Textoris and Carozzi, 1964), winnowing of sediment from between thrombolite colonies (Pratt, 1982), winnowing of sediment from beneath submarine crusts (Bathurst, 1980, 1982), slumping (Schwarzacher, 1961), dewatering and collapse (Heckel, 1972), dynamic metamorphism in a tensional stress regime (Logan and Semeniuk, 1976; Logan, 1984) and aragonite dissolution (Playford, 1984; Kerans, 1985).

There is general agreement on the following features of stromatactis structures:-

- 1) The masses of spar constituting stromatactis are generally accepted as cement-filled cavities (Bathurst, 1959, 1977).
- 2) Stromatactis cavities generally have an irregular top and a smooth base. The smooth base is thought to be due to internal sedimentation (Bathurst, 1982).
- 3) Stromatactis cavities are believed to be products of syndepositional marine diagenesis (e.g. Schwarzacher, 1961; Lees, 1964; Bathurst, 1980; Pratt, 1982).

4) The cements filling stromatactis cavities are generally believed to be of marine origin and often have the characteristics of radiaxial fibrous calcite (Kendall and Tucker, 1973; Lohmann and Meyers, 1977; Playford, 1984; Kendall, 1985).

While it is clear that a wide variety of spar features ranging from large fenestrae (Flügel, 1982) to interskeletal porosity (Kukal, 1971), have been termed stromatactis in the past, it is equally clear that there exists a major group of structures which have all of the features described above and are comparable to the structures originally described as stromatactis by Dupont (1881) and Lecompte (1937). These "classic" stromatactis structures are virtually identical, regardless of where they are found in the world and this fact has prompted Bathurst (1980) to suggest that all share a common origin.

The Devonian reef complexes of the Canning Basin are among the best preserved and most spectacularly outcropping ancient reef complexes in the world. The stromatactis structures occurring in the reef complexes are equally spectacular and several authors have described them (Playford and Lowry, 1966; Logan and Semeniuk, 1976; Playford, 1976, 1980, 1984; Bathurst, 1980, 1982; Logan, 1984, Kerans, 1985; Kerans *et al.*, 1986). The most detailed study was that of Kerans (1985) who considered stromatactis and stromatactis-like cavities from a variety of facies in the reef complexes. Kerans (1985) described several types of stromatactis-shaped cavities and demonstrated that each had a different origin:

- A) Stromatactis cavities formed by the breakdown of sponges ("doughnut" and "head-dress" sponges, discussed later).
- B) Laminar stromatactis cavities (zebra limestones) formed by soft-body decay and possibly by pull-apart in some cases.
- C) Stromatactis-shaped cavities developed as growth cavities within cyanobacterial bindstones.
- D) Stromatactis-shaped cavities formed by early marine dissolution of aragonitic skeletal components.

This report deals only with the first two types of stromatactis cavities as these appear to be most closely related to the "classic" stromatactis described by Dupont (1881) and Lecompte (1937). In the Devonian reef complexes, stromatactis and associated structures are most abundant in platform marginal environments (i.e. reef-flat, reef-margin, reefal-slope, and upper fore-reef subfacies) and are restricted to lithologies which have been subject to extensive submarine cementation (Kerans *et al.*, 1986) (Fig. 13).

Stromatactis cavities have generally been considered as a problem in themselves and few researchers have considered the cavity types with which they are associated. In this study, it is observed that a number of other unusual lithologies are associated with stromatactis cavities. These include wackestones with an abundance of shelter cavities, and zebra limestones. It is suggested that all of these lithologies are the result of extensive syndepositional internal erosion and sedimentation which occurred after the breakdown and decay of various soft-bodied organisms (Wallace, 1987). It is further suggested that these soft-bodied organisms played a major role in stabilizing many deeper water Palaeozoic buildups.

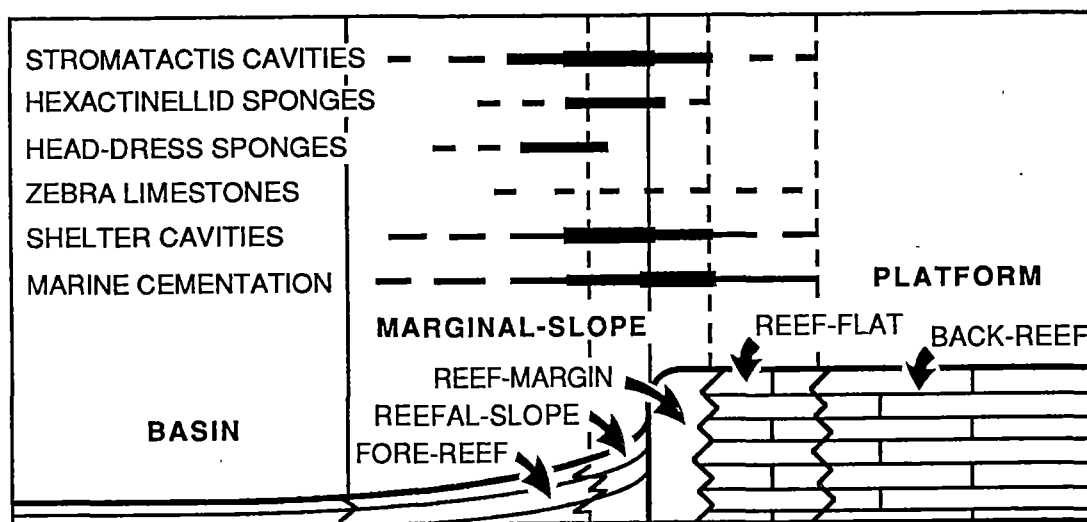


Figure 13. Distribution of stromatactis and associated structures in the Devonian reef complexes of the Canning Basin.

Stromatactis Cavities

Occurrence

Stromatactis structures are abundant in the both Frasnian and Famennian reefal-slope, reef-margin and upper fore-reef subfacies (Figs. 13), and are a minor component of Frasnian coralline reef-flat subfacies. In marginal-slope facies, stromatactis cavities occur within the clasts of debris flow deposits and within in-situ lithologies. Stromatactis cavities also commonly occur within internal sediments in neptunian dykes and other cavity types of the platform margin (Fig. 15A, D; 16A, B, C).

Description

The host sediment containing the stromatactis cavities generally consists of lime mud and/or peloidal grainstones and wackestone. Stromatactis cavities range in size from 30 x 10 cm vugs to microscopic pores. The cavities are generally elongate in a plane close to the depositional geopetal plane. The roofs of stromatactis cavities are generally irregular on a small scale (Fig. 14A). Skeletal components are commonly found hanging from the roofs of cavities and projecting into the cavities (Fig. 16C).

The base of cavities is generally smooth and the material of the cavity floor commonly has the appearance of being an internal sediment (Fig. 14A). In many cases, there is a distinct layer of internal sediment lining the floor of cavities which has a recognizably different composition from the host (Fig. 16B). The internal sediment generally rests on the smooth surface of the underlying host. The host material commonly grades down without break into the roof material of the underlying cavity (Fig. 14A). Where the host lithology is a lime mud, the floor material becomes darker (in transmitted light) in a downward direction (Fig. 14A).

Figure 14. Sponge-associated stromatactis cavities of the reefal-slope subfacies.

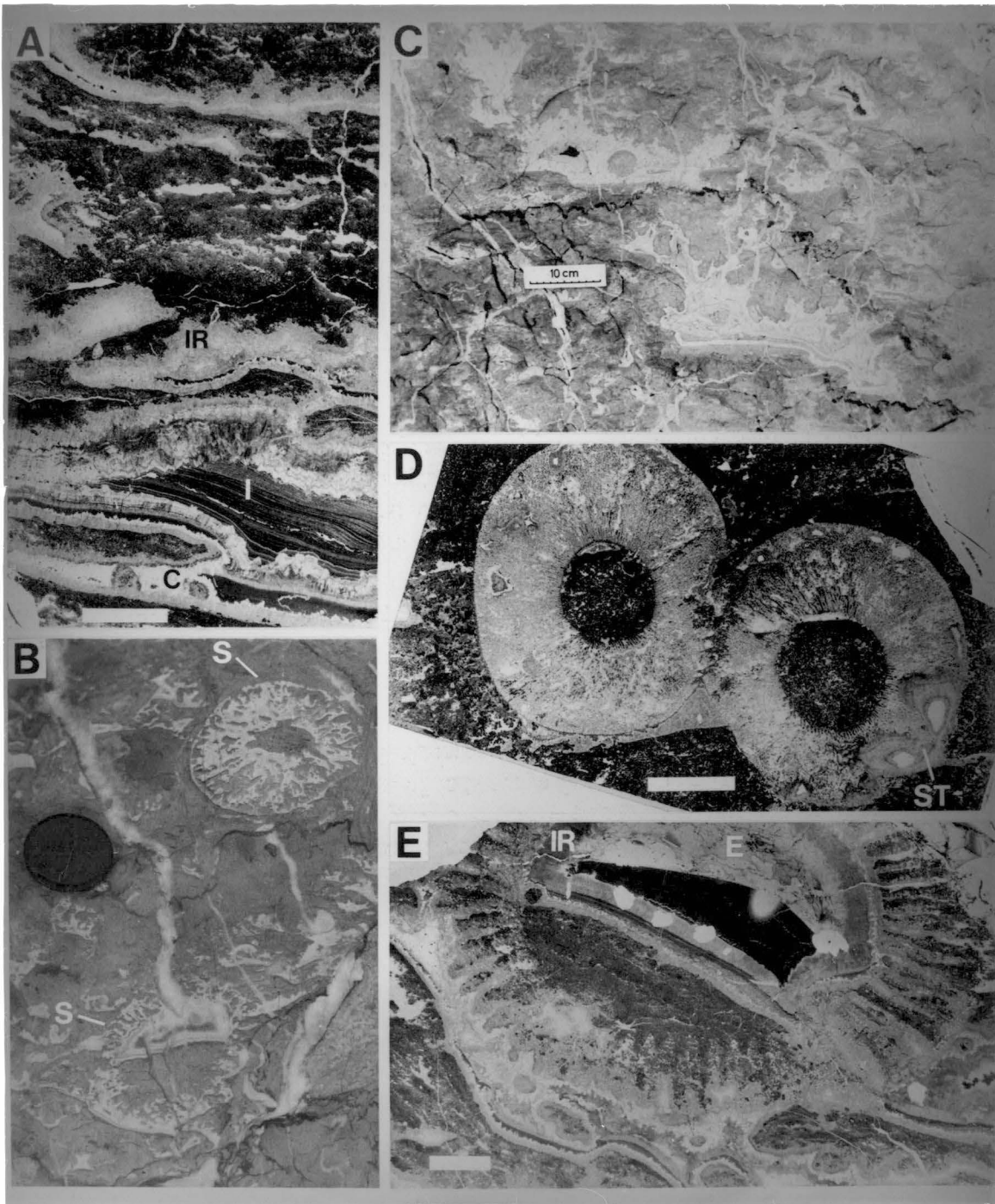
A) Vertically oriented thin-section photo-micrograph illustrating a typical stromatactis lime mudstone. Stromatactis cavities are filled by internal sediments (I), inclusion-rich (IR) and inclusion-poor (C) radiaxial fibrous calcite cements. Internal sediments commonly overlie radiaxial fibrous calcite. Note that it is difficult to distinguish internal sediments from the host at the smooth base of cavities. Napier Formation, Copley Valley; scale bar = 1 cm. UTGD sample no. 70318

B) Vertical outcrop view of the reefal-slope subfacies containing sponges (S) and abundant stromatactis cavities. The upper sponge is not well preserved, but the radial structure is still recognizable. The lower sponge is poorly preserved, only recognizable by a circular concentration of stromatactis cavities. Napier Formation, Geikie Gorge; Lens cap is 55 mm in diameter.

C) Vertical outcrop view of the reefal-slope subfacies with two large stromatactis cavities. The irregularity of the cavity roofs is, in part, due to the growth of encrusting cyanobacterial forms like *Renalcis* from the roofs. The host sediment contains sponges and abundant small stromatactis cavities. Napier Formation, Copley Valley.

D) Thin-section photomicrograph illustrating two relatively well-preserved sponges. Stromatactis-shaped cavities (ST) have developed within the sponge bodies. Note the shelter cavities beneath the sponges. From an allochthonous block in the fore-reef subfacies of the Napier Formation, Geikie Range. Scale bar = 1 cm. UTGD sample no. 70304

E) Vertically oriented thin-section photo-micrograph of a sponge with a well-preserved spicular network. The body cavity of the sponge is filled by internal sediment, radiaxial fibrous calcite (IR) and equant calcite (E). The host sediment contains abundant stromatactis cavities. Note the shelter cavity beneath the sponge. Napier Formation, Copley Valley; scale bar = 1 cm. UTGD sample no. 70317



Hexactinellid sponges are commonly (though not invariably) associated with stromatactis structures of the reefal-slope subfacies, and stromatactis cavities have commonly developed within the framework of these sponges (Figs. 14B, D, E). In fact, as indicated by Kerans (1985), all transitions exist between well-preserved sponge bodies and classic stromatactis mudstones having no recognizable sponges (Fig. 14B, E). In many cases, sponges can only be recognized by a vague circular concentration of stromatactis cavities (Figs. 14B).

Small mound-like masses of stromatactis are common in the reefal-slope and upper fore-reef subfacies (Fig. 15B, C) and these have been termed "head-dress" sponges by Kerans (1985) because of their resemblance to the North American Indian feather head-dress. These structures commonly have a planar base, a convex top, and are generally around 30-40 cm wide and 10-15 cm high. Commonly the small mounds consist of a mass of almost randomly oriented stromatactis cavities, but in some specimens, a vaguely concentric spiral structure is observed (Fig. 15C). Kerans (1985) has observed a poorly preserved spicular framework in some examples.

Zebra Limestone

Occurrence

Zebra limestone is a relatively uncommon lithology within the Canning Basin reefs. Zebra limestone occurs within Frasnian stromatoporoid-coral-cyanobacteria reef-flat subfacies (e.g. Lloyd Hill platform atoll) and in the internal sediment of neptunian dykes and cavities of the reef-margin subfacies (Fig. 15D, E; 16B).

Description

The term "zebra limestone" (Ross *et al.*, 1975; laminar stromatactis of Pratt, 1982) is used here to describe a series of multiply stacked cement-filled laminar cavity systems separated by thin sheets of bioclastic carbonate. The cavities are usually less than 1 cm in height but may be up to 10 cm high (Fig. 15D). The lateral extent of cavities ranges from several meters to a few centimetres and the cavities are completely gradational with stromatactis cavities (Fig. 16A, B, E). The division into stromatactis or zebroid structures is purely arbitrary and based on the lateral extent of cavities.

The laminar cavities of zebra limestone are identical to stromatactis cavities in detail. The roofs of laminar cavities are generally irregular on a fine scale and skeletal fragments often hang from, or partly line the irregular roofs. The cavities have a smooth floor and there may or may not be a layer of recognizable internal sediment on the floor. The host sediment in zebra limestones includes lime mudstones, wackestones and grainstones.

Kerans (1985) described several interesting structures in zebra limestones from the Devonian reefs of the Lennard Shelf. Deflection of host sediment layers below rigid objects like intraclasts and skeletal components led Kerans (1985) to suggest that the host sediment layers were not completely rigid at deposition. A similar deflection structure is illustrated from the Ordovician Micklejohn mound (Ross *et al.*, 1975).

Figure 15.

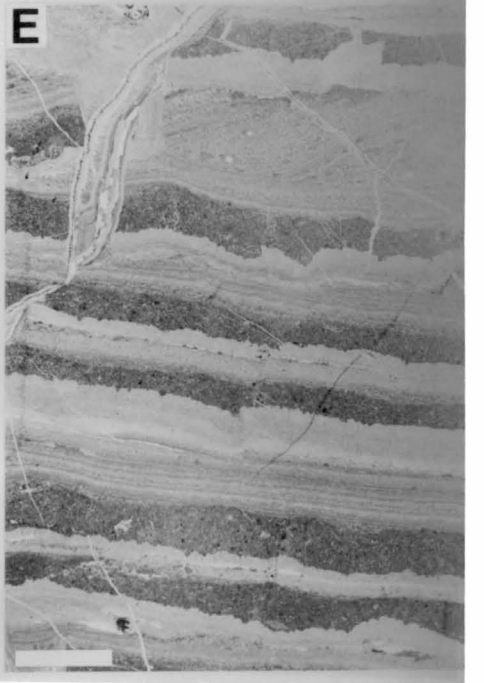
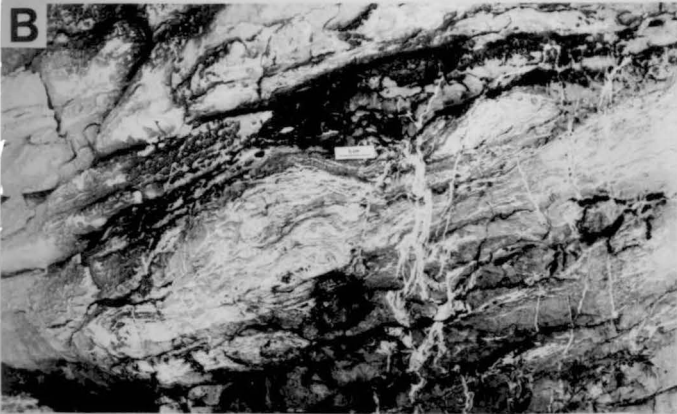
A) Stromatactis cavities in the internal sediment of a neptunian dyke within the reef-margin subfacies. The dyke is lined by radiaxial fibrous calcite and cyanobacterial encrustations (left side of photo) and these are overlain by stromatactis internal sediment. Pillara Limestone, Copley Valley; scale bar in centre is 10 cm long.

B) Vertical outcrop view of small stromatactis mounds known as "head-dress sponges" in the fore-reef subfacies. The dip reflects the palaeo-slope in the marginal-slope facies. Napier Formation, Copley Valley; scale bar in centre = 5 cm.

C) Vertical outcrop view of head-dress sponge mound in the fore-reef subfacies. Napier Formation, Copley Valley; scale bar = 5 cm.

D) Neptunian dyke filled by zebra limestone within the reefal-slope subfacies. Napier Formation, Copley Valley; scale bar in centre = 10 cm.

E) Vertically-oriented thin-section photomicrograph of zebra limestone from the neptunian dyke in Fig. 15 (D). The host sediment is a peloidal packstone. The cavities are filled by internal sediment, radiaxial fibrous calcite and cyanobacterial material. Note the neptunian fracture in the upper left. Scale bar = 1 cm. UTGD sample no. 70257



Wackestones and Bindstones with Abundant Shelter and Stromatactis Cavities

Occurrence

Lithologies with an abundance of shelter cavities are common in Frasnian and Famennian reefal-slope subfacies. Shelter cavities are also abundant in Frasnian stromatoporoid-coral-cyanobacteria reef-flat subfacies.

Description

Shelter cavities beneath skeletal constituents are almost invariably found in association with stromatactis mudstones (e.g. Figs. 14D, E; 16D, E). In many lithologies *there is a shelter cavity beneath every skeletal constituent, irrespective of whether the components are in position of growth or not* (Fig. 16D, E). Within these lithologies, all transitions exist from shelter cavities beneath skeletal constituents, to stromatactis cavities with part of the roof sheltered by a skeletal component, to stromatactis cavities with small skeletal constituents hanging from the roof (Fig. 16E).

The structure of the host sediment in shelter cavity lithologies is identical to that found in stromatactis mudstones.

Cavity-Filling Materials

The first generation of cavity fill is generally internal sediment (discussed below) and/or marine encrusting organisms like *Renalcis*. The roofs of stromatactis and associated cavity types are commonly lined by *Renalcis*. First generation cements are most commonly fibrous inclusion-rich cements (Fig. 14A,E) which commonly have the characteristics of radiaxial fibrous calcite (Bathurst, 1959). Inclusion-poor radiaxial fibrous cements (Kendall, 1985; Saller, 1986) with large crystal terminations (scaleno-hedral calcite of Kerans, 1985) are commonly interlayered with the inclusion-rich radiaxial cements (Fig. 14A).

These early cement types are very commonly interlayered with internal sediments (Fig. 16C). A coarse, equant calcite cement generally overlies these cements and fills all remaining porosity (Fig. 14E, 16D).

Marine Origin of Cavity Systems

The early diagenetic marine origin for the cavity systems described is demonstrated by:

- a) The growth of marine encrusting organisms on the roofs of cavities.
- b) Partial infill of the cavity systems by internal sediment (Fig. 14A, 15E, 16B, C).
- c) Reworking of cemented cavity systems in fore-reef debris flows.

Figure 16.

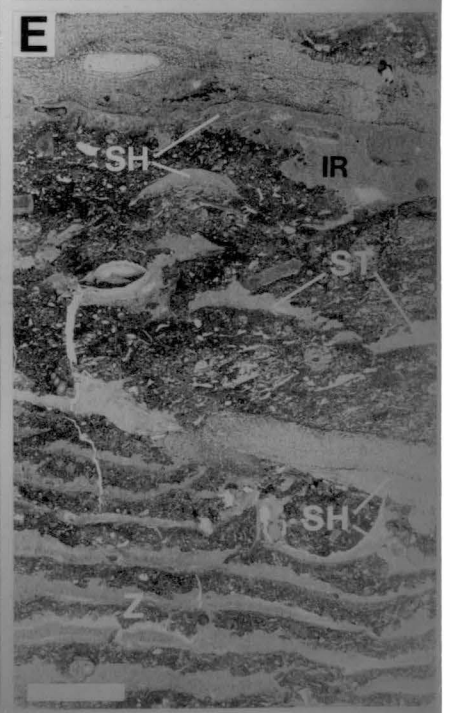
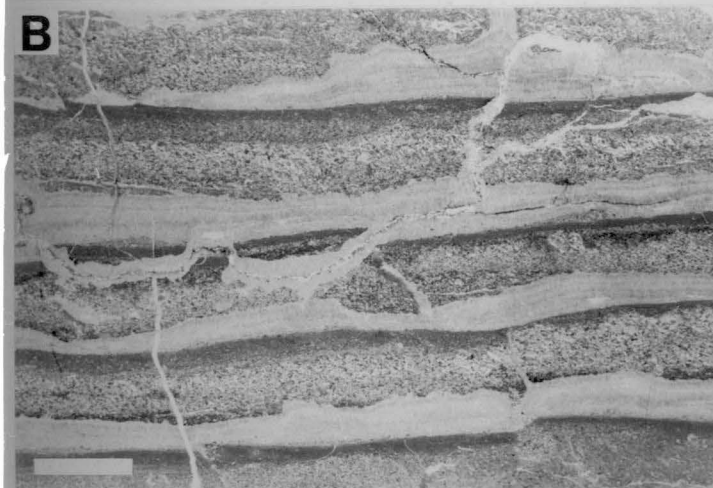
A) Vertical outcrop view of stromatactis cavities in the internal sediment of the neptunian dyke illustrated in Fig. 15(A). Note that there is a gradation from stromatactis cavities through to the sheet cavities of zebra limestone. Scale bar = 5 cm.

B) Vertically oriented thin-section photomicrograph of zebra limestone from the neptunian dyke illustrated in Fig. 15(A). The cavities are filled by internal sediment and radiaxial fibrous calcite. Scale bar = 1 cm. UTGD sample no. 70259

C) Vertically oriented thin-section photomicrograph of stromatactis cavities in the internal sediment of the same neptunian dyke. The cavities are filled by radiaxial fibrous cement and internal sediment. In the large central cavity, internal sediments and cements are interlaminated. The boundary between internal sediment and the host is unclear in most cavities. Note the brachiopod (**B**) hanging from the roof of the large cavity. Scale bar = 1 cm. UTGD sample no. 70260

D) Vertically oriented thin-section photomicrograph from an allochthonous block within the fore-reef subfacies. The block was probably dislodged from the reefal-slope subfacies and contains abundant shelter cavities. The cavities are filled by inclusion-rich radiaxial fibrous calcite and equant calcite. The roof of each cavity is sheltered by a thin laminar skeletal constituents. Stromatactis cavities are also present (**ST**). Napier Formation, Copley Valley; scale bar = 1 cm. UTGD sample no. 70309

E) Vertically oriented thin-section photomicrograph from small patch reef illustrating the intimate association between stromatactis, shelter and sheet cavities. Shelter cavities (**SH**) are abundant and occur beneath virtually every large skeletal constituent. Stromatactis (**ST**) and sheet cavities (**Z**) are also common. Emanuel Range (locality 3 from Playford, 1981); scale bar = 1 cm. UTGD sample no. 70268



In addition, there is ample evidence of a marine syndepositional origin for radiaxial fibrous cements filling the cavity types described:

- a) Intergrowths between radiaxial fibrous cement and encrusting marine organisms.
- b) Interlamination of internal sediment and radiaxial fibrous cement (Fig. 14C).
- c) Reworking and truncation of radiaxial fibrous cements in fore-reef debris flows and allochthonous blocks.

The Stromatactis, Shelter-Cavity and Sheet-Cavity Association

There is strong evidence that all of the cavity types described (stromatactis cavities; sheet cavities of zebra limestones and shelter cavities) share a common origin. Firstly, all the cavity types are gradational with one another. All transitions exist from unsheltered stromatactis cavities with small skeletal fragment projecting from the roof, to stromatactis cavities with part of the roof sheltered by skeletal fragments, to shelter cavities (Fig. 16E). A similar gradational relationship exists between stromatactis cavities and the sheet cavities of zebra limestone (Fig. 15A, 16E).

Secondly, there is a strong association in space between stromatactis, shelter and sheet cavities both on a macro- and micro-scale (e.g. Fig. 16E). All three cavity types are most abundant in platform marginal environments. Outside these environments, stromatactis and sheet cavities are generally absent and shelter cavities are only moderately common. Shelter cavities are invariably present in stromatactis-bearing lithologies (assuming there are skeletal fragments in the lithology). In many reefal-slope and reef-flat lithologies, there is a shelter cavity beneath every large skeletal component regardless of whether it is in the position of growth or not. This is not observed in lithologies away from the platform margin (back-reef subfacies for example).

The association between stromatactis and sheet cavities has been documented by a number of authors (Lees, 1964; Ross *et al.*, 1975; Bathurst, 1982; Pratt, 1982), whereas the association between shelter and stromatactis cavities has only been rarely documented (Heckel, 1972; Bathurst, 1982). This is probably because shelter cavities are not generally considered as problematic in origin and have not been considered relevant to the origin of stromatactis structures. All shelter cavities are generally considered to be of primary origin, and as the name implies, are believed to form by the sheltering effect of the overlying skeletal fragment.

The Roof of Stromatactis and Sheet Cavities

The roof of stromatactis cavities (and the laminar cavities of zebra limestone) from the Lennard Shelf and elsewhere (Bathurst, 1982) is generally irregular on a fine scale. Commonly small skeletal fragments hang from the roof and project into the cavities. "Where the roof is nearly horizontal and is made of a single piece of skeleton, then the adjacent mud-supported roof takes a sharp turn upwards where the skeletal support ends" Bathurst (1982, See also Fig. 16E). These features have prompted several researchers to suggest that the roof has been subject to erosion and upward stoping (Schwarzacher, 1961; Bathurst, 1980, 1982). Using this hypothesis, the irregularity of the roof is due to "the greater physical resistance of outward projections to erosion"

(Dunham, 1969, p. 169) and skeletal components project from the roof due to their resistance to erosion.

On the other hand, Heckel (1972) suggested the irregular roof in stromatactis cavities is due to simple pull apart and downward collapse without significant lateral water movement or erosion. There is evidence to support this contention in some stromatactis and sheet cavities from the Canning Basin reef complexes. Series of small *en echelon* cavities (gravitational pull-apart structures) in zebra limestones and stromatactis mudstones suggest that large fragments of host material have partially fallen into the underlying cavity. Bourque and Gignac (1986) suggested that the roof and original floor of sheet cavities (from the zebra limestones in Frasnian Belgium mounds) match each other and that they represent pull-apart walls. Kerans (1985) suggested a similar hypothesis for the genesis of some sheet cavities.

Internal Sediment - Host Rock Relationships

The distinction between "host-rock" and internal sediment is particularly important in considering the origin of stromatactis and associated cavities. Many authors have distinguished between internal sediment and "host rock" in order to determine the morphology of the original unfilled cavity system (Bathurst, 1959; Lees, 1964; Pratt, 1982). However, in stromatactis cavities of the Canning Basin, *the interface between internal sediment and host rock is commonly unclear* (Fig. 14A, 16C). Bathurst (1982) also noted this as a common feature in stromatactis lithologies.

When the interface between internal sediment and host rock is unclear, the internal sediment of one cavity often has the appearance of being continuous with the roof material of the underlying cavity (Fig. 14A, 16C). This gives the impression that the roof of one cavity is within the internal sediment pile of the overlying cavity. These observations suggest that stromatactis cavities are not simple partially sediment-filled cavities as has been suggested by numerous authors (Lees, 1964; Pratt, 1982).

A Soft-Body Decay Model for Stromatactis and Associated Cavity Systems

From the above evidence, it is suggested that the following sequence of events occurred:-

- a) At the sediment surface, the carbonate sediments contained, or were bound by one or more soft-bodied organism(s) (Fig. 17A).
- b) At a shallow depth below the sediment-water interface (perhaps only a few centimetres depth) the organic matter began to break down (Fig. 17B). This led to local sediment collapse which produced a pervasive cavity system. This may have included shelter, laminar and stromatactis cavities.
- c) The resulting pervasive cavity system was then subject to the influence of through-flowing marine waters (Fig. 17C). Material from the top of cavities was removed by internal erosion and subsequently deposited on the floor of cavities, either directly below the point of erosion, or down-stream from it. In this way, cavities migrated upward through the sediment, leaving an extended trail of internal sediment. Where large skeletal constituents were present in the lithology, upward migrating cavities were trapped beneath them, producing shelter cavities.

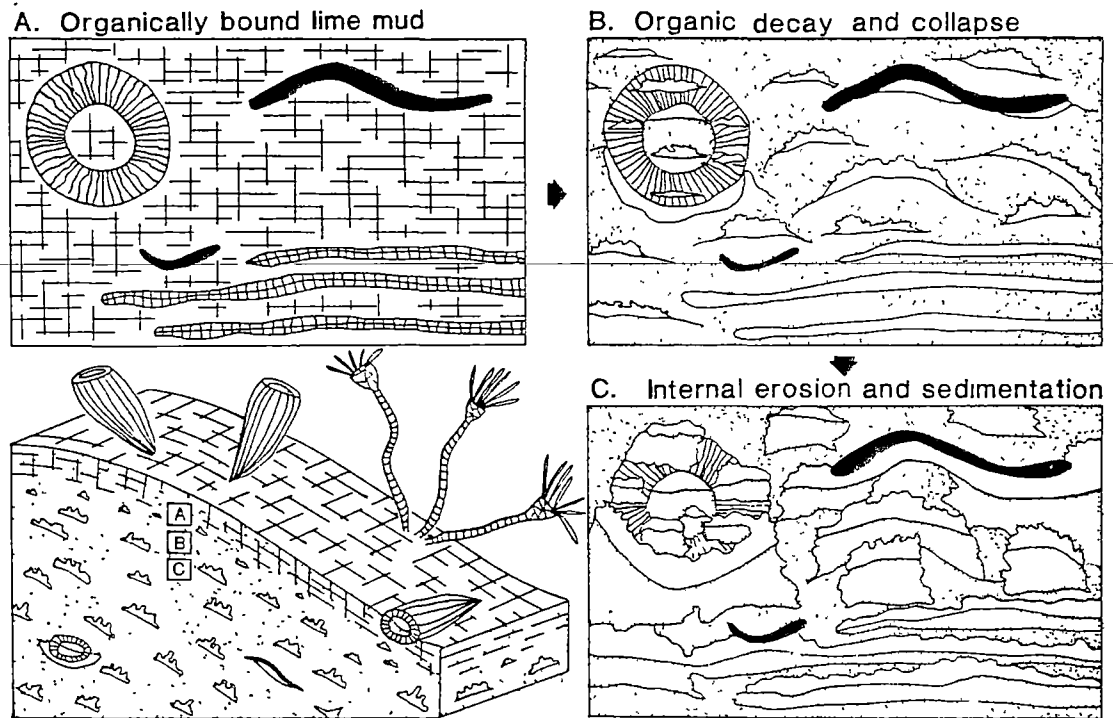


Figure 17. Schematic diagram illustrating the suggested process for the formation of stromatactis and associated structures. (A) It is suggested that at the sediment-water interface the host sediment contained, or was bound by, soft-bodied organisms (represented by cross pattern). In some lithologies the organisms may have had a laminar morphology (represented in the lower portion of the diagram). (B) At a shallow depth below the sediment-water interface the organic matter broke down causing sediment collapse. Collapse beneath skeletal components may have formed shelter cavities and collapse within the sediment may have formed stromatactis cavities. Where the organic matter had a laminar fabric, sheet cavities may have formed by collapse and pull-apart along organic laminae. (C) Because the environment was subject to significant wave and tidal action, large volumes of sea water passed through the cavity systems. This resulted in extensive internal erosion occurring at the roofs of the cavities and internal sediment being deposited on the floor of the cavities. Cavities migrated upwards through the sediment leaving a trail of internal sediment beneath the cavity. Where the cavities encountered a large skeletal component, a shelter cavity was formed.

The model presented above explains many of the features of stromatactis and related structures:-

1) *The association between stromatactis, shelter and sheet cavities.* This is a consequence of organic breakdown and subsequent internal reworking. When the process occurred in lime mudstones and fine grainstones, stromatactis cavities developed. When the organic breakdown occurred in carbonates with large skeletal constituents sediment would sometimes collapse beneath skeletal components, forming shelter cavities (Heckel, 1972). During subsequent internal erosion and sedimentation upward-migrating cavities would be trapped beneath bioclasts resistant to erosion and shelter cavities would again be formed.

The sheet cavities of zebra limestone may have developed where the organic material within the sediment had a laminar fabric. During the breakdown of the dispersed organic matter, the sediment may have broken along laminar zones having a greater concentration of organic matter. The sheet cavities may also be in part, the moulds of the soft-bodied organisms. In the majority of cases, zebra limestones have

not been subject to extensive internal erosion and sedimentation following organic breakdown.

2) *The gradation between internal sediment and host-rock.* This is a consequence of the internal erosion and sedimentation (internal reworking) following breakdown of the soft-bodied organisms. In migrating upwards through the sediment, cavities would migrate into the internal sediment of the overlying cavity. If internal reworking continues to completion, there may be no host material remaining, all of the sediment having been re-deposited internally.

3) *The sponge-stromatactis association.* The intimate association between sponges and stromatactis cavities in the Canning Basin reef complexes appears particularly significant. A stromatactis-sponge association has also been noted in the Silurian mud mounds of Gaspé (Bourque and Gignac, 1983) and in the Frasnian carbonates of Belgium (Bourque and Gignac, 1986). Bourque and Gignac (1983) suggested that stromatactis cavities were the result of early cementation of growth cavities within a sponge network and of cavities created by the decay of local uncemented sponge tissue.

Two possibilities exist to explain the development of stromatactis cavities within the bodies of sponges. It may be that the spicular network of the sponges broke down at a shallow depth below the sediment-water interface (Bourque and Gignac, 1983; Kerans, 1985). In this way, stromatactis cavities would have developed as a direct result of the decay of soft-bodied organisms, namely sponges.

Alternatively, a cavity system may have developed (by the decay of soft-bodied organisms) independently of the sponges. The internal erosion and sedimentation which followed may have eroded the spicular networks of the sponges, producing stromatactis-shaped cavities within the sponge bodies. This would appear to be the case in Fig. 14D where the cavities are largely developed in the lower parts of the sponge. Upward-migrating cavities would at first encounter the lower wall of the sponge and produce shelter cavities. Through-flowing waters might then begin to erode into the spicular network.

Significance and Conclusions

Stromatactis appears to be present in mounds ranging in age from Early Cambrian (James and Gravestock, 1986) through to Early Carboniferous (Bathurst, 1959; Lees, 1964) and appears to be rare or completely absent in older and younger mounds. Several post-Palaeozoic structures have been compared with stromatactis (Shinn, 1968b; Ginsburg and James, 1976; Mathur, 1975; Neumann *et al.*, 1977; Flugel, 1982) but it is doubtful that any of these structures have all of the features of "classic" stromatactis cavities.

As suggested by Bourque and Gignac (1983), this distribution strongly suggests a biological influence on stromatactis formation rather than a purely inorganic control, which would occur uniformly throughout the geologic record. The most likely explanation appears to be that the inferred soft-bodied organisms producing the initial cavity system were most abundant in the Palaeozoic.

Stromatactis cavities are most commonly found in mud mound environments which are generally thought to be of deeper water origin (Wilson, 1974, 1975). Based on the presence or absence of components like calcareous algae, micritization, plurilocular foraminifera and hyalosteliid sponges, Lees *et al.* (1985) estimate that

some Waulsortian buildups probably developed at water depths exceeding 300 m. Evidence from the Lennard Shelf reef complexes also suggests a deeper water origin for stromatactis and related structures. Lithologies most closely resembling Waulsortian lithologies and containing abundant stromatactis cavities are most common in the reefal-slope subfacies. Stromatactis cavities are rarely found in the shallow-water fenestral lithologies of the platform facies.

Stromatactis mud mounds are often characterized by a lack of skeletal framebuilders and an abundance of lime mud. The steep palaeo-slopes found in many mud mounds are difficult to explain without skeletal framebuilders. A pervasive soft-bodied binder would explain mound development and is compatible with the proposed hypothesis for cavity development. Lees and Miller (1985) have similarly suggested that the primary micrite of the Waulsortian buildups had a "gel-like consistency" and that the mound surface was probably mucilaginous. Bourque and Gignac (1983) have also proposed that some stromatactis mounds were bound by sponges.

The water energy in stromatactis mud mound environments is difficult to assess. Clearly there was enough current activity to carry internal sediments through the mounds. The mounds are often surrounded by low energy subtidal lime mudstones, wackestones and calcareous shale suggesting a low energy setting. However many mud mounds are flanked by coarse crinoidal grainstone beds which contain virtually no lime mud (Wilson, 1975). This indicates there was enough water energy to deposit the grainstones and to remove all lime mud from them. However, moving up-slope into the mound facies (into shallower water and theoretically into higher energy conditions), the grainstones are gradually replaced by muddy lithologies. This apparent reversal in water energy is most easily explained if, as suggested, the surface of the mud mound is baffled or bound by soft-bodied organisms.

Because internal erosion and sedimentation was generally quite extensive, the nature of the inferred organic binder is difficult to assess. The pervasive nature of many stromatactis and shelter cavity systems (Fig. 16D,E) suggests the organism must have been dispersed throughout much of the sediment and may indicate an endolithic organism. The common association between stromatactis structures and sponge spicules or sponge bodies may indicate the binder was a sponge (or group of sponges). Endolithic sponges described by Weidenmayer (1978) as forming small bioherms in the Bahamas may represent modern analogues.

Whatever the nature of the soft-bodied organisms, it appears likely that they played an important role in the development and stabilization of many Palaeozoic mud buildups which lack a true growth framework. If this hypothesis is correct, it becomes important to be able to identify lithologies which have been stabilized in this manner. An abundance of stromatactis-shelter cavities may be the only indication of this type of "bindstone". In addition, if there is an abundance of skeletal constituents in the lithology, stromatactis cavities may be absent and the only evidence of organic binding may be an over-abundance of shelter cavities.

In summary, it is proposed that at least one group of non-preservable organisms existed in the Palaeozoic which probably acted as sediment binders. The abundant stromatactis and shelter cavities occurring in many Palaeozoic carbonate mounds are believed to be the indirect result of the collapse and breakdown of these organic binders. Organic breakdown probably occurred within a few centimetres of the sediment-water interface, leaving a mass of porous, unconsolidated lime mud. Because such mound environments were probably subject to some current activity, extensive

internal erosion and sedimentation (internal reworking) probably occurred within the unconsolidated lime mud. The resulting stromatactis-shelter cavity network was then preserved by the marine cementation which followed the internal reworking.

In the past, it has been proposed that non-preservable, or soft-bodied, organisms may have been responsible for the construction of carbonate buildups lacking an organic framework (e.g. Lees, 1964). These proposals have largely been rejected on the basis that there is not sufficient direct evidence in the sediment to prove the existence of these organisms. But can we realistically expect to see this evidence? One glance at almost any modern marine environment reveals a whole host of organisms which will not be preserved in any form. It appears probable that at least one group of non-preservable organisms were important sediment binders in the Palaeozoic.

5. MARINE DIAGENESIS IN THE DEVONIAN REEF COMPLEXES OF THE GEIKIE GORGE AREA

Introduction

Near-surface diagenesis in the Devonian reef complexes of the Lennard Shelf is dominated by marine diagenetic processes (Playford, 1984; Kerans, 1985; Kerans *et al.*, 1986; Hurley, 1986). Marine diagenesis is most intense around the platform margins (reef-flat, reef-margin and reefal-slope subfacies) and includes internal erosion (Chapter 4) and sedimentation, carbonate precipitation and syndimentary fracturing. Evidence for the marine origin of the diagenetic phases includes interlamination with marine internal sediments, overgrowth by marine encrusting organisms, and reworking in the marginal-slope deposits. This evidence is further discussed under each diagenetic phase.

During early marine diagenesis, organic processes commonly induce carbonate precipitation and it is difficult to separate organic from purely inorganic processes. In the following discussion, those cavity-filling materials which have a morphology suggesting an organic origin have been termed "encrustations". The remainder of the precipitates have been termed "cements". However, using this terminology is not intended to imply that cements are purely inorganic precipitates.

Internal Sediments

A wide range of sediment types fill cavities and neptunian fractures in the platform-margin lithologies. Sediment types include lime mudstones, grainstones and packstones (peloid, ooid, skeletal), and skeletal rudstones and floatstones. Many of these internal sediments have similar compositions to overlying lithologies and appear to be derived by downward percolation from the depositional interface (Kerans *et al.*, 1986). Other internal sediments may be derived by internal erosion of the host sediments (Chapter 4).

However many cavities within the reef-margin, reef-flat and reefal-slope subfacies are filled by deep-red peloidal grainstones, packstones and lime mudstones which only occur as internal sediments. The red peloids commonly have a distinctive rod-shaped morphology (Fig. 18A).

Figure 18. Marine diagenetic phases in reef complexes of the Geikie Gorge region

A) Thin-section photomicrograph of red peloidal internal sediments filling a cavity within a cyanobacterial framestone of the reef-margin subfacies. The cyanobacterial framestone consists of *Renalcis* (R) and *Uralinella* (U). Pillara Limestone, western Copley Valley. Scale bar = 1 mm. UTGD sample no. 70254

B) Vertical exposure of internal sediment within a neptunian dyke. The internal sediment is a breccia with large fragments of fibrous marine cement and internal sediment. Pillara Limestone, western Copley Valley. Scale bar = 10 cm.

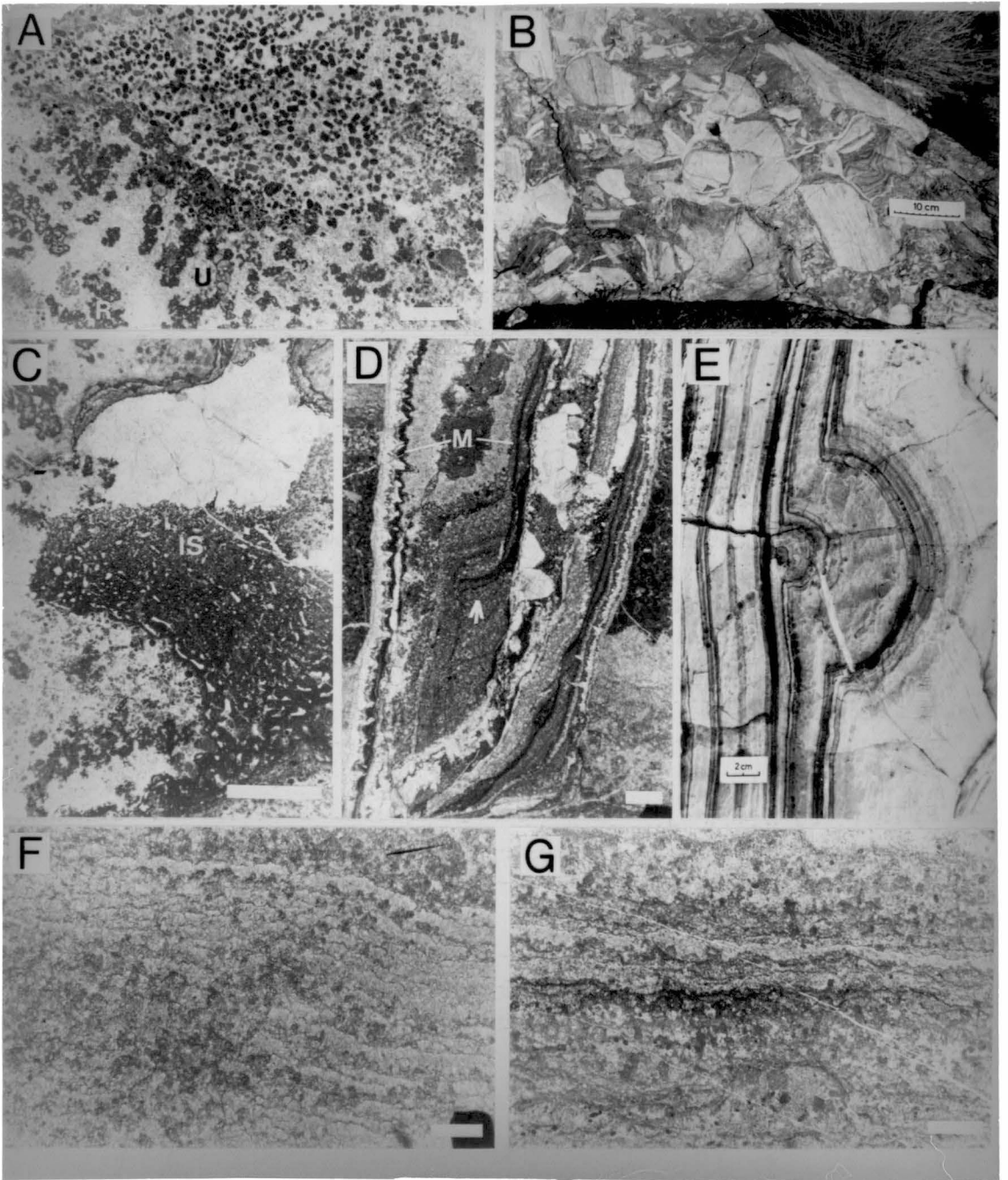
C) Thin-section photomicrograph of internal sediment (IS) filling a cavity within a cyanobacterial framestone. The internal sediment has a very fine vermiform fenestral fabric. Pillara Limestone, western Copley Valley. Scale bar = 1 mm. UTGD sample no. 70242

D) Thin-section photomicrograph of a neptunian dyke with a variety of infilling materials. Micritic encrustations (M) are prominent. Note the way in which the micritic encrustations thicken and grade into internal sediment at the base of the cavity (arrow). Pillara Limestone, western Copley Valley. Scale bar = 1 mm. UTGD sample no. 70257

E) Horizontal exposure of a longitudinal non-fenestral stromatolite within a neptunian dyke. The stromatolite is underlain, overlain, and laterally equivalent to marine fibrous cements. The darker laminae within the fibrous cements have a microlenticular fabric similar to the stromatolite. Pillara Limestone, western Copley Valley. Scale bar = 2 cm.

F) Thin-section photomicrograph of a non-fenestral stromatolite within a neptunian dyke. Numerous micrite columns are separated by laminae of fibrous calcite and microlenticular calcite. Pillara Limestone, western Copley Valley. Scale bar = 1 mm. UTGD sample no. 70261

G) Thin-section photomicrograph of a non-fenestral stromatolite within a neptunian dyke. The stromatolite consists of micrite columns and micrite laminae interlaminated with microspar and fibrous calcite. Pillara Limestone, western Copley Valley. Scale bar = 1 mm. UTGD sample no. 70262



There has been much debate over the origin of magnesium-calcite peloids associated with submarine cementation in Holocene reefs (James *et al.*, 1976; Macintyre, 1977). Macintyre (1985) noted that the peloids were largely restricted to skeletal cavities and suggested that they were chemical precipitates. The red peloidal sediments of the Canning Basin reef complexes appear to have developed within the reefal cavity systems and may have a bacterial origin (Playford, 1984; Kerans *et al.*, 1986).

Breccias consisting of lithified fragments of internal sediment and cement crusts occur in many large neptunian dykes (Fig. 18B). These unusual internal sediments probably developed when filled neptunian fractures were re-opened and pre-existing cavity fills were broken from the fracture surfaces.

A variety of cavity systems are found within internal sediments of the platform margin and these include sheet cavities (zebra limestone of Ross *et al.*, 1975) and stromatactis cavities (Fig. 15 A, D, E). Micro-fenestral (spongiform and vermiform of Pratt, 1982) cavity systems are also common in internal sediments within the reef-margin subfacies (Fig. 18C). These cavity systems appear to be of organic origin and may have developed by the action of various soft-bodied organisms which inhabited the reefal cavities. Extensive internal sedimentation occurred in lithologies with stromatactis (Chapter 4).

The frequent occurrence of normal-marine skeletal components (particularly ostracods) within internal sediments suggests a marine origin.

Micritic Encrustations

Micritic encrustations commonly line neptunian fractures in the platform margin lithologies. In outcrop, the micritic encrustations commonly have an orange or light brown colouration. The micrite is generally finely laminated and commonly peloidal (Fig. 18D). The lamination can be isopachous with the margins of the cavity but can also have a wavy or rippled texture (Fig. 20E). When the micrite completely encircles a cavity, it is generally thickest and commonly grades into internal sediment at the base of the cavity (Fig. 18D). Individual laminae can be traced around the walls and thicken at the base. Micritic encrustations are generally overlain by (and commonly interlaminated with) fibrous cements and internal sediments and this suggests a marine origin for the encrustations.

The micritic encrustations from the Geikie Gorge region may be similar to the micrite cements described by Kerans *et al.* (1986) from the reef complexes. The encrustations may have been precipitated directly onto the walls of the cavity. Alternatively, the micrite may have been carried through the cavity systems by pore waters and collected on the cavity walls by adhering to organic films. The latter explanation is supported by the greater thickness of micrite observed at the base of cavities. Similar micritic crusts were described by Reid (1987) from Triassic reefs.

Micro-lenticular Encrustations

In many large neptunian fractures and growth cavities in the reef-margin subfacies, micro-lenticular calcite encrustations are intergrown with fibrous cements. Commonly,

these encrustations fill a significant proportion of the primary porosity. In addition, microlenticular encrustations commonly form a substantial portion of many reef-margin lithologies (Kerans, 1985). Deeper water stromatolites have very similar microlenticular fabrics (described previously under section "deeper water stromatolite unit", Chapter 3) and for this reason, microlenticular encrustations in reefal cavities are believed to have a similar stromatolitic origin (Fig. 18F, G). In large neptunian fractures, microlenticular calcites commonly grade laterally into true detrital deeper water stromatolite heads and this again suggests a cyanobacterial or bacterial origin for the microlenticular encrustations (Fig. 18E).

In hand specimen, microlenticular encrustations have a milky-white appearance and commonly look very similar to fibrous marine cements. However, in many samples, the lamination is more irregular than in fibrous marine cements. As in deeper water stromatolites, the microlenticular encrustations consist of stacked lenticular accretionary units. Each lenticular unit consists a microspar core and a thin outer margin of micrite. Micritic columns are also common in the microlenticular encrustations (Fig. 18F, G). Commonly, microlenticular encrustations display gradational relationships with fibrous marine cements (Fig. 18F). In samples where this occurs, individual lenticular accretionary units may be quite large (up to 2 mm diam.) and commonly consist of spar, rather than microspar. In other cases, the micritic laminae and columns (which normally fringe the lenticular accretionary units) are interlaminated with fibrous marine cements. The transitions between fibrous marine cements and microlenticular encrustations suggest that both inorganic and organic processes have contributed to form the encrustations (Kerans, 1985).

Stromatolitic encrustations have been described from several Holocene reefs (James and Ginsburg, 1979; Land and Moore, 1980; Marshall, 1983). However, the Holocene crusts do not display a well-developed microlenticular fabric.

Dendritic Encrustations

Microstromatolitic and dendritic encrustations commonly fill large volumes of primary porosity in neptunian fractures and growth cavities within the platform margin lithologies (reef-flat, reef-margin and reefal-slope subfacies). The general morphology of these encrustations varies from micro-columnar to dendritic (Fig. 19A).

Encrustations commonly show a gradation from an early micro-columnar form to later dendritic morphologies (Fig. 19A). The internal structure of the micro-columns and dendritic colonies varies from laminated (convex toward growth direction as in stromatolites) to homogeneous and may consist of micrite, microspar or spar (Fig. 19A,B).

Micro-columnar and dendritic encrustations commonly have high concentrations of iron and manganese oxides, and in some cases, may consist almost entirely of these oxides (Fig. 19A). However, more commonly the iron contents are around 1-2 % (by microprobe analysis). The oxides are extremely finely crystalline (less than the 10 μm beam size on the microprobe) and dispersed throughout the calcite. Minute amounts of finely dispersed iron oxides gives the calcite of the micro-columns a bright yellow or red colour.

Figure 19. Marine diagenetic phases in the reef complexes of the Geikie Gorge area.

A) Thin-section photomicrograph of a dendritic encrustation within a neptunian dyke. The dark material consists of iron oxides. The encrustation is surrounded by microcrystalline calcite cement (MC). Pillara Limestone, western Copley Valley. Scale bar = 1 mm. UTGD sample no. 70242

B) Thin-section photomicrograph of a dendritic encrustation within a neptunian dyke. Individual shrubs consist of micrite and are surrounded by microspar. The encrustation is overlain by fibrous marine cement. Pillara Limestone, western Copley Valley. Scale bar = 1 cm. UTGD sample no. 70256

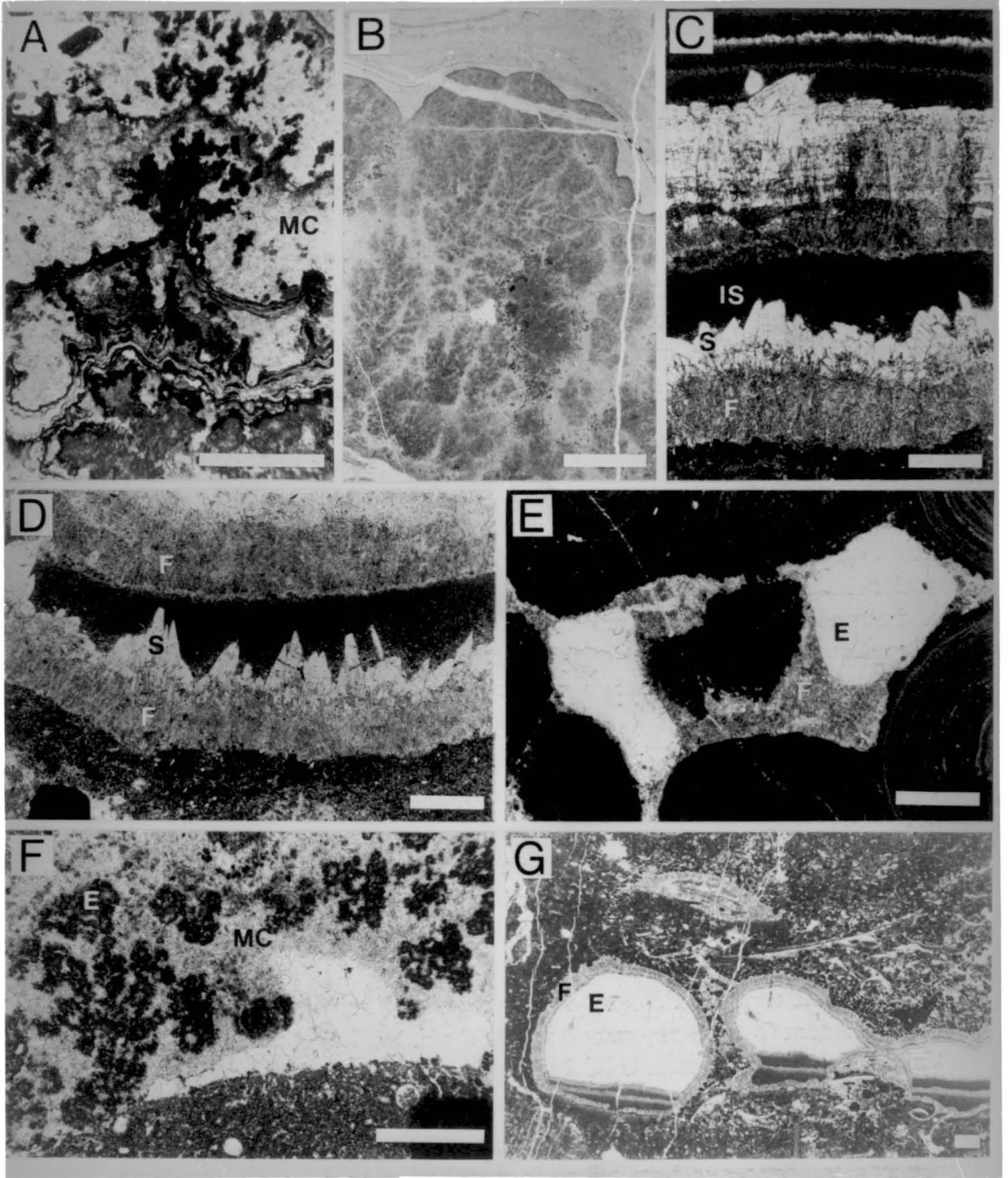
C) Thin-section photomicrograph of a typical sequence of marine cements and internal sediments at the base of a large cavity within the reefal-slope subfacies. Inclusion-rich radiaxial fibrous cement (F) is overlain by inclusion-free scalenohedral cement. The scalenohedral cement is overlain by micritic internal sediment (IS). Radiaxial fibrous cement overlies the internal sediment and this is again overlain by scalenohedral calcite. The sequence of internal sediment overlain by fibrous marine cement overlain by scalenohedral marine cement is very common. The interlamination of internal sediment and cement supports a marine origin for the cements. Note that the upper radiaxial fibrous cement has irregular inclusion-free areas within it. Frasnian Napier Formation, western Copley Valley. Scale bar = 1 mm. UTGD sample no. 70318

D) Thin-section photomicrograph of radiaxial fibrous marine cement overlain by well-developed inclusion-free scalenohedral marine cement. Reefal-slope subfacies of the Frasnian Napier Formation, western Copley Valley. Scale bar = 1 mm. UTGD sample no. 70317

E) Thin-section photomicrograph of fibrous meniscus cement (F) overlain by equant calcite cement (E) within pisoid rudstones from the back-reef subfacies of the fenestral peloidal calcarenite unit. Pillara Limestone, southern Copley Valley. Scale bar = 1 mm. UTGD sample no. 70300

F) Thin-section photomicrograph of *Epiphyton* (E) surrounded by microcrystalline calcite cement (MC). Reef-margin unit of the Pillara Limestone, western Copley Valley. Scale bar = 1 mm. UTGD sample no. 70242

G) Thin-section photomicrograph of molluscan moulds filled by internal sediments, fibrous marine cement (F) and equant calcite cement (E). This suggests that penecontemporaneous dissolution of aragonite occurred. Fore-reef subfacies of the Famennian Napier Formation, western Copley Valley. Scale bar = 1 cm. UTGD sample no. 70245



The encrustations are commonly overlain by internal sediments (containing marine fossils) and this indicates a marine origin for the encrustations. An organic origin for the encrustations is indicated by: 1) their micro-stromatolitic morphology; and 2) the similarity in form and habit to *Renalcis*. Reid (1987) suggested a bacterial origin for similar "knobby crusts" within Triassic reefs. Pratt (1984) has suggested that *Renalcis* is a marine calcified cyanobacterium. The encrustations described above may be the result of calcification of other species of cyanobacteria or bacteria. As with *Renalcis*, the cavity-filling nature of the encrustations suggests that the organisms responsible for growth were either tolerant of very low light conditions or were non-phototrophic (bacterial). The high concentrations of iron-manganese oxides suggest that iron and manganese oxidizing bacteria may have been associated with the encrustations. Playford *et al.* (1976) also suggested this origin for iron oxides in deeper water stromatolites from the reef complexes (discussed above).

Manganese-iron encrustations have been observed in modern reef-framework lithologies (James and Ginsburg, 1979) and are very common in deep sea environments. It has been suggested that the abundant manganese crusts found in modern deep sea settings are bacterial stromatolites (Monty, 1973).

Microcrystalline Cement

Renalcis colonies and the dendritic encrustations described above were observed to be invariably associated with, and surrounded by a microcrystalline cement (Fig. 19F). The microcrystalline calcite cement commonly occupies up to 50% of some reef-margin lithologies and is an important constituent of cyanobacterial framestones. Microcrystalline cement has been previously described from the Lennard Shelf reef complexes by Kerans (1985) and Kerans *et al.* (1986).

Microcrystalline calcite precipitation most commonly predates geopetal sedimentation (and radial calcite precipitation) and appears to have occurred penecontemporaneously with the growth of cyanobacterial colonies. As proposed by Kerans (1985), the close association with cyanobacteria suggests that precipitation of the microcrystalline calcite was organically induced.

Fibrous Cements

Fibrous calcite cements are spectacularly developed in platform-margin lithologies in the Geikie Gorge region (Fig. 20). Fibrous cements line neptunian fractures and almost all primary porosity types in the reef-flat, reef-margin and reefal-slope subfacies.

In the Geikie Gorge region, the majority of fibrous cements have a radial fibrous mosaic (Bathurst, 1959, 1977, 1982; Kendall and Tucker, 1973) although minor amounts of fascicular optic calcites (Kendall, 1977) are also present. Radial fibrous calcite is characterized by a pattern, within each crystal, of subcrystals that diverge away from the substrate and optic axes that converge away from the substrate. Fascicular optic calcite has similar diverging subcrystals but also has diverging optic axes.

Figure 20. Neptunian dykes of the platform margins.

A) Horizontal exposure of a neptunian dyke filled by fibrous marine calcite cement (F) overlain by *Renalcis* colonies (R). This supports a syndepositional marine origin for the fibrous calcite cement. Reef-margin unit of the Pillara Limestone, western Copley Valley. Scale bar = 2 cm.

B) Vertically oriented polished slab of a neptunian dyke which is filled by *Renalcis* (R) and fibrous marine calcite cement (F). The darker band within the fibrous cement has a microlenticular fabric. Reef-margin unit of the Pillara Limestone, western Copley Valley. Scale bar = 1 cm. UTGD sample no. 70254

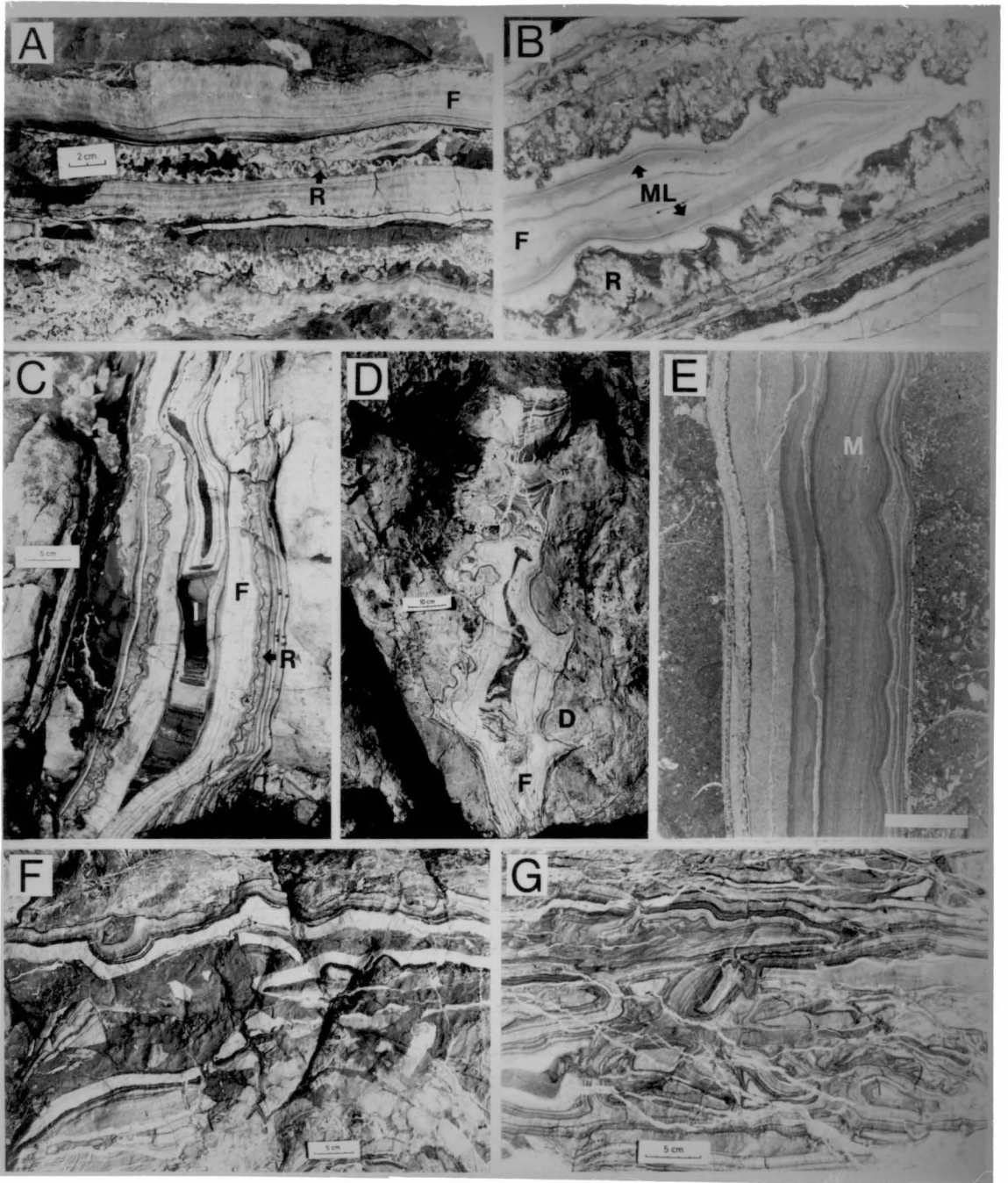
C) Vertical exposure of a large neptunian dyke within the reef-margin unit. The dyke has an extended fracture history, but in the major fracture, *Renalcis* (R) grew first and this was overlain by fibrous marine cement (F). In the central part of the dyke, fibrous marine cement is interlaminated with red peloidal internal sediment (I). Pillara Limestone, western Copley Valley. Scale bar = 5 cm.

D) Vertical exposure of a large neptunian dyke within the reef-margin unit. The dyke was first lined by a thick dendritic encrustation (photomicrograph in Fig. 19B) (D) and this was overlain by fibrous marine cement (F). The dark material in the centre is red peloidal internal sediment. Pillara Limestone, western Copley Valley. Scale bar = 10 cm.

E) Thin-section photomicrograph of a small neptunian dyke in the reef-flat subfacies of the fenestral peloidal calcarenite unit. The dyke is filled by a micritic encrustation (M) and fibrous marine cement. Note the rippled texture in the micritic encrustation. Pillara Limestone, western Copley Valley. Scale bar = 1 cm. UTGD sample no. 70265

F) Horizontal exposure of a neptunian dyke within the reef-margin unit. The dyke was first lined by fibrous cement and microlenticular calcite. The dyke was then refractured and filled with internal sediment, producing a breccia. Pillara Limestone, western Copley Valley. Scale bar = 5 cm.

G) Horizontal exposure of cavity fill within a large neptunian dyke. Large fragments of fibrous cement have been re-cemented by later fibrous cement and microlenticular calcite. The dark material is microlenticular calcite. Reef-margin unit of the Pillara Limestone, western Copley Valley. Scale bar = 10 cm.



The fibrous cements typically have a cloudy appearance in thin-section due to the abundance of micro-inclusions (Fig. 19C, D). In studying similar cements from McWhae Ridge, Kendall (1985) suggested that the majority of the inclusions were fluid-filled micro-cavities. Kerans *et al.* (1986) also commented on the abundance of micro-dolomite inclusions in the fibrous cements from the reef complexes. Fibrous cements commonly have irregular areas of inclusion-free calcite (Fig. 19C) and Kendall (1985) has suggested that these areas result from infill of the micro-cavities within the cements by calcite. It appears possible that the areas of inclusion-free calcite are the result of incipient neomorphism (chapter 6).

Layering in the fibrous cements is approximately isopachous but, as noted by Kerans *et al.* (1986), the cement layers commonly thin over protuberances on the cavity walls. This occasionally gives a meniscus fabric to the fibrous calcites (Fig. 20B). Fibrous calcites in the back-reef lithologies commonly have well developed meniscus textures (Fig. 19E). Fibrous calcites from the Geikie Gorge region typically display non-luminescence to very dull luminescence with numerous micron-sized luminescent inclusions and are non-ferroan (Fig. 23D).

The fibrous calcites are interpreted to have been precipitated in a marine environment because: 1) fibrous cements are commonly overlain by, and interlaminated with internal sediments (Fig. 16C; 19C, D, G, also see Kerans *et al.*, 1986); 2) fibrous calcites are commonly overgrown by *Renalcis* colonies and deeper water stromatolites (Fig. 20A); and 3) fibrous calcites are commonly reworked in the marginal-slope deposits. Meniscus textures suggest a marine vadose (intertidal) origin for some fibrous cements (Fig. 19E).

Radiaxial fibrous and fascicular optic calcites are uncommon in Cenozoic carbonates. Radiaxial fibrous calcite has been observed in cores from Enewetak atoll (Videtich, 1985; Saller, 1986) and in Pleistocene limestones from Japan (Sandberg, 1985). The high magnesium concentrations in these Cenozoic radiaxial fibrous calcites and the common micro-dolomite inclusions in Palaeozoic examples indicate the cement was originally precipitated as high-magnesium calcite (Lohmann and Meyers, 1977).

Kendall and Tucker (1973) concluded that radiaxial fibrous calcites are a replacement of an acicular cement. However, several researchers have recently challenged this interpretation (Sandberg, 1985; Kendall, 1985; Saller, 1986) and suggest that radiaxial calcite was precipitated with its present fabric.

In the Geikie Gorge region, the common interlamination between radiaxial fibrous calcite and internal sediments (and the overgrowth of radiaxial fibrous calcite by cyanobacteria) suggests that much of the radiaxial calcite was precipitated close to the depositional interface. However, it is probable that radiaxial fibrous calcite precipitation also continued in marine-burial conditions (Halley and Scholle, 1985; Saller, 1986).

Fibrous calcites from the Geikie Gorge region have $\delta^{18}\text{O}$ values ranging between -6.5 and 4.5 ‰ (PDB) and $\delta^{13}\text{C}$ values ranging between 1.0 and 4.0 ‰ (PDB) (Fig. 21). The most positive $\delta^{18}\text{O}$ values are consistent with Hurley's (1986) estimate for pristine Late Devonian marine radiaxial fibrous cements { $\delta^{18}\text{O} = -4.5$ ‰ (PDB) and $\delta^{13}\text{C} = +2.0$ ‰ (PDB)} from the Oscar Range reef complex. Using Hurley's (1986) estimate, and assuming radiaxial fibrous calcite originally had magnesium

contents similar to those of modern marine high-magnesium calcites, Devonian marine low-magnesium calcite should have a $\delta^{18}\text{O}$ value of approximately -6.4 ‰ (PDB) {using Gonzalez and Lohmann's (1985) $\Delta^{18}\text{O}$ low mag-high mag calcite }.

Scalenoedral Cements

Inclusion-poor scalenoedral cements (Kerans, 1985; Kerans *et al.*, 1986, inclusion-poor cement of Kendall, 1985) are common in large cavities and neptunian dykes of the platform-margin lithologies (Fig. 19C, D). Individual crystals have unit extinction and display little or no growth banding. In a typical cementation sequence, inclusion-poor scalenoedral cements overlie fibrous cements. However, cyclical cement sequences from internal sediment to radial fibrous cement to scalenoedral cement (Fig. 19C, D) are common in large cavities (Kendall, 1985; Kerans, 1985; Kerans *et al.*, 1986). Scalenoedral cements are non-luminescent and non-ferroan.

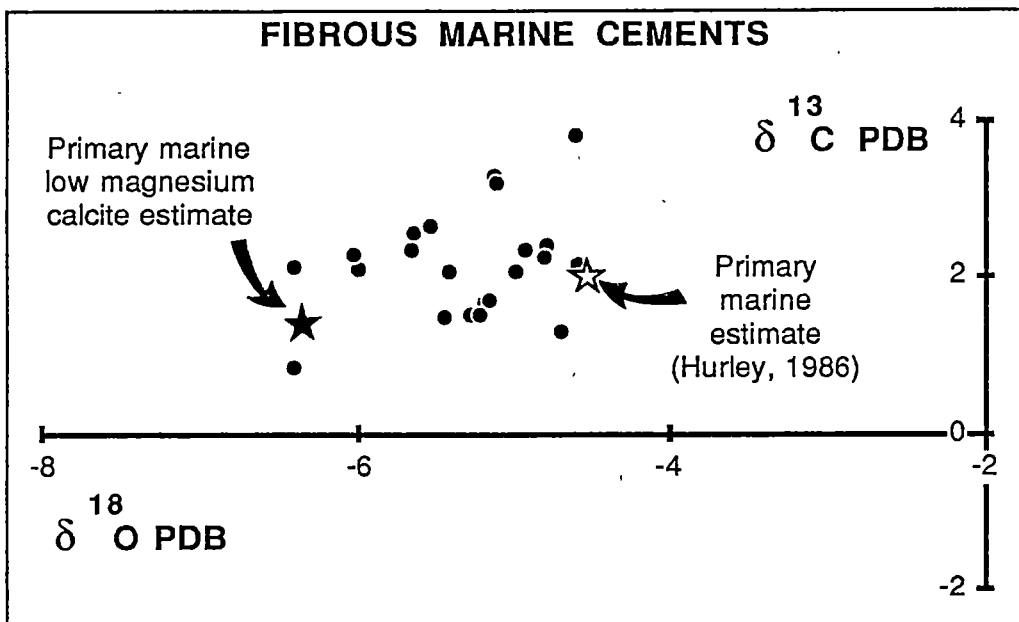


Figure 21. Carbon and oxygen isotope values for marine fibrous cements from the Geikie Gorge region. Hurley's (1986) estimate for primary marine radial fibrous cement is given. An estimate of the Upper Devonian marine low-magnesium calcite composition is also plotted. This is based on Hurley's marine estimate in combination with Gonzalez and Lohmann's (1985) $\Delta^{18}\text{O}$ low mag-high mag calcite estimated value.

The frequent interlamination of scalenoedral cements with radial fibrous cements and with internal sediments indicate a marine origin for the scalenoedral cement. Because of the absence of micro-dolomite inclusions, Kerans *et al.* (1986) and Kendall (1985) suggested that the scalenoedral cement was originally precipitated as low-magnesium calcite.

Saller (1986) described inclusion-poor radial cements from Enewetak atoll which have a morphology and occurrence almost identical to scalenoedral cements from the Geikie Gorge region. Inclusion-poor radial cements from Enewetak also have a high magnesium content (Saller, 1986) and this may suggest that the Devonian scalenoedral cements were originally precipitated as high-magnesium calcite. The

mean $\delta^{18}\text{O}$ value of -4.3 ‰ (PDB) for scalenohedral cements analyzed by Kerans *et al.* (1986) is also significantly higher than predicted for Devonian marine low-magnesium calcite $\{-6.4$ ‰ (PDB) $\}$ and is more consistent with an original high-magnesium calcite mineralogy.

Scalenohedral marine cements are rarely recorded from ancient carbonates (Schlager, 1974; James and Klappa, 1983). This may be because they are generally the latest marine cements to be precipitated, are relatively inclusion-free, and hence could easily be grouped with the clear burial cements which often directly overlie them.

Aragonite Dissolution

Aragonitic skeletal components within the reef complexes are generally preserved as cement-filled moulds and in the platform-margin lithologies, the moulds are commonly filled by internal sediments and radiaxial fibrous marine cements (Fig. 19G). This suggests that aragonite dissolution occurred in a near-surface environment. Kerans *et al.* (1986) noted that early aragonite dissolution occurred in both shallow and deep water environments in the reef complexes and suggested that aragonite dissolution took place in marine waters. No aragonitic marine cements have been observed in the reef complexes and it appears probable that shallow Devonian sea water was undersaturated with respect to aragonite (Kerans *et al.*, 1986). Saller (1986) noted a similar relationship between radiaxial fibrous calcite and aragonite dissolution in Enewetak atoll and suggested a deep marine origin for aragonite dissolution.

Subaerial exposure of the reef complexes could also explain the early aragonite dissolution. The Frasnian carbonates in the Geikie Gorge region may have been subject to subaerial exposure during latest Frasnian-Early Famennian time as there is a disconformity of this age in the Oscar Range (Hurley, 1986). Aragonite dissolution would almost certainly have occurred below this disconformity. In modern environments, aragonite can dissolve within 400,000 years when subject to subaerial exposure (Reeckmann and Gill, 1981). It is therefore possible that some aragonite dissolution occurred in meteoric water.

Neptunian Dykes and Sills

In the Geikie Gorge region, neptunian dykes and sills occur in two major environments: 1) within platform margin lithologies (reefal-slope, reef-margin and reef-flat); 2) associated with faulting.

Those neptunian dykes associated within the platform-margin lithologies are generally oriented approximately parallel to the reef margin (Playford, 1984; Kerans *et al.*, 1986). Neptunian dykes in the reef-flat and reef-margin lithologies generally have a near-vertical orientation while those in the reefal-slope lithologies commonly dip steeply towards the platform. Neptunian dykes may be up to 20 m wide but are generally much smaller. The sills and dykes have a large variety of marine cavity-filling materials within them, including marine internal sediments, cyanobacterial crusts (*Renalcis*), micritic encrustations, deeper water stromatolites, dendritic encrustations and marine cements (Fig. 20). Larger neptunian dykes are almost invariably composite and have suffered a long and complex history of filling and refracture (Fig. 20C, F, G). Playford *et al.* (in press) suggested several factors were responsible for symsedimentary fracturing and these include early cementation, contemporary

earthquakes, unsupported reef scarps, compaction of basin sediments and periodic slippage along marginal-slope bedding.

Neptunian fractures associated with faulting occur in linear zones which may be several kilometres long (see map enclosure). Fault-associated neptunian dykes have composite widths of up to 50 m and may occur in back-reef, reef-margin or marginal-slope lithologies. Fault-associated neptunian dykes have similar infills to those around the platform margins but commonly have a greater abundance of breccias. Many of the breccias appear to have been formed by shear movement along the dykes and are commonly similar to fault breccias.

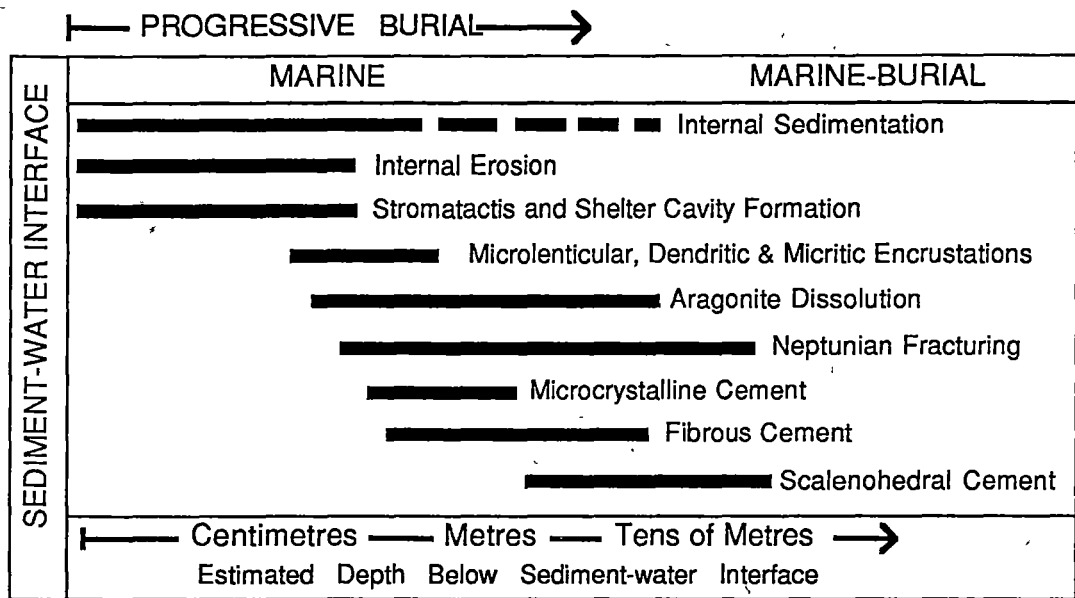


Figure 22. Interpreted paragenetic sequence of the major marine diagenetic processes which occurred in the Devonian reef complexes of the Geikie Gorge region. The interpreted depth of formation (below the sediment-water interface) is also estimated.

Discussion

Near-surface diagenesis in the reef complexes is dominated by marine diagenetic processes which are most intense at the platform margins. Marine diagenesis in the reef complexes is unlike that found in Holocene tropical reef complexes. Marine aragonite cements were not precipitated in the Devonian reef complexes and there is evidence for marine aragonite dissolution. The spectacular quantities of marine radial fibrous calcite cements in the reef complexes are also not found in Holocene shallow water environments. These observations are consistent with the idea of Early Palaeozoic "calcite seas" (Sandberg, 1975, 1983; Wilkinson, 1979, 1982; James and Choquette, 1983). Early Palaeozoic shallow seas are believed to have precipitated calcitic inorganic constituents and this is supported by textural data on ooids, marine cements and skeletal constituents. The interpreted paragenesis of the major marine diagenetic processes is illustrated in figure 22.

The marine diagenetic phases in the Devonian reef complexes of the Geikie Gorge region strongly resemble those observed in Holocene low-latitude deeper water (400 to 800 m) environments (Aissaoui *et al.*, 1986; Saller, 1986). High-magnesium

calcite marine cements are abundant in these environments and aragonite dissolution also occurs (Saller, 1986).

The estimated primary oxygen isotopic composition of Devonian marine high-magnesium calcite is substantially different (-4.5 ‰) from that of modern marine high-magnesium calcite cements (Hurley, 1986). There is growing evidence that the isotopic composition of both organic and inorganic carbonate precipitates show systematic variations through the Phanerozoic (Given and Lohmann, 1985; Meyers and Lohmann, 1985; Popp *et al.*, 1986; Veizer *et al.*, 1986).

The lack of definite near-surface meteoric diagenetic features in the carbonates of the Geikie Gorge region is problematic. Sedimentological and stratigraphical evidence indicates that the carbonates of the platforms were deposited very close to sea level. In this environment, it is difficult to envisage a situation in which the platform carbonates would never have been exposed to meteoric water. However, no definite near-surface Devonian meteoric cements have been recognized (even below the Frasnian-Famennian disconformity in the Oscar Range, Hurley, 1986).

The lack of early diagenetic meteoric cements may be linked to the lack of aragonite in the primary sediments. James and Choquette (1984), suggested that the dissolution of aragonite in meteoric water is a major source of carbonate for meteoric cementation. Without metastable aragonite to supply carbonate for cementation, most Tertiary deeper water chalks remain uncemented in the subaerial environment (James and Choquette, 1984). Therefore, the carbonates of the Devonian reef complexes may have suffered little or no cementation when subject to meteoric diagenesis because they were largely composed of calcite rather than aragonite.

Synthesis of Marine Diagenesis

Marine diagenetic processes first affected the Upper Devonian reef complexes of the Geikie Gorge region and occurred penecontemporaneously with reef growth. Marine diagenetic processes were most intense within the platform-margin lithologies (reef-margin, reef-flat and reefal-slope subfacies) and include stromatactis and shelter cavity development, internal sedimentation, neptunian fracturing, marine cementation (fibrous cements, microcrystalline cements, scalenohedral cements) and the formation of biogenic encrustations (microlenticular calcite, micritic, dendritic). No aragonite marine cements were precipitated in the reef complexes and the majority of marine cements probably had a high-Mg calcite mineralogy. Much of the primary porosity in the reef-margin subfacies was occluded by marine diagenetic phases so that the reef-margin facies acted as a permeability barrier during later diagenesis. Away from the platform margins, marine diagenesis was much less intense.

There is widespread evidence of synsedimentary aragonite dissolution and this may have occurred in both marine and meteoric waters. The reef-complexes were exposed to meteoric waters at least once (during latest Frasnian-early Famennian times, Hurley, 1986) but apparently did not suffer any significant cementation during this period. This may be because of the lack of primary aragonite in the sediments. Without extensive meteoric aragonite dissolution, there was probably no major source of CaCO_3 for cementation (James and Choquette, 1984).

The fibrous and particularly the scalenohedral marine cements probably continued to precipitate into the shallow-burial diagenetic environment (Halley and Scholle, 1985).

6. POST-MARINE DIAGENESIS IN THE DEVONIAN REEF COMPLEXES OF THE GEIKIE GORGE AREA

Introduction

Following Devonian synsedimentary diagenesis, the reef complexes of the Geikie Gorge region were subject to a variety of diagenetic environments. The consequences of these later diagenetic environments include equant calcite cementation, dolomitization, pressure solution, karstification, dedolomitization and calcite recrystallization. In fact, while the synsedimentary diagenetic features around the platform margins are the most visually striking (fibrous marine cements, internal sediments etc.), the later diagenetic processes had a much more profound effect on porosity destruction.

In this study, individual diagenetic phases were distinguished using a combination of optical petrography, cathodoluminescence petrography, and isotope geochemistry (carbon and oxygen). The overall diagenetic history of the sequence was deduced by combining the paragenetic sequence of the diagenetic phases with the burial history of the sequence. The carbonates of the Geikie Gorge region were subject to: 1) Late Devonian-Early Carboniferous burial; 2) Late Carboniferous - Early Permian uplift and subaerial exposure; 3) Permian - Cenozoic burial; and 4) Cenozoic subaerial exposure.

In summary, it is believed that almost all porosity was destroyed by Late Devonian - Early Carboniferous burial cementation (equant calcite cements). Karstification and minor cementation occurred during Late Carboniferous - Early Permian uplift and subaerial exposure. Minor secondary porosity was occluded by calcite cements during Permian-Cenozoic burial. During Cenozoic subaerial exposure, karstification, dedolomitization and calcite recrystallization occurred locally.

Clear Equant Calcite Cements

Clear equant calcite cements directly overlie skeletal components and marine cements in the Geikie Gorge region. Cathodoluminescence petrography and staining (Dickson, 1966) indicate the presence of five major zones in the clear equant calcite cements. From oldest to youngest, these are:

- a) Non-luminescent, non-ferroan cement.
- b) Bright-luminescent, mixed-ferroan cement.
- c) Dull-luminescent, ferroan cement.

- d) Late brightly banded luminescent cement.
- e) Late-dull-luminescent, ferroan cement.

Non-Luminescent Cement

Non-luminescent calcite cements, where present, directly overlie marine cements (radial fibrous, cloudy microcrystalline and scalenohedral calcite cements) and depositional components. Non-luminescent cements fill intergranular, fenestral and intragranular porosity, have an equigranular crystal fabric and display a low nucleation density relative to earlier marine cements (Figs. 23B, F). Under cathodoluminescence, the cement is either black or very weakly luminescent (Figs. 23B, F). Thin brightly luminescent bands are commonly present within the cement (Fig. 23B). The cement is never stained by potassium ferricyanide, indicating a non-ferroan composition.

Non-luminescent cements have a restricted distribution, being most abundant in coarse-grained back-reef lithologies. The cement also occurs in coarse-grained lithologies of the marginal-slope subfacies. In the platform abutting the Precambrian basement in the northern Geikie Gorge region, non-luminescent cements fill over 95% of all primary porosity and also fill pressure-solution-related tension gashes in this region. Non-luminescent cements are commonly absent from marine cemented platform margin and fine-grained marginal-slope lithologies.

Non-luminescent cements have $\delta^{18}\text{O}$ values ranging from -6.7 to -3.5 ‰ (PDB) and $\delta^{13}\text{C}$ values ranging from 1.1 to 3.2 ‰ (PDB). There is a slight covariance between oxygen and carbon isotope ratios (Fig. 24).

Bright Cement

Skeletal components, marine cements, and non-luminescent cements are commonly overgrown by brightly luminescing, zoned cements which are commonly ferroan (Fig. 23B, D, F). The bright cements generally form thin zones (100 μm to 2 mm) and grade into weakly zoned, dull-luminescent cements by an overall decrease in luminescence.

There is commonly an alternation between bright and dull bands in the younger portions of the bright cement. Bright cements tend to become ferroan (stain purple) in the youngest portions. Bright cements are most common in the marginal-slope subfacies. Bright cements post-date dolomitization and are therefore demonstrably of post-stylolite origin. (discussed below).

Because of the very thin nature of the bright cements, only two samples could be isotopically analyzed and both had values of around $\delta^{18}\text{O} = -10$ ‰ (PDB) and $\delta^{13}\text{C} = 1.5$ ‰ (PDB) (Fig. 24).

Figure 23. Thin-section photomicrographs of clear equant cement generations in plane light and cathodoluminescence.

A) A cement-filled cavity within a pisoid rudstone filled by a fibrous meniscus cement (F) and clear calcite cement (plain light). Back-reef subfacies of the fenestral peloidal calcarenite unit, Pillara Limestone, southern Copley Valley. Scale bar = 1 mm. UTGD sample no. 70300

B) Same area in A under cathodoluminescence. The fibrous meniscus cement (F) has a patchy low-intensity luminescence. Non-luminescent scalenohedral cements (S) rim the cavity. The clear equant cement consists of an early non-luminescent cement (N), overlain by a bright-luminescent cement (B), which is in turn overlain by a dull-luminescent cement (D).

C) A cement-filled cavity within a lithoclast breccia filled by radiaxial fibrous calcite (F) and clear cements (plain light). Fore-reef subfacies of the Famennian Napier Formation, western Copley Valley. Scale bar = 1 mm. UTGD sample no. 70306

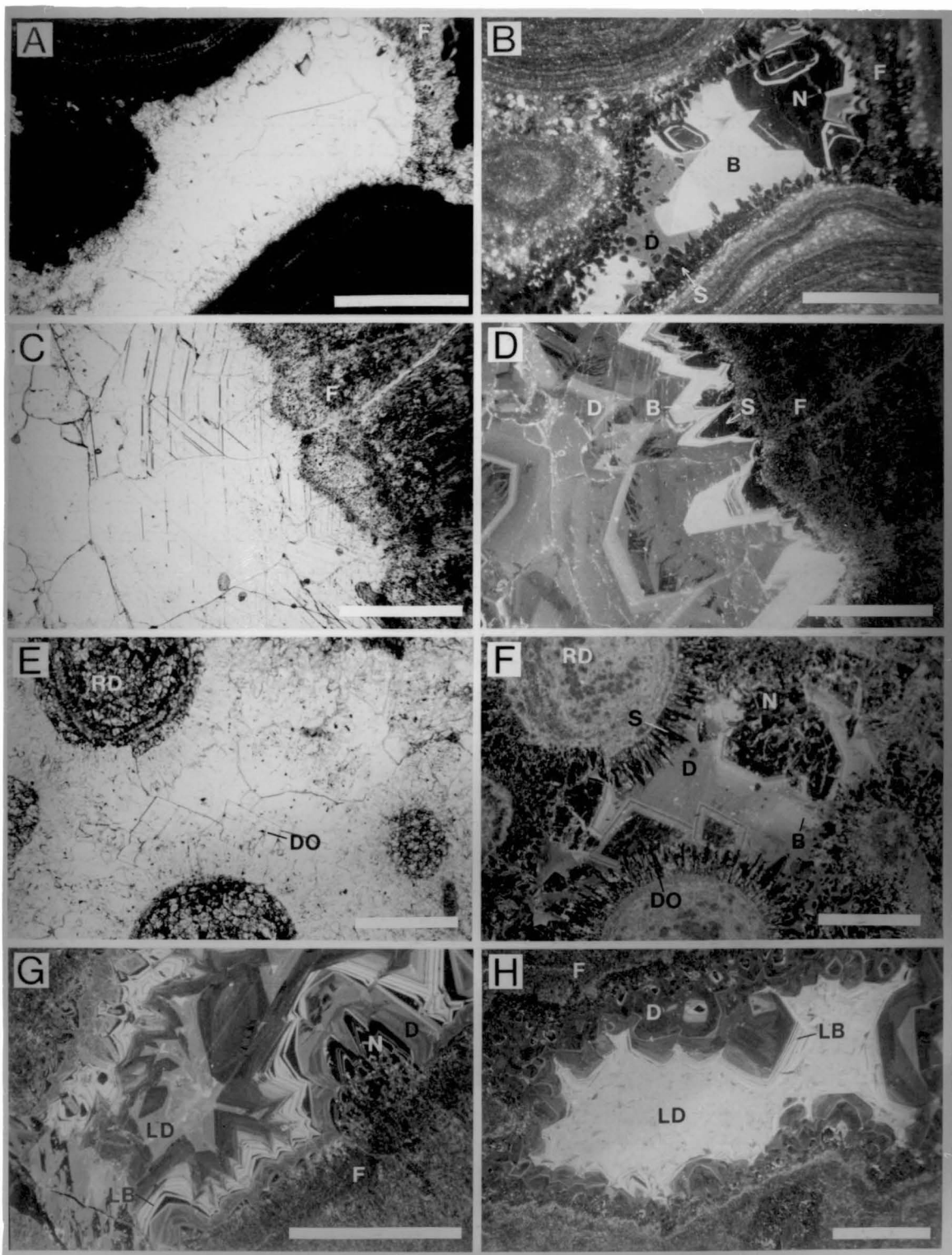
D) Same area in C under cathodoluminescence. The radiaxial fibrous calcite has a patchy low intensity luminescence. The radiaxial fibrous calcite is overlain by a non-luminescent scalenohedral cement generation which was not visible in plain light. The scalenohedral cement is overlain by a bright-luminescent cement and this is in turn overlain by a final dull-luminescent cement.

E) A cement-filled cavity within a partially dolomitized ooid grainstone (plain light). The ooids have been partially replaced by dolomite (RD). The cavity is filled by clear calcite cements and a dolomite cement (DO). Fore-reef subfacies of the Frasnian Napier Formation, north-eastern Copley Valley. Scale bar = 1 mm. UTGD sample no. 70299

F) Same area in E under cathodoluminescence. The clear calcite cements consist of the following cement generations from oldest to youngest - non-luminescent scalenohedral (S), non-luminescent equant (N), bright-luminescent equant (B), dull-luminescent equant (D). The dolomite cement (DO) has an early non-luminescent zone followed by a complexly banded bright- and dull-luminescent rim. The dolomite cement directly overlies the scalenohedral marine cement. The replacement dolomite (RD) has the same non-luminescent to bright-banded luminescent rim.

G) Cathodoluminescence photomicrograph of a cement-filled cavity within the fore-reef subfacies of the Frasnian Napier Formation. The cavity shows an extended record of cementation and is filled, from oldest to youngest, by fibrous marine cement (F), non-luminescent equant cement (N), dull-luminescent equant cement (D), late-banded cement (LB), late-dull cement (LD). The late-banded and late-dull cements are relatively rare as most cavities are filled by the dull cement generation. Northern Geikie Gorge. Scale bar = 1 mm. UTGD sample no. 70293

H) Cathodoluminescence photomicrograph of a cavity within the reef-margin unit of the Pillara Limestone. The cavity is filled, from oldest to youngest, by fibrous marine cement (F), dull-luminescent cement (D), late-banded cement (LB), and late-dull cement (LD). The late-dull cement has been neomorphosed and now has a blotchy bright luminescence. Western Copley Valley. Scale bar = 1 mm. UTGD sample no. 70252



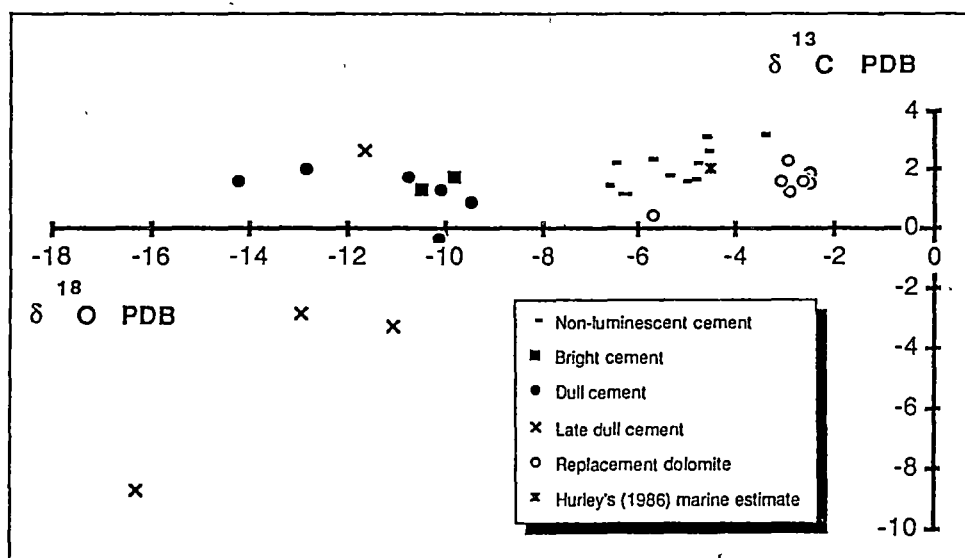


Figure 24. Carbon and oxygen isotope analyses for equant calcite cements and replacement dolomite from the Geikie Gorge region.

Dull Cement

Dull cement occludes virtually all of the primary porosity left after precipitation of the bright cement and is the final void fill in most primary cavities (Figs 23A-F). Under cathodoluminescence, the cement has a dull-orange luminescence which is zoned in earlier portions and weakly or unzoned in later portions. Dull cements are commonly ferroan (stain purple).

Dull cements generally occupy a large proportion of porosity in the fine-grained lithologies of the marginal-slope facies but also occur within the reef-margin and more rarely within the back-reef subfacies. Dull cements are commonly absent from the coarse-grained platform lithologies.

Dull cements have $\delta^{18}\text{O}$ values ranging from -9.5 to -14.2 ‰ (PDB) and $\delta^{13}\text{C}$ values ranging from -0.4 to 2.0 ‰ (PDB) (Fig. 24).

Late-Banded Cement

Late-banded cement has only been observed in primary porosity within strongly marine-cemented platform margin lithologies and is volumetrically unimportant as a porosity occluder. Where it occurs, the cement post-dates the dull cement (Figs. 23G, H). Under cathodoluminescence, banded cements display finely interlaminated bright and non-luminescent zones (Figs. 23G, H). The cement generation commonly has an unusual growth morphology. Smaller calcite crystals of the banded cement often nucleate on the very coarse dull cements (Figs. 23G). In addition, there is often very strong preferential growth on particular crystal faces, and adjacent crystal faces may show no growth (Fig. 23G). This gives the appearance of planar truncation surfaces on the crystals. The cement commonly contains thin ferroan zones.

Late-Dull Cement

Dull-luminescent, weakly zoned calcite cements overlie late-banded cements in primary pore space within marine cemented lithologies of the platform margin (Fig. 23G). The dull cements have both strongly ferroan (stain blue) and non-ferroan zones. Late-dull cements also occur in mouldic porosity within dolostones and in large dissolution-related caverns. When occurring in larger pores, late-dull cements have a poikilitic morphology. The late-dull cements have a restricted distribution and are volumetrically unimportant as porosity occluders.

Large caverns filled by late-dull cements occur at numerous localities in the Geikie Gorge area. These cement-filled caverns commonly occur along faults and neptunian fractures and are often up to 10 m across. Individual crystals are commonly over 40 cm in length. The caverns are believed to be the result of dissolution during Late Carboniferous - Permian subaerial exposure. The commonly linear nature and occurrence along faults and joints of the cement-filled caverns may be due to these features acting as conduits for Permian vadose-meteoric water.

Very few samples of late-dull cement were isotopically analyzed. Those that were analyzed have $\delta^{18}\text{O}$ values ranging from -16.3 to -11.0 ‰ (PDB) and $\delta^{13}\text{C}$ values ranging from -8.7 to 2.6 ‰ (PDB) (Fig. 24).

Timing and Origin of Clear Equant Cements

Non-luminescent cement: The non-luminescent cement is invariably non-ferroan and this suggests that it was precipitated from oxygen-rich waters (Meyers, 1974, 1978; Frank *et al.*, 1982). Pressure-solution-associated tension veins filled by non-luminescent cement indicate that it was precipitated contemporaneously with pressure solution. The common restriction of the cement to coarse-grained lithologies suggests that the cement was precipitated from oxidized waters which flowed through the more permeable zones in the carbonates during Late Devonian - Early Carboniferous burial diagenesis.

The distribution and timing of the non-luminescent cement is compatible with a topography-driven meteoric water model (Grover and Read, 1983; Meyers and Lohmann, 1985; Dorobek, 1987). In this model, meteoric pore waters are derived from recharge areas in basin margin uplands. The uplands provide the hydraulic gradient to drive the waters into the carbonates under shallow burial conditions. However, the high carbon and oxygen isotope ratios of many non-luminescent cements (relative to estimated Devonian marine composition) are not compatible with this meteoric water model.

Kerans (1985) analyzed samples of non-ferroan, non-luminescent cement from Geikie Gorge with relatively high $\delta^{18}\text{O}$ and $\delta^{13}\text{C}$ values and suggested the heavy carbon was the result of bacterial fermentation of organic matter (Irwin *et al.*, 1977; Matsumoto and Matsuhisa, 1985). Irwin *et al.* (1977) suggested that organic matter can be bacterially fermented during burial diagenesis, producing methane which has a very light carbon isotope ratios and carbon dioxide which has very heavy carbon. However, this explanation cannot explain the high oxygen ratios. In addition, bacterial fermentation is believed to occur below the zone of sulphate reduction (Irwin *et al.*, 1977). Non-luminescent cements were probably precipitated from relatively oxidized waters.

A marine-burial origin for the cements (Kerans, 1985) is most compatible with their petrographic and geochemical characteristics. The high $\delta^{18}\text{O}$ and $\delta^{13}\text{C}$ values of the cements (relative to the estimated Devonian marine composition) are compatible with a cold-sea-water origin for the cements. Similar enriched isotope compositions (relative to marine components) were found in deep-marine cements from the Bahama Escarpment (Freeman-Lynde *et al.*, 1986).

Bright cement; Bright-luminescent cements have slightly-ferroan zones and this suggests they were precipitated from slightly reduced waters. This would have allowed the incorporation of manganese into the calcite, causing the bright luminescence. The bright cement is known to have been precipitated after some stylolite development, suggesting the cement was formed at depths of at least a few hundred meters in a Late Devonian - Early Carboniferous burial environment.

The low $\delta^{18}\text{O}$ values of the bright cement (two analyzed samples) suggest relatively high temperatures of precipitation. If the difference in the $\delta^{18}\text{O}$ value of the bright cement (-10‰) from the primary marine composition (-4.5‰) is caused by temperature alone, the bright cement would have been precipitated at approximately 50°C (assuming sea water temperature of 25°C and using Friedman and O'Neil's (1977) calcite-water fractionation curve).

Dull cement; The weakly-zoned dull-luminescent cements are commonly ferroan and presumably formed from relatively reduced pore fluids in a Late Devonian - Early Carboniferous burial environment (Grover and Read, 1983; Choquette and James, 1987). The abundance of dull cements in the fine-grained marginal-slope lithologies suggests the cements occluded porosity in the impermeable lithologies which were not cemented by earlier cement generations.

The low $\delta^{18}\text{O}$ values of the dull cements probably reflect higher temperatures of precipitation. Applying the same temperature estimate (described above) for the lowest $\delta^{18}\text{O}$ value suggests precipitation temperatures of around 70°C .

Late-banded cement; The strongly-zoned bright- and non-luminescent character of the banded cements suggests rapid changes in pore water composition and this suggests a near-surface environment of precipitation. Bright and non-luminescent cements are characteristic of relatively oxidized pore waters (Grover and Read, 1983). This cement is therefore interpreted to have precipitated in a Late Carboniferous - Early Permian near-surface environment as the limestones were subject to subaerial exposure and karstification during this period.

Banded cements have only been observed in marine-cemented lithologies and this probably reflects the relative rarity of primary porosity in the carbonates after burial cementation. The marine-cemented lithologies apparently preserved a small amount of primary porosity during burial because of their very impermeable nature.

Late-dull cement; Large dissolution caverns filled by the late-dull cement indicate the cement was precipitated after Late Carboniferous-Early Permian exposure. The cement has a weakly-zoned dull luminescence and is commonly strongly ferroan. These

features suggest a Late Permian - Cenozoic deep-burial environment of precipitation (Scholle and Halley, 1985; Choquette and James, 1987). Hurley (1986) found similar cements in the Oscar Range (Hurley's diagenetic event VI ferroan blocky cement) and also suggested a Late Permian - Cenozoic burial origin for the cements.

The low $\delta^{18}\text{O}$ values may reflect high temperatures of precipitation and/or a meteoric water contribution. The very light carbon isotopic ratios of some late-dull cements probably reflects a contribution from organic carbon. Isotopically light carbon can be released into pore waters from organic matter during several processes:

- a) Oxidation of organic matter during soil formation (Meyers and Lohmann, 1985).
- b) Microbial oxidation of organic matter and microbial sulphate reduction during the early stages of burial (Irwin et al., 1977).
- c) Thermocatalytic decarboxylation of organic matter at elevated temperatures during burial (Irwin et al., 1977; Pisciotto and Mahoney, 1981).
- d) Oxidation of biogenically produced methane (Hathaway and Degens, 1969; Roberts and Whelan, 1975; Nelson and Lawrence, 1984).

A contribution from light soil carbon appears improbable because of the wide range in the $\delta^{18}\text{O}$ values. A relatively uniform oxygen isotopic composition is expected during meteoric diagenesis because rainwater will be the dominant source of oxygen in these environments (Meyers and Lohmann, 1985). It appears more likely that the low $\delta^{13}\text{C}$ values in the late-dull cements were produced via an organic reaction during burial. This may suggest that the pore waters which precipitated the late-dull cements interacted with, or were derived from, organic-rich sediments. Isotopically light carbon appears to be quite common in carbonates within terrigenous host rocks (Irwin et al., 1977; Nelson and Lawrence, 1984; Hennessy and Knauth, 1985) and it may be that the pore waters which precipitated the late-dull cements were largely derived from the overlying Upper Carboniferous - Permian Grant Formation or other terrigenous units.

Regional Correlation of Equant Calcite Cements

Kerans (1985) carried out a regional analysis of cements in the reef complexes. Kerans' (1985) non-luminescent, banded and homogeneous luminescent cement correspond to the non-luminescent, bright-luminescent and dull-luminescent cements respectively of this paper. However, Kerans (1985) included marine scalenohedral cements in his non-luminescent group.

Hurley (1986) also presented a detailed investigation of calcite cements from the Oscar Range reef complexes and his cementation sequence was quite different from that in the Geikie Gorge area. Hurley's (1986) first-generation banded-luminescing blocky calcite cement (Hurley's diagenetic event II) appears to be equivalent to the bright cement of this study (the non-luminescent cement of the Geikie Gorge area is apparently absent in the Oscar Range). However, Hurley (1986) documented his banded-luminescent cement as being overlain by a non-luminescent non-ferroan calcite cement (Hurley's diagenetic event III). In the Geikie Gorge area, the bright cements are overlain by dull-luminescent ferroan calcite cements. In summary, Hurley's (1986) cementation sequence from the Oscar Range 1) lacks the early non-luminescent non-ferroan blocky cements of the Geikie Gorge area; 2) lacks the ferroan dull-luminescent

cements which are so common in the Geikie Gorge region; and 3) places a greater importance on Late Carboniferous subaerial exposure and later burial diagenesis than is apparent in the Geikie Gorge area.

Dolomitization and Dolomite Cementation

Dolomite occurs as a cement and as a replacement phase throughout the Devonian carbonates of the Geikie Gorge region but massive dolostones are only extensively developed on the platform abutting Precambrian basement (Fig. 25). On this platform, a narrow rim of completely dolomitized lithologies occurs on the back-reef side of the reef-flat subfacies. Dolomite is also present in the upper marginal-slope facies of this platform.

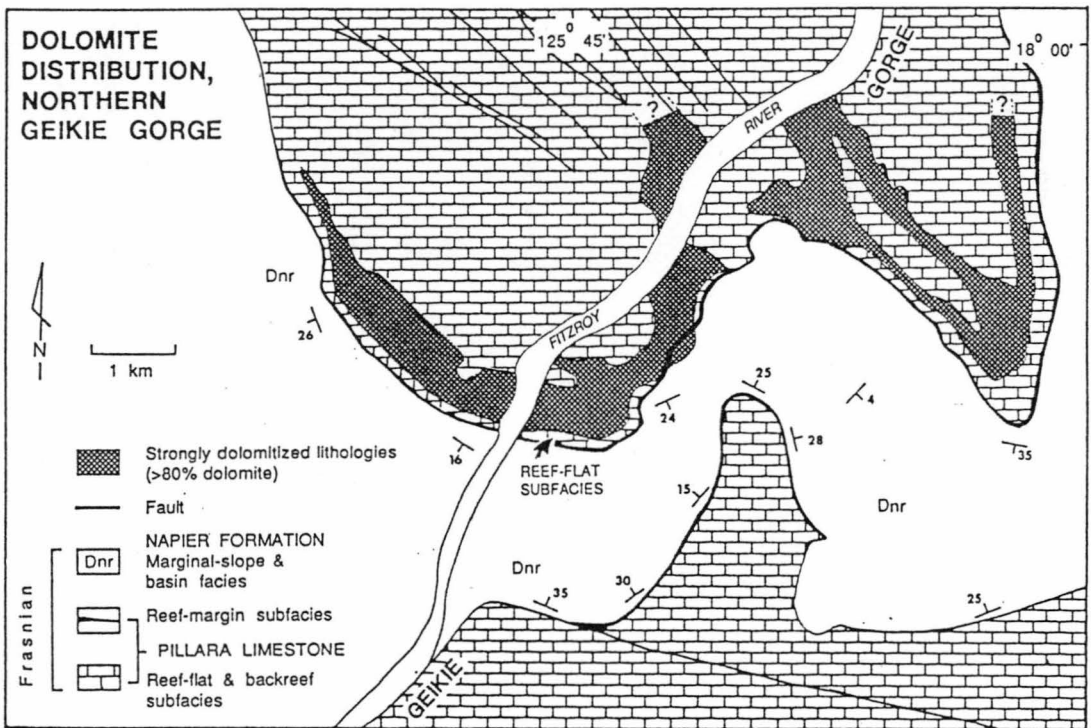


Figure 25. Map showing the distribution of strongly dolomitized lithologies in the northern Geikie Gorge region. Dolomite is most abundant in a narrow zone (<1 km wide) on the platform side of the reef-flat subfacies.

Replacement Dolomite

The majority of dolomite in the sequence is a replacement of the finely crystalline depositional components. The crystal size of the replacement dolomite most commonly ranges from 80 to 200 μm. Dolomite may occur as isolated replacement crystals or as a pervasive mosaic of dolomite crystals. Crystal mosaics in completely dolomitized lithologies are generally subhedral to anhedral. Crystals generally display straight extinction but commonly display weakly to moderately undulose extinction and could

be termed xenotopic (Gregg and Sibley, 1984). In transmitted light, many dolomite crystals have clear rims and cloudy centres (Fig. 26A).

The general order of susceptibility to dolomitization, from most to least susceptible is: geopetal micrite; micritic matrix; ooids and peloids; skeletal components; and marine and blocky cements (Kerans, 1985). Fenestral and coarse grainstone lithologies appear to have been resistant to dolomitization as fenestral grainstone beds often remain as limestones even when all surrounding lithologies have been pervasively dolomitized. Stylolites are also preferentially dolomitized, demonstrating that dolomitization occurred after stylolites had developed (Fig. 26E).

Kerans (1985) suggested that the order of susceptibility to dolomitization is due to a permeability control, but it seems likely that crystal size also played a significant role in determining which components were dolomitized (Bullen and Sibley, 1984). This is illustrated in dolomitized marginal-slope breccias. The breccias are generally extremely well cemented by marine fibrous calcite and yet the clasts of micrite within the breccias can be strongly dolomitized. Dolomitizing fluids must have been able to penetrate the radial fibrous calcites to reach the clasts, but did not dolomitize the marine fibrous calcite.

In completely dolomitized lithologies, calcite dissolution commonly occurred during the later stages of dolomitization. Thus secondary mouldic and intercrystalline porosity is common in completely dolomitized lithologies (Fig. 26A). Fracture porosity is also common in these lithologies.

Under cathodoluminescence, replacement dolomites of the Geikie Gorge region have an early non-luminescent core followed by a thinner, brightly luminescent and finely banded outer rim (Fig. 23F, 26B). At some localities, the central non-luminescent zone may be partly or completely neomorphosed and display a bright luminescence similar to that found in later dolomite zones (Fig. 26B).

The majority of replacement dolomites examined in this study are from the northern Geikie Gorge platform (Fig. 2) and show uniform isotopic compositions, with $\delta^{18}\text{O}$ values clustering around -2.5 ‰ (PDB) and $\delta^{13}\text{C}$ values around $+1.5$ ‰ (PDB) (Fig. 24). One sample of dolomitized geopetal sediment from the western Copley Valley has significantly lower oxygen and carbon isotopic ratios. Dolomites from the northern Geikie Gorge platform have high $\delta^{18}\text{O}$ values compared with other Devonian burial dolomites from Canadian reefs (Mattes and Mountjoy, 1980) and from the Barbwire Terrace. In fact, the Geikie Gorge dolomites have only slightly lighter oxygen ratios than the value estimated for Devonian marine dolomite ($\delta^{18}\text{O} = -2$ ‰ (PDB), chapter 8).

Dolomites from Geikie Gorge are calcium-rich, (56-61.5 mol% Ca). Strontium, sodium, iron and manganese values for the replacement dolomites are illustrated in figure 27.

Figure 26 Thin-section photomicrographs illustrating dolomitization and dedolomitization fabrics.

A) A cement-filled cavity within a completely dolomitized *Amphipora* wackestone (plain light). The dolomite rhombs have cloudy centres and clear rims. The cavity is an *Amphipora* mould and is filled by a poikilitic calcite cement (C). Back-reef subfacies of the stromatoporoid unit, Pillara Limestone, northern Geikie Gorge. Scale bar = 1 mm. UTGD sample no. 70286

B) Same area in A under cathodoluminescence. Dolomite rhombs have non-luminescent centres and bright-luminescent rims. Many of the non-luminescent centres have been neomorphosed to a blotchy dull luminescence. The poikilitic calcite cement has a very dull unzoned luminescence.

C) A cement-filled cavity within a partially dolomitized fenestral peloidal grainstone (plain light). Most of the cavity is filled by clear equant calcite cements. A small dolomite rhomb (D) is located within the calcite cement sequence. Note the small protuberances on outer margins of the dolomite rhomb (arrows). Reef-flat subfacies of the stromatoporoid unit, Pillara Limestone, northern Geikie Gorge. Scale bar = 100 μm . UTGD sample no. 70297

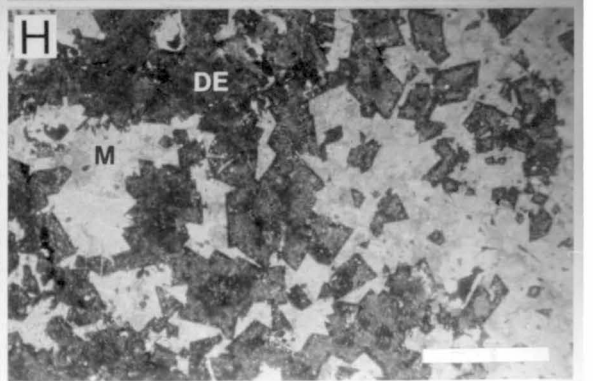
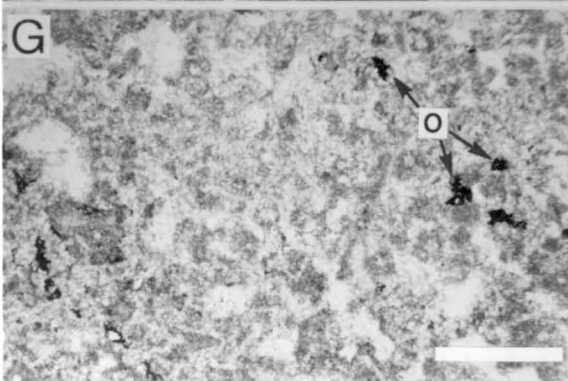
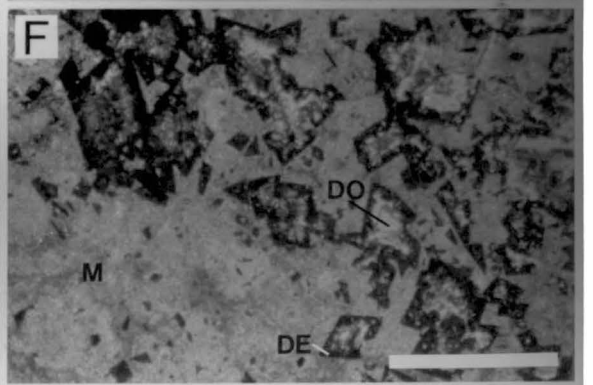
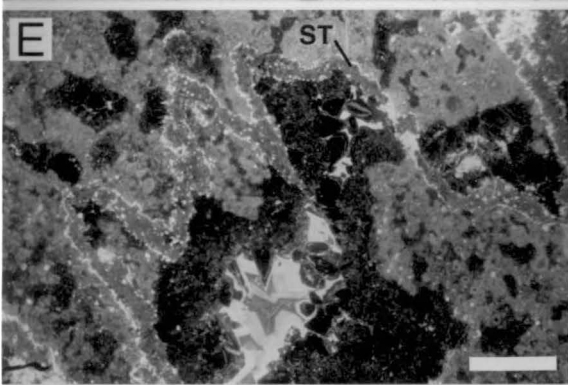
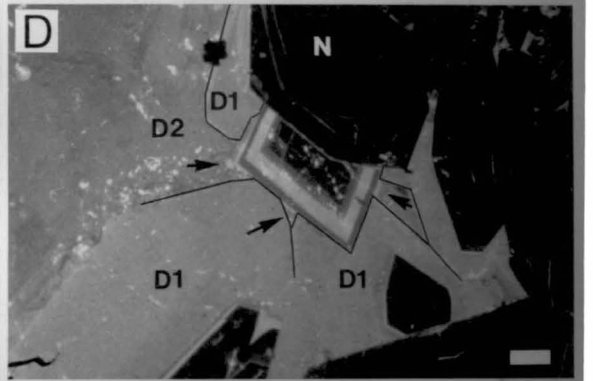
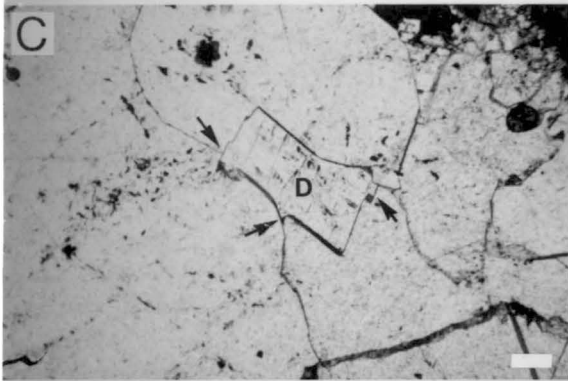
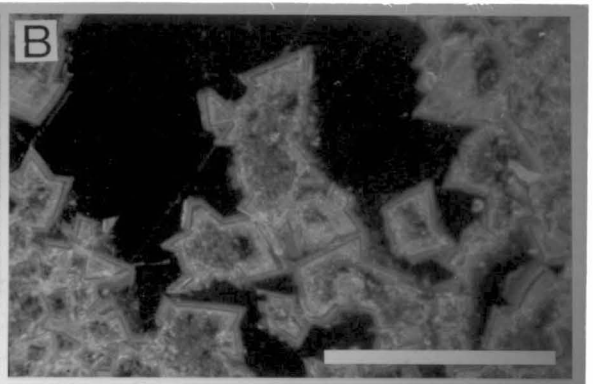
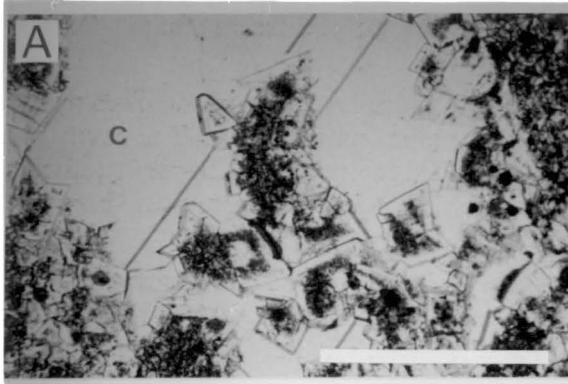
D) Same area in C under cathodoluminescence. The dolomite rhomb post-dates the non-luminescent calcite (N). The dolomite rhomb consists of an earliest non-luminescent zone followed by a banded bright and dull-luminescent zone. Weakly zoned dull-luminescent calcite cements (D1 and D2) post-date the non-luminescent calcite cement. The boundary between the D1 and D2 dull-luminescent calcite cements is marked (black lines). Note that the dull-luminescent dolomite protuberances on the dolomite rhomb (arrows) are only present where the dull-luminescent calcite cement D1 did not cover the dolomite rhomb. This indicates that the dolomite protuberances were precipitated after the precipitation of dull-luminescent D1 calcite cements. Thus, the overall cementation sequence is, from oldest to youngest, non-luminescent calcite (N), non-luminescent dolomite, banded bright- and dull-luminescent dolomite, dull-luminescent D1 calcite, dull-luminescent dolomite (protuberances arrowed) and finally dull-luminescent D2 calcite. This complex alternation between dolomite and calcite cementation is observed in many partially dolomitized lithologies.

E) A cathodoluminescence photomicrograph of a dolomitized stylolite (ST) within a partially dolomitized fenestral peloidal grainstone. The replacement dolomite along the stylolite has the same early non-luminescent and a late bright-luminescent zonation that is observed in all dolomite from the Geikie Gorge area. This demonstrates that dolomitization occurred after some stylolites had developed. Reef-flat subfacies of the stromatoporoid unit, Pillara Limestone, northern Geikie Gorge. Scale bar = 1 mm. UTGD sample no. 70297

F) A cathodoluminescence photomicrograph of a partially dedolomitized lithology. Scattered dolomite rhombs have dolomite cores (DO) and non-luminescent dedolomitized rims (DE). The dolomite cores have embayed and irregular margins. The rhombs are within dull-luminescent lime mud (M). Back-reef subfacies of the stromatoporoid unit, Pillara Limestone, northern Geikie Gorge. Scale bar = 1 mm. UTGD sample no. 70281

G) A completely dedolomitized lithology (plain light). The lithology has a peloidal texture which is largely due to dedolomitization. Note the dispersed oxides (O). Back-reef subfacies of the stromatoporoid unit, Pillara Limestone, northern Geikie Gorge. Scale bar = 1 mm. UTGD sample no. 70281

H) Same area in G under cathodoluminescence. Calcitized dolomite rhombs (DE) are non-luminescent and are surrounded by dull-luminescent micrite (M).



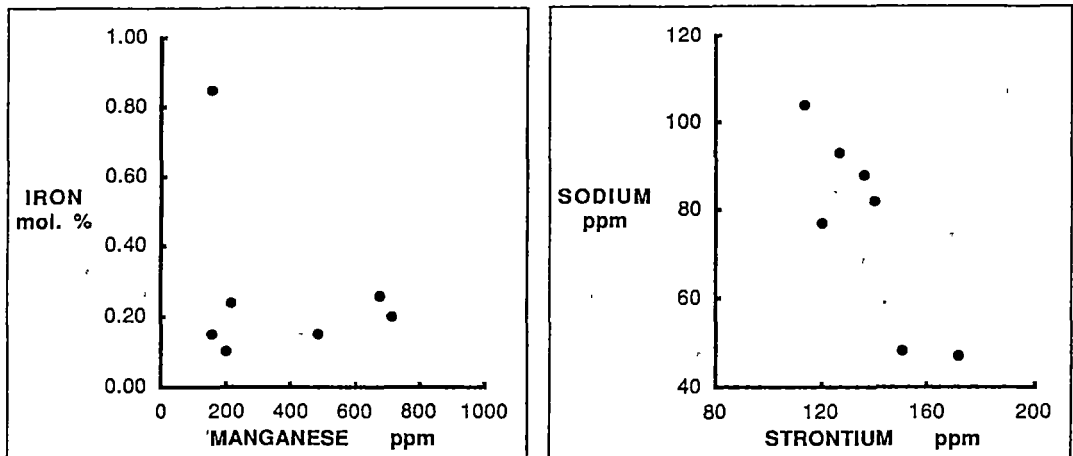


Figure 27. Iron vs. manganese and sodium vs. strontium values for replacement dolomites from the northern Geikie Gorge region.

Dolomite Cements

Dolomite cements occur in completely and partially dolomitized lithologies. In the completely dolomitized lithologies, dolomite cements fill mouldic, fracture, intercrystalline and primary porosity, whereas in partially dolomitized lithologies, dolomite cements fill primary porosity. Dolomite cements are inclusion-poor and have weak to strong lattice curvature (in many instances the cements could be classified as saddle dolomite, Radke and Mathis, 1980).

Under cathodoluminescence, dolomite cements of the northern Geikie Gorge region have an early non-luminescent zone and a later strongly zoned bright and dull-luminescent zone (Figs. 23F, 26D). The cathodoluminescence zonation in the dolomite cements is always identical to the zonation in the associated replacement dolomite (except where there has been neomorphism in the replacement dolomite). This indicates that the replacement dolomites and dolomite cements were precipitated from the same pore fluids.

Dolomite cements generally directly overlie marine cements and skeletal components (Fig. 23E, F). However, dolomite cements commonly display complex relationships with the non-luminescent, bright and dull-luminescent calcite cements. Figures 26C and D illustrate the complex relationships between the dolomite and calcite cements. A dolomite cement crystal (non-luminescent to bright-luminescent to dull-luminescent) overlies a non-luminescent calcite cement crystal. The dolomite crystal was then largely enveloped by the dull-luminescent calcite cement. Portions of the dolomite crystal still exposed to pore fluids were then overgrown by a zoned dull-luminescent dolomite. Finally, dull calcite cements grew over the dolomite.

These relationships demonstrate that, in some instances, dolomite cementation (and dolomitization) post-dated the non-luminescent cement generation. In the same sample, dolomite having the same cathodoluminescence zonation preferentially replaces stylolites and this demonstrates that stylolites had developed prior to

dolomitization and dolomite cementation. It appears significant that there is an alternation between dolomite and calcite precipitation.

Elsewhere in the back-reef subfacies of the northern Geikie Gorge region, the early non-luminescent portion of dolomite cement is overgrown by non-luminescent calcite cement. Alternation between dolomite and calcite cements is a common feature of many partially dolomitized lithologies. It is important to note that dolomite and calcite cements will generally only precipitate on dolomitic and calcitic substrates respectively. Therefore, alternation between dolomite and calcite precipitation can only be recognized where the two minerals are in direct contact and compete for growth space.

In completely dolomitized lithologies, dolomite cementation was preceded by calcite dissolution.

Timing and Origin of Dolomite

Dolomitization in the Geikie Gorge region began after stylolites had developed. This suggests that dolomitization occurred at depths of at least a few hundred metres. Hurley (1986) estimated the thickness of Famennian carbonates in the Oscar Range to have been at least 160 m. If similar thicknesses existed over Frasnian carbonates at Geikie Gorge, it appears improbable that stylolites could have developed in Frasnian carbonates during Famennian times and that stylolites would most likely not have developed until Early Carboniferous times. Therefore dolomitization probably took place during Early Carboniferous time, when the reef complexes were buried beneath the Fairfield Group.

Dolomite in the Geikie Gorge region is largely restricted to the platform which abuts the Precambrian basement. As suggested by Kerans (1985), the distribution of dolomite on this platform appears to be largely controlled by the permeability of the carbonates at the time of dolomitization. Dolomitization was not extensive in the reef-margin subfacies because it was strongly marine cemented. Dolomitization was not extensive in the back-reef subfacies of the northern Geikie Gorge platform probably because it was already cemented by early non-luminescent equant calcite. The resistance of fenestral carbonates to dolomitization was probably due to their early cementation by non-luminescent calcite.

Very similar dolomites occur throughout the Oscar Range in Frasnian and Famennian carbonates. Selectively dolomitized geopetal micrite within fractures and cavities suggests a similar timing for dolomite in the Oscar Range reef complex (Kerans, 1985). Hurley (1986) noted that the dolomite of the Oscar Range was most extensive in the Frasnian back-reef lithologies immediately adjacent to the Precambrian basement core.

The dolomites of the Geikie Gorge region share many similarities with the dolomites of Holocene reefal atolls (Saller, 1984; Aissaoui *et al.*, 1986; Aharon *et al.*, 1987). Dolomite in the Mururoa atoll is best developed in a zone on the platform side of the platform margin (Aissaoui *et al.*, 1986) as are the dolomites at Geikie Gorge. At Niue Island, the core of the atoll is strongly dolomitized (Aharon *et al.*, 1987) as in the Oscar Range reef complex (Hurley, 1986). The paragenesis of the atoll dolomites is also very similar to that of the Geikie Gorge dolomites. Saller (1986) noted that dolomite cements occasionally overgrew radial calcite cements. This is the most

common sequence of dolomite cementation in the Devonian reefs of the Geikie Gorge region.

Isotopically, the Geikie Gorge dolomites are closely comparable with the atoll dolomites. The $\delta^{18}\text{O}$ and $\delta^{13}\text{C}$ values of the Geikie Gorge dolomites is very similar to the estimated composition of Devonian "marine dolomite" (discussed earlier). Similarly, Holocene atoll dolomites have isotopic compositions in equilibrium with cold Cenozoic sea water (Saller, 1984). Atoll dolomites are generally considered to have been precipitated from sea water (Saller, 1984; Aharon *et al.*, 1987) although Aissaoui *et al.* (1986) favour a meteoric-marine mixing model.

However, the post-stylolite origin for the dolomites of the Geikie Gorge region is not compatible with the atoll dolomitization model. A basinal brine model is more compatible with the timing and distribution of dolomite in the reef complexes. The distribution of the dolomites could be explained if basinal dolomitizing brines migrated upwards along the basin margin and into the more permeable platform lithologies of the reef complexes. The marine-cemented platform margins may have acted as a permeability barrier and prevented the dolomitizing fluids from entering the marginal-slope lithologies (Fig. 28). The high $\delta^{18}\text{O}$ values of the dolomite implies that the basinal brines had heavy $\delta^{18}\text{O}$ compositions, particularly if the brines were at elevated temperatures.

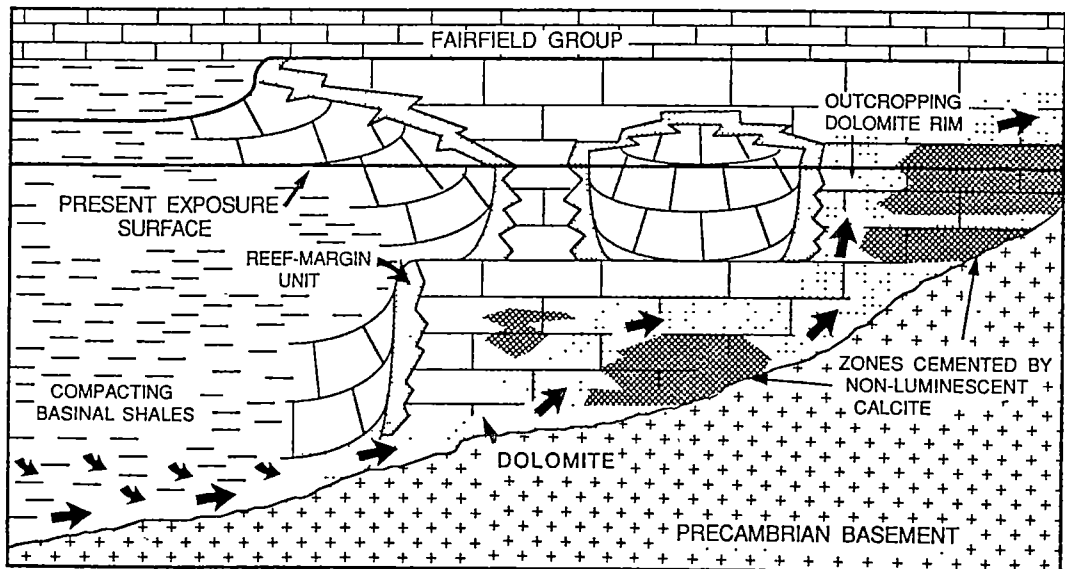


Figure 28. Model for dolomitization in the Devonian reef complexes of the Geikie Gorge region. Dolomitization is believed to have occurred in an early burial diagenetic environment during Early Carboniferous time, when the reef complexes were buried beneath the Fairfield Group. Basinal dolomitizing brines are suggested to have migrated through permeable zones along the basin margin. The path of the dolomitizing fluids was controlled by the strongly marine cemented reef-margin subfacies and zones cemented by non-luminescent calcite cements of early burial origin. In the northern Geikie Gorge region, the dolomitizing waters were forced through a narrow permeable, uncemented zone between the marine cemented reef-margin subfacies and the back-reef subfacies (cemented by non-luminescent calcite).

Playford (1984) and Kerans (1985) have also suggested a burial compaction model for dolomitization on the Lennard Shelf, similar to that proposed by Mattes and Mountjoy (1980) for the Miette dolomite. Kerans (1985) suggested that a major phase of basinal fluid expulsion may have taken place during the mid-Carboniferous period of rapid subsidence in the Fitzroy Trough (Middleton, 1984), causing warm basinal brines to be forced through the basin margin carbonates.

Compaction

Both physical compaction and pressure solution (chemical compaction) have occurred within the carbonates of the Geikie Gorge region. Minor grain-breakage in the sandy lithologies is the only unequivocal evidence for physical compaction in the carbonates. Pressure solution appears to have been a more important compaction process and stylolites are the most obvious pressure solution features in the carbonates.

Stylolites most commonly follow the bedding in the carbonates. Hence, in the platform carbonates, stylolites are subhorizontal, while in the marginal-slope beds, stylolites have basinward dips ranging from 20 to 30°. Stylolite teeth in all facies are generally oriented subvertically, suggesting that overburden pressure was the dominant control on pressure solution. Stylolites are most abundant in the grainstones of the back-reef and fore-reef subfacies. In the fore-reef subfacies, two sets of stylolites are occasionally present; one set following bedding and another set having a subhorizontal orientation. In the reef-flat and reefal-slope subfacies, stylolites most commonly follow bedding, and ^{are} quite widely spaced. In the reef-margin subfacies, stylolites are more irregularly oriented. ae

Subvertical stylolites with subhorizontal teeth are present at some localities in the Geikie Gorge region. Vertical stylolites are occasionally dolomitized, indicating that some of the vertical stylolites developed during early burial diagenesis.

Playford (1980) and Hurley (1986) have made quantitative estimates of the amount of pressure solution which has taken place in the reef complexes of the Lennard Shelf. By measuring the peak to trough amplitude of stylolites, Hurley (1986) found that the marginal-slope and back-reef subfacies of the Oscar Range reef complexes had suffered the most compaction due to pressure solution (means of 14.7 and 11.0% respectively) while the reef-flat and reef-margin subfacies had suffered the least (mean of 6.3%). Playford (1980) gave similar estimates and suggested that the amount of pressure solution compaction was inversely related to the amount of marine cement in the carbonates. Playford (1980) also suggested that the slightly dished shape of many carbonate platforms on the Lennard Shelf was due to preferential pressure solution compaction in the back-reef portions of the platforms.

Other pressure-solution features include intergranular pressure solution (overly close packing of grains), microstylolites and clay seams. Clay seams are common in the impure fine-grained lithologies of the stromatoporoid unit. Nodular structures are also common in these lithologies (Fig. 6F). The clay seams and nodular textures are believed to be due largely to pressure solution (see chapter 7).

Logan and Semeniuk (1976) presented a model involving dynamic metamorphism to explain the macro- and microstructure of the carbonates on the Lennard Shelf. In their dynamic metamorphic model, Logan and Semeniuk (1976) suggested that the major structures in the Napier Formation (bedding, breccias, allochthonous blocks) were not of sedimentary origin but were the result of intense

pressure solution and shear. They also suggested that the reef-margin lithologies were the result of intense deformation and were not of sedimentary origin. Logan (1984) further emphasized the importance of pressure solution and shear in the formation of the carbonates of the Lennard Shelf.

Playford (1980, 1984) refuted the dynamic metamorphic model citing the following observations:

1) The structures of the Napier Formation and the reef-margin unit of the Pillara Limestone are sedimentary features which have been *modified* by pressure solution. They are not the *result* of pressure solution.

2) Geothermal studies on the carbonates of the Lennard Shelf (vitrinite reflectance and conodont colour alteration) do not support the metamorphic model (greenschist facies) of Logan and Semeniuk (1976).

Kerans (1985) concluded that most of the features documented by Logan and Semeniuk (1976) were of synsedimentary or early burial origin.

A significant proportion of Logan and Semeniuk's field evidence was based in the Geikie Gorge area and many of the outcrops illustrated by them were examined in this study. All of the outcrop structures examined in this study (which Logan and Semeniuk (1976) illustrated and attributed to a metamorphic origin) were found to be of early diagenetic or sedimentary origin. The following are examples:

1) Stromatactid vugs illustrated by Logan and Semeniuk (Fig. 52A of Logan and Semeniuk, 1976) are not metamorphic strain cavities. They are stromatactis cavities filled by fibrous marine cements and internal sediments (this study, chapter 4).

2) The vein structure illustrated by Logan and Semeniuk (Fig. 47A of Logan and Semeniuk, 1976) is not of metamorphic origin. It is a neptunian fracture filled by marine fibrous cements and internal sediments. It is likely that synsedimentary faulting produced the neptunian fracture.

3) Megabreccias illustrated by Logan and Semeniuk (Figs. 78A, B of Logan and Semeniuk, 1976) are not metamorphic shear breccias. They are sedimentary mass-flow deposits.

In summary, the structural-metamorphic hypothesis of Logan and Semeniuk (1976) is not consistent with the observed field or microstructural relationships in the carbonates.

Cenozoic Cave Precipitates

Dendritic encrustations commonly line the surfaces of large dissolution cavity systems and caves in the Geikie Gorge region (Fig. 29E, F). The encrustations consist of branching club-shaped columns (up to 1 cm diam.). Red clayey micritic sediments with quartz silt commonly lie between the columns and this may be carbonate cemented wind-blown material. Individual columns consist of micrite and have a laminated micro-fenestral fabric (Fig. 30F). Three samples of the encrustations were isotopically analyzed and these had $\delta^{18}\text{O}$ values ranging from -0.5 to 0 ‰ (PDB) and $\delta^{13}\text{C}$ values ranging from -2 to $\bar{-7}$ ‰ (PDB). The high $\delta^{18}\text{O}$ values of the dendritic encrustations are presumably due to non-equilibrium calcite precipitation. The dominant process in the development of the encrustations is probably evaporation.

Speleothem calcites from caves in the area also have oxygen isotopic compositions $\{\delta^{18}\text{O} = -6.5 \text{ to } -7.5 \text{ ‰ (PDB)}\}$ which are similar to the estimated modern meteoric calcite composition (Fig. 30, discussed below).

Karstification

The limestone ranges in the Geikie Gorge region have suffered extensive karstification (Fig. 29D). A near-planar surface bounds the top of the limestone ranges and this is interpreted to be the exhumed Late Carboniferous-Early Permian erosion surface (Playford and Lowry, 1966; Hurley, 1986). Depressions in the limestone ranges occasionally have Grant Group sandstones within them, suggesting that the depressions are karst features which developed during Late Carboniferous-Early Permian subaerial exposure. Hurley (1986) documented similar features from the Oscar Range.

The near-planar surface at the top of the limestone ranges is deeply dissected and strongly karstified (Fig. 29D). Joints are commonly enlarged to form clefts and chasms. Steep-sided pinnacles and ridges are commonly developed in the platform lithologies. Many of the exposed limestone surfaces have well-developed rillenkarren. These features appear to have developed during Cenozoic subaerial exposure.

Figure 29. Cenozoic diagenetic fabrics.

A) Vertical exposure of a dolomitized *Amphipora* floatstone. The lithology has been dedolomitized along fractures and joints (dolomite = DO, dedolomite = DE). Back-reef subfacies, stromatoporoid unit, Pillara Limestone, northern Geikie Gorge. Scale bar = 10 cm.

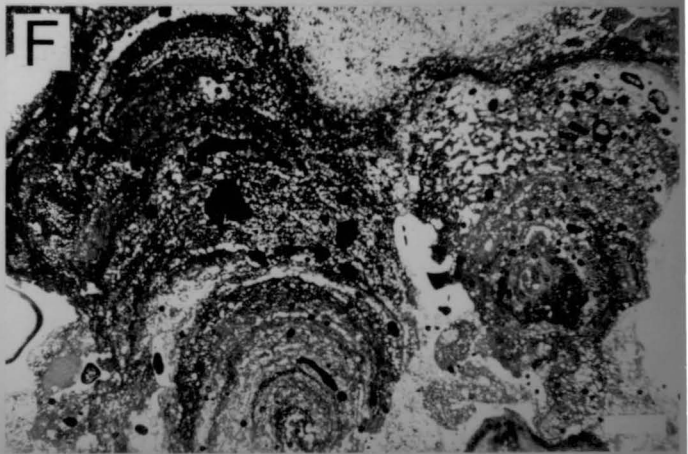
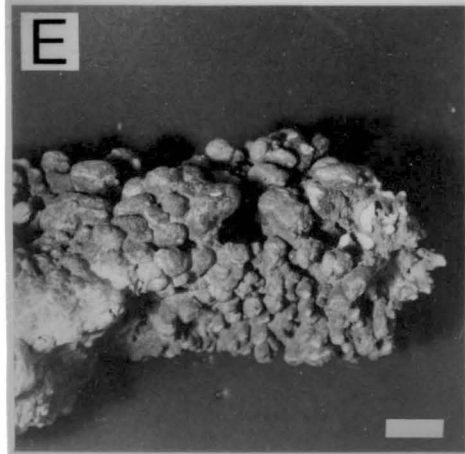
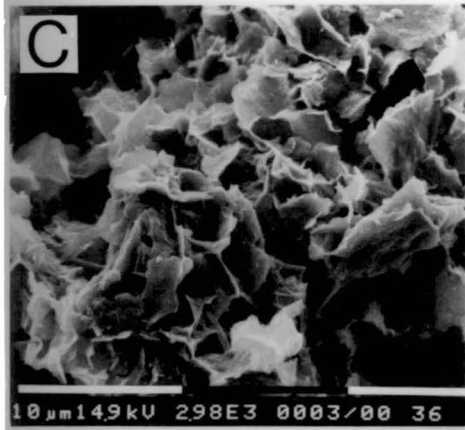
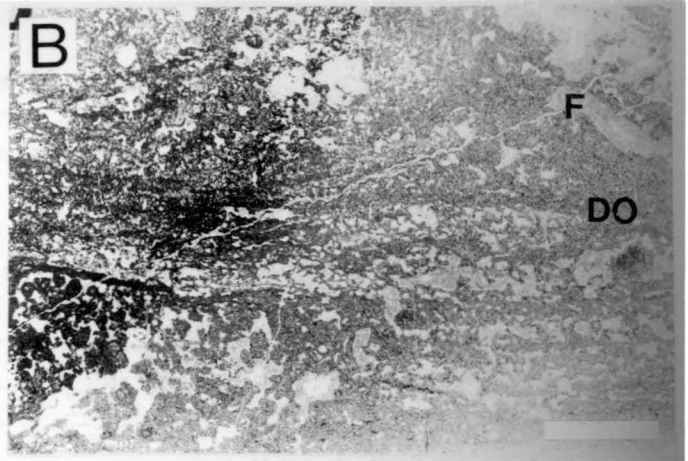
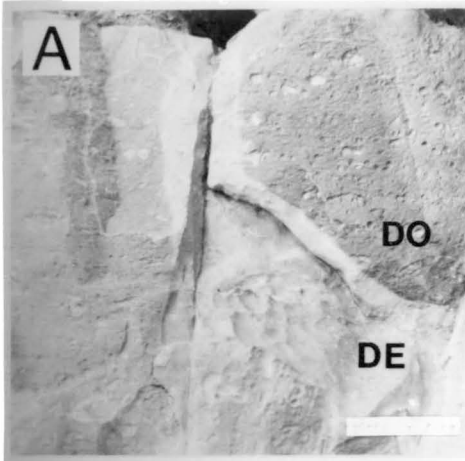
B) Thin-section photomicrograph of a partially dolomitized (dolomite = DO) fenestral peloidal grainstone. The micrite was preferentially dolomitized, leaving the inclusion-rich fibrous calcite cements undolomitized (F). In the upper left corner, the dolomite has been calcitized (darker material is dedolomite). Note that the sparry calcite within the fenestrae in the dedolomitized portion of the thin-section is inclusion-free. Reef-flat subfacies, stromatoporoid unit, Pillara Limestone, northern Geikie Gorge. Scale bar = 1 cm. UTGD sample no. 70295

C) Scanning electron micrograph of an oxide mass within a dedolomitized lithology. The oxide has a platy character. Back-reef subfacies, stromatoporoid unit, Pillara Limestone, northern Geikie Gorge. Scale bar is in 10 μm intervals. UTGD sample no. 70281

D) Upper surface of a limestone range in the western Copley Valley. The approximately planar nature of the upper surface is believed to be the result of Permian-Carboniferous subaerial exposure. The superimposed dissection and karstification is probably a result of Cenozoic subaerial exposure.

E) A dendritic encrustation from a cave in the region. Western Copley Valley. Scale bar = 1 cm. UTGD sample no. 70315

F) Thin-section photomicrograph of a dendritic cave encrustation. Individual columns have a fenestral fabric. Western Copley Valley. Scale bar = 1 mm. UTGD sample no. 70314



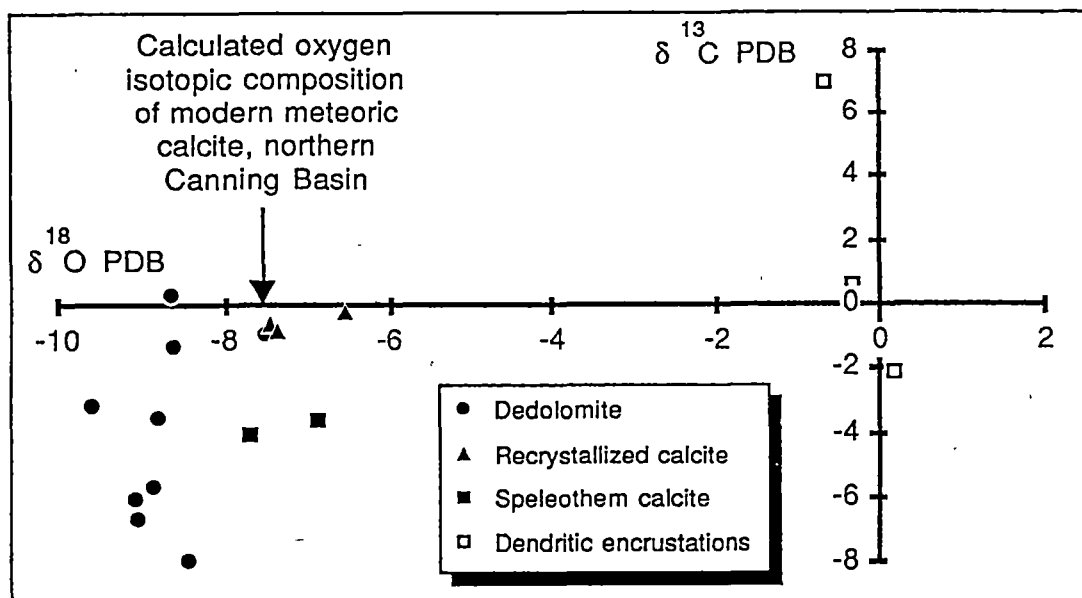


Figure 30. Carbon and oxygen isotope analyses for dedolomite, recrystallized calcite, speleothem calcite and dendritic cave encrustations.

Dedolomitization and Associated Calcite Recrystallization

Dedolomitization

Calcitized dolomite is common in alteration zones around joints, stylolites and large dissolution cavities within both completely and partially dolomitized lithologies (Fig. 29A, B). The alteration zones around these features may be up to 20 cm thick. Within the alteration zones, dolomite rhombs are replaced (or partially replaced) by low-magnesium calcite microspar and micrite (microprobe and X.R.D. analysis).

Dedolomitization began around the edges of dolomite rhombs, producing dolomite crystals with embayed and irregular margins (Fig. 26F). The process continued until the entire dolomite crystal was replaced by finely crystalline low-magnesium calcite (Figs. 26G, H). Dolomite crystals surrounded by calcite spar were replaced by sparry low-magnesium calcite. This resulted in the partial regeneration of the pre-dolomitization fabric during dedolomitization as suggested by Evamy (1967). All of the calcitized dolomite is non-luminescent and non-ferroan (Fig. 26F, G, H).

Dedolomitized lithologies commonly have a peloidal texture (Fig. 26G) and this appears to be a product of dedolomitization. Calcitized dolomite commonly has a coarser crystal size than depositional micrite and scattered calcitized dolomite crystals in a micrite matrix gives a peloidal appearance to the lithology.

Dedolomitized lithologies often contain minute (<50 μm), finely disseminated dendritic opaque minerals (Fig. 26G). The dendritic accumulations contain dominantly manganese with significant amounts of titanium, and are presumably hydrated oxides. Microprobe analyses indicate areas rich in Mn, Fe, Ti, and S, suggesting the presence of sulphate phases. The dendritic masses have a poorly developed platy character (Fig. 30C), but this may be due to intergranular growth, rather than a true crystallographic form. In hand specimen, dedolomitized lithologies have a pink-red colouration and this is presumably due to very finely dispersed iron oxides.

Calcitized dolomites have a relatively narrow range of $\delta^{18}\text{O}$ values, with $\delta^{18}\text{O}$ ranging from -7.5 to -9.5 ‰ (PDB) (Fig. 30). The carbon isotopic composition of calcitized dolomites is quite variable with $\delta^{13}\text{C}$ ranging from 0 to -8 ‰ (PDB) (Fig. 30 31).

Calcite Recrystallization

Depositional components, marine cements, and equant cements have been strongly recrystallized in the alteration zones surrounding joints, stylolites and dissolution cavities (Fig. 30B). The intensity of recrystallization increases towards the centre of the alteration zone (i.e. moving closer to the joint, stylolite etc.). The crystal size of the recrystallized carbonates is greater than that in the unaltered carbonates. Where recrystallization was the least intense, finely crystalline carbonates were converted to microspar. Finely crystalline carbonates were converted to pseudospar (with a crystal size up to 3 mm) (Bathurst, 1975) where recrystallization was most intense. Fibrous marine and equant calcite cements were recrystallized to a clear poikilitic calcite. Calcite which has suffered intense recrystallization is invariably non-luminescent and non-ferroan (Figs. 31I, J). Dendritic manganese-titanium oxides (similar to those found in calcitized dolomites) are disseminated throughout recrystallized calcites. Recrystallized calcites also have a pink colouration, indicating the presence of finely dispersed iron oxides.

Figure 31 illustrates the various stages of recrystallization in fibrous marine cements. From least to most recrystallized, these stages are as follows:

- 1) In the earliest stages of recrystallization (Figure 31A & B), portions of the radiaxial fibrous calcite become inclusion-poor and slightly more coarsely crystalline than the unaltered radiaxial fibrous calcite. Under cathodoluminescence, the recrystallized portion of the calcite has an overall dull luminescence (in contrast to the almost non-luminescent unaltered radiaxial fibrous calcite). When examined in detail, the recrystallized portion of calcite has a complex luminescence pattern consisting of needle shaped non-luminescent centres surrounded by dull-luminescent calcite.
- 2) All of the radiaxial fibrous calcite has become inclusion-poor and more coarsely crystalline (Figure 31C & D). The columnar crystal mosaic of the original radiaxial fibrous calcite has become less distinct and grades into an equant mosaic. Under cathodoluminescence, the recrystallized calcite displays the same complex pattern described above but with a coarser zonation.
- 3) The neomorphic calcite has a clear equant fabric (Figure 31E & F). Under cathodoluminescence, the neomorphic calcite has well defined concentric euhedral zonations which nucleate from centres within the calcite.
- 4) The neomorphic calcite has a coarse clear equant mosaic (Figure 31G & H). Under cathodoluminescence, the calcite has well developed euhedral zonations which nucleate from the edges of the spar. The zonation consists of an early bright-banded zone which grades into a non-luminescent zone.
- 5) The neomorphic calcite has a clear poikilitic fabric and is almost entirely non-luminescent (Figure 31I & J).

Figure 31. Sequence of paired plain light and cathodoluminescence photomicrographs illustrating the recrystallization of radiaxial fibrous calcite. The sequence begins with the least-altered spars (Figs. A and B) and concludes with the most altered spars (Figs. I and J). All photomicrographs are from a partially dolomitized fenestral peloidal grainstone of the reef-flat subfacies, stromatoporoid unit, Pillara Limestone, northern Geikie Gorge. UTGD sample no. 70295

A) A fenestral cavity filled by inclusion-rich radiaxial fibrous marine calcite (F) and clear equant calcite (E) (plain light). The radiaxial fibrous calcite has suffered minor recrystallization in the upper left corner of the cavity (arrows). The recrystallized area is relatively inclusion-free. Scale bar = 1 mm.

B) Same area in A under cathodoluminescence. The radiaxial fibrous calcite has a blotchy very dull luminescence. The recrystallized radiaxial fibrous calcite (arrows) consists of numerous minute (<20 μm) nucleation centres which have a non-luminescent core and a bright-luminescent rim.

C) A radiaxial fibrous calcite-filled fenestral cavity in which recrystallization is further advanced (plain light). The recrystallized spar is relatively inclusion-free and has a coarser crystal size than the primary radiaxial calcite. The radial crystal arrangement is only partially preserved. The fenestral cavity is surrounded by dolomitized micrite (RD). Scale bar = 1 mm.

D) Same area in C under cathodoluminescence. The recrystallized spar consists of numerous non-luminescent nucleation centres. Each nucleation centre is surrounded by dull-luminescent calcite.

E) A fenestral pore filled by strongly recrystallized radiaxial calcite (plain light). The spar is inclusion-free and coarsely crystalline. The radial crystal arrangement has been totally destroyed. The spar is surrounded by dedolomite (DE). Scale bar = 100 μm .

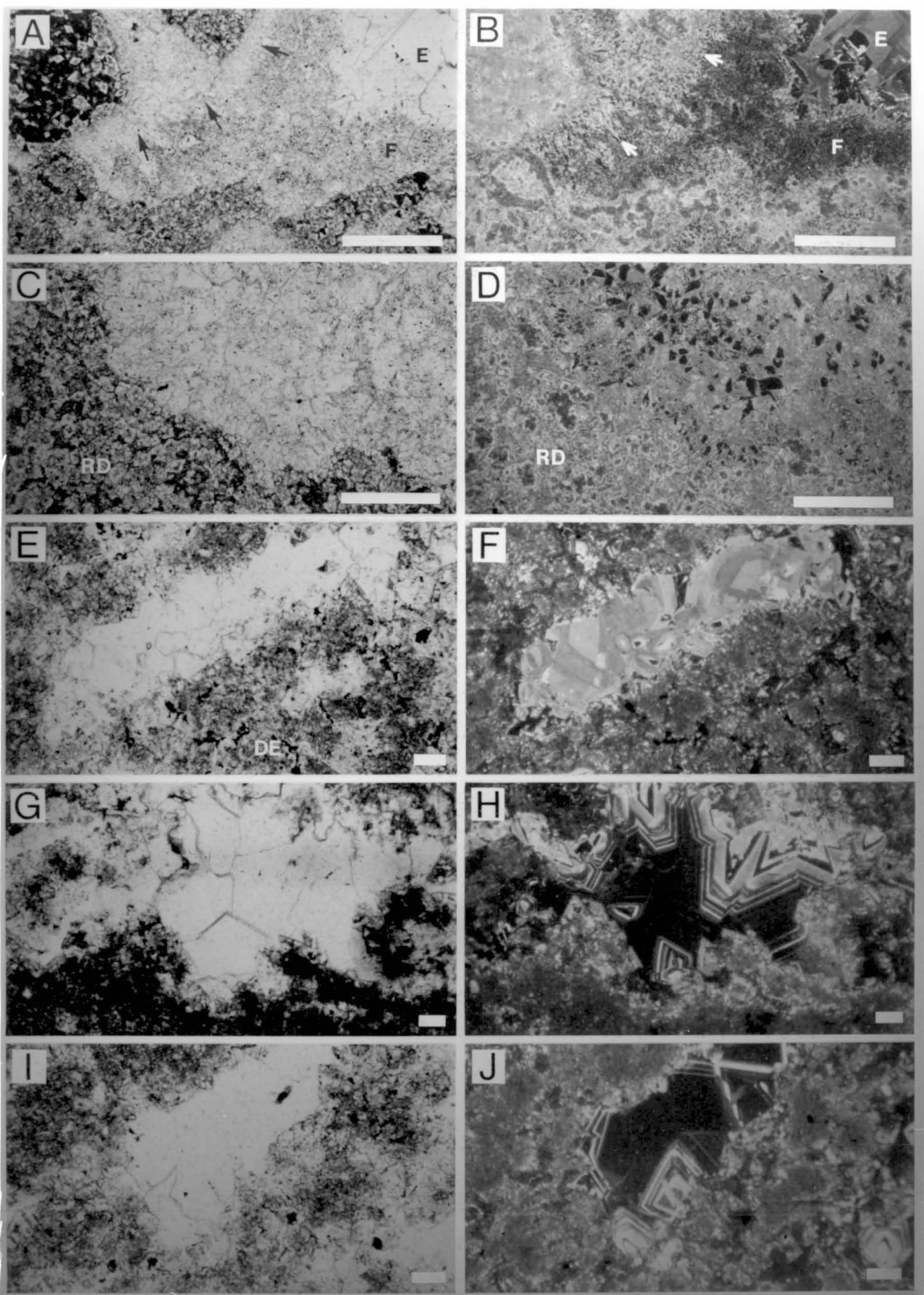
F) Same area in E under cathodoluminescence. The recrystallized spar has a series of large nucleation centres with zoned bright and dull luminescence. The nucleation centres appear to nucleate from the walls of the cavity and from within the spar. However those nucleation centres within the spar may nucleate from cavity walls outside the plane of the thin-section. Comparing the plain light (Fig. E) and cathodoluminescence views, it is observed that each nucleation centre corresponds to a single crystal. The crystal boundaries are the result of competitive growth, as is the case in cements.

G) A fenestral pore filled by strongly recrystallized calcite (plain light). The spar is inclusion-free and has a coarse equant character. Scale bar = 100 μm .

H) Same area in G under cathodoluminescence. The recrystallized spar consists of nucleation centres which largely nucleate from the walls of the cavity. The nucleation centres have strongly zoned bright and non-luminescence. The cathodoluminescence zonation could be mistaken for a cementation sequence. Comparing the plain light (Fig. G) and cathodoluminescence views, it can again be seen that the crystal boundaries are the result of competitive crystal growth, as is the case in cement spars.

I) A fenestral pore filled by strongly recrystallized calcite (plain light). The spar has an inclusion-free poikilitic character. Scale bar = 100 μm .

J) Same area in I under cathodoluminescence. The spar is largely non-luminescent with thin bright-luminescent bands. Nucleation centres grow from the walls of the spar.



Three isotopic analyses of recrystallized calcite were performed and $\delta^{18}\text{O}$ values ranged from -6.5 to -7.5 ‰ (PDB) and $\delta^{13}\text{C}$ values ranged from -0.25 to -0.75 ‰ (PDB) (Fig. 30).

Timing and Origin of Dedolomitization and Calcite Recrystallization

Dedolomites and recrystallized calcites occur in alteration zones which surround joints, stylolites and large dissolution cavities. The joints and cavities are not lined by any cements and appear to have been subject to dissolution. These features suggest that the dissolution and the alteration zones are a product of Cenozoic meteoric diagenesis.

The non-luminescent nature of the dedolomite and the most recrystallized calcite is consistent with the interpreted near-surface meteoric origin. Oxidizing conditions would be expected in such diagenetic environments and the trace elements responsible for cathodoluminescence (dominantly manganese, Pierson, 1981; Fairchild, 1983; Machel, 1985) could not be incorporated into the carbonates (Frank *et al.*, 1982; Machel, 1985). Non-luminescent calcite is a common precipitate in near-surface meteoric environments (e.g. Meyers, 1978; Solomon and Walkden, 1985).

The presence of dispersed ferro-manganese oxides within the dedolomite and recrystallized calcite also suggests an oxidizing diagenetic environment. Iron oxides are almost invariably associated with near-surface meteoric alteration in carbonates (Folkman, 1969; Chafetz, 1972; Al-Hashimi and Hemingway, 1973; Abbott, 1974; Frank, 1981). Evamy (1963) suggested that dolomite often contained iron in excess of the amount required to saturate the calcite lattice and that the excess iron would be precipitated as colloidal ferric hydroxides. Mirsal and Zankl (1985) suggested that the presence of iron oxides in association with calcitized dolomites may be related to the action of chelated iron catalysts.

The isotopic signature for the dedolomites is consistent with a near-surface meteoric origin, with low $\delta^{13}\text{C}$ values and relatively constant $\delta^{18}\text{O}$ values (Allan and Matthews, 1982; James and Choquette, 1984; Meyers and Lohmann, 1985). Recrystallized calcites have similar $\delta^{18}\text{O}$ values and low $\delta^{13}\text{C}$ values.

The estimated $\delta^{18}\text{O}$ value for calcite in equilibrium with modern rainwater in the northern Canning Basin region is -7.6 ‰ (PDB) (Fig. 30). This estimate is based on a long term projected oxygen isotopic composition for modern rainfall of $\delta^{18}\text{O} = -5.2$ ‰ (SMOW) (Hughes and Allison, 1984) and a mean annual temperature of 27°C at Fitzroy Crossing (Bureau of Meteorology, 1975) using Friedman and O'Neil's (1977) calcite-water fractionation equation. It is commonly found that the vadose rock temperature is approximately equal to the mean annual temperature in the region (Goede *et al.*, 1982). Therefore, the mean annual temperature is probably a reasonable estimate for the temperature at which most near-surface meteoric reactions occur today.

Dedolomite and recrystallized calcite have $\delta^{18}\text{O}$ values $\{\delta^{18}\text{O} = -7.5$ to -9.5 ‰ (PDB) $\}$ which are similar to the $\delta^{18}\text{O}$ value estimated for modern meteoric calcite and observed values for speleothem calcite. This observation is consistent with a Cenozoic origin for the calcitized dolomite and recrystallized calcite. The slightly different ranges

could easily be accounted for by varying temperatures and rainfall compositions during the Cenozoic.

Hurley (1986) found that carbonates associated with the Late Carboniferous - Early Permian period of meteoric exposure in the Oscar Range had $\delta^{18}\text{O}$ values -7.0 to -9.0 ‰ (PDB). These values are remarkably similar to those for the Cenozoic period of meteoric exposure. The Canning Basin is thought to have been in a cool, high-latitude setting during Late Carboniferous-Early Permian times (Embleton, 1984; Towner and Gibson, 1983). High-latitude meteoric waters generally have low $\delta^{18}\text{O}$ values and it appears unusual that Permo-Carboniferous high-latitude meteoric carbonates should have identical $\delta^{18}\text{O}$ values to Cenozoic low-latitude carbonates.

The majority of dedolomites in the geological record have been assigned to a near-surface meteoric origin. However, a few occurrences of dedolomite have been shown to be of burial origin (Land and Prezbindowski, 1981; Budai *et al.*, 1984). A burial origin for the dedolomites from the Geikie Gorge region can be ruled out on the basis of: 1) the non-luminescent non-ferroan and apparently oxidized nature of the dedolomite; 2) the association with large dissolution cavities and other conduits for near-surface meteoric waters; and 3) the low $\delta^{13}\text{C}$ values and uniform $\delta^{18}\text{O}$ values of the dedolomites which indicate a substantial contribution from biogenic soil carbon. These features are more consistent with a Cenozoic near-surface meteoric origin.

Calcite Recrystallization versus Cementation

There has been considerable debate in the geological literature concerning the origin of calcite spars in limestones. The two major hypotheses for the formation of spar are: 1) Precipitation of calcite into an open pore (cementation); and 2) neomorphism of a precursor material without the formation of mouldic porosity. Bathurst (1975) presented a number of fabric criteria to distinguish between neomorphic spars and cements. Two of the most important criteria suggested for distinguishing cements were 1) a high proportion of plain intercrystalline boundaries; and 2) a high percentage of enfacial junctions among the triple junctions (Bathurst, 1975). In contrast, neomorphic spar was suggested to be characterized by irregular intercrystalline boundaries and a low proportion of enfacial junctions.

With the advent of cathodoluminescence petrography, the internal growth zonation characteristics of spar crystals could be determined. Using this technique, Dickson (1983) found that cements may have a high proportion of irregular intercrystalline boundaries (in thin-section) and low proportion of enfacial junctions. These observations led Dickson (1983) to suggest that the practice of using a list of textural criteria for the general recognition of all cements should be abandoned.

The morphology of cathodoluminescence zonations in calcite and dolomite spars is now commonly used to distinguish neomorphic spar from cavity-filling cement spar (e.g. Sippel and Glover, 1965; Meyers, 1974; Fairchild, 1980; James and Klappa, 1983; Tucker, 1983; Walkden and Berry, 1984). Zonations with a euhedral morphology which appear to have been produced by growth from the walls of a cavity are generally taken to indicate the spar is a cement. Where recrystallization fronts or nucleation centres are recognized, the spar is interpreted to be of neomorphic origin (Fairchild, 1980; Machel, 1985).

The recrystallization sequence described (Fig. 31) for fibrous cements from the Geikie Gorge region presents several problems in interpretation. In less recrystallized

spars, multiple closely-spaced nucleation centres are observed throughout the spar (under cathodoluminescence) (Fig. 31A - F) and the spar is clearly of neomorphic origin. However, spars which are interpreted to have undergone more intense recrystallization have luminescence zonations which nucleate from the margins of the spar (Fig. 31G - J). Taken in isolation, this luminescence zonation would be universally interpreted as a cementation sequence.

However, evidence indicating the luminescence zonations are of neomorphic origin and are not cements includes:

- 1) Luminescence zonations in altered spars are unlike the zonations in primary and secondary porosity in the surrounding lithologies.
- 2) Luminescence zonations in altered spars cannot be correlated from cavity to cavity. In fact, the zonations systematically change (over a distance of 3 to 4 cm) towards meteoric conduits. Towards the meteoric conduit, individual luminescence zonations contain a greater proportion of non-luminescent spar. Spars closest to the conduit are totally non-luminescent.
- 3) Systematic crystal size changes accompany the luminescence zonation changes towards meteoric conduits. All transitions can be observed from unaltered cement spars like radial fibrous calcite furthest from meteoric conduits, through to clear poikilitic spar closest to the conduits.
- 4) No remnant porosity was observed in transitions from unaltered cements to the most altered poikilitic spars.

Fairchild (1980) noted that dolomite replacements of calcite may be petrographically identical (plane light and cathodoluminescence petrography) to dolomite cements. This occurred where dolomite nucleation was restricted to the margins of the replaced calcite unit. This situation is exactly analogous to the calcite recrystallization process described here. In the later stages of sparry calcite recrystallization, nucleation tends to be restricted to the margins of the spar and this produces zonations which mimic cementation fabrics.

These observations suggest that neomorphic luminescence zonations may mimic cementation fabrics.

Synthesis of Post-Marine Diagenesis

Marine cements and depositional components are overlain by non-luminescent non-ferroan clear equant calcite cements in platform lithologies and coarse-grained marginal-slope lithologies. Non-luminescent calcite cements probably formed in a shallow-burial environment.

Replacement dolomite and dolomite cements were precipitated during and after non-luminescent calcite cementation. Pressure solution had already commenced and stylolites were commonly dolomitized. Dolomitization and dolomite cementation was widespread, but dolomitization was most extensive on the northern Geikie Gorge platform, where completely dolomitized lithologies are restricted to a narrow zone on the platform side of the reef-flat subfacies (Fig. 25). The distribution of dolomite on this platform was controlled by the permeability distribution at the time of dolomitization. Lithologies on the platform side of the dolomitized lithologies had probably already been cemented by non-luminescent calcite and the platform margin

lithologies had been marine cemented. Mouldic porosity developed during the later stages of dolomitization in the completely dolomitized lithologies.

Depositional components, marine cements, non-luminescent cements and dolomite cements were overgrown by brightly-luminescing calcite cements. The bright cements are overgrown by dull-luminescent ferroan-calcite cements which filled virtually all the remaining primary porosity in the reef complexes. The dull ferroan-calcite cements are interpreted to have formed in a deep-burial environment.

The cathodoluminescent cement sequence from non-luminescent to bright-luminescent to dull-luminescent is very common in carbonate sequence and is interpreted to represent a gradual decrease in the oxygen content of pore waters during progressive burial (Grover and Read, 1983; Machel, 1985). However, it appears probable that the cement transitions were partly diachronous (Grover and Read, 1983; Dorobek, 1987). In the general sequence of cementation from non-luminescent calcite to dolomite to bright calcite to dull calcite, there is a progressive trend towards lower $\delta^{18}\text{O}$ values (allowing for the dolomite to calcite fractionation factor) in later diagenetic phases while the $\delta^{13}\text{C}$ values remain the same (Fig. 24). This isotopic signature is best explained by increasing temperatures during progressive burial and is consistent with a connate marine burial diagenetic model (Kerans, 1985).

By Late Carboniferous time, virtually all of the primary porosity in the carbonates had been occluded by dull-luminescent calcite cements. Rare primary porosity was largely restricted to the marine cemented reef-margin subfacies and mouldic porosity was present in the completely dolomitized lithologies.

During Late Carboniferous - Early Permian times, the carbonates were exhumed and karstified. Rare banded-luminescent cements were precipitated in the remaining primary porosity in the reef-margin subfacies. Hurley (1986) found similar banded-luminescent cements in the Oscar Range reef complexes and these had a meteoric isotopic signature.

The carbonates were then deeply buried during post-Carboniferous time and dull-luminescent ferroan-calcite cements were precipitated in the rare remaining primary porosity, in large dissolution cavities beneath the Grant unconformity, and in mouldic porosity within the completely dolomitized lithologies. These cements have low $\delta^{18}\text{O}$ values and variable $\delta^{13}\text{C}$ values which may indicate high temperatures of precipitation and the incorporation of biogenic carbon due to organic reactions in the subsurface.

During the Cenozoic, the reef complexes were again exhumed and karstified. Dedolomitization and calcite recrystallization occurred along conduits for meteoric waters during this period. Strongly recrystallized calcite is non-ferroan and non-luminescent. Calcite cements were recrystallized to poikilitic non-luminescent neomorphic spar. The dedolomites and recrystallized calcites have relatively uniform $\delta^{18}\text{O}$ values and variably low $\delta^{13}\text{C}$ values consistent with a near-surface meteoric origin.

The carbonates have therefore suffered a long and complex diagenetic history. Visually, the most spectacular diagenetic phases are the marine cements of the platform margin lithologies. However, Devonian - Early Carboniferous burial diagenesis was the most important episode in the history of carbonates. Virtually all of the primary porosity was occluded and the major dolomitization event occurred during this period.

A summary diagram of the diagenetic history in the carbonates is presented in figure 32.

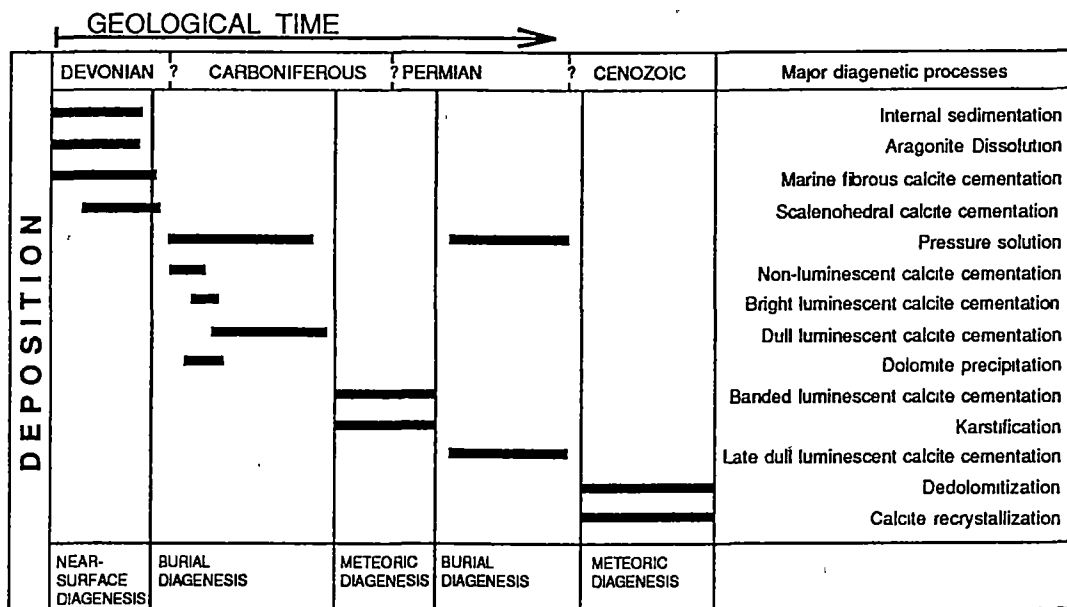


Figure 32. Summary diagram illustrating the interpreted paragenetic sequence and timing of the major diagenetic processes which occurred in the Devonian reef complexes of the Geikie Gorge region.

7. SEDIMENTOLOGY OF THE DEVONIAN CARBONATES ON THE BARBWIRE TERRACE

Introduction

A thick, areally extensive sequence of Upper Devonian carbonates occurs on the Barbwire Terrace, located on the southern margin of the Fitzroy Trough, in the Canning Basin (Fig. 1). The sequence is not exposed, but has been penetrated by a number of wells (Fig. 33). The carbonates are of Frasnian-Famennian age (Ashton, 1984) and are laterally equivalent to the Devonian reef complexes of the Lennard Shelf. Therefore, the Frasnian and Famennian portions of the sequence have been termed the Pillara Limestone and Nullara Limestone respectively (Fig. 34). The uppermost carbonates in the sequence are equivalent to the Fairfield Group. The Upper Devonian carbonates are unconformably overlain by the Upper Carboniferous - Lower Permian Grant Formation and extensive karstification has taken place up to 200 m below this unconformity (Fig. 34).

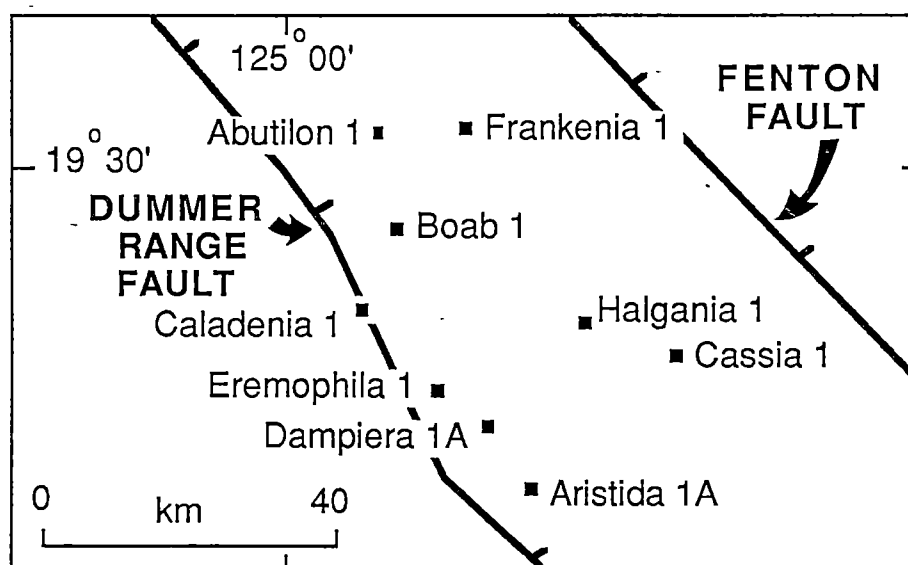


Figure 33. Well location map of the study area on the Barbwire Terrace (see Fig. 1 for location of study area).

Most of the Upper Devonian carbonates form an upward shallowing sequence in which the impure, deeper subtidal lithologies have remained as limestones and the more pure, peritidal lithologies have been very thoroughly dolomitized (Fig. 34). No true reefal carbonates (e.g. reef-margin framestone lithologies) have been recognized in the carbonates examined from the Barbwire Terrace. Most of the carbonate lithologies are either of peritidal or shallow-subtidal origin.

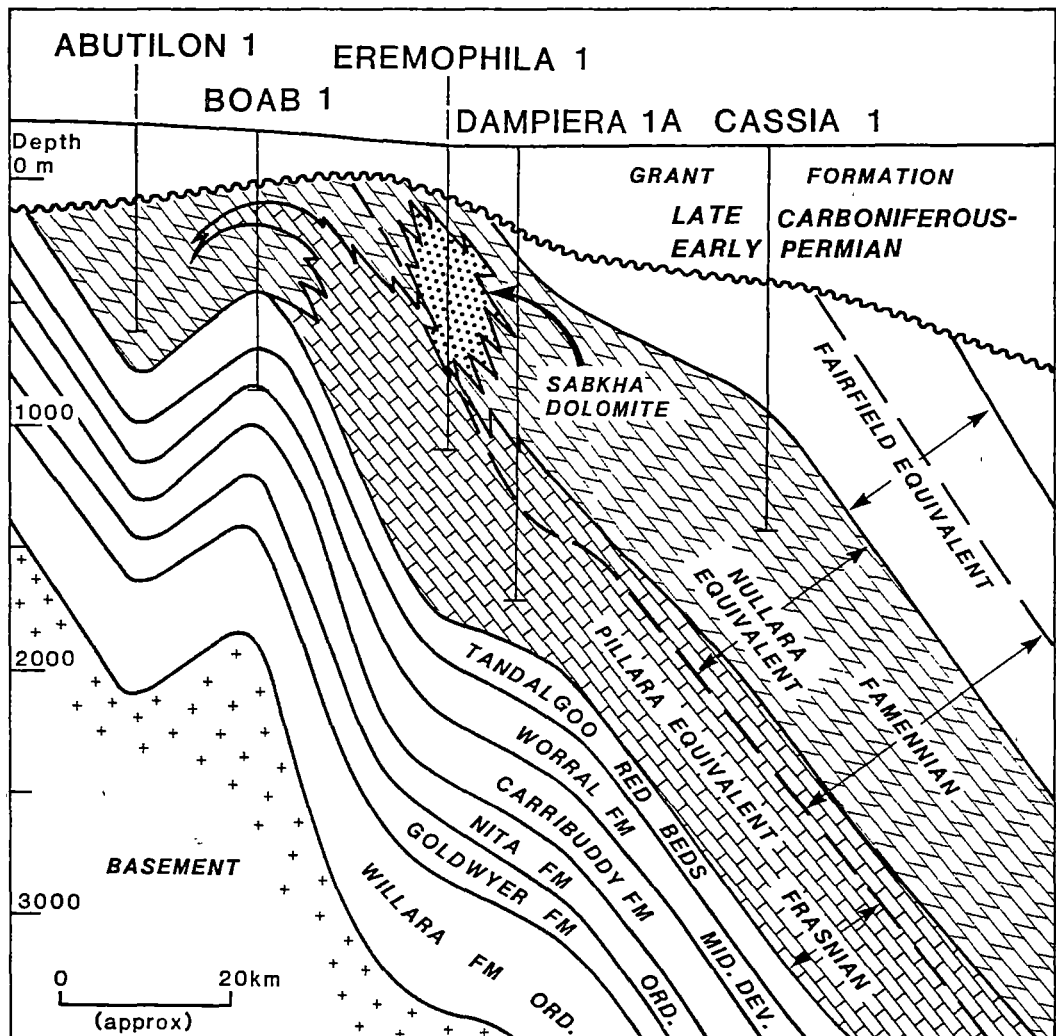


Figure 34. Diagrammatic section across the Barbwire Terrace illustrating the stratigraphy in the region and the distribution of dolomite in the Devonian carbonates. Devonian limestones have a brick pattern and regionally dolomitized lithologies have a slanted brick pattern.

The lithologies in the sequence are quite varied and in order to examine their environmental significance, the lithologies have been grouped into nine lithotopes (Fig. 35). Each of the lithotopes contains lithologies which are interpreted to have been deposited in several closely related depositional environments (e.g. the laminated dolomudstone lithotope most likely includes lithologies which represent supratidal levee deposits, supratidal pond deposits, and supratidal cryptalgal laminites).

Lithotope	Characteristics	Interpretation
A- Laminated dolomudstone *	Red-brown or light grey colour, mudcracks and nodular anhydrite occasionally present	Lower supratidal-upper intertidal
B- Clayey dolomudstone	Red-brown colour, no lamination, nodular anhydrite abundant	Upper supratidal, desert loess?
C- Fenestral dolomite *	Abundant laminoid or bubble fenestrae	Upper intertidal, cyanobacterial mat
D- Massive carbonate mudstone *	Unlaminated carbonate mudstone, burrow-mottled	Intertidal
E- Skeletal wackestone *	Normal marine skeletal components in a carbonate mudstone matrix	Normal marine, shallow subtidal
F- Skeletal grain-packstone	Grainstone with large, unbroken skeletal components and a partially infiltrated matrix	Subtidal mound
G- Laminated organic-rich lime mudstone	Finely laminated mudstones and organic-rich clays	Subtidal cryptalgal laminite, hypersaline?
H- Skeletal-lithoclast breccias	Matrix and grain-supported breccias, rotated geopetals and grading common	Allochthonous sediment gravity flows
I-Clayey lime mudstones and marls *	Impure lime mudstones, marls and calcareous shales, nodule and seam structure common	Low energy, normal marine subtidal

Figure 35. Summary of lithotope characteristics. Asterisks denote major lithotopes.

Five of these lithotopes are believed to be of peritidal and shallow subtidal origin. Virtually all of the peritidal and shallow subtidal lithologies have been completely replaced by coarsely crystalline dolomite. Regional dolomitization has destroyed much of the depositional microfabric in the carbonates (sometimes to the extent that it is impossible to determine the original grain size of the carbonate). Peritidal carbonates unaffected by regional dolomitization only occur in the well Eremophila #1 (Fig. 36) and this is probably due to the abundance of anhydrite in the supratidal carbonates of this well. It is likely that the anhydrite formed an effective seal against the pore waters causing regional dolomitization (discussed later). The following sedimentological analysis is therefore necessarily biased towards the carbonates which have suffered the least destructive diagenesis.

Supratidal Facies

Laminated Dolomudstone (Lithotope A)

Description; These carbonates consist of red, buff or light grey finely laminated impure carbonate mudstones which are invariably completely dolomitized (Figs. 37C, D, E). Laminae range from 0.1 to 5 mm in thickness. Lamination is defined by variations in the crystal size, the organic matter and clay content of the carbonate. The non-carbonate fraction of the lithology commonly constitutes up to 50% by weight. The carbonate crystal size ranges from 4 to 25 microns. Angular silt-size quartz grains are common and laminated dolomudstones occasionally grade into laminated dolomitic quartz siltstones. Normal grading is common within laminae (Fig. 37C).

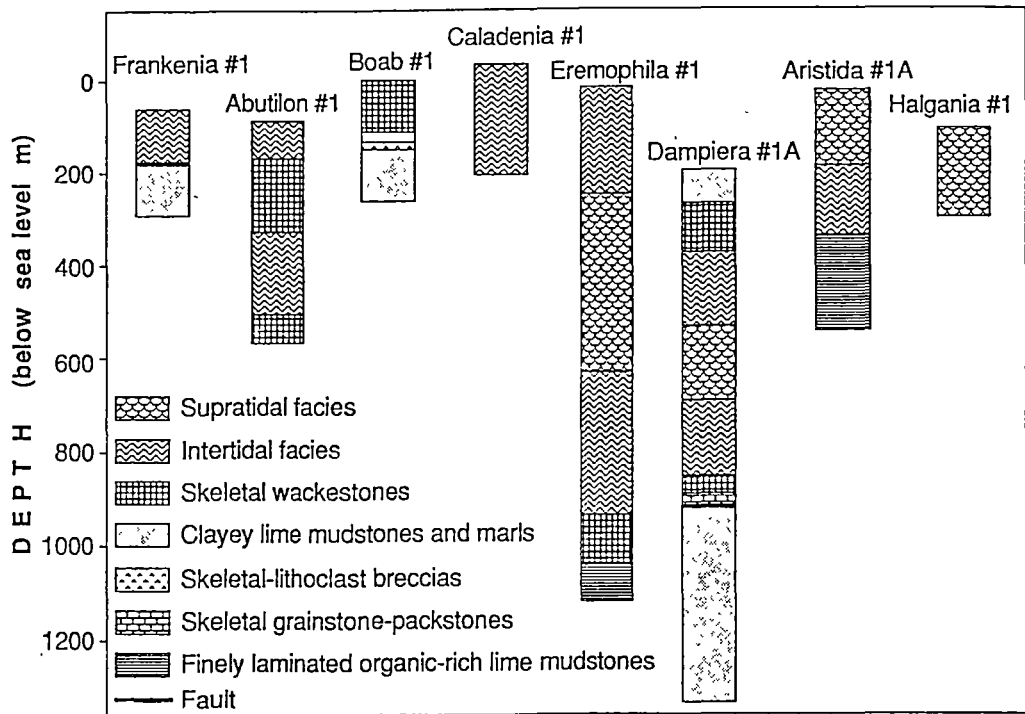


Figure 36. Distribution of the lithotypes in the Devonian carbonates. Because the peritidal lithotypes are generally interbedded on a scale of metres, the peritidal sections have been grouped into predominantly supratidal or intertidal facies. The horizontal distance between the wells is not to scale.

Nodular anhydrite is common at some localities (Eremophila #1, Fig. 37E) and displays a felted texture. Interlaminated dolomite and anhydrite occurs sporadically (Fig. 37D). Sulphate escape structures and other syndimentary deformation features are commonly found in association with nodular anhydrite (Fig. 37D) and mudcracks are also common.

Distribution; Laminated dolomudstones occur sporadically throughout the upper parts of the sequence but are most abundant within the well Eremophila #1 where they occur in association with abundant nodular anhydrite. Together with massive red dolomudstones (Lithotope B) laminated dolomudstones make up over 300 m of section in Eremophila #1 (Fig. 36).

Laminated dolomudstones commonly occur in association with fenestral dolostones and mottled mudstones. In sections of the well Eremophila #1, laminated dolomudstones are interbedded with poorly laminated lime mudstones (Lithotope D).

Figure 37. Supratidal and intertidal lithologies of the Devonian carbonates, Barbwire Terrace.

A) Cut core of unlaminated red clayey dolomudstone with early diagenetic anhydrite nodules (A). Eremophila #1, 611.16 m. Scale bar = 1 cm.

B) Thin-section photomicrograph of unlaminated red dolomudstone with numerous small anhydrite nodules. Eremophila #1, 513.13 m. Scale bar = 1 cm. UTGD sample no. 70321

C) Thin-section photomicrograph of laminated dolomudstone with well developed normally graded laminae. Note the fine crystal size of the dolomite. Dampiera #1A, 886.60 m. Scale bar = 1 mm. UTGD sample no. 70335

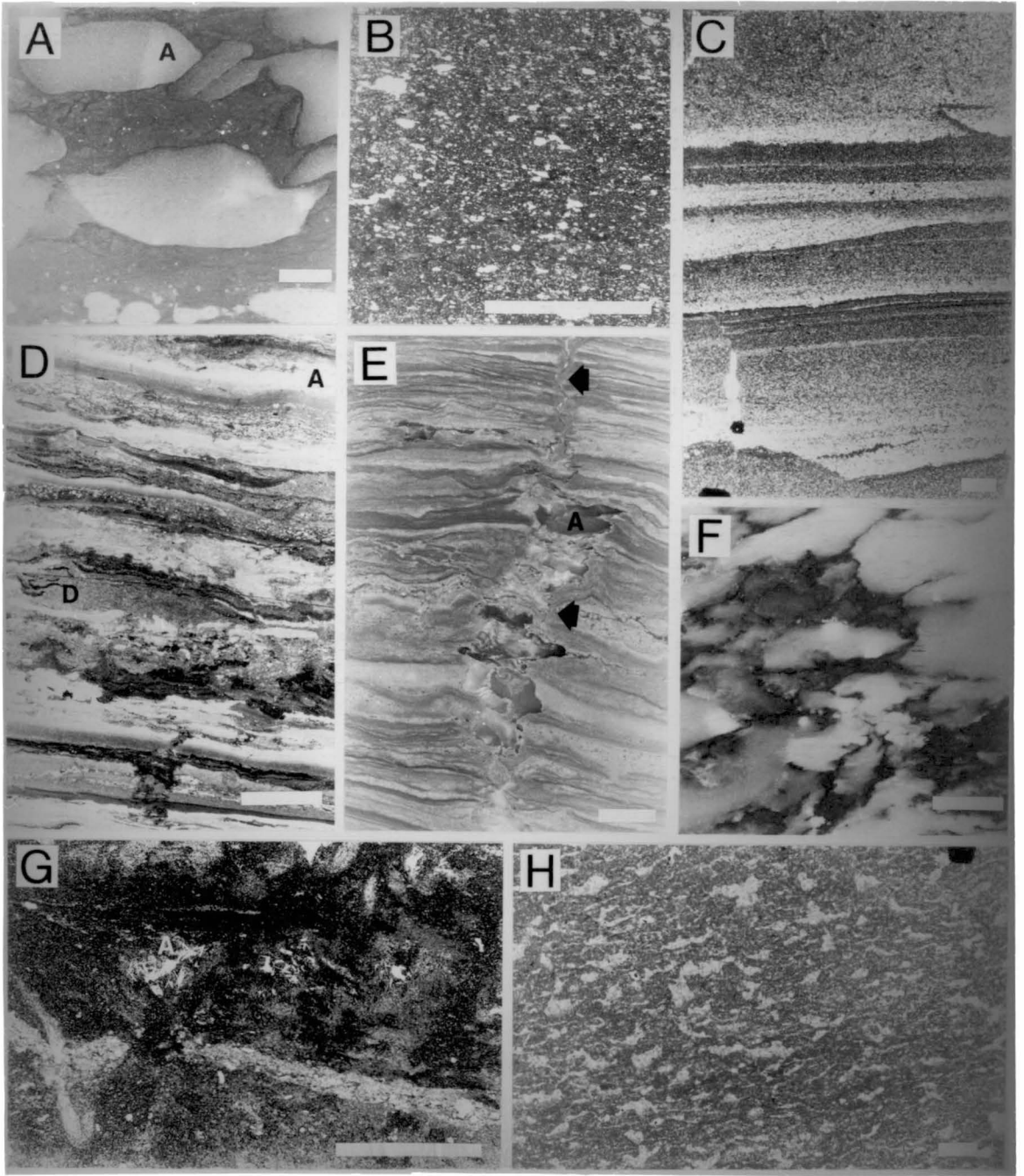
D) Thin-section photomicrograph of interlaminated dolomudstone (D) and anhydrite (A). Eremophila #1, 550.57 m. Scale bar = 1 cm. UTGD sample no. 70322

E) Cut core of laminated dolomudstone with an anhydrite escape structure (arrows). Anhydrite (A) is present along this structure. Eremophila #1, 732.87 m. Scale bar = 1 cm. UTGD sample no. 70323

F) Cut core of chicken wire anhydrite. Eremophila #1, 492.78 m. Scale bar = 1 cm. UTGD sample no. 70320

G) Thin-section photomicrograph of burrow-mottled dolomudstone with anhydrite (A). Eremophila #1, 864.90 m. Scale bar = 1 cm. UTGD sample no. 70326

H) Thin-section photomicrograph of fenestral dolomite. Both laminoid and irregular fenestrae are present and are filled by dolomite spar. Dampiera #1A, 493.94 m. Scale bar = 1 mm. UTGD sample no. 70332



Interpretation; These carbonates are believed to have developed on arid supratidal and upper intertidal flats on the basis of: a) the presence of lamination; b) the presence of mud cracks; c) the presence of nodular and laminated anhydrite; d) the oxidized nature of the carbonates (their red or light grey colouration); and e) the absence of skeletal constituents.

The abundance of nodular anhydrite indicates an arid climate, enabling the development of hypersaline pore waters below the sediment-water interface. The presence of laminated anhydrite suggests direct precipitation and deposition of sulphates from a hypersaline water body (Lucia, 1972). These conditions commonly develop in partly restricted supratidal ponds.

The normal grading within laminated dolomudstones may be due to episodic influx of sediment during storm or spring tidal flooding on the flats. Similar lithologies are found in modern tidal-channel levee sediments (Shinn, 1983b). The silt-size quartz grains and dolomitic quartzose siltstones commonly associated with the laminated dolomudstones may be aeolian in origin.

Laminated carbonate mudstones have commonly been interpreted as cryptalgal laminites (Aitken, 1967). In this case, definite evidence for a cyanobacterial influence is lacking. However, it appears likely that some of the lamination may be due to colonization of the sediment surface by cyanobacterial mats.

Clayey Dolomudstone with Anhydrite (Lithotope B)

Description; This lithotope consists of unlaminated red clayey dolomite with abundant anhydrite nodules (Fig. 37A). Anhydrite nodules vary in size from microscopic aggregates to masses up to 2 cm in diameter. Occasionally, the anhydrite nodules coalesce to form the commonly observed "chicken-wire anhydrite" texture (Fig. 37F). Many smaller anhydrite aggregates (around 2 mm in diameter) have a lath-shaped outline and these may represent anhydrite replacement of single gypsum crystals (Fig. 37B). The lithotope lacks bedding or lamination.

Distribution; Massive dolomudstones with anhydrite are restricted to the upper section of the well Eremophila #1 where they generally occur as thin beds (several centimetres) and are interbedded with the laminated dolomudstone lithotope (Fig. 36).

Interpretation; This lithotope appears to have been deposited in the upper-supratidal zone of an arid tidal flat environment. This is suggested by a) the intimate association with laminated dolomudstones; b) the abundance of nodular anhydrite; c) the absence of skeletal components; and d) the oxidized nature of the sediment (red colouration).

The morphology of the larger anhydrite nodules in this lithotope (and in lithotope A) is very similar to that of the sulphate nodules found in many modern sabkhas (Shearman, 1966; Butler, 1969; Ali and West, 1983). The original mineralogy of sulphate nodules in ancient sabkha deposits has been much debated in the geological literature as both gypsum and anhydrite nodules occur in modern sabkhas (Ali and West, 1983). Indeed the question of whether any of the modern anhydrite nodules of the Trucial Coast were originally precipitated as anhydrite has not been fully resolved (Butler, 1969; Bush, 1973). In addition, the effects of burial probably make the

distinction between primary and secondary anhydrite nodules impossible. The development of diagenetic evaporite minerals in sabkha environments is generally explained by the upward movement of brines (by capillarity) and surface evaporation (Ali and West, 1983).

The absence of lamination in this lithotope would appear to argue against a supratidal origin (Shinn, 1983b). However, this lithotope has been illustrated by a number of researchers (Lucia, 1972, Fig. 7; Lowenstein, 1987, Fig. 7) and is generally associated with supratidal lithologies. Ali and West (1983) have described gypsiferous deposits from northern Egypt which have many similarities with lithotope B. The material is apparently unlaminated, contains nodular gypsum and consists of a mixture of silt-size argillaceous material and carbonate. Ali and West (1983) suggest the deposit is a "desert loess" (Whalley *et al.*, 1982) of aeolian origin.

Unlaminated clayey aeolian deposits occur as lunettes around playa lakes in north-western Victoria (Stephens and Crocker, 1946). Macumber (1970) has suggested that the lunettes developed when the lakes were dry and salts are precipitated at the surface. This broke up the clays into aggregates which were transported by saltation. It appears likely that similar aeolian processes occurred in many ancient arid sabkha settings. The clayey dolomudstones are therefore tentatively interpreted as an aeolian deposit, similar to the "desert loess" described by Ali and West (1983). Development of vegetation with consequent rhizoid disruption and incipient soil formation would also be expected in such a setting.

Fenestral Dolomite (Lithotope C)

Description; Laminoid, irregular and bubble-like fenestral fabrics (Grover and Read, 1978) are common in these carbonates (Fig. 37H). The lithotope is always completely replaced by coarsely crystalline (>20 microns) dolomite and the host sediment textures are poorly preserved. Host sediments generally appear to have been deposited as carbonate mudstones but it is likely that minor grainstone and packstone lithologies were also present. Regional dolomitization makes positive identification of the host sediment fabrics difficult.

Distribution; Fenestral dolomites occur sporadically in the upper parts of the sequence and occur in association with the laminated and poorly laminated dolomite lithotopes. No fenestral dolomites were found in association with anhydrite.

Interpretation; Fenestral or bird's-eye structures have been considered reliable indicators of supratidal and upper-intertidal deposition. However, Playford *et al.* (1976) have demonstrated that fenestral fabrics can also occur in shallow-subtidal environments. In the Devonian reef complexes of the Lennard Shelf, fenestral stromatolites and bindstones occur in the reef-flat and reef-margin subfacies (Kerans, 1985). Shinn (1983a) has also documented the presence of fenestral fabrics within subtidal carbonates. Shinn (1983a) suggested that early lithification plays an important role in preserving fenestral cavities and that fenestral cavities are most commonly preserved in supratidal conditions because of early lithification, while fenestral fabrics formed in subtidal environments are generally destroyed during compaction.

In the Barbwire Terrace sequence, it appears unlikely that there was extensive subtidal marine cementation (because of the low energy nature of the sequence) and the fenestral fabrics were most likely developed in supratidal or upper-intertidal conditions.

Intertidal Facies

Massive and Poorly Laminated Carbonate Mudstones (Lithotope D)

Description; Massive and poorly laminated buff and grey coloured dolostones are particularly common in all wells and there is generally little non-carbonate material in the lithotope. The dolomite is usually coarsely crystalline (>20 microns) and textural preservation is commonly poor. The lithotope appears to have been deposited mainly as carbonate mudstones but some fine packstones and grainstones may have been present. Fracturing and brecciation is very common. Where lamination is present, it is defined by variations in crystal size and non-carbonate content. Skeletal components are absent.

In the well Eremophila #1, this lithotope is not affected by regional dolomitization and the fabrics are well preserved. Here the lithotope often has a mottled texture and burrow structures are common (Fig. 37G). In addition, the lithotope commonly grades into laminated dolomudstones through a burrowed partially laminated intermediate lithology. In Eremophila #1, the lithotope commonly has small (<3 mm) nodules and individual lath-shaped crystals of anhydrite.

Distribution; Massive and poorly laminated dolostones are present in the upper sections of almost all wells examined (Fig. 36). The lithotope is unaffected by regional dolomitization only in Eremophila #1, below a thick sequence of evaporitic supratidal sediments. The lithotope is most commonly interbedded with the laminated dolomudstone lithotope, the fenestral dolostone lithotope, and the skeletal wackestone lithotope.

Interpretation; This lithotope is interpreted to have been deposited in intertidal conditions on the basis of a) the absence of lamination; b) the absence of skeletal components; c) the association with both supratidal laminated dolomudstones and subtidal skeletal wackestones; d) the presence of anhydrite masses; and e) the presence of abundant burrow structures. The mottled, unlaminated nature of the lithotope is probably due to extensive bioturbation and this is a characteristic feature of many intertidal sediments (Shinn, 1983b).

Subtidal Facies

Skeletal Wackestone (Lithotope E)

Description; This lithotope consists of wackestones with various quantities of skeletal material (Fig. 38A). Generally the lithology is completely dolomitized. Skeletal components are most commonly preserved as dolomite cement-filled molds (Fig. 38A)(discussed later) and include crinoid ossicles, brachiopods, tabulate and rugosan corals, stromatoporoids and green algae.

Figure 38 Subtidal lithologies from the Devonian carbonates on the Barbwire Terrace.

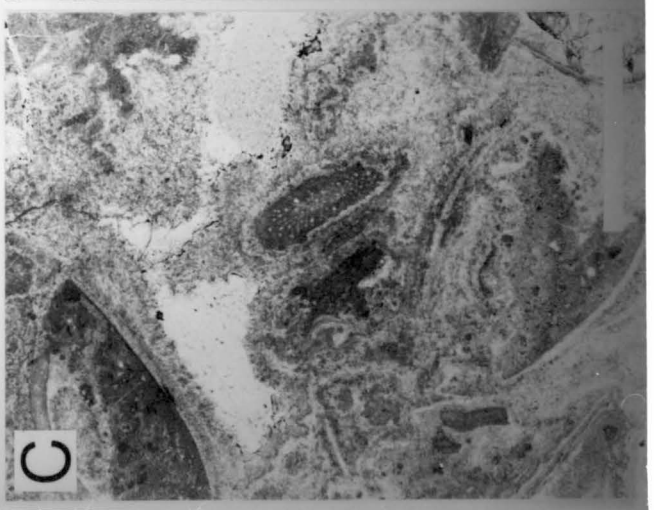
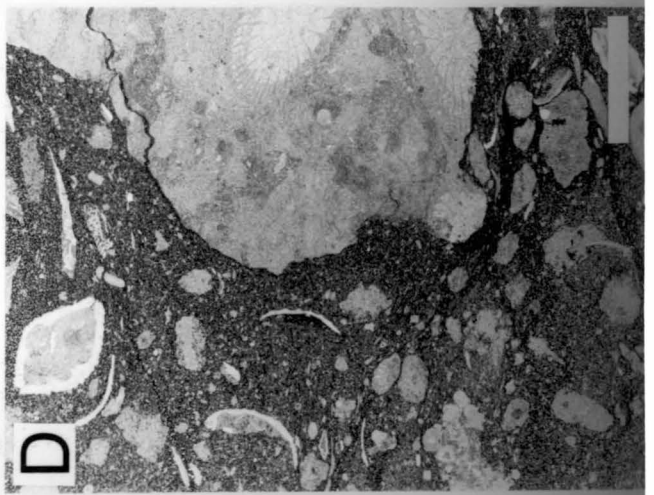
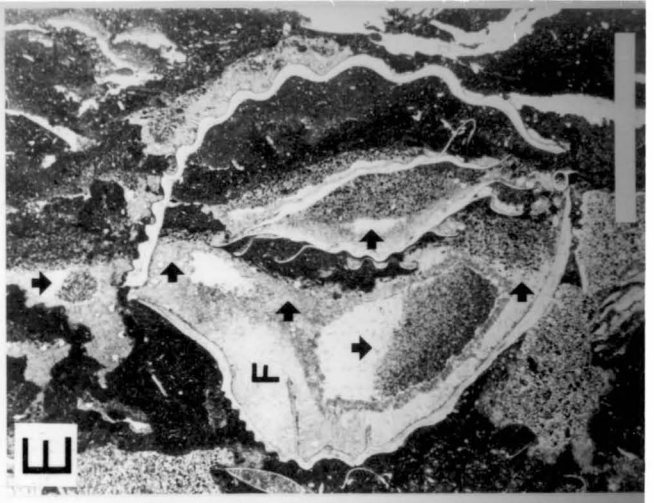
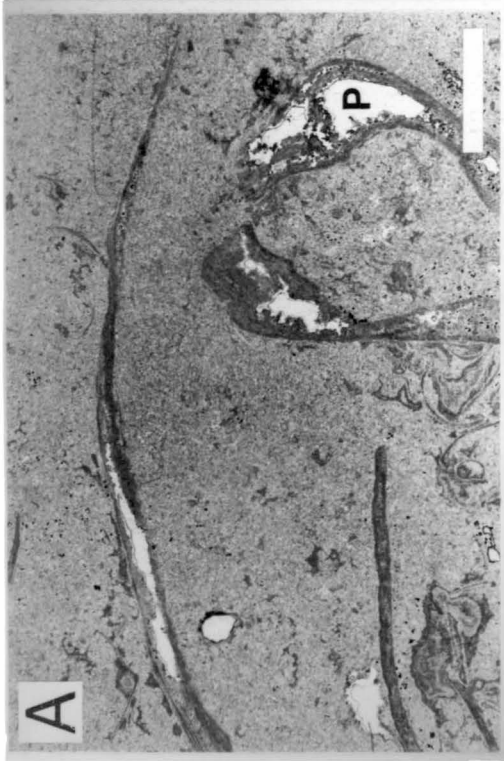
A) Thin-section photomicrograph of a dolomitized skeletal floatstone with large bivalves in a dolomudstone matrix. Note mouldic porosity (P). Cassia #1, 1234.00 m. Scale bar = 1 cm. UTGD sample no. 70344

B) Thin-section photomicrograph of a finely laminated organic-rich lime mudstone. The lime mudstone (M) laminae are separated by thin organic-rich laminae (O). Note the gypsum crystals (G). Eremophila #1, 1220.40 m. Scale bar = 1 mm. UTGD sample no. 70330

C) Thin-section photomicrograph of a dolomitized skeletal rudstone. Bivalves dominate the skeletal constituents. Dampiera #1A, 1082.10 m. Scale bar = 1 cm. UTGD sample no. 70336

D) Photomicrograph of a peel taken from a skeletal-lithoclast breccia. Skeletal components and large lithoclasts are within a clayey lime mudstone matrix. Note the rugosan corals within the large lithoclast to the right. Boab #1, 367.00 m. Scale bar = 1 cm. UTGD sample no. 70354

E) Thin-section photomicrograph of a brachiopod within a large lithoclast from a skeletal-lithoclast breccia. Two sets of geopetals are visible in the lithology. One set of geopetals is now oriented vertically (marked by horizontal arrows). The second set of geopetals is approximately horizontal (marked by vertical arrows). The second set of geopetals is produced by internal sediments which overlie fibrous cements (F) and have been preferentially dolomitized. These features indicate that the lithoclast was rotated after the fibrous cements had developed. Boab #1, 356.45 m. Scale bar = 1 cm. UTGD sample no. 70353



Distribution; Skeletal wackestones are found in all wells but are seldom preserved as limestones. Thick sequences of the lithotope are found in the wells Boab #1, Eremophila #1A and Dampiera #1 and there is commonly a gradation from skeletal wackestones to nodular limestones in a downward direction (Fig. 36).

Interpretation; This lithotope is believed to have been deposited in a normal-marine, shallow-subtidal environment. This is indicated by: a) the abundance of normal-marine organisms like brachiopods and echinoderms; b) the lack of features like fenestrae or mud cracks indicative of subaerial exposure; c) the often thick nature of the lithotope. The abundance of lime mud would appear to suggest relatively low energy conditions. However, the lack of clay minerals in most lithologies suggests the water energy was high enough to keep particulate clays and organic matter in suspension.

Skeletal Grainstone-Packstones

Description; Coarse skeletal grainstones with a partially infiltrated carbonate mud matrix are uncommon in the sequence (Fig. 38C). Both undolomitized and completely dolomitized examples of this lithotope are present. Large unbroken skeletal components form the framework for the lithotope and carbonate muds partially fill the interskeletal cavities leaving abundant shelter cavities. Stromatactis cavities are present within the carbonate mud matrix. In undolomitized lithologies, these cavities are lined by thick isopachous coatings of inclusion-rich radiaxial fibrous calcite cements. The fibrous cements are occasionally overlain by internal sediments. In dolomitized lithologies, the cavities are lined by a similar dolomitized inclusion-rich isopachous cements (Fig. 38C).

Skeletal components present include brachiopods, bryozoans, tabulate corals, gastropods and bivalves.

Distribution; This lithotope is relatively uncommon and was only encountered in two wells: a) in Dampiera #1A where the lithotope is completely dolomitized ; b) in Boab #1 as undolomitized clasts within a debris-flow deposit (Fig. 36).

Interpretation; The presence of radiaxial fibrous calcite is significant. Radiaxial fibrous calcite cements are generally interpreted as being precipitated from marine waters (see chapters 3 and 6) especially where they are overlain by internal sediments. Extensive marine cementation generally only occurs in environments which are subject to much turbulence in the form of tidal or wave action. These conditions are found in mound and reefal environments. This would suggest that the lithotope was probably formed in a mound environment, or at a steep platform margin.

The presence of stromatactis structures also suggests either a mound or steep platform-margin environment.

Finely Laminated Organic-Rich Lime Mudstones

Description; This lithotope consists of finely interlaminated lime mudstones and organic-rich clays (Fig. 38B). Lime mudstone laminae are commonly only 0.3 to 0.5 mm thick while the clayey laminae are generally much thinner. Silt-size quartz grains are abundant in the clayey laminae but are virtually absent from the lime mudstone laminae. There is virtually no grading within the laminae and contacts between the laminae are generally sharp. Lime mud laminae commonly have a fine hummocky surface. Gypsum crystals frequently occur within lime mud laminae. In many cases the crystals have a rounded outline, possibly indicating a detrital origin.

Evidence of soft-sediment deformation in the form of slumping and shear along laminae is common. The lithotope is generally preserved as limestones but is sometimes partially dolomitized. Occasionally dolomites and limestones are finely interlaminated.

Distribution; This lithotope is most well developed in the basal section of Eremophila #1 where it is around 100 m thick. It occurs beneath the subtidal skeletal wackestone lithotope (Fig. 36).

Interpretation; The lithotope is here interpreted as a cryptalgal laminite (Aitken, 1967). The thin films of organic-rich material with quartz silt may represent periodic colonization by cyanobacterial mats. Similar fabrics were described by Gebelein and Hoffman (1973) from stromatolites. The quartz silt within the organic laminae may result from the accumulation of wind-blown silt on the cyanobacterial mats.

Stromatolites and other cyanobacterial laminites are commonly assumed to be indicators of the intertidal and supratidal environment. However recent studies suggest that cryptalgal structures may occur in a wide variety of environments including marine-subtidal environments (Playford and Cockbain, 1969; Playford *et al.*, 1976). Several features suggest the laminites described here are of subtidal origin; a) the large continuous thickness of the lithotope; b) the association with subtidal wackestones; c) the absence of features like mud-cracks and fenestrae indicative of subaerial exposure. However the presence of gypsum crystals and the general absence of burrowers and skeletal constituents within the lithotope may suggest a hypersaline environment. The development of the lithotope within restricted lagoonal environment may explain the above observations.

Skeletal-Lithoclast Breccias

Description; These carbonates consist of both matrix and clast-supported breccias. Many of the grain-supported breccias show normal grading. The clasts range in size from a few metres to millimetres in diameter. Small clasts generally consist of individual skeletal components while the large blocks are generally lithoclasts (Fig. 38D). The clasts commonly display evidence of post-lithification transport in the form of rotated geopetal fabrics (Fig. 38E). Skeletal components occasionally show evidence of growth *in-situ*.

Distribution; This lithotope is a minor lithology and only occurs in a small section of the well Boab #1 (Fig. 36).

Interpretation; This lithotope is interpreted as a series of allochthonous sediment gravity flow deposits. The allochthonous origin is demonstrated by the rotation and truncation of geopetal fabrics. The matrix-supported breccias are interpreted as debris flows while the grain-supported matrix-free lithologies are interpreted as grain flows.

This interpretation is important because it suggests there was a depositional dip on the sediments. In addition, the presence of blocks containing stromatolite structures and cemented by marine radial fibrous calcite suggests that there may have been a buildup structure up-slope.

Impure Lime Mudstones and Marls

Description; This lithotope consists of calcareous shales, marls and impure limestones which have textures ranging from nodular through to irregular clay seam networks (Fig. 39A-D). The lithotope is rarely dolomitized. In the nodular marls, nodules range from 1 mm up to 4 cm thick and consist of lime mudstone with various proportions of clay and silt-size quartz grains. Nodule boundaries are generally sharp. Nodules are separated by calcareous shale seams which are commonly greater than 1 cm thick. Where the internodular calcareous shale is thin, nodular textures grade into irregular clay seam networks (Fig. 39A, B)

The most commonly occurring skeletal components within these rocks are brachiopods (Fig. 39E). Skeletal components occur within the nodules and within the internodular material. Skeletal components in the internodular calcareous shale are almost invariably filled by lime mudstone which has a similar composition to that found in the nodules (Fig. 39E)

Distribution; Impure lime mudstones occur in the basal sections of the wells Dampiera #1A, Eremophila #1, Frankenia #1 and Boab #1. The lithotope may be up to 400 m thick (Dampiera #1A) and commonly grades upward into the skeletal wackestone lithotope (Fig. 36).

Interpretation; Nodular limestones are common in deeper water carbonate sequences (Jenkyns, 1974; Mullins *et al.*, 1980). However, the nodular limestones of the Barbwire Terrace are here interpreted as normal-marine, moderately shallow water subtidal carbonates on the basis of a) The presence of normal-marine benthonic faunas; b) The fine grain size of the carbonate. The presence of abundant clay minerals suggests the sediments were deposited below normal wave base.

Figure 39. The fabrics of clayey lime mudstones and marls from the Devonian carbonates of the Barbwire Terrace. Figures A -D shows a gradation from an anastomosing clay seam network within a clayey lime mudstone through to a nodular marl.

A) Photomicrograph of a stained (alizarin red-s) peel taken from a clayey lime mudstone with numerous anastomosing clay seams. The clay seams (dark) consist of clay minerals, quartz silt, carbonate and organic matter. Dampiera #1A, 1174.85 m. Scale bar = 1 cm. UTGD sample no. 70341

B) Photomicrograph of a stained (alizarin red-s) peel taken from a clayey lime mudstone with thick clay seams (dark) and swarms of microstylolites. Dampiera #1A, 1169.20 m. Scale bar = 1 cm. UTGD sample no. 70338

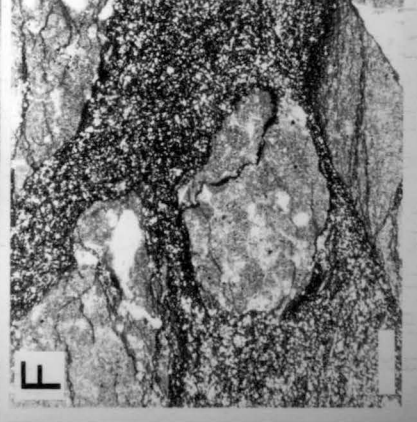
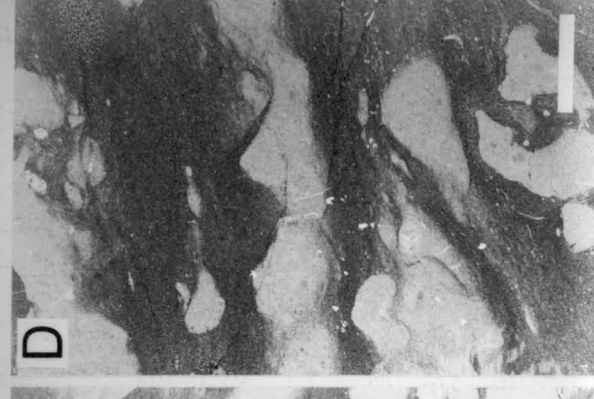
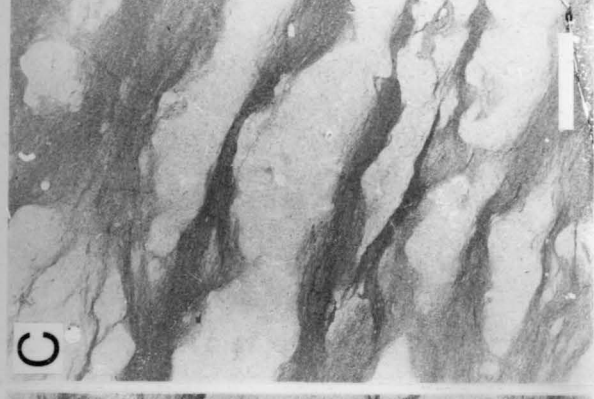
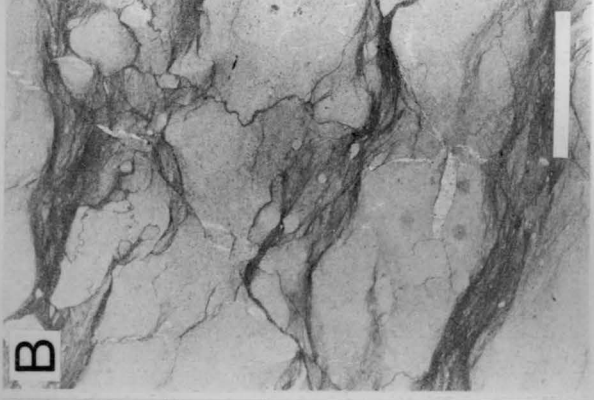
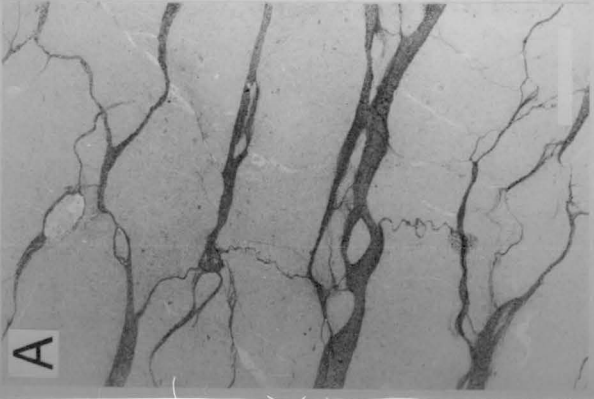
C) Photomicrograph of a stained (alizarin red-s) peel taken from a marl with a nodular structure. The nodules (light) consist of a carbonate mud with a high proportion of clay minerals and quartz silt. Note that the nodules commonly have gradational boundaries. Dampiera #1A, 1169.90 m. Scale bar = 1 cm. UTGD sample no. 70339

D) Photomicrograph of a stained (alizarin red-s) peel taken from a marl with a nodular structure. The marly nodules are separated by thick seams of calcareous shale (dark). Dampiera #1A, 1170.00 m. Scale bar = 1 cm. UTGD sample no. 70340

E) Photomicrograph of a stained (alizarin red-s) peel taken from a clayey brachiopod rudstone. The lithology has a matrix of calcareous shale. Each brachiopod or group of brachiopods contains sediment with a greater proportion of carbonate (lighter material) than the matrix. Boab #1, 395.30 m. Scale bar = 1 cm. UTGD sample no. 70357

F) Thin-section photomicrograph of nodules within a clayey lime mudstone. The inter-nodular material consists of clay minerals, quartz silt and organic matter. The nodules have both sharp and gradational boundaries. Where the boundary is gradational, it consists of a swarm of microstylolites. Dampiera #1A, 1145.30 m. Scale bar = 1 mm. UTGD sample no. 70337

G) Photomicrograph of a stained (alizarin red-s) peel taken from a clayey brachiopod rudstone. The material within the brachiopod (lighter material) has a higher proportion of carbonate than the shaley matrix. In addition, the brachiopod skeletons have been subject to extensive pressure dissolution (arrows). Boab #1, 395.30 m. Scale bar = 1 mm. UTGD sample no. 70357



The origin of the nodule and seam structures has been much debated in geological literature. The hypotheses which have been put forward include:

- a) differential cementation and concretionary growth during early diagenesis (Garrison and Fischer, 1969; Jenkyns, 1974; Nobel and Howells, 1974; Kennedy and Garrison, 1975; Jones *et al.*, 1979)
- b) differential physical compaction and sedimentary boudinage (McCrossan, 1958; Nichols, 1966; Ricken, 1986).
- c) differential carbonate removal during late diagenetic pressure solution (Logan and Semeniuk, 1976; Wanless, 1979; Choquette and James, 1987).
- d) the activities of burrowing organisms (Fursich, 1973; Abed and Schneider, 1980).

Nodular limestones are almost certainly polygenetic. Clearly nodular limestones have been formed by the action of burrowers and by a number of other early diagenetic processes like concretionary growth. However, there are a number of problems with the early diagenetic models. Firstly, there are relatively few reports of modern deep-water nodular carbonates (Mullins *et al.*, 1980). Secondly, it appears that virtually all ancient marls or impure limestones which have been deeply buried have a nodular structure. This is not the case with uncompacted marls. Empirically, this would suggest that many nodular structures develop during burial.

It is suggested that the nodular fabrics and clay seam networks in the marls in the Barbwire Terrace are largely a result of pressure solution. This hypothesis is further discussed in Chapter 8.

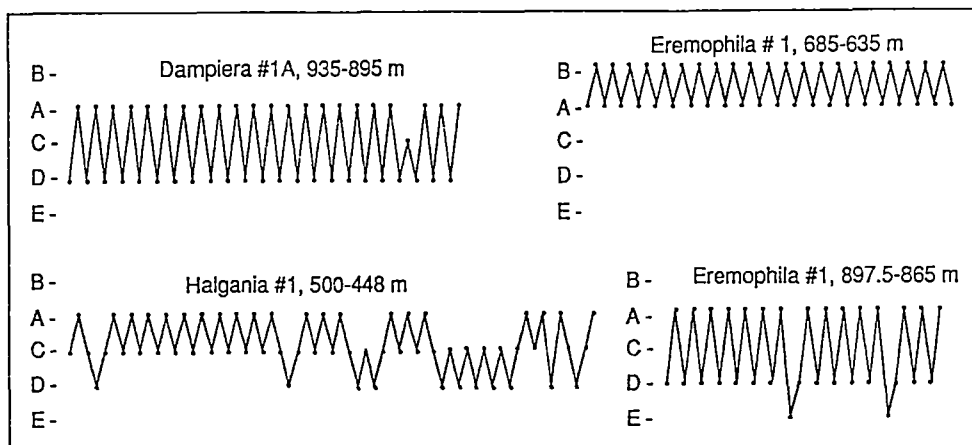


Figure 40. Plot of the lithotope sequences from four sections in the wells Dampiera #1A, Halganian #1 and Eremophila #1 with stratigraphic top to the right. The lithotopes are arranged from subtidal at the base and upper supratidal at the top. The horizontal distance between dots is not to scale.

Discussion

Peritidal Lithotope Associations and Sequences

The peritidal lithotopes occur as thin, interlaminated beds varying from several centimetres to a metre thick. Examination of several detailed sections failed to show any significant cyclic relationships between the various peritidal lithotopes (Fig. 40). In order to determine the relationships between the peritidal lithotopes, the semi-quantitative method of Selley (1970) was employed. A matrix was constructed to display the observed number of over- and underlying contacts between each lithotope for the three well sections examined in detail (Fig. 41). Another matrix was then constructed to display the predicted number of contacts if the lithotopes were arranged randomly (Selley, 1970). The random matrix was then subtracted from the observed matrix in order to construct a matrix which shows those contacts which occur more frequently than would be expected if the lithotope sequence was random. The very symmetrical nature of this matrix (Fig. 41) indicates that the dominant lithotope sequence is an interbedding between two lithotopes.

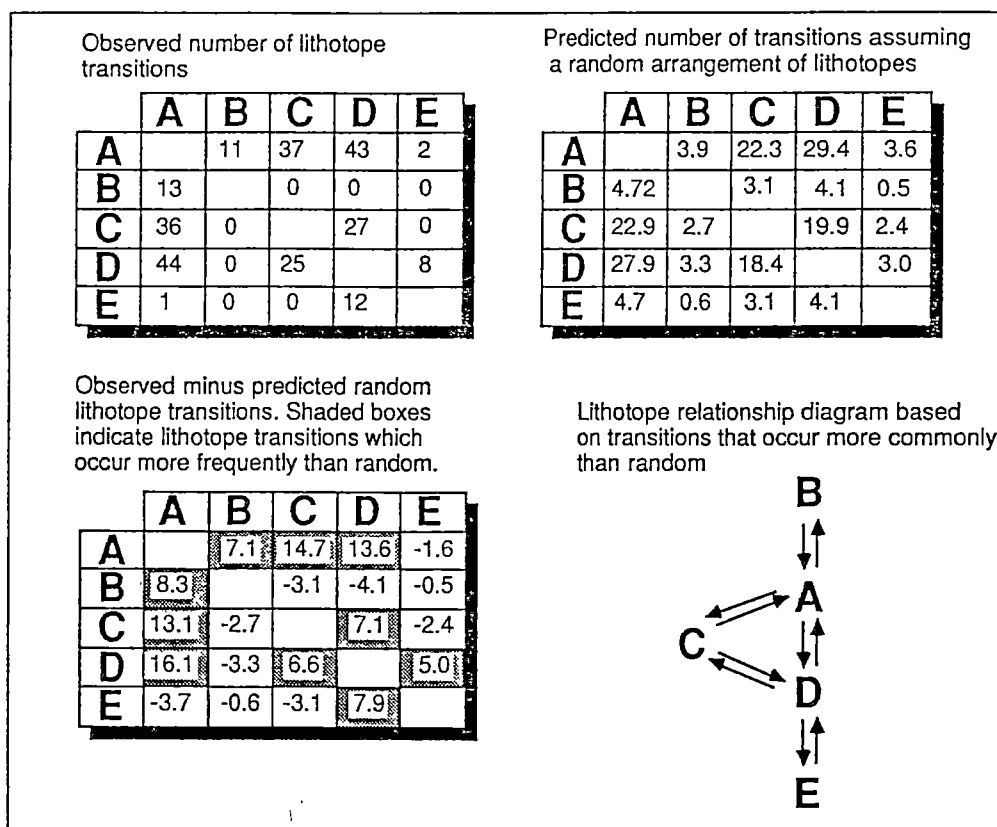


Figure 41. Analysis of the relationships between the peritidal lithotopes using the method of Selley (1970). Each column of the matrices records the number of times that the lithotope at the top of the column overlies the lithotope shown in the rows beneath. The data were taken from the wells Eremophila #1, Dampiera #1A and Halgania #1. Lithotope A = laminated dolomudstone. Lithotope B = Clayey dolomudstone with anhydrite. Lithotope C = fenestral dolomite. Lithotope D = massive carbonate mudstone. Lithotope E = Skeletal wackestone.

A facies relationship diagram (De Raaf *et al.*, 1965) was then constructed which displays those contacts between lithotopes which occur more frequently than would be expected from a random lithotope sequence (Fig. 41). From this facies relationship diagram, an idealized peritidal facies sequence (incorporating all of the petrographic evidence given above) was constructed for the Barbwire Terrace carbonates (Fig. 42). The resulting idealized lithotope sequence is comparable to that constructed for the arid tidal flats of the Persian Gulf (McKenzie *et al.*, 1980; Shinn, 1983b).

However, there are several important differences between the lithotope sequence for the Barbwire Terrace and idealized peritidal facies sequences based on modern and ancient peritidal carbonates; 1) Massive carbonate mudstones with nodular anhydrite (Lithotope B) are abundant in supratidal facies. In modern arid tidal flats, laminated lithotopes dominate the supratidal zone (Shinn, 1983b); 2) No erosion surfaces were recognized within the supratidal sediments. Erosional surfaces appear to be an important part of the supratidal sequence in many modern and ancient carbonates (Warren and Kendall, 1985); 3) Supratidal sediments commonly occur in very thick sections (e.g. 300 m of supratidal sediments in Eremophila #1). This great thickness appears to be at odds with almost all peritidal facies models developed on modern tidal flat environments; 4) The peritidal sediments lack the well developed peritidal cycles which have been predicted from modern peritidal environments and documented in many ancient peritidal sequences.

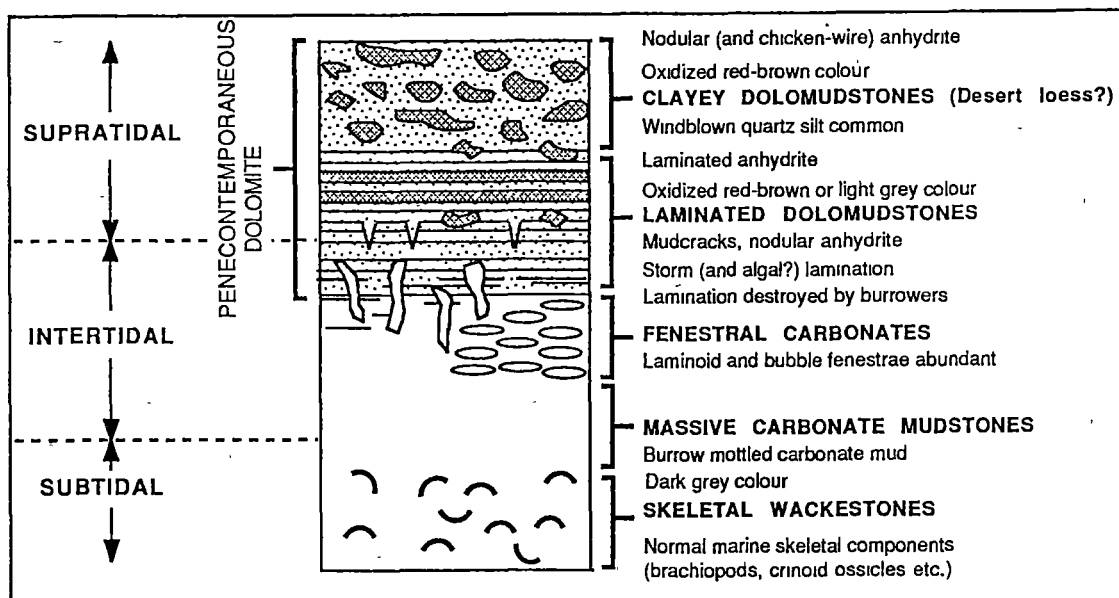


Figure 42. Idealized lithotope sequence for the Devonian peritidal carbonates of the Barbwire Terrace. This is derived from the facies relationship diagram of figure 41 and from the petrographic data given above.

Lack of Peritidal Cycles

Studies on peritidal carbonates often stress the small scale cyclic nature of many sequences. The most common type of cycle documented is an asymmetrical shallowing-upward unit and these have been termed "punctuated aggradational cycles" (PACs) by some authors (Goodwin and Anderson, 1980). The principal processes invoked to

explain the cycles include eustatic sea-level fluctuation, subsidence and the lateral migration of local carbonate facies. Eustatic sea-level fluctuation has been emphasized by many researchers (e.g. Read *et al.*, 1986), while subsidence mechanisms have been emphasized by others (Read, 1973a; Goodwin and Anderson, 1980).

Wong and Oldershaw (1980) and Ginsburg (1971) have invoked a mechanism of lateral peritidal facies migration ("autocycles" of Ginsburg, in Bosellini and Hardie, 1973). In this explanation, tidal flats are thought to prograde over the adjacent subtidal areas until the subtidal sediment supply is choked off completely. The next cycle begins when the subtidal area has expanded under the influence of continued subsidence.

However, the peritidal carbonates of the Barbwire Terrace do not display the small scale cycles described above. The idealized lithotope sequence which was constructed for the carbonates (on the basis of lithotope associations) never occurs in a single cycle. In fact, the dominant small-scale vertical lithotope sequence is almost always an interbedding of two lithotopes (Figs. 40, 41). The origin of this type of sequence is obscure. Pratt and James (1986) have similarly found that ideal upward shallowing cycles are quite rare in the Ordovician peritidal carbonates of the St. George Group, and have stressed the heterogeneous nature of typical lithologic sequences. Pratt and James (1986) developed an "autocyclic" model based on laterally migrating supratidal islands to explain the heterogeneous lithotope sequences of the St. George Group.

More recently, Morrow (1986) and Read *et al.* (1986) have suggested a combination of constant subsidence and an oscillating eustatic sea level to explain small scale carbonate cycles. Using several variables (depth-dependent sedimentation rate, amplitude and period of sea level oscillation, linear rate of subsidence, lag time of sedimentation and tidal range), Read *et al.* (1986) attempted to model carbonate cycle generation. Using their model, Read *et al.* (1986) suggested that erosional surfaces did not develop when sea level fall was balanced by subsidence. This situation is favoured when 1) subsidence rates are high; and/or 2) the amplitude of sea level oscillation is low; and/or 3) the period of sea level oscillation is long. These conditions may explain the lack of erosional breaks in the peritidal sequences of the Barbwire Terrace.

Using the model of Read *et al.* (1986), the thick sequences of supratidal sediments in the Barbwire Terrace carbonates may be explained by a combination of short lag times (time after transgression of emergent shelf when sediment production is not fully operative) and a small amplitude of sea level oscillation.

Large Scale Evolution of the Carbonates

In most of the wells studied, a lower regressive sequence and an upper transgressive sequence of carbonates is present (Fig. 36). The basal subtidal carbonates of the lower regressive sequence appear to be of Frasnian age on the basis of 1) the presence of *Amphipora* and 2) the abundance of atrypid brachiopods. Because of the absence of fossils, it is difficult to estimate the age of the intertidal and supratidal lithotopes in the upper portions of the regressive sequence.

The upper transgressive sequence of carbonates may be equivalent to the Lower Carboniferous Fairfield Group on the Lennard Shelf. If this correlation is correct, the

thick supratidal and intertidal carbonates of the Barbwire Terrace would be equivalent to the Nullara Limestone. On the Lennard Shelf, the Famennian reef complexes are characterized by their strongly advancing nature and this indicates low subsidence rates and stable sea levels (Playford, 1980; Begg, 1987). However, correlation between the Barbwire Terrace and Lennard Shelf carbonates is likely to be complicated by local tectonic events and subsidence rates.

Environmental Synthesis

The thick sequence of supratidal evaporites suggests that the Devonian climate was arid. Kerans (1985) has also suggested that the Canning Basin may have been subject to arid climatic conditions in the Late Devonian. This suggestion was based on the chemically immature nature of Upper Devonian siliciclastics on the Lennard Shelf. Palaeomagnetic data from the Upper Devonian carbonates of the Lennard Shelf (Hurley, 1986) indicate a palaeolatitude of around 15 degrees. This equatorial palaeolatitude is consistent with the presence of well developed reef complexes on the Lennard Shelf. Hence, the peritidal carbonates of the Barbwire Terrace were probably developed in a warm, arid equatorial climate. This may suggest that the climatic regimes of the Late Devonian were different from modern climatic regimes as the modern equatorial belt is subject to humid climatic conditions.

The total absence of any sandy lithologies from the peritidal facies and their rarity in subtidal facies suggest very low energy conditions. This may be due to several factors: a) the development of an outer shelf barrier (reefs, bars or mounds); b) the presence of a very wide shelf which acted as an oceanographic barrier; c) local oceanographic and climatic conditions damping wave and storm activity. The outer shelf barrier hypothesis is supported by the presence of buildup lithologies (Lithotope F) in the sequence. However, not enough information is available on the outer shelf lithologies to speculate on the reason for the very low energy conditions on the Barbwire Terrace.

In such low energy conditions, nodular, marly and shaley carbonates (Lithotope D) may have been deposited in much shallower waters than are generally associated with these lithologies. This may explain the great abundance of nodular impure carbonates in the sequence.

A wide, shallow water, low energy shelf model is invoked to explain the major lithologies of the Barbwire Terrace carbonates. As suggested by Pratt and James (1986), the peritidal sections of the shelf may have been composed of a series of supratidal islands. The peritidal areas were probably rimmed by a zone of shallow-subtidal skeletal wackestones (Lithotope E). In slightly deeper waters (below wave base), impure (nodular) limestones were deposited.

8. DIAGENESIS IN THE DEVONIAN CARBONATES OF THE BARBWIRE TERRACE

Introduction

The majority of the Frasnian-Famennian carbonates on the Barbwire Terrace display a relatively simple diagenetic history. This is because most of the peritidal and shallow subtidal carbonates have been very thoroughly dolomitized. This regional dolomitization event destroyed many of the earlier, more subtle, diagenetic textures and inhibited further cementation. This also makes paragenetic interpretation difficult. In general, only the most impermeable and non-porous carbonates escaped regional dolomitization. However, these impermeable carbonates never possessed any substantial primary porosity and so did not record an extended cementation history. Only in the well Boab #1 did limestones with significant primary porosity escape dolomitization and so display the most diverse diagenetic fabrics.

The Devonian carbonates of the Barbwire Terrace suffered a burial history similar to the reef complexes of the Lennard Shelf (chapter 6). After Devonian synsedimentary diagenesis, the carbonates were subject to Late Devonian - Early Carboniferous burial diagenesis. During the the Late Carboniferous, the whole basin was subject to massive uplift and the Barbwire Terrace carbonates were subject to peneplanation and subaerial diagenesis (Begg, 1987). The carbonates of the Barbwire Terrace were then subject to a long period of burial diagenesis and remain buried to the present day. As on the Lennard Shelf (chapter 6), the episode of Late Carboniferous subaerial diagenesis provides a useful paragenetic marker by which earlier and later diagenetic phases can be dated (using petrographic criteria).

Devonian Synsedimentary Diagenesis

Supratidal Dolomitization

A thick section of the well, Eremophila #1, consists of a sequence of evaporitic peritidal lithologies (Fig. 36). In this sabkha sequence, dolomite is almost entirely restricted to the supratidal lithologies which are always pervasively dolomitized. In some sections, supratidal lithologies are interbedded with burrowed intertidal lime mudstones. In these sections, dolomitization has only occurred within and around the supratidal lithologies, producing a sequence of interbedded supratidal dolomites and intertidal limestones.

The supratidal dolomite generally has an anhedral crystal shape with a crystal size ranging from 4 to 25 microns. The supratidal dolomicrite displays none of the

compaction features found in similarly impure limestones, indicating that dolomitization was probably a pre-compaction phenomena.

Supratidal dolomites have $\delta^{18}\text{O}$ values ranging from -2 to 0 ‰ (PDB) and $\delta^{13}\text{C}$ values ranging from 0 to 2 ‰ (PDB) (Fig. 43). The supratidal dolomites have high strontium (150 to 750 ppm) and sodium contents (850 to 1500 ppm) (Fig. 44). The manganese contents range from 330 to 780 ppm and the iron contents range from 0.5 to 4 mole percent (Fig. 45). The supratidal dolomite has calcium contents ranging between 48 and 55.7 mole percent.

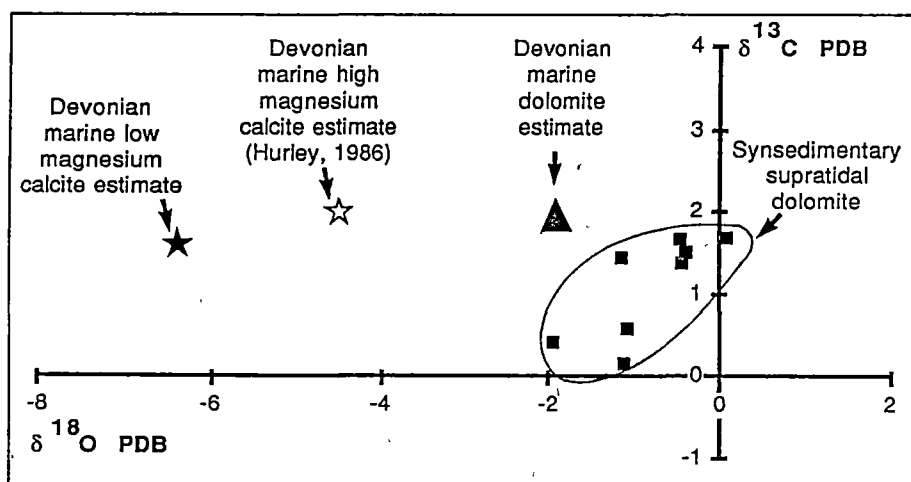


Figure 43. Carbon and oxygen isotope values for the synsedimentary supratidal dolomites of Eremophila #1. An estimate of the Devonian marine dolomite composition is made which is based on the lowest $\delta^{18}\text{O}$ values for the synsedimentary supratidal dolomites. Estimates for Devonian high magnesium and low magnesium calcite are also shown (see Fig. 21).

Supratidal Sulphate Precipitation

Nodular anhydrite is common within the supratidal lithotopes of 1 Eremophila #1 (Fig. 37A, B, E, F) and their synsedimentary origin has been discussed previously (chapter 7).

Marine Cementation

Marine cementation is rare in the Devonian carbonates of the Barbwire Terrace. Inclusion-rich fibrous cements interpreted to be of marine origin have been observed within Boab #1 and Dampiera #1A. In Dampiera #1A, the cements have been thoroughly dolomitized and much of the textural detail has been destroyed (Fig. 38C). In Boab #1, radiaxial fibrous calcite cements are present in large allochthonous blocks within a mass-flow deposit (Fig. 38E).

The marine origin of the radiaxial fibrous calcite is consistent with: A) its occurrence as a first generation cement; B) internal sediment overlying the cement; C) allochthonous blocks containing truncated radiaxial fibrous cements.

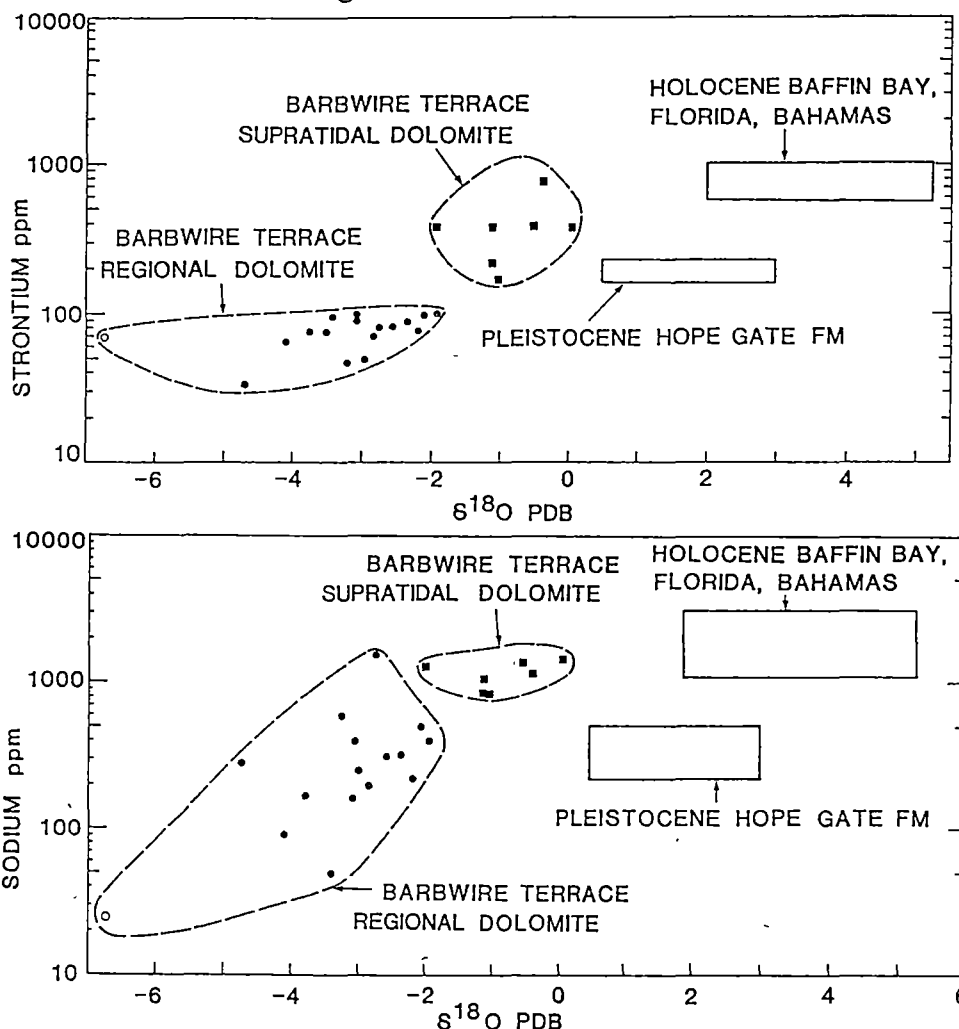


Figure 44. Strontium and sodium values for the Barbwire Terrace dolomites plotted against $\delta^{18}\text{O}$. Supratidal dolomite = solid squares. Replacement dolomite of regional dolomite = solid circles. Cloudy dolomite cements of regional dolomite = open circles. Also shown are data from Holocene marine dolomites (Baffin Bay, Bahamas, Florida; Behrens and Land, 1972), and Pleistocene dolomites interpreted to be of mixed-water origin (Hope Gate Formation; Land, 1973).

Discussion of Synsedimentary Diagenesis

Volumetrically, the most important synsedimentary diagenetic phase in the Barbwire Terrace carbonates is the supratidal dolomite. A synsedimentary, hypersaline-supratidal origin for the dolomite described is supported by: A) the restriction of dolomite to supratidal lithologies; B) the association with early diagenetic evaporite minerals; C) the fine-grained nature of the dolomite and D) the petrographic evidence for a pre-compaction origin.

Poorly ordered calcian dolomite has been found in the Holocene arid supratidal flats of the Persian Gulf (Wells, 1962; Curtis *et al.*, 1963; Illing *et al.*, 1965). Sea water beneath the supratidal flats is believed to be progressively concentrated by evaporation. Subsequent precipitation of gypsum produces an increase in the Mg/Ca ratio of the water and this produces dolomitization (Butler, 1969). This "sabkha"

dolomitization model has been used to explain many ancient peritidal dolomites (e.g. West *et al.*, 1968; Budai *et al.*, 1987).

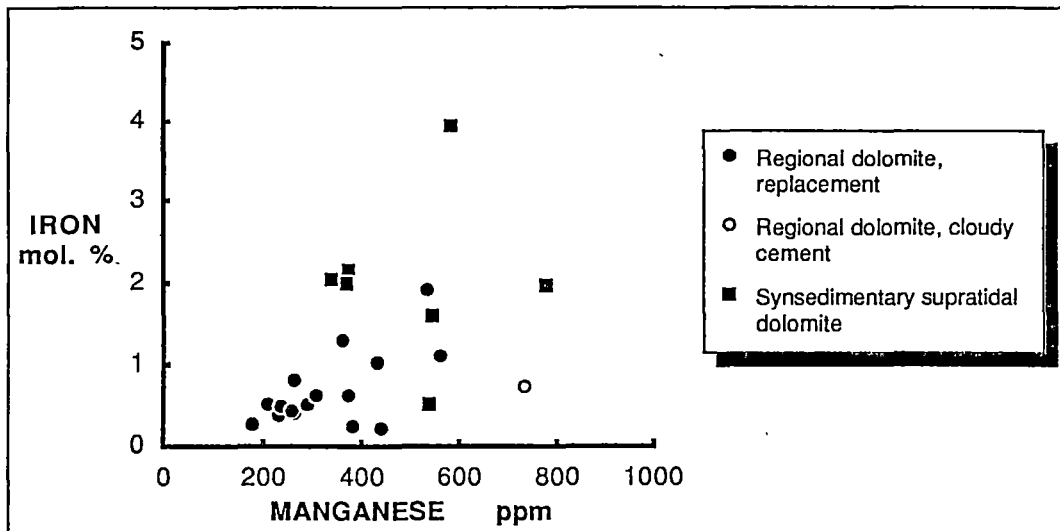


Figure 45. Iron and manganese values for the Barbwire Terrace dolomites.

The relatively high $\delta^{18}\text{O}$ values of the supratidal dolomite also support a model of dolomitization from highly evaporated pore waters. The slight positive covariance between $\delta^{18}\text{O}$ and $\delta^{13}\text{C}$ values may be a result of CO_2 degassing by capillary evaporation near the sediment-air interface (Pierre *et al.*, 1984). Supratidal dolomites from the Barbwire Terrace have strontium values less than or equal to modern marine and hypersaline dolomites (Behrens and Land, 1972) (Fig. 44). The sodium contents of the supratidal dolomites correspond roughly with those from modern supratidal dolomites (Land and Hoops, 1973) (Fig. 44). The reason for the high iron and manganese content of the supratidal dolomite is obscure as the dolomite is interpreted to have formed in an oxidized supratidal environment (Fig. 45). The iron and manganese may have entered the dolomite during a recrystallization event.

The oxygen isotopic composition of Upper Devonian marine dolomite can be estimated by using the synsedimentary supratidal dolomite as a reference. Since the supratidal dolomite is interpreted to have formed from hypersaline waters at surface temperatures, the best estimate of Upper Devonian normal-marine dolomite would probably have $\delta^{18}\text{O}$ values overlapping with the lowest hypersaline values; i.e. around -2‰ (PDB) (Fig. 43).

Comparison of this $\delta^{18}\text{O}$ value for Upper Devonian marine dolomite with the estimated oxygen isotopic composition of Upper Devonian radiaxial fibrous marine cements from the Oscar Range reef complex $\{\delta^{18}\text{O} = -4.5 \pm 0.5\text{‰}$ (PDB), Hurley, 1986} suggests a dolomite to calcite enrichment factor of around -2.5‰ (subtracting the dolomite phosphoric acid fractionation of Sharma and Clayton (1965) would reduce this to around 1.7‰). Given that radiaxial fibrous cements were probably precipitated as high-magnesium calcite (Lohmann and Meyers, 1977), this estimate for $\Delta^{18}\text{O}_{\text{Dol-Mag Calcite}}$ is not unreasonable (Land, 1980).

The lack of marine cementation in the sequence is consistent with the suggested low energy depositional environment of the carbonates (chapter 7). Marine cementation

requires large volumes of sea water to be pumped through the sediments and this is not possible in low energy environments.

Limestone Cementation

Only the clayey limestones and marls in the sequence escaped regional dolomitization. Almost all porosity in these impure limestones is filled by ferroan-calcite cements. However, minor silica, anhydrite and ferroan-dolomite cements are also present in these carbonates.

Ferroan-Calcite Cementation

In the marly lithologies which escaped regional dolomitization, scalenohedral and equant calcite cements directly overlie the depositional components (Figs. 46A, 47A). In general, the earliest cements have a scalenohedral morphology and frequently have a cloudy inclusion-rich appearance (Fig. 47A) and later cements have a clear equant character. The cements are generally ferroan and display a dull, weakly-zoned luminescence (Fig. 46A). Occasionally, there is a first-generation non-ferroan non-luminescent stage. The cements fill interskeletal, intraskeletal and fracture porosity, suggesting that they were, at least in part, precipitated after significant mechanical compaction had taken place.

Silica Cementation

Minor quartz cementation and silicification has occurred within the marly lithologies. Quartz cements are coarsely crystalline (~1mm diam), generally fill intraparticle porosity and post-date ferroan dull-luminescent scalenohedral calcite cements (Fig. 47A). Ferroan, dull-luminescent, equant-calcite cements occasionally overlie the quartz cements. Silicification of skeletal fragments is commonly associated with quartz cementation and silicification generally preserves the microstructure of skeletal components. Partially silicified skeletal components filled by quartz cements have been observed within regionally dolomitized lithologies (Fig. 47B) and this suggests that silicification occurred prior to regional dolomitization.

Anhydrite Cementation

Minor anhydrite cements fill fracture porosity in the impure limestones of the sequence. The anhydrite has a coarsely crystalline felted texture. Ferroan-dolomite crystals occasionally replace the anhydrite cements.

Ferroan Dolomite Precipitation

Ferroan-dolomite cements and replacement dolomites occur within marly limestones in the sequence. In Boab #1, strongly-ferroan, non-luminescent saddle dolomite occurs as a cement and as a replacement of internal sediment (Fig. 46A, 38E). The saddle dolomite cements occur within, and interrupt the ferroan dull-luminescent calcite cement sequence. Ferroan saddle dolomite cements fill fracture and primary porosity.

Figure 46. Thin-section photomicrographs illustrating diagenetic fabrics in the Devonian carbonates of the Barbwire Terrace.

A) Cathodoluminescence photomicrograph of a brachiopod within an undolomitized lithoclast breccia. The non-luminescent brachiopod is surrounded and partially filled by dull luminescent lime mud (M). The remaining upper portion of the brachiopod was filled by carbonate cements. The earliest cement is a dull luminescent inclusion-rich scalenohedral calcite cement (S). Non-luminescent, strongly ferroan saddle dolomite cements (DO) directly overlie the scalenohedral cement. A sequence of zoned dull luminescent ferroan calcite cements (D) post-date the saddle dolomite cements fill the remaining pore space. Boab #1, 367.4 m. Scale bar = 1 mm. UTGD sample no. 70355

B) Cathodoluminescence photomicrograph of a regionally dolomitized crinoidal wackestone. A crinoid ossicle (C) has been syntaxially replaced by dull luminescent unzoned dolomite. Intercrystalline porosity (P) has been partially filled by a dull luminescent unzoned poikilitic calcite cement (PD). Cassia #1, 1088.80 m. Scale bar = 1 mm. UTGD sample no. 70342

C) Thin-section photomicrograph illustrating the principal diagenetic phases within regionally dolomitized lithologies (plain light). Replacement dolomite (R) forming the wall of a mouldic cavity, is overlain by cloudy dolomite cement (C), which is overlain by limpid dolomite cement (L). The final cavity filling material is a poikilitic calcite cement (PD). *Eremophila* #1, 424.40 m. Scale bar = 1 mm.

D) Same area in C under cathodoluminescence. The replacement dolomite (R) and cloudy dolomite cement (C) have an identical unzoned luminescence. The limpid dolomite cement (L) is zoned. The poikilitic calcite cement (PD) has a dull weakly-zoned luminescence.

E) Cathodoluminescence photomicrograph of a fracture within a regionally dolomitized lithology. Unzoned replacement dolomite = (R). The fracture was lined by limpid dolomite cement (L) and this suggests that fracturing took place during the later stages of regional dolomitization. The fracture was later filled by poikilitic weakly zoned dull luminescent calcite cement (PD). Cassia #1, 1303.10. Scale bar = 1 mm. UTGD sample no. 70345

F) Cathodoluminescence photomicrograph illustrating hollow zones within the limpid dolomite cement. An intercrystalline pore has been partially filled by cloudy dolomite (C) and limpid dolomite cement (L). Pore space = P. Ferroan zones within the limpid dolomite cement were then selectively dissolved, leaving narrow hollow zones within the limpid dolomite crystals (arrows). Boab #1, 254.13 m. Scale bar = 1 mm.

G) Thin-section photomicrograph of non-ferroan equant calcite calcite cement (E) filling dissolution porosity within replacement dolomite (RD) of the regional dolomite type. Pore space = P. *Eremophila* #1, 409.13 m. Scale bar = 1 mm.

H) Same area in G under cathodoluminescence. The non-ferroan equant calcite cement consists of an early non-luminescent zone (N) overlain by a bright luminescent zone (B) and a final dull luminescent zone (D). Note the area of blotchy dull luminescent neomorphic spar (arrow) within the non-luminescent zone. Pore space = P.

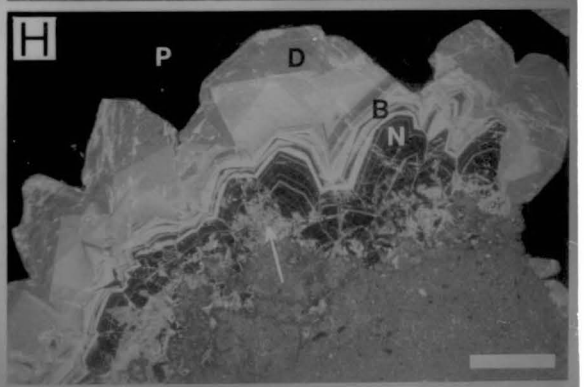
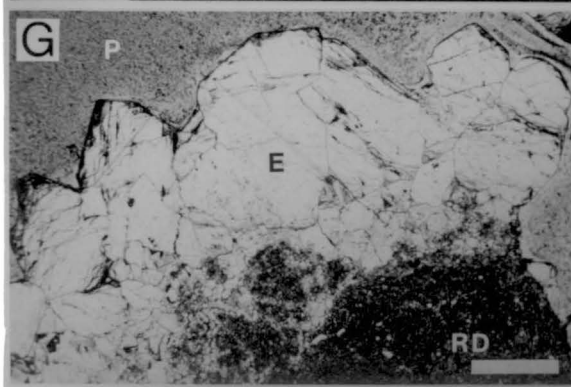
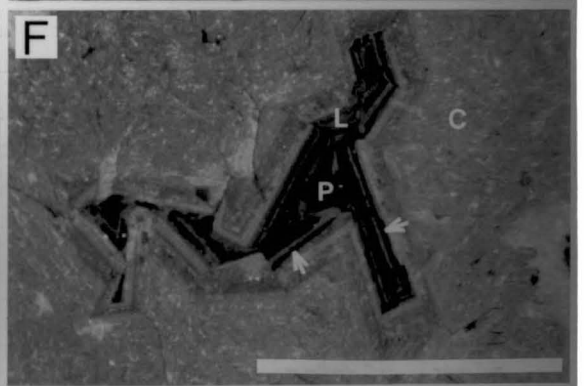
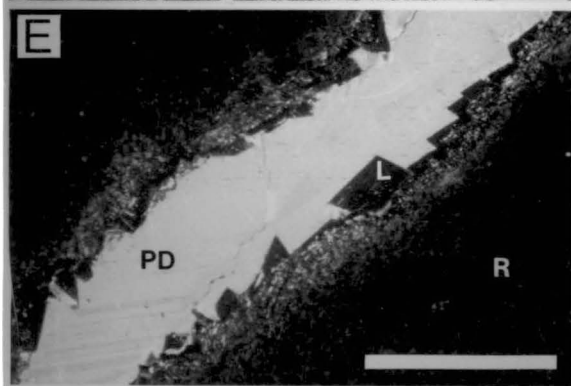
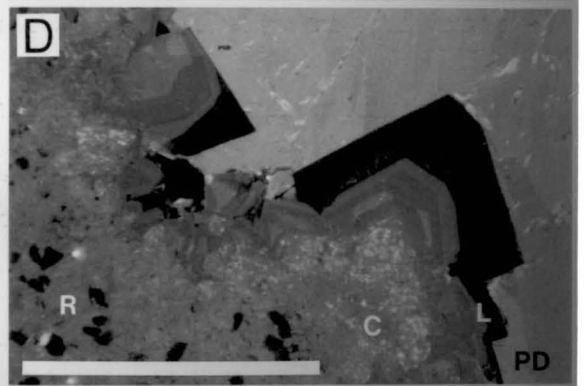
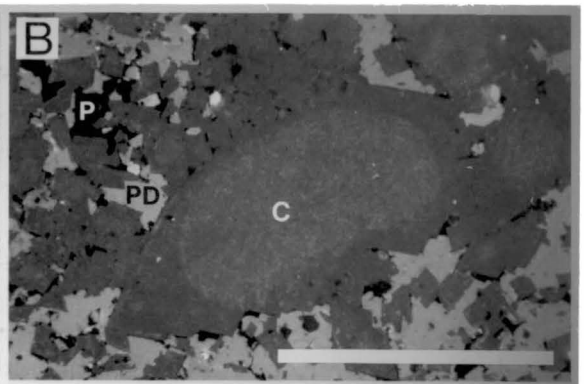
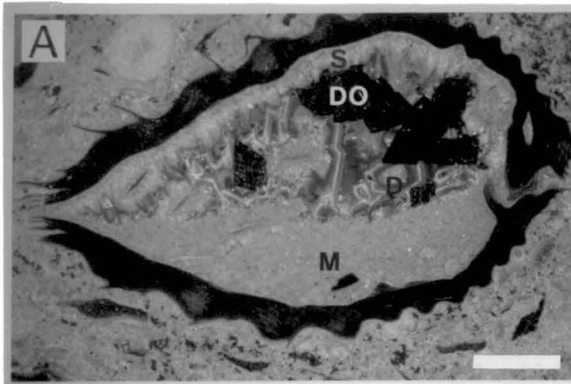


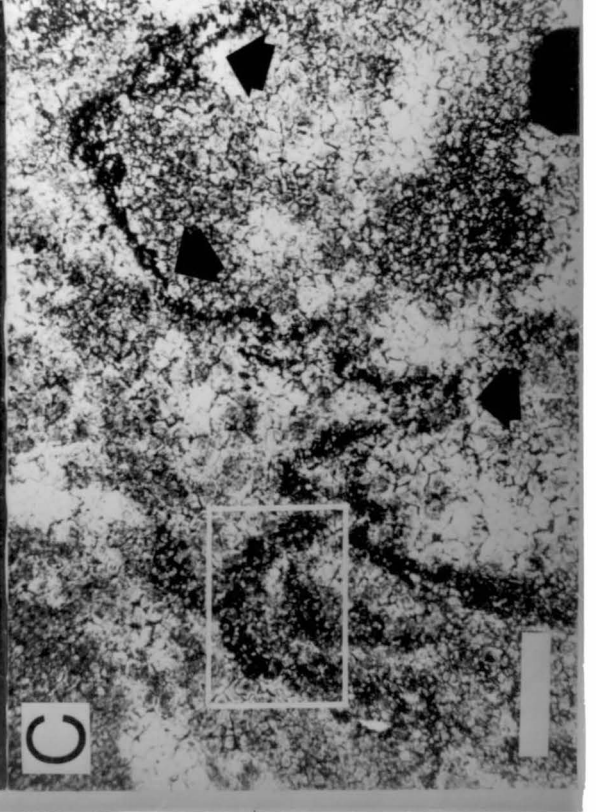
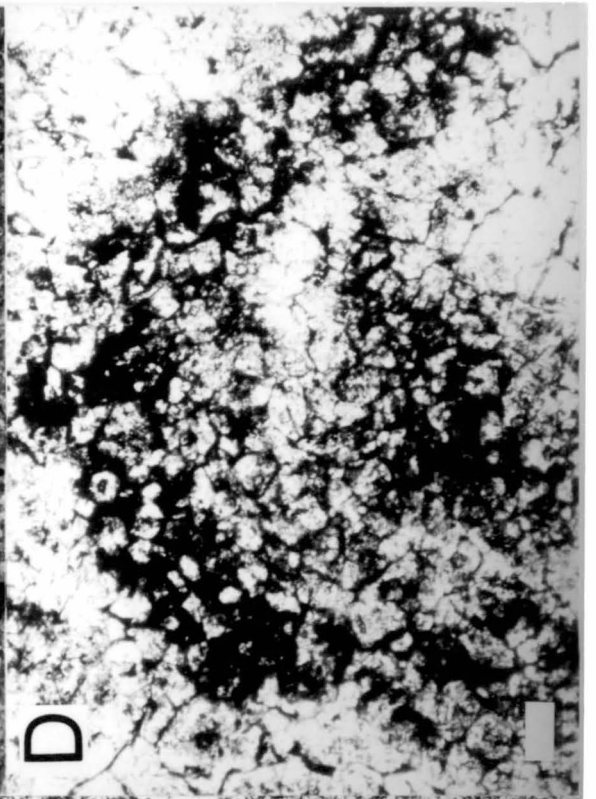
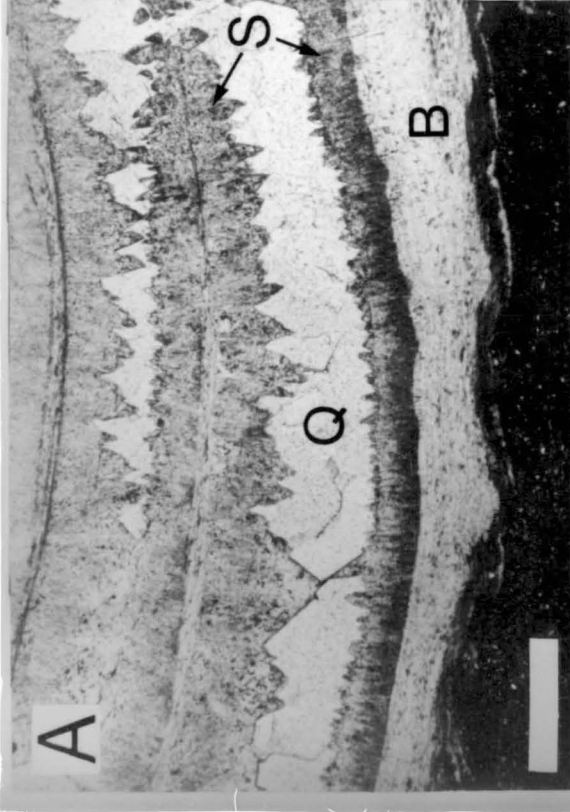
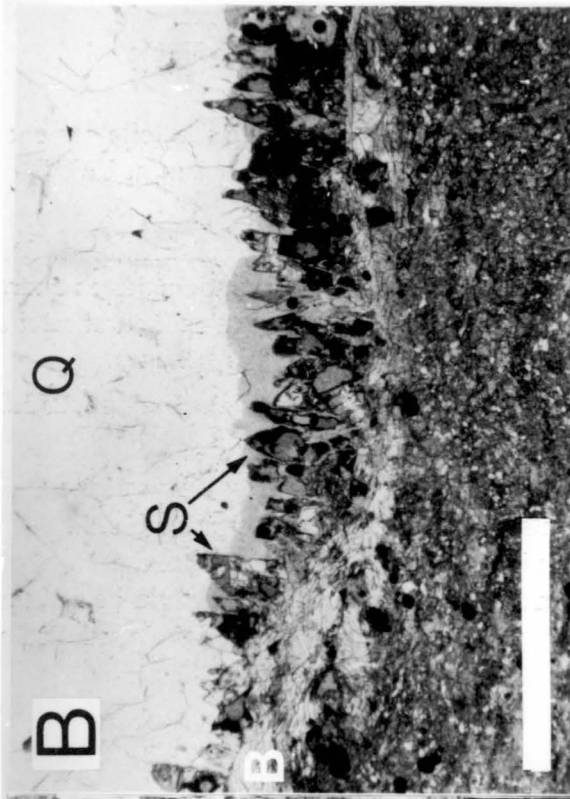
Figure 47. Thin-section photomicrographs illustrating the timing of regional dolomitization.

A) Cements filling atrypid brachiopod (B) lined first by scalenohedral calcite cement (S) and then by quartz cement (Q). Boab #1, 387.31 m. Scale bar = 1 mm. UTGD sample no. 70356

B) Regionally dolomitized equivalent of area in A, with dolomitized brachiopod (B), partially dolomite filled molds of scalenohedral calcite cement (S) and unaltered quartz cement (Q). This indicates regional dolomitization occurred after scalenohedral calcite cementation and quartz cementation. Boab #1, 408.44 m. Scale bar = 1 mm.

C) A regionally dolomitized lithology with a relict stylolite (arrows). Boab #1, 253.00 m. Scale bar = 1 mm. UTGD sample no. 70349

D) Enlargement of area outlined in C. The relict stylolite consists of a crystalline dolomite mosaic in which dolomite crystals are surrounded by clay minerals. In addition, the margins of the stylolite are quite diffuse. This indicates that the replacement dolomite crystals grew within the organic material of the stylolite and thus suggests that regional dolomitization occurred after the stylolite had developed. Scale bar = 100 μ m.



Discussion of Limestone Diagenesis

Dull-luminescent ferroan-calcite cements are interpreted to have precipitated during Devonian - Carboniferous burial diagenesis. This is consistent with a) their position as first generation cements; b) their high iron content; and c) their post-compaction timing. The high iron content is probably related to the abundance of clay in the host lithologies (Oldershaw and Scoffin, 1967). The cements also partially pre-date regional dolomitization (discussed later). Regional dolomitization is known to have occurred prior to Late Carboniferous subaerial exposure (as dolomites have been eroded and karstified beneath the Late Carboniferous unconformity, discussed below).

Silica precipitation is interpreted to have occurred during Late Devonian - Early Carboniferous burial because they a) post-date ferroan calcite cements; b) fill primary pore space; and c) pre-date regional dolomitization. Anhydrite cements are interpreted to be of burial diagenetic origin because they fill fracture porosity.

Ferroan saddle dolomites are interpreted to be of Late Devonian - Early Carboniferous burial origin because they a) fill fracture and primary porosity; and b) pre- and post-date ferroan-calcite cements. Preferential dolomitization of internal sediments also suggests an early burial origin, similar to the dolomitization in the Geikie Gorge region (chapter 6). It is possible that the ferroan-saddle dolomites in the clayey carbonate lithologies precipitated from the waters which were responsible for regional dolomitization in the pure carbonates (discussed below).

Regional Dolomitization

Virtually all of the pure carbonate lithologies on the Barbwire Terrace have been completely dolomitized. Most of the dolomite is not restricted to supratidal, or even peritidal lithologies. Thick sections of purely subtidal carbonate (containing normal-marine faunas) are generally completely dolomitized. The dolomite distribution appears to be most closely related to the clay content of the carbonate, rather than to the depositional facies. Carbonates with more than 50% clay are seldom dolomitized. Where dolomitization has occurred, there is generally no primary calcite remaining within the lithology. Partially dolomitized lithologies are not common. Transitions from limestone to dolomite are generally quite narrow and occur over a scale of one or two metres. Dolomitized sections range from 200 m to 500 m thick.

The majority of the dolomitized lithologies are poorly to unlaminated micrites. Other lithologies include fenestral mudstones and fossiliferous mudstones and wackestones (chapter 6). Most of the dolomitized lithologies are moderately to strongly fractured. Fracturing directly below the Late Carboniferous-Early Permian unconformity is related to karstification. However, the majority of the fracturing and brecciation appears to have occurred penecontemporaneously with the dolomitization event (discussed below).

Replacement Dolomite

The majority of dolomite in the sequence is a replacement of lime mud. Replacement dolomite has a cloudy appearance with a crystal size ranging from 20 to 70 microns. Crystal mosaics are generally anhedral to subhedral (Fig. 48A) and crystals generally have weakly to moderately undulose extinction (xenotopic, Gregg and Sibley, 1984).

Figure 48. Photomicrographs illustrating features of the regional dolomite type. Scale bar = 1 mm in all photomicrographs.

A) Thin-section photomicrograph illustrating the subhedral to anhedral crystal mosaic in the replacement dolomite. Boab #1, 434.50 m. UTGD sample no. 70360

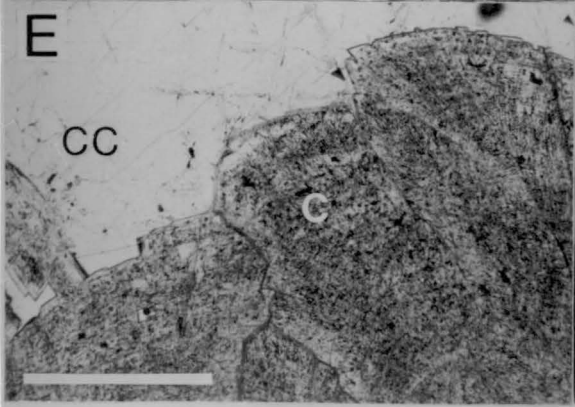
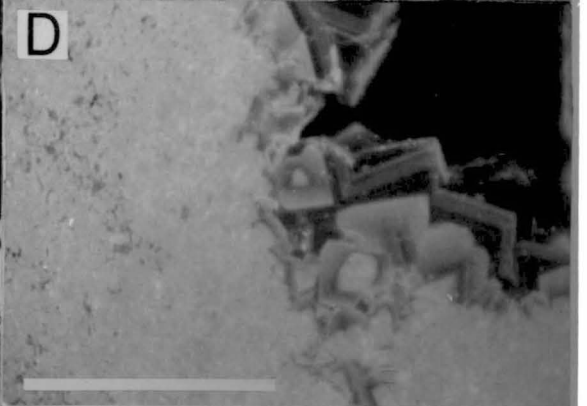
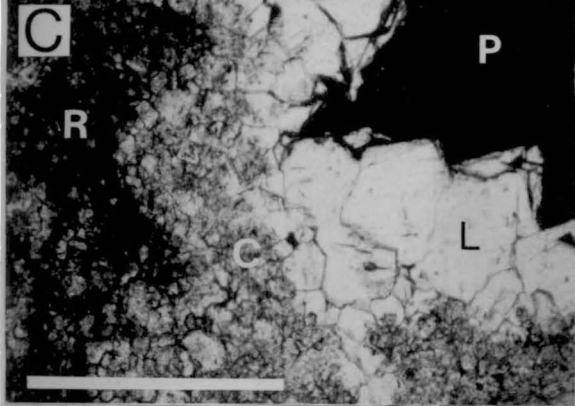
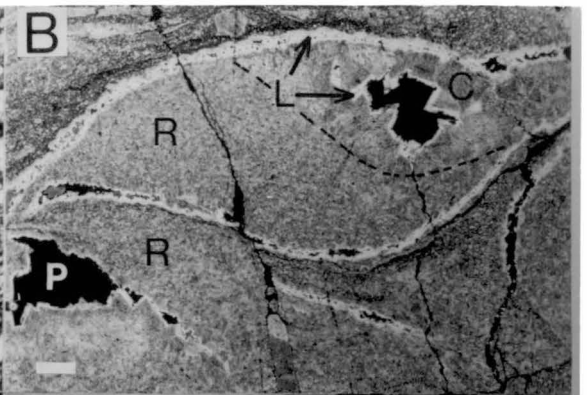
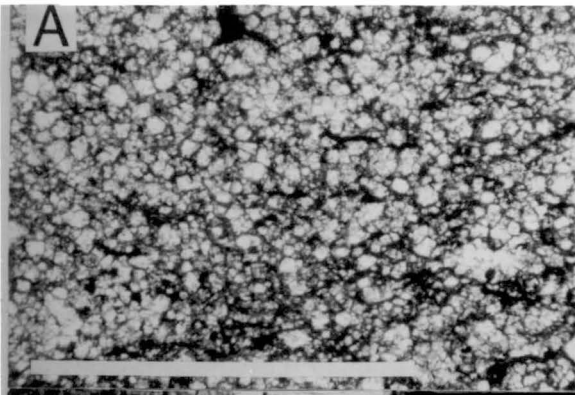
B) Thin-section photomicrograph of dolomitized brachiopod wackestone illustrating dolomite paragenesis. R = replacement dolomite, C = cloudy dolomite cement, L = limpid dolomite cement, P = pore space. Dashed line within brachiopod delineates the upper boundary of the internal sediment. The cloudy dolomite cement fills primary porosity within the brachiopod. The limpid dolomite cement fills skeletal moulds and remaining primary porosity. Note the extensive fracturing. Boab #1, 414.55 m.

C) Thin-section photomicrograph illustrating dolomite cements. Replacement dolomite (R) forming wall of cavity, overlain by cloudy dolomite cement (C), which is overlain by limpid dolomite cement (L). P = pore space. Boab #1, 434.50 m. UTGD sample no. 70360

D) Area in C under cathodoluminescence. Note the identical unzoned luminescence of the replacement dolomite and the cloudy dolomite cement. The limpid dolomite cement is zoned and has decreased luminescence in younger zones.

E) Thin-section photomicrograph illustrating cloudy saddle dolomite cement (C) overlain by poikilitic calcite cement (CC). Cassia #1, 1169.22 m. UTGD sample no. 70343

F) Electron micrograph of saddle dolomite cement, Cassia #1, 1538.00 m. UTGD sample no. 70348



Skeletal elements are less frequently dolomitized and are generally preserved as cement-filled moulds. However, crinoids, coralline forms, oncoids and brachiopods are in some cases partially or completely replaced by dolomite. Crinoids are generally the only skeletal components to be replaced syntaxially, and if replaced, retain unit extinction. Crinoids are also the most common skeletal constituents to be replaced by dolomite. Other skeletal constituents are less frequently dolomitized, and almost never retain their primary crystallographic form.

Under cathodoluminescence, dolomitized lime mud and skeletal constituents have identical uniform orange-red luminescence (Fig. 46B). Replacement dolomite luminescence remains uniform over the scale of a hand specimen (Fig. 46B-F), but over a distance of metres, luminescence may gradually change. The intensity of luminescence ranges from nil to dull.

Dolomite Cements

Cloudy Unzoned Dolomite Cement; This is the earliest dolomite cement generation and fills primary, mouldic, and fracture porosity (Fig. 46D, 48B,C). Numerous micro-inclusions of unknown origin give the cement a cloudy appearance. Individual crystals have weak to strong lattice curvature (Fig. 48B,E,F), and in many instances could be classified as saddle dolomite (Radke and Mathis, 1980). Cloudy saddle dolomite cements are very conspicuous in the well Cassia #1 (Fig. 48E,F).

Cloudy dolomite cements invariably display precisely the same luminescence characteristics as the replacement dolomite (Fig. 46C,D, 48C,D). The cement shows no zonation in transmitted light or under cathodoluminescence.

Limpid Dolomite Cement; This is the last dolomite cement lining most cavities and precipitation of this cement usually followed dissolution of all remaining primary calcite. It is therefore commonly found lining skeletal moulds but also fills fractures and unfilled primary porosity (Figs. 46C, 48B,C). Strongly ferroan zones (up to 12 mole percent by microprobe analysis) are common in this cement generation. In cathodoluminescence, the cement may be finely zoned and there is generally a decrease in the intensity of luminescence in younger zones (Figs. 46D, 48D). Luminescent zones in the limpid dolomite cement do not appear to be regionally continuous, and can only be correlated on a scale of metres.

The substrate for the limpid dolomite cement is generally the cloudy cement generation. The boundary between the two cement types is often distinct (Fig. 46C). However, there is sometimes a gradation from the cloudy to the limpid generation by a gradual decrease in the number of inclusions or by an alternation between limpid and cloudy cement.

Dolomite Paragenesis

The following evidence was used to interpret the paragenesis of the major dolomite type:

- 1) Skeletal constituents are most commonly preserved as moulds, suggesting that there was preferential dolomitization of the carbonate mud matrix (Figs. 48B).

- 2) Primary porosity is generally filled by the cloudy dolomite cement (Fig. 48B), suggesting the cloudy dolomite cement was precipitated in available pore space penecontemporaneously with the major phase of replacement dolomitization. The identical geochemistry of the replacement and cloudy dolomite cement (discussed later) supports this interpretation.
- 3) Skeletal moulds are mostly filled by the limpid dolomite cement (Fig. 48B), indicating that the remaining skeletal calcite was removed by dissolution during the later stages of dolomitization, prior to the precipitation of the limpid dolomite cement.
- 4) Fracturing and brecciation is very common in the dolomite and often the fractures are lined by cloudy and clear dolomite cements (Fig. 46E). This suggests fracturing was initiated early in the history of dolomitization.

Timing of Regional Dolomitization

Regional dolomitization of the shallow-water carbonates in the sequence was the most widespread and important diagenetic event affecting the carbonates and it is therefore important to be able to establish the timing of this major event. Dolomite clasts occur in the basal conglomerates of the Grant Formation which unconformably overlies the Devonian carbonates and this indicates that dolomitization occurred prior the Late Carboniferous.

The presence of dolomitized wavy stylolites (Fig. 47C,D), microstylolites in dolomitized muddy lithologies and pressure solution impaction structures between dolomitized skeletal components suggests that regional dolomitization occurred after significant pressure solution had taken place. This suggests that regional dolomitization took place while the carbonates were subject to Late Devonian - Early Carboniferous burial diagenesis. Figure 49 diagrammatically illustrates the interpreted paragenesis and timing for the regional dolomites in Boab #1.

Dolomite Geochemistry

Isotope data for the regionally dolomitized lithologies of the Barbwire Terrace are presented in Fig. 50. The replacement dolomite of the major dolomite type has $\delta^{18}\text{O}$ values ranging from -9 to -2 ‰ (PDB). Where analysed, dolomitized skeletal components have identical isotope ratios to the dolomitized carbonate mud that surrounds them.

Cloudy dolomite cements of the major dolomite type have similar $\delta^{18}\text{O}$ and $\delta^{13}\text{C}$ values to the replacement dolomite that surround them. This supports the interpretation that the replacement dolomite and the cloudy dolomite cement are derived from the same solutions. Very few limpid cements were collected, due to the difficulty of sampling the thin rims. Those that were collected have $\delta^{18}\text{O}$ values ranging from -7 to -4 ‰ (PDB) and $\delta^{13}\text{C}$ values ranging from -2 to -1 ‰ (PDB) which are lower than the cloudy dolomite cement.

There appear to be regional variations in the oxygen isotope ratios of the major dolomite type (both replacement dolomite and cloudy dolomite cement). In Cassia #1 for example, the dolomite has $\delta^{18}\text{O}$ values ranging from -9 to -7 ‰ (PDB). In the well closest to Cassia #1 (Halgalania #1) the dolomites also have low $\delta^{18}\text{O}$ values { -7

to -6‰ (PDB)}. This may indicate a basinward lightening trend for oxygen isotopes. However, there are too few wells in the region to confirm this.

Trace element data for the regional dolomites is shown in Figs. 44 and 45. Replacement dolomite from the regional dolomites have strontium contents ranging from 30 to 100 ppm and sodium contents ranging from 50 to 1600 ppm. Iron contents range from 0.2 to 2 mole percent and manganese contents range from 180 to 560 ppm. Manganese and iron values are positively correlated. Replacement dolomite from the regional dolomite contains between 50.0 and 51.5 mole percent calcium.

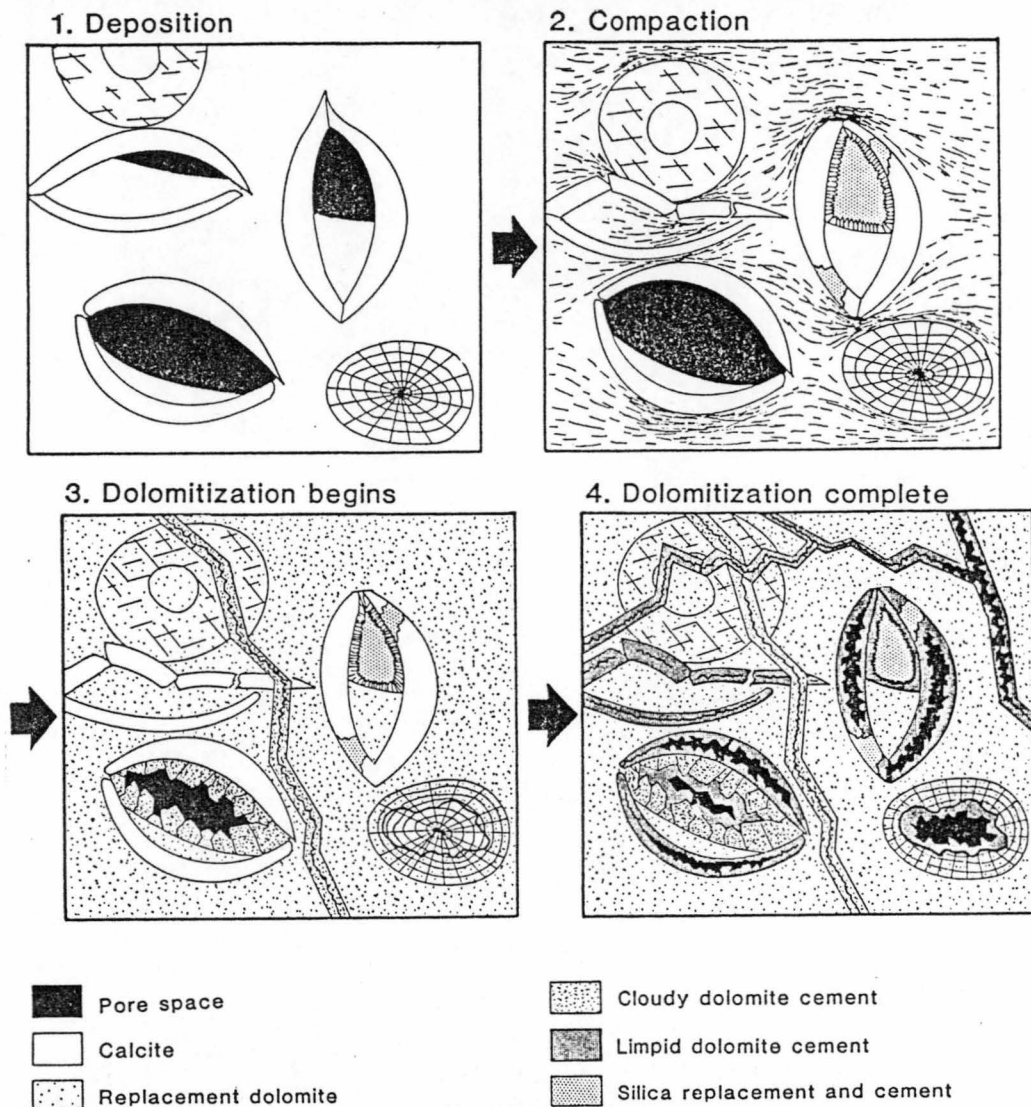


Figure 49. Diagram illustrating the interpreted paragenetic sequence for the regional dolomites in Boab #1. 1) The lithology at deposition with brachiopods, crinoid, coralline skeletal component and primary porosity. 2) The lithology was subject to mechanical compaction and pressure solution. Ferroan calcite cementation, silicification and quartz cementation occurred sporadically. Clay seams and microstylolites develop within the matrix. 3) During the initial stages of regional dolomitization, the matrix and some skeletal constituents were preferentially dolomitized. Cloudy dolomite cements precipitated in primary and fracture porosity. 4) During the final stages of regional dolomitization, calcite dissolution occurred, producing mouldic porosity. Limpid dolomite cement precipitated in mouldic, fracture and primary porosity.

Origin of Regional Dolomitization

Petrographic Interpretation

The paragenesis of the regional dolomite type suggests initial preferential dolomitization of the more finely crystalline carbonate in fluids saturated with calcite. The cloudy dolomite cement was precipitated during this phase. Dissolution of calcite appears to have begun just prior to the transition from cloudy to limpid dolomite cement precipitation in most cases. The cloudiness of the early cement may be analogous to the "swiss cheese" texture of Katz and Matthews (1977), who concluded the texture resulted from the dissolution of high magnesium calcite inclusions formed during the transformation of calcite to dolomite.

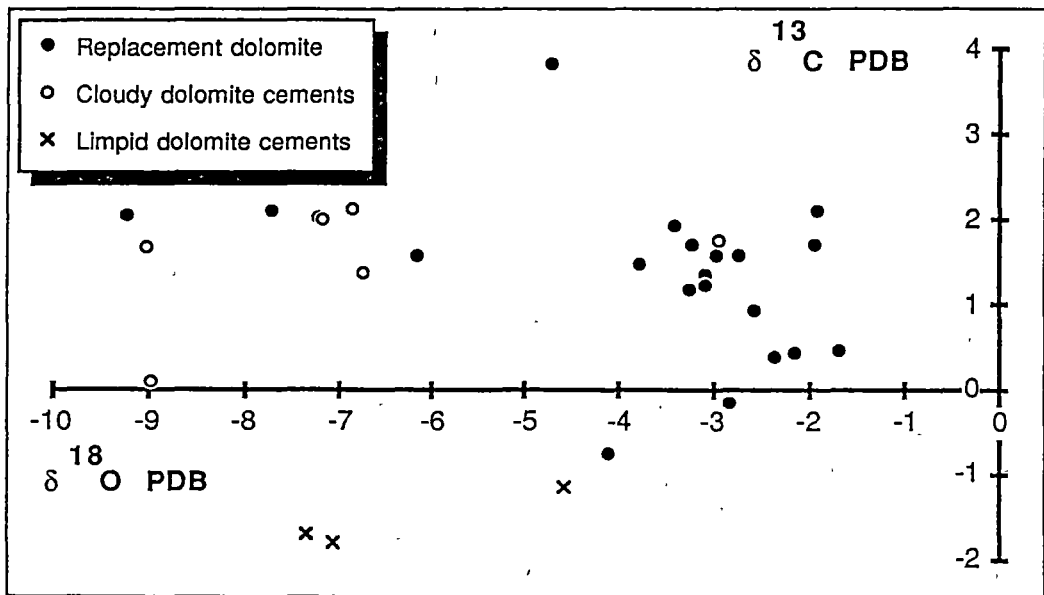


Figure 50. Carbon and oxygen isotope values for the regional dolomites

The transition from early cloudy to late limpid dolomite is a common feature of dolomites and Sibley (1980) suggested this phenomenon was due to pore waters changing from calcite-saturated to calcite-undersaturated during diagenesis. In the major dolomite type of the Barbwire Terrace, the dissolution of calcite is approximately but not exactly coeval with the change from cloudy to limpid dolomite, as in some cases, the cloudy dolomite cement lines mouldic porosity.

Geochemical Interpretation

Carbon and oxygen isotope ratios; The highest $\delta^{18}\text{O}$ values found in the major dolomite type roughly correspond to the estimated Devonian marine dolomite composition ($\delta^{18}\text{O} = -2.0/00$ (PDB)). However, the majority of samples from the major dolomite type have much lower $\delta^{18}\text{O}$ values {as low as $-9.0/00$ (PDB)}. This could be due to :-

- dolomitization at elevated temperatures and/or
- non-marine pore fluids participating in dolomitization.

It appears unlikely that oxygen isotope ratios of the dolomite could be inherited from the precursor carbonate. For example, using sea water as the dolomitizing agent,

the volume of water required to dolomitize a given volume of rock far exceeds the requirement for an open system with respect to oxygen (using Taylor's (1978) approximation to an open system). The oxygen isotope ratio of the dolomite should therefore reflect the oxygen isotopic composition of the dolomitizing waters.

Dolomite strontium contents; Estimates of the strontium content of modern marine dolomite range from 245 ppm (Baker and Burns, 1985) up to 600 ppm (Veizer, 1983) depending on the dolomite-water partition coefficient that is used (Katz and Matthews, 1977; Jacobson and Usdowski, 1976; Baker and Burns, 1985). The strontium contents of some modern dolomite types are shown in Fig. 44.

The regional dolomite has strontium contents ranging from 30 to 100 ppm and are thus lower than the lowest estimate for modern marine dolomites (Katz and Matthews, 1977). As indicated by Veizer et al. (1978), dolomites with strontium contents lower than marine values cannot be explained by meteoric-marine mixing dolomitization. For the range of mixing over which dolomite is saturated and calcite is undersaturated (Wigley and Plummer, 1976), the strontium to calcium ratio remains essentially the same as marine water so that any dolomite precipitated will have a marine strontium content.

Low strontium contents are quite common in ancient dolomite sequences (Weber, 1964; Tucker, 1983). Veizer *et al.*, (1978) have proposed that dolomitization in systems with low water/rock ratios can account for the low strontium content of ancient dolomites. However, it appears more likely that relatively high water/rock ratios would be needed for complete dolomitization and the strontium content of the dolomite would be largely, if not completely controlled by the pore water composition.

Other alternatives to explain the low strontium contents in the major dolomite type are:-

- a) A reduction of the strontium partition coefficient at high temperatures. Katz and Matthew's (1977) experiments at 250 to 300°C suggest a partition coefficient which is lower than most other estimates. In addition, Moore (1985) found very low strontium contents (<100 ppm) in calcite cements which appear to have been precipitated from highly hypersaline strontium-rich brines in a burial environment.
- b) A reduction in the strontium partition coefficient due to an increased rate of precipitation (Lorenz, 1981). This appears to be the case for magnesium substitution in calcite (Given and Wilkinson, 1985). However the high strontium content of the sabkha dolomite (presumably formed at rates of precipitation higher than those of the major dolomite type) does not support this hypothesis.
- c) Diagenetic removal of strontium. Brand and Veizer (1980) found that the strontium values of carbonates is reduced during diagenesis by recrystallization in meteoric water. Clearly it is possible that meteoric pore waters invaded the Barbwire Terrace dolomites at some stage in their diagenesis and it is possible that the low strontium content of the major dolomite type is due to recrystallization in meteoric water.

Dolomite sodium contents; The sodium contents of the Barbwire Terrace dolomite types and modern dolomite types are shown in Fig. 44. The interpretation of sodium contents in dolomite is difficult because sodium can be held within the dolomite lattice and within inclusions as NaCl. The possibility of sodium contamination from clay minerals during analysis cannot be excluded (Baum, Harris, and Drez, 1985). Since

sodium partition coefficients are poorly known (Land, 1980) and the element is thought to be more mobile during diagenesis than strontium (Veizer, 1983), little emphasis has been placed on the interpretation of sodium data.

Iron and manganese content of dolomites; Iron and manganese are redox sensitive and the high contents of these elements in the regional dolomites probably indicates that the dolomitizing fluids were reduced (Fig. 45).

Major element composition of dolomites; Morrow (1982) summarized the available data on dolomite stoichiometry and divided dolomites into three groups based on the calcium content. Near stoichiometric dolomites like the regional dolomite (with compositions ranging from 50 to 51.5 mole percent calcium) are interpreted by Morrow (1982) to have precipitated from very dilute waters possibly at elevated temperatures in a subsurface environment. This interpretation appears to be based largely on a few modern dolomites, where it is observed that the Mg/Ca ratio of the precipitating waters partially controls the calcium content of the precipitated dolomite. Morrow (1982) believes this is due to the kinetic difficulties of precipitating dolomite in surface waters. However, it may be possible to produce stoichiometric dolomite in solutions with a wide range of Mg/Ca ratios in pore solutions of burial environments owing to possible variations of thermodynamic conditions. For this reason, little emphasis has been placed on the interpretation of the stoichiometry of the dolomite on the Barbwire Terrace.

Regional Dolomitization Models

Petrographic evidence from the regional dolomite type suggests dolomitization was a relatively late diagenetic event (post-compaction, post-silica and calcite cementation). The xenotopic form of replacement dolomite and the saddle shape of the cloudy dolomite cement are often considered to indicate elevated temperatures of precipitation (Choquette, 1971; Radke and Mathis, 1980; Gregg and Sibley, 1984;). The $\delta^{18}\text{O}$ values in the dolomites are very low where saddle dolomite cements are well developed, suggesting that the oxygen isotopic variation in the dolomites may be partially temperature controlled. The greatest isotopic variation in the dolomites occurs over a regional scale, rather than with depth. This would appear to rule out the possibility of sequential dolomitization in near-surface environments (near-surface dolomitization should produce "layer cake geochemistry", Machel and Mountjoy, 1986).

With regard to the geochemistry of the major dolomite type, it appears significant that in any one sample of dolomite, dolomitized lime mud, dolomitized skeletal constituents and the cloudy dolomite cement have no chemical zonation and are all geochemically identical. The limpid dolomite cement is generally the only constituent which may be geochemically distinct and is zoned. This indicates a major recrystallization event and open system conditions prior to the precipitation of the limpid dolomite cement.

The range of oxygen isotope ratios for the major dolomite type can be explained by postulating Upper Devonian marine waters (estimated earlier) as agents for dolomitization at temperatures ranging from 30 to 70°C (using the dolomite-water fractionation curve of Sheppard and Schwarz, 1970). However, if solutions with

$\delta^{18}\text{O}$ values higher than Devonian marine waters were involved in dolomitization, even higher temperatures of precipitation would be indicated.

A burial dolomitization model would seem to be most compatible with the petrographic evidence for a late diagenetic origin, elevated temperatures of dolomitization, regional geochemical variations and low $\delta^{18}\text{O}$ values. Several dolomitization models ~~are~~ which appear compatible with the above data are discussed below. X

Model 1 - Burial compaction; It appears possible that large volumes of heated basinal compaction brines entered and dolomitized the carbonates of the Barbwire Terrace during Late Devonian - Early Carboniferous burial diagenesis. Playford (1984) and Kerans (1985) have suggested a similar model for dolomites of a similar age associated with Mississippi Valley type lead-zinc deposits in the Lennard Shelf reef complexes (it should be noted that small amounts of galena and sphalerite are dispersed throughout the dolomites of the Barbwire Terrace, discussed earlier). Kerans (1985) has suggested that a major subsidence and dewatering event in the Mid-Carboniferous (Middleton, 1984) may have caused large volumes of heated basinal water to be expelled from the Fitzroy Trough into shallow basin-margin settings.

However, a vast volume of dolomite is present on the Barbwire Terrace (greater than 500 m thick over an area of several hundred km^2) and consequently an equally vast amount ^{of} magnesium is required for dolomitization. Land (1985) calculated that 432 volumes of sea water are required to dolomitize 1 volume of limestone initially having 6.3 mole percent MgCO_3 at 25°C , assuming constant partial pressure of CO_2 {Land (1985) presented the result as 648 pore volumes to completely dolomitize a sediment with 40% porosity}. ^

The volume of dolomite in the study area on the Barbwire Terrace is estimated to be about 1250 km^3 ($2500 \text{ km}^2 \times 500 \text{ m}$ thick). Given that the combined porosity and argillaceous matter content is approximately 30%, the total volume of the mineral dolomite is estimated to be approximately 875 km^3 ($1250 \text{ km}^3 \times 70\%$). This volume of dolomite would have required $3.8 \times 10^5 \text{ km}^3$ ($432 \times 875 \text{ km}^3$) of pore water if dolomitization had occurred in a solution with a Mg/Ca ratio similar to sea water.

The Fitzroy Trough contains approximately $1.8 \times 10^5 \text{ km}^3$ (100 km wide x 600 km long x 3 km thick) of Devonian-Lower Carboniferous sediment and this could not have produced a sufficient volume of marine-like connate water during compaction to dolomitize the sediments of the Barbwire Terrace, even if all the compaction fluids were concentrated into the one region.

But to add to this problem: a) the volume of dolomite on the Barbwire Terrace is probably much greater than that estimated because the dolomite almost certainly continues outside the study area; b) basinal brines are commonly depleted in magnesium relative to sea water (Land, 1985).

It is therefore difficult to explain the Barbwire Terrace dolomitization by means of a burial compaction model if the only supply of magnesium is from connate sea water. However if there was some other source of magnesium within the basin (e.g. magnesium salts, connate magnesium-rich evaporitic brines or rock-water interactions like clay mineral transformations), it might be possible to produce larger volumes of dolomitizing fluids.

Model 2 - Burial dolomitization by topography driven flow; This has been suggested as a mechanism to move large volumes of water in burial environments and has been suggested as a way of producing regionally extensive dolomites (Gregg, 1985; Machel and Mountjoy, 1986). This burial flow model is theoretically capable of pumping greater volumes of water through carbonate sequences than is the burial compaction model because surface meteoric water is brought into the burial environment. However it is unlikely that meteoric water would supply magnesium for dolomitization and if the only source of magnesium is connate sea water, the same volume problems will be encountered as in burial compaction models. In addition, the Barbwire Terrace is situated approximately 200 km from the nearest basin margin and it is difficult to envisage topography driven flow being important during the Late Devonian-Early Carboniferous period of active subsidence.

Model 3 - Burial dolomitization by deep thermal convection; Deep thermal convection is a process which could theoretically circulate sufficient volumes of marine or evaporitic brines from the surface into deep burial environments to dolomitize large volumes of carbonate. Fanning *et al.* (1981) have suggested that dolomitization is occurring by this mechanism in Florida. However there have been no examples of massive dolomites formed by deep thermal convection reported to date.

Model 4 - Karstic dolomitization; Dolomites from the Zohar and Shderot Formations of Israel of Israel (Buchbinder *et al.*, 1984) have many characteristics in common with the Barbwire Terrace dolomites (similar $\delta^{18}\text{O}$ and $\delta^{13}\text{C}$ values, similar petrographic characteristics). Based largely on the hydrogen isotope composition of fluid inclusion waters from saddle dolomites and the association with a regional unconformity, Buchbinder *et al.* (1984) have suggested a meteoric karstic-related origin for the dolomites. The Barbwire Terrace dolomites are also associated with a regional unconformity and a similar karstic mixing-zone model could be applied. However, several features of the dolomites are difficult to explain using this model:

a) The $\delta^{13}\text{C}$ values of the dolomites are relatively high and suggest there was no contribution from biogenic soil carbon. Soil carbon would be expected to participate in karstic-related dolomitization.

b) It is difficult to envisage a sufficiently large source of magnesium for dolomitization if the system, was dominated by meteoric water.

Model 5 - Dolomitization in a near-surface environment with a major recrystallization event superimposed during burial diagenesis; As discussed, the lack of geochemical zonation in the replacement dolomite suggests a major recrystallization event. In this model, the geochemistry of the dolomites can be explained as simply reflecting the burial recrystallization event and the original geochemistry of the dolomite has been obliterated (Land, 1980; Hardie, 1987). Some of the petrographic features of the dolomite can be similarly explained. The coarse crystal size and xenotopic form of the dolomite may have been produced during recrystallization. Saddle dolomite cements may have been precipitated during burial recrystallization. Dolomitized stylolite textures may have developed by crystal growth during recrystallization. Dolomitized calcite and silica cements may have been dolomitized during the recrystallization event.

Such wholesale geochemical and fabric alteration could only occur if a) the dolomite was originally precipitated as metastable partly ordered phase; or b) The dolomite was precipitated as ordered dolomite but immense volumes of pore water passed through the dolomites during burial diagenesis. The second alternative appears unlikely as such massive recrystallization does not occur in similarly stable low-magnesium calcites in the burial environment. In addition, Land (1980) has suggested that dolomite is less susceptible to recrystallization than is calcite. It therefore seems likely massive recrystallization could only occur if the dolomite was originally precipitated as a metastable phase and this hypothesis is analogous to the recrystallization of aragonite to low magnesium calcite during diagenesis (Land, 1980).

If such a recrystallization event has occurred during burial, virtually all of the present petrographic and geochemical characteristics of the dolomite would be irrelevant to the problem of the initial dolomitization mechanism. Without more data on the initial dolomite type, several near-surface dolomitization models could be used to explain the origin of the dolomites on the Barbwire Terrace (hypersaline reflux, shallow-subtidal dolomitization, etc.).

Dolomite Diagenesis

The regionally dolomitized lithologies display a quite different set of diagenetic phases from those in the undolomitized lithologies. Fracturing and brecciation is very common in the regional dolomites. The major cements in the dolomites are poikilitic dull cements. Minor sulphides are also present. Directly below the Grant unconformity, dolomite dissolution and equant calcite cementation is common.

Sulphide Precipitation

Pyrite, and more rarely galena and sphalerite, occur sporadically as cements throughout the carbonates. These sulphides overlie and post-date the limpid dolomite cements associated with the regional dolomitization event.

Dolomite Dissolution

Extensive dissolution of dolomite has occurred to a depth of 200 m beneath the Late Carboniferous unconformity. Dolomite dissolution has produced vuggy, cavernous, intercrystalline and intracrystalline porosity. From petrographic and geochemical observations, the following factors appear to affect dolomite dissolution:

- 1) The greater the iron content, the more susceptible the dolomite is to dissolution. Hollow dissolution zones in dolomite crystals (Fig. 46F) can be correlated with strongly ferroan zones (up to 12 mole% by microprobe analysis) (Fig. 51). Ward and Halley (1985) have similarly suggested that calcian dolomites can be more readily dissolved than more stoichiometric dolomites.
- 2) More impure dolomites appear to be less susceptible to dissolution than are the clay-free dolomites. In dolomite lithologies with anastomosing clayey seams, the more pure dolomites between the seams have been preferentially dissolved. If the dissolution is extensive, the more pure dolomites are completely dissolved, leaving vugs which are bounded by anastomosing clayey dolomite seams.

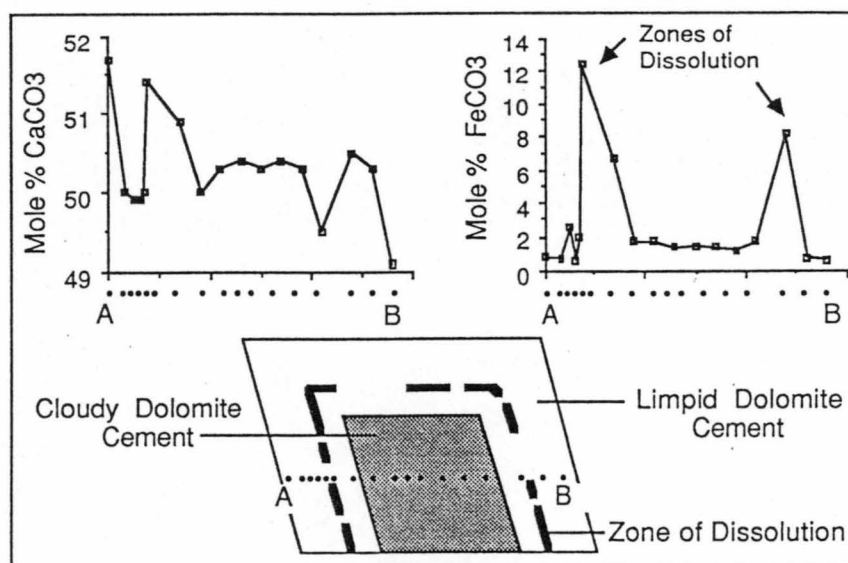


Figure 51. Diagram of microprobe traverse across a dolomite cement crystal. Hollow dissolution zones correspond to strongly ferroan zones. Boab #1, 311.00 m, UTGD sample no. 70352.

Equant Calcite Cements

Clear scalenohedral and equant calcite cements are common to a depth of 200 m beneath the Upper Carboniferous unconformity (Fig. 46G). These cements display a non-luminescent to brightly banded luminescent to dull luminescent zonation sequence (Fig. 46H). The non-luminescent portion of the cements is non-ferroan and later zones are ferroan. The non-luminescent portion of the cements is commonly partially neomorphosed and displays a patchy dull luminescence (Fig. 46H). Fracture, mouldic and vuggy dissolution porosity is occluded by the cements. The equant calcite cements have $\delta^{18}\text{O}$ values ranging from -13 to -8 ‰ (PDB) and $\delta^{13}\text{C}$ values ranging from -6.5 to -4 ‰ (PDB) (Fig. 52).

Fracturing and Brecciation

Fracturing is widespread and intense in the regionally dolomitized lithologies. The fractures are commonly lined by cloudy and limpid dolomite cements suggesting that these fractures developed during regional dolomitization (Fig. 46E). Intense fracturing and brecciation also occurs directly beneath the Upper Carboniferous unconformity.

Poikilitic Dull Calcite Cements

Poikilitic dull-luminescent calcite cements are restricted to, and occur throughout the regionally dolomitized lithologies. The cements are commonly ferroan and have a weakly-zoned dull-luminescence (Fig. 46B-E).

Poikilitic calcite cements fill mouldic, intercrystalline, fracture and primary porosity. The cements are coarsely crystalline (often >1 cm), and commonly contain

two-phase fluid inclusions. Coarse poikilitic calcite cements overlie and post-date both sulphides and limpid dolomite cements. Poikilitic calcite cements do not occur in association with the equant calcite cements beneath the Late Carboniferous unconformity.

The dull luminescent poikilitic calcite cements have $\delta^{18}\text{O}$ values ranging from -18 to -12 ‰ (PDB) and $\delta^{13}\text{C}$ values ranging from -6.5 to -2.5 ‰ (PDB) (Fig. 52).

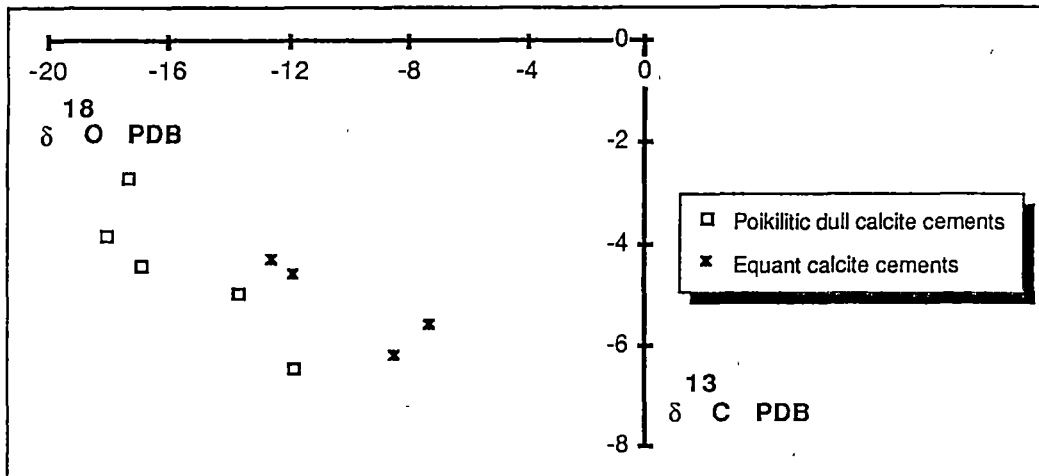


Figure 52. Carbon and oxygen isotope compositions of calcite cements within the regional dolomites.

Discussion of Dolomite Diagenesis

Sulphide Precipitation

Sulphide precipitation is interpreted to have occurred during burial diagenesis. There is insufficient data to positively assign the sulphides to Devonian - Carboniferous burial or Permian - Cenozoic burial diagenesis. However, it seems most likely that the sulphides developed during Devonian-Carboniferous burial diagenesis.

Dolomite Dissolution

Dolomite dissolution is interpreted to have occurred during Late Carboniferous - Early Permian meteoric diagenesis because dissolution is restricted to the zone beneath the Grant unconformity. It appears likely that the ferroan dolomites were preferentially dissolved because the meteoric waters were strongly oxidized. The clayey dolomites were probably not subject to extensive dissolution because of their low permeability.

Equant Calcite Cements

These cements are interpreted to be of Late Carboniferous - Early Permian meteoric origin because they: a) only occur in close proximity the Grant unconformity; b) post-date dolomite dissolution; and c) have low $\delta^{13}\text{C}$ values suggesting a contribution from biogenic soil carbon (Allan and Matthews, 1982).

Hurley (1986) also found that calcite cements associated with the Late Carboniferous unconformity on the Lennard Shelf had $\delta^{18}\text{O}$ values that range from -7 to -9.5 ‰ (PDB).

Fracturing and Brecciation

The regional dolomites of the Barbwire Terrace appear to have been subject to several episodes of fracturing and brecciation. Many fractures were developed contemporaneously with dolomitization. Other fractures developed after dolomitization and it appears likely that these are a reaction to the overburden (and tectonic?) stress applied to the dolomites.

Fracturing in the regional dolomites is particularly common beneath the Grant unconformity. These fractures are interpreted to be the result of meteoric leaching followed by sediment loading during Permian - Cenozoic burial diagenesis. Much of the vuggy dissolution porosity probably collapsed during mechanical and chemical compaction, causing extensive fracturing.

Poikilitic Dull Cements

Poikilitic dull cements are interpreted to be of Permian - Cenozoic deep-burial origin because they a) display a weakly-zoned dull-luminescence and are ferroan; b) contain abundant two-phase fluid inclusions suggesting precipitation at elevated temperatures; c) are the youngest diagenetic phases in the carbonates; and d) have strongly negative $\delta^{18}\text{O}$ values, also suggesting precipitation at elevated temperatures. However, it is possible that they are partly of Devonian - Carboniferous age.

The poikilitic nature of the cements is interpreted to be the result of a very low nucleation density. This is likely to have been due to: a) the absence of a calcitic substrate for syntaxial crystal growth; and b) the low saturation level of the precipitating waters.

The dull-luminescent zone overlying non-luminescent and brightly banded luminescent equant calcite cements beneath the Grant unconformity may be equivalent to the poikilitic dull calcite cements occurring elsewhere in the dolomites. Dull-luminescent calcite neomorphism may also have occurred during Permian - Cenozoic burial diagenesis.

The low $\delta^{18}\text{O}$ values of the dull poikilitic calcite cements are consistent with a deep-burial origin and high temperatures of precipitation. The low $\delta^{13}\text{C}$ values may indicate that organic reactions took place during burial which released organic carbon into the pore waters. The isotopic composition of the poikilitic dull cements on the Barbwire Terrace is similar to the late dull cements in the Geikie Gorge region, also interpreted to be of Permian - Cenozoic burial origin. Hurley (1986) also found coarsely-crystalline ferroan-calcite cements in the Oscar Range reef complexes which had similar isotopic compositions and which he suggested were of Permian or later age.

Compaction

Both physical compaction and pressure solution (chemical compaction) were important processes in the diagenetic history of the Devonian carbonates on the Barbwire

Terrace. Unequivocal compaction features observed in these carbonates include grain-breakage, pressure solution at grain contacts, and pressure solution along larger surfaces (stylolites). However, petrographic evidence (described below) suggests that the most important compaction structures may be the abundant anastomosing clay seams in the carbonates.

In the Devonian carbonates of the Barbwire Terrace, anastomosing clay seams are very common and range in thickness from less than a millimetre, up to a centimetre. Three major types of clay seam networks can be recognized in the carbonates (Fig. 39). The principal variant controlling the type of structures developed is the amount of argillaceous matter in the carbonates: 1) In relatively pure lithologies (skeletal wackestone lithotope), thin isolated anastomosing clay seams and classical stylolites are developed; 2) In more impure carbonates (skeletal wackestone and impure lime mudstone lithotopes), networks of anastomosing clay seams are developed and this gives the lithology a "breccoid" appearance (Fig. 39A,B); 3) In marls and calcareous shales, very thick clay seams are developed and this gives a nodular appearance to the lithologies (Fig. 39C,D). The following petrographic observations give clues to the origin of the clay seams:

- 1) Skeletal components within clay seams invariably have intraskeletal sediment which has a much higher proportion of carbonate than in the surrounding clay seam (Fig. 39E).
- 2) The boundary between clay seams and the host commonly consist of a zone of microstylolites (Fig. 39F).
- 3) Skeletal components within the clay seams have commonly suffered extensive pressure solution (Fig. 39G). Skeletal components within the host carbonate have generally not suffered such extensive pressure solution.
- 4) All transitions from thin isolated clay seams and sutured stylolites, to breccoid networks of clay seams, to nodular structures can be observed (Fig. 39A-D).

Observation 1 is best explained if the clay seams are a result of a compaction phenomena. Intraskeletal sediments were sheltered from compaction and so clay seams did not form. Observations 2 and 3 suggest that pressure solution has occurred within the clay seams. Observation 4 suggests that all of the clay seam structures share a common origin.

Origin of Clay Seams

From the above observations, it is concluded that the clay seams in the Barbwire Terrace carbonates are largely the result of chemical compaction during burial (i.e. the clay seams are non-sutured solution seams, Wanless, 1979; Choquette and James, 1987). However it appears likely that depositional features played a role in the distribution and development of clay seams. For example, Shinn and Robbin (1983) have demonstrated that wavy organic "stylolite-like" laminae can develop from primary organic structures (sea grass blades and roots) by simple mechanical compaction. Shinn and Robbin (1983) suggested that these might later act as sites for preferential pressure dissolution. Early diagenetic nodule or burrow structures would also influence the geometry of diagenetic clay seams. In addition, any depositional lamination in the carbonates is likely to be accentuated during compaction (Ricken, 1986).

Porosity Development and Occlusion

Significant porosity development is restricted to the regionally dolomitized carbonates. The porosity distribution is therefore controlled by a Late Devonian - Early Carboniferous burial diagenetic event. However, the regional dolomite distribution was probably controlled by the porosity distribution in the primary carbonates (discussed above). The end result is that the sediments which had the most porosity during early diagenesis (peritidal and shallow subtidal lithotopes) were regionally dolomitized and their porosity was further enhanced. In contrast, impermeable, clayey carbonates were not dolomitized and were subject to pressure solution and calcite cementation, effectively removing all primary porosity.

The major factors governing porosity in carbonates are, in order of priority: a) regional burial dolomitization; b) meteoric leaching during subaerial exposure; c) calcite cementation during subaerial exposure and later burial diagenesis.

Regional dolomitization was by far the most significant process which produced and preserved porosity in the sequence. There are several reasons for this:

- a) Calcite dissolution occurred during the later stages of dolomitization.
- b) Extensive fracturing occurred during and after dolomitization.
- c) Porosity in the dolomites was not destroyed by pressure solution or cementation.

Porosity types developed and preserved as a result of Late Devonian - Early Carboniferous regional dolomitization include intercrystalline, mouldic, fracture, fenestral, primary interparticle and primary intraparticle porosity. Of these, fracture and intercrystalline porosity is the most important. Although primary interparticle and intraparticle porosity is still present within the regional dolomites, they are very minor porosity types. This is probably a result of: a) the original paucity of primary porosity in this fine-grained low-energy peritidal sequence; b) the loss of primary porosity during compaction and pressure solution which occurred prior to the regional burial dolomitization event. Primary fenestral porosity is locally significant in the regionally dolomitized upper intertidal lithotopes.

In ancient peritidal sequences, it is common for the intertidal and shallow subtidal facies to be the most porous units at deposition (Rogers, 1971). Shinn (1983b) presented a stratigraphic trap model for peritidal carbonates in which evaporitic supratidal sediments formed the seals and porous subtidal and intertidal carbonates formed the reservoir facies. In the Devonian carbonates of the Barbwire Terrace, the initial porosity in the intertidal and shallow-subtidal lithologies was greatly increased during burial dolomitization. It therefore seems likely that stratigraphic (and structural) traps may have developed within the porous dolomitized intertidal and shallow-subtidal lithologies which flank supratidal sabkha island lithologies in the sequence.

Late Carboniferous - Early Permian meteoric leaching of the regional dolomites produced intercrystalline and intracrystalline, vuggy and cavernous solution porosity directly below the Grant unconformity (selective ferroan-dolomite dissolution, discussed above).

The major porosity-reducing diagenetic phases in the carbonates include the limp dolomite cements associated with regional burial dolomitization, the Upper

Carboniferous - Lower Permian meteoric calcite cements, and the poikilitic dull calcite cements (discussed above). The interpreted porosity paragenesis within the regionally dolomitized carbonates is illustrated in Figure 53.

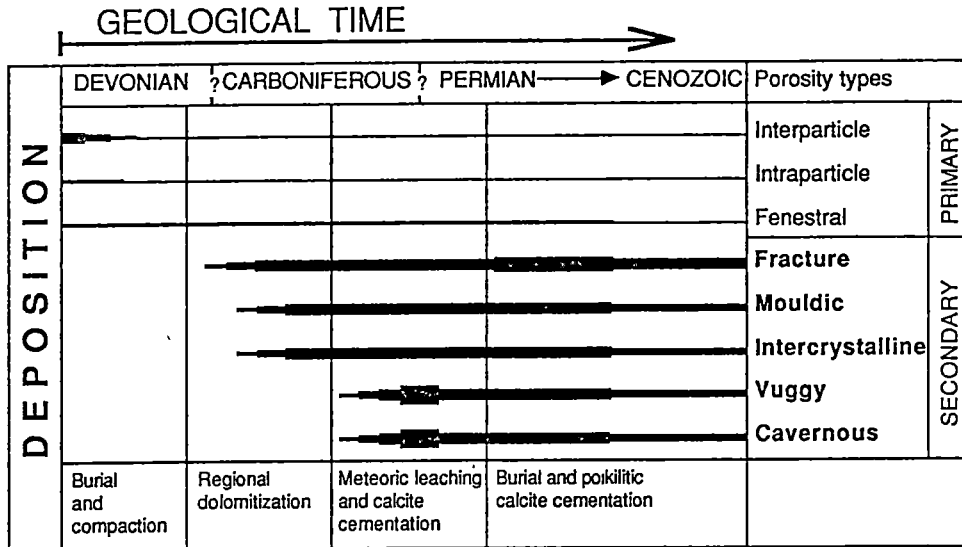


Figure 53. Interpreted porosity paragenesis in the regionally dolomitized lithologies.

Synthesis of Diagenesis

Figure 54 illustrates the interpreted paragenetic sequence for the major diagenetic processes which occurred in the Devonian carbonates on the Barbwire Terrace.

The first major diagenetic processes occurred in the Late Devonian near-surface environment and include supratidal dolomitization and supratidal anhydrite precipitation (Eremophila #1). Marine cementation was very minor in the sequence and this is probably explained by the low energy nature of the sequence. Based on the lowest oxygen isotopic values of the synsedimentary supratidal dolomite, the $\delta^{18}\text{O}$ value of Devonian marine dolomite is estimated to be around -2‰ (PDB).

The carbonates were then subject to Late Devonian - Early Carboniferous burial diagenesis. During this period, the clay-free shallow-water carbonates were completely dolomitized, with consequent mouldic, intercrystalline and fracture porosity development. The only peritidal lithologies not affected by regional dolomitization are those in the well Eremophila #1 which contain abundant early diagenetic evaporite minerals and probably acted as a permeability barrier. The more clayey carbonates were not dolomitized and were subject to extensive compaction and cementation, losing virtually all of their primary porosity. Nodular fabrics developed in the clayey lithologies as a result of pressure solution. Cements precipitated in the clayey carbonates include dull-luminescent ferroan-calcites, ferroan-dolomites, silica and anhydrite cements. The $\delta^{18}\text{O}$ values of the regional dolomites range from -9 to -2‰ (PDB) suggesting elevated temperatures of precipitation.

9. SUMMARY AND CONCLUSIONS

Sedimentology

The outcropping Devonian reef complexes of the Geikie Gorge region consist of reef-fringed carbonate platforms flanked by dipping marginal-slope deposits. The platform carbonates are all of Frasnian age and consist predominantly of shallow-water, high-energy grainstones. The older Frasnian platforms in the region have a well-developed lagoonal facies which consists of finer-grained lithologies with abundant *Amphipora* and bulbous stromatoporoids. The latest Frasnian platform carbonates consist of peloidal or ooid grainstones which commonly have a fenestral fabric. The platforms are fringed by a narrow rim (commonly less than 50 m wide) of framestones. These lithologies consist of a framework of cyanobacteria including *Renalcis* and *Sphaerocodium*. Stromatoporoids are present in the older Frasnian reef margins.

The marginal-slope carbonates of the reef complexes consist predominantly of Frasnian-Famennian peloidal grainstones and lithoclast breccias which are interpreted to have been deposited as grain-flows and debris-flows. The Frasnian-Famennian boundary is marked by a horizon of deeper water stromatolites which can be traced across the Geikie Gorge region for a distance of over 20 km. Most commonly, the stromatolites encrust steep eroded platform scarps. However, the stromatolite horizon also occurs within the fore-reef facies as a series of scalloped stromatolite beds.

Stromatactis and shelter cavities are important constituents of the upper fore-reef, reefal-slope, reef-margin and reef-flat subfacies of the Devonian reef complexes of the Canning Basin. The closely-related laminar stromatactis cavities (sheet cavities of zebra limestone) are also present in these subfacies. It is suggested that these cavity types are largely the result of the breakdown and decay of soft-bodied organisms. The cavity morphology (excluding laminar stromatactis) is probably only vaguely related to the geometry of the soft-bodied organism. It is likely that downward collapse during organic decay and subsequent internal erosion and sedimentation controlled the morphology of the final cavity system. In lithologies lacking large skeletal components, stromatactis cavities were dominant. In lithologies with large skeletal constituents, shelter cavities dominated. Where the soft-bodied organisms had a dominantly laminate morphology, zebra limestones were formed. The nature of the soft-bodied organism(s) is difficult to assess, but the common association between sponges and the various cavity types may indicate that sponges participated in cavity development. The described cavity types are commonly found in Palaeozoic mud buildups which often show a lack of preserved stabilizing organisms and it is suggested that the soft-bodied

organisms responsible for cavity development may have played an important sediment stabilizing role. It may be that a deeper water soft-bodied organic community often initiated buildup development during the Palaeozoic.

In contrast to the Lennard Shelf reef complexes, the subsurface carbonates of the Barbwire Terrace consist predominantly of low-energy peritidal and shallow-subtidal lithologies. Most of the clay-free carbonates have been very thoroughly replaced by coarsely crystalline dolomite and this has obscured much of the depositional microfabric in the lithologies. However, nine distinct lithotypes were recognized in the sequence: a) laminated dolomudstone; b) clayey dolomudstone; c) fenestral dolomite; d) massive carbonate mudstone; e) skeletal wackestone; f) skeletal grainstone-packstone; g) laminated organic-rich lime mudstone; h) skeletal-lithoclast breccia; and i) clayey lime mudstones and marls. Each of these lithotypes contains lithologies which are interpreted to have been deposited in several closely related depositional environments ranging from upper-supratidal to normal-marine subtidal conditions.

Cycles are not well developed within the peritidal lithologies. By examining the relationships between the peritidal lithotypes using the method of Selley (1970), it was possible to construct an idealized lithotype sequence. This sequence resembles that constructed for the arid tidal flats of the Persian Gulf. Because of the abundance of evaporites in the supratidal carbonates, the carbonates are interpreted to have been deposited in a warm arid environment.

The low-energy peritidal carbonates of the Barbwire Terrace are very different from the relatively high energy reef-fringed platforms of the Lennard Shelf and several hypotheses would account for these differences: a) the Barbwire Terrace carbonates of the study area may be part of a large lagoonal area on a wide reef-fringed shelf, the reefal carbonates being located in the more deeply buried basinward areas of the Barbwire Terrace; or b) the Barbwire Terrace carbonates may be leeward of a wide shelf which damped wave and storm activity.

Diagenesis

The Devonian reef complexes of the Geikie Gorge region have suffered a long and complex diagenetic history which began in Devonian sea water. Intense marine cementation and internal sedimentation occurred in the platform-margin lithologies and this occluded much of the primary porosity in the reef-margin subfacies. High-magnesium calcite cementation is inferred to be the dominant marine diagenetic phase and aragonite cements appear to have been absent. This situation is quite different from that found in modern tropical carbonate environments where aragonite is the major marine cement. The Devonian marine diagenetic processes resemble those found in Holocene low-latitude deeper-water (400 to 800 m) carbonate environments and this suggests that the chemistry of Devonian sea water was quite different from that of modern sea water. The carbonate precipitating zones of modern sea water may have been elevated during the Devonian (Fig. 55). If this hypothesis is correct, the calcite compensation depth would have been considerably higher in Devonian sea water. The different chemistry of the Devonian ocean may be related to variations in sea water CO₂ (and Mg?) concentrations (Wilkinson and Given, 1986).

In contrast, the dominant syngenetic diagenetic process in the Devonian carbonates of the Barbwire Terrace was hypersaline supratidal dolomitization. Isotope

analyses of this supratidal dolomite enable an estimate of the $\delta^{18}\text{O}$ value for Devonian marine dolomite to be made $\{\delta^{18}\text{O} = -2 \text{ ‰ (PDB)}\}$. This estimate is consistent with Hurley's (1986) estimate for radial fibrous calcite $\{\delta^{18}\text{O} = -4.5 \text{ ‰ (PDB)}\}$.

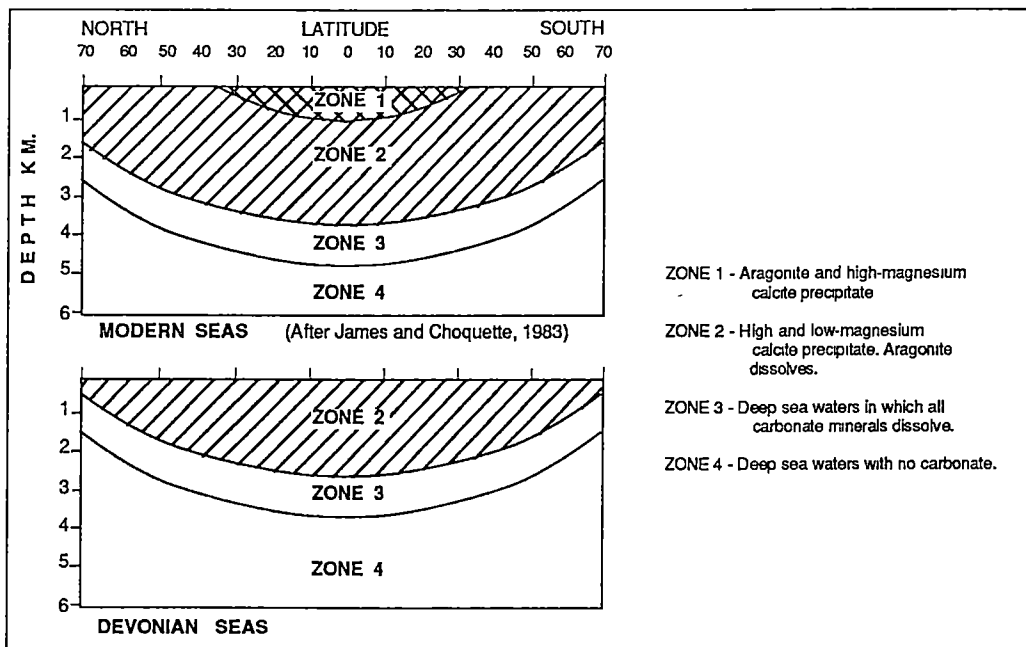


Figure 55. Diagrammatic illustration of the zones of carbonate mineral stability in the modern oceans and the interpreted zones in the Devonian oceans. The aragonite stability zone appears to have been absent in Devonian sea water. Tropical Palaeozoic sea water is believed to be similar to modern deep or non-tropical sea water.

Post-synsedimentary diagenesis in the carbonates of the Barbwire Terrace and Lennard Shelf show many similarities. In both sequences, the Devonian - Early Carboniferous burial environment was the most important episode of diagenesis. On the Lennard Shelf, almost all porosity was destroyed by calcite cementation (non-luminescent to bright-luminescent to dull-luminescent zonation) and dolomitization occurred during Devonian - Carboniferous burial. On the Barbwire Terrace, the clayey lithologies were cemented by ferroan-calcite (dull-luminescent) and the clay-free lithologies were completely dolomitized during Devonian-Carboniferous burial. Both sequences were subject to meteoric diagenesis during Late Carboniferous - Early Permian times and extensive karstification took place. Following this episode of meteoric diagenesis, both sequences were subject to burial diagenesis. Dull-luminescent calcite cements were precipitated in both sequences. The Lennard Shelf carbonates were later exhumed and subject to meteoric diagenesis during the Cenozoic. Karstification, dedolomitization and calcite recrystallization were the dominant diagenetic processes during this episode of diagenesis.

Regional dolomitization in the Barbwire Terrace carbonates produced significant secondary porosity and this was preserved during later diagenesis. On the other hand, the Lennard Shelf carbonates were not regionally dolomitized and most primary porosity in the limestones was occluded by clear-equant calcite cements of Devonian -

Carboniferous burial origin. The greater porosity preservation in the regional dolomites of the Barbwire Terrace may be due to the greater resistance of dolomite to pressure solution. This would inhibit chemical compaction and would also starve the pore waters of a source of CaCO_3 for cementation.

Some preliminary generalizations can be made about the isotopic record of diagenesis in the carbonates of the Barbwire Terrace and the Lennard Shelf (Fig. 56). Devonian - Early Carboniferous burial diagenetic phases have uniformly positive $\delta^{13}\text{C}$ values and a wide range in $\delta^{18}\text{O}$ values. The most positive $\delta^{18}\text{O}$ values correspond approximately to the estimated Devonian marine (dolomite or calcite) signatures. This isotopic signature could be interpreted to indicate that diagenesis took place in Devonian sea water-like fluids with temperatures of precipitation ranging from 25 to 70°C.

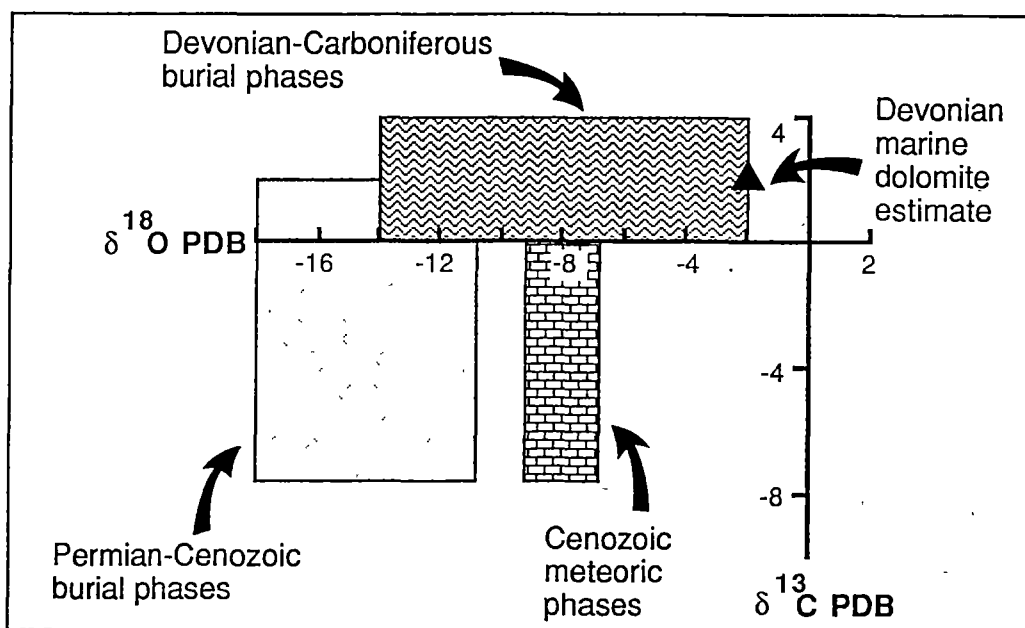


Figure 56. Generalized carbon and oxygen isotopic compositions of the diagenetic phases in the carbonates of the Barbwire Terrace and Lennard Shelf regions.

In both sequences, inferred Permian-Cenozoic burial calcite cements have variable $\delta^{13}\text{C}$ values and strongly negative $\delta^{18}\text{O}$ values. The variable $\delta^{13}\text{C}$ values suggest a biogenic carbon contribution. It may be that the pore waters were derived from terrigenous organic-rich sediments. The strongly negative $\delta^{18}\text{O}$ values indicate high temperatures of precipitation and/or low $\delta^{18}\text{O}$ meteoric waters participating in diagenesis.

The inferred Cenozoic meteoric diagenetic phases (from the Lennard Shelf carbonates) have relatively uniform $\delta^{18}\text{O}$ values ranging from -7 to -9 ‰ (PDB) and variably negative $\delta^{13}\text{C}$ values.

The Late Carboniferous isotopic signature was not positively identified in this study. Hurley's (1986) isotope data for inferred Late Carboniferous meteoric diagenetic phases suggest that it may overlap with the Cenozoic meteoric signature.

Suggestions for Further Research

Because of the outstanding exposure on the Lennard Shelf, both areally and in section, the Devonian reef complexes of the Lennard Shelf offer a unique opportunity to study the processes involved in the development of carbonate platforms with steep reef-rimmed margins. It appears probable that a greater understanding of carbonate reef sedimentology will be gained from study of these ancient reefs than is possible even from modern reefs. Potential subjects for detailed sedimentological analysis include a) the mass-flow deposits of the marginal-slope facies; b) the mechanism of reef-framework accretion; c) the regional back-reef stratigraphy and its relationship to eustatic and/or tectonic events; d) the Frasnian-Famennian boundary. Each of these subjects would be worthy of a major study.

A regional study of the back-reef subfacies on the Lennard Shelf would yield information on the sea level history of the region. Selected and detailed sections in the Pillara and Nullara Limestones (similar to the approach used by Hall, 1984; Benn, 1984; Cooper *et al.*, 1984) would provide a firm basis for regional correlations across the Lennard Shelf. For example, at the moment, it is not possible to correlate the back-reef subfacies of the Geikie Gorge region with the Oscar Range region (Hurley, 1986). Particular attention to disconformities and subaerial exposure surfaces would be important as these appear to be strangely absent from the back-reef subfacies of the reef complexes.

A study of the Frasnian-Famennian boundary within the reef complexes would also be of interest. This might include a general study of the sedimentology of the boundary sediments. The reasons for the widespread occurrence of horizons like the deeper water stromatolite unit, the *Frutexites* bed and the straight nautiloid bed (Playford, 1980; Kerans, 1985) are, at present, obscure. Resolution of the sea level history during this interval appears particularly important. The origin of prominent red colouration in the Virgin Hills Formation and the deeper water stromatolite unit also appears obscure. A detailed study to determine the distribution of platinum group elements within the sediments and the presence or absence of shocked quartz and microspherules within insoluble residues might help to resolve the meteoroid impact hypothesis.

The origin of dolomitization on the Lennard Shelf appears particularly important as the secondary porosity associated with the dolomites makes them potential petroleum reservoirs. In addition, the Mississippi Valley type mineralization is associated with dolomitization. The dolomites in the Geikie Gorge region are known to be of early burial origin and can be accurately timed relative to the calcite cement generations. The dolomites also appear to have uniform cathodoluminescent and geochemical characteristics over a wide area (Kerans, 1985).

Fluid inclusion studies on the dolomites would give important information on the temperatures of precipitation and the character of the dolomitizing fluids (salinity and hydrogen isotope characteristics of inclusion waters). This information in combination with the isotopic composition of the dolomites would characterize the types of fluids involved in dolomitization. The relationship between dolomitization and mineralization also appears important. This study would provide a rare opportunity to link the regional diagenesis of a carbonate sequence with its mineralization history.

The calcite cementation history in the carbonates of the Lennard Shelf also deserves further attention. In this report, the cementation history in primary porosity was studied in detail. However, since primary porosity was largely filled by Late Carboniferous time, this only gives a small portion of the fluid history in the carbonates. A study which concentrated on secondary porosity cementation would give a more extended record of cementation. The secondary porosity in pervasively dolomitized lithologies would provide a relatively complete record of cementation as it was relatively early formed (Late Devonian-Carboniferous early burial) and some porosity is still present in the dolomites.

The Late Carboniferous karst-related cavernous dissolution porosity should provide a detailed record of Late Carboniferous meteoric cementation, as well as later burial cementation. The Late Carboniferous meteoric isotopic signature is problematic at present. Hurley (1986) suggested a Late Carboniferous meteoric signature which is very similar to the present-day meteoric signature.

A basin-wide approach to carbonate diagenesis might also be useful in the Canning Basin. As discussed above, the carbon and oxygen isotopic composition of Devonian - Early Carboniferous burial diagenetic phases on the Barbwire Terrace and Lennard Shelf are similar. The Permian-Cenozoic burial diagenetic phases also show a similar relationship. This suggests that it may be possible to correlate the diagenetic phases over large distances. Such a study might provide data for developing models of basin hydrology.

REFERENCES

- ABBOTT, P.L., 1974, Calcitization of Edwards Group Dolomites in the Balcones fault zone aquifer, South-Central Texas: *Geology*, v. 2, p. 359-362.
- ABED, A.M., and SCHNEIDER, W., 1980, A general aspect in the genesis of nodular limestones documented by the Upper Cretaceous limestones of Jordan: *Sed. Geology*, v. 26, p. 329-335.
- ADELEYE, D.R., 1975, Derivation of fragmentary oolites and pisolites from dessication cracks: *Jour. Sed. Petrology*, v. 45, p. 794-798.
- AHARON, P., SOCKI, R.A., and CHAN, L., 1987, Dolomitization of atolls by sea water convection flow: test of hypothesis at Niue, South Pacific: *Jour. Geology*, v. 95, p. 187-203.
- AISSAOUI, D.M., BUIGUES, D., and PURSER, B.H., 1986, Model of reef diagenesis: Mururoa Atoll, French Polynesia: *in* Schroeder, J.H., and Purser, B.H., *eds.*, Reef Diagenesis: Berlin Heidelberg, Springer-Verlag, 455p.
- AITKEN, J.D., 1967, Classification and environmental significance of cryptalgal limestones and dolomites, with illustrations from the Cambrian and Ordovician of southwestern Alberta: *Jour. Sed. Petrology*, v. 37, p. 1163-1178.
- AL-HASHIMI, W.S., and HEMINGWAY, J.E., 1973, Recent dedolomitization and the origin of the rusty crusts of Northumberland: *Jour. Sed. Petrology*, v. 43, p. 82-91.
- ALI, Y.A., and WEST, I., 1983, Relationships of modern gypsum nodules in sabkhas and loess to compositions of brines and sediments in northern Egypt: *Jour. Sed. Petrology*, v. 53, p. 1151-1168.
- ALLAN, J.R., and MATTHEWS, R.K., 1982, Isotope signatures associated with early meteoric diagenesis: *Sedimentology*, v. 29, p. 797-818.
- ALVAREZ, L.W., ALVAREZ, W., ASARO, F., and MICHEL, H.V., 1980, Extraterrestrial cause for the Cretaceous-Tertiary extinction: *Science*, v. 208, p. 1095-1108.
- ASHTON, S.M., 1984, Slim hole drilling in the Canning Basin, Philosophy and application: *in* Purcell, P.G., *ed.*, The Canning Basin, W.A.: Perth, Proc. Geological. Soc. Australia/Petroleum Exploration Soc. Australia Symposium, p. 521-531.

- BAKER, P.A., and BURNS, S.J., 1985, Occurrence and formation of dolomite in organic-rich continental margin sediments: *Am. Assoc. Petroleum Geologists Bull.*, v. 69, p. 1917-1930.
- BAKER, P.A., and KASTNER, M., 1981, Constraints on the formation of sedimentary dolomite: *Science*, v. 213, p. 214-216.
- BALME, B.E., and HASSELL, C.W., 1962, Upper Devonian spores from the Canning basin, Western Australia: *Micropaleontology*, v. 8, p. 1-28.
- BATHURST, R.G.C., 1959, The cavernous structure of some Mississippian Stromatactis reefs in Lancashire, England: *Jour. Geology*, v. 67, p. 506-521.
- BATHURST, R.G.C., 1975, Carbonate sediments and their diagenesis: Amsterdam, Elsevier, 658p.
- BATHURST, R.G.C., 1977, Ordovician Meiklejohn bioherm, Nevada: *Geol. Mag.*, v. 114, p. 308-311.
- BATHURST, R.G.C., 1980, Stromatactis - Origin related to submarine cemented crusts in Paleozoic mud mounds: *Geology*, v. 8, p. 131-134.
- BATHURST, R.G.C., 1982, Stromatactis- Origin related to submarine-cemented crusts in Palaeozoic carbonate mud buildups: *Jour. Geol. Soc. London*, v. 139, p. 165-181.
- BATHURST, R.G.C., 1983, Neomorphic spar versus cement in some Jurassic grainstones: significance for evaluation of porosity evolution and compaction: *Jour. Geological Soc. Lond.*, v. 140, p. 229-237.
- BAUM, G.R., BURLEIGH HARRIS, W., and DREZ, P.E., 1985, Origin of dolomite in the Eocene Castle Hayne Limestone, North Carolina: *Jour. Sed. Petrology*, v. 55, p. 506-517.
- BEARD, J.S., and WEBB, M.J., 1974, Great Sandy Desert, 1:1,000,000 vegetation series, explanatory notes to sheet 2: Nedlands, W.A., University of Western Australia Press, 66p.
- BEGG, J., 1987, Structuring and controls on Devonian reef development on the north-west Barbwire and adjacent Terraces, Canning Basin: *Jour. Australian Petroleum Exploration Assoc.*, v. 27, p. 137-151.
- BEHRENS, E.W., and LAND, L.S., 1972, Subtidal Holocene dolomite, Baffin Bay, Texas: *Jour. Sed. Petrology*, v. 42, p. 155-161.
- BELLANCA, A., and NERI, R., 1986, Evaporite carbonate cycles of the Messinian, Sicily: stable isotopes, mineralogy, textural features, and environmental implications: *Jour. Sed. Petrology*, v. 56, p. 614-621.
- BELLIERE, J., 1953, Note sur le calcaire Famennien de Baelen et ses stromatactis: *Ann. Soc. Geologique Belgique*, v. 76B, p. 115-128.
- BENN, C.J., 1984, Facies changes and development of a carbonate platform, East Pillara Range: *in Purcell, P.G., ed., The Canning Basin, W.A.: Proc. Geological Soc. Aust./Petroleum Exploration Soc. Aust. Symposium Perth*, p. 223-228.
- BLACK, W.W., 1952, The origin of the supposed tufa bands in Carboniferous reef limestones: *Geological Magazine*, v. 89, p. 195-201.

- BLATTNER, P., and HULSTON, J.R., 1978, Proportional variations of geochemical $\delta^{18}O$ scales - an interlaboratory comparison: *Geochim. Cosmochim. Acta*, v. 42, p. 59-62.
- BOSELLINI, A., and HARDIE, L.A., 1973, Depositional theme of a marginal marine evaporite: *Sedimentology*, v. 20, p. 5-27.
- BOURQUE, P.-A., and GIGNAC, H., 1983, Sponge-constructed stromatactis mud mounds, Silurian of Gaspé, Quebec: *Jour. Sed. Petrology*, v. 53, p. 521-532.
- BOURQUE, P.-A., and GIGNAC, H., 1986, Sponge-constructed stromatactis mud mounds, Silurian of Gaspé, Quebec- Reply: *Jour. Sed. Petrology*, v. 56, p. 461-463.
- BRAND, U., and VEIZER, J., 1980, Chemical diagenesis of a multicomponent carbonate system - 1: Trace elements: *Jour. Sed. Petrology*, v. 50, p. 1219-1236.
- BRIGGS, D.E.G., and ROLFE, W.D.I., 1983, New Concavicularida (New order: ?Crustacea) from the Upper Devonian of Gogo, Western Australia, and the palaeoecology and affinities of the group: *Spec. Papers Paleontology*, v. 30, p. 249-276.
- BUCHBINDER, L.G., MARGARITZ, M., and GOLDBERG, M., 1984, Stable isotope study of karstic-related dolomitization: Jurassic rocks from the coastal plain, Israel: *Jour. Sed. Petrology*, v. 54, p. 236-256.
- BUDAI, J.M., LOHMANN, K.C., and OWEN, R.M., 1984, Burial dedolomite in the Mississippian Madison Limestone, Wyoming and Utah thrust belt: *Jour. Sed. Petrology*, v. 54, p. 276-288.
- BUDAI, J.M., LOHMANN, K.C., and WILSON, J.L., 1987, Dolomitization of the Madison Group, Wyoming and Utah Overthrust Belt: *Am. Assoc. Petroleum Geologists Bull.*, v. 71, p. 909-924.
- BULLEN, S.B., and SIBLEY, D.F., 1984, Dolomite selectivity and mimic replacement: *Geology*, v. 12, p. 655-658.
- BURCHETTE, T.P., 1981, European Devonian reefs: a review of current concepts and models: *in* Toomey, D.F., *ed.*, *European Fossil Reef Models*: Soc. Econ. Paleontologists Mineralogists Spec. Pub. No. 30, p. 85-142.
- BUREAU OF METEOROLOGY, 1975, *Climatic Averages Australia (Metric Edition)*: Canberra, Aust. Govt. Publ. Service, various pagings.
- BUSH, P., 1973, Some aspects of the diagenetic history of the sabkha in Abu Dhabi, Persian Gulf: *in* Purser, B.H., *ed.*, *The Persian Gulf*: Berlin, Springer-Verlag, p. 395-407.
- BUTLER, G.P., 1969, Modern evaporite deposition and geochemistry of coexisting brines, the sabkha, Trucial Coast, Arabian Gulf: *Jour. Sed. Petrology*, v. 39, p. 70-89.
- CAPUTO, M.V., 1985, Late Devonian glaciation in South America: *Palaeogeography, Palaeoclimatology, Palaeoecology*, v. 51, p. 291-317.
- CAPUTO, M.V., and CROWELL, J.C., 1985, Migration of glacial centers across Gondwana during the Paleozoic era: *Geological Soc America Bull.*, v. 96, p. 1020-1036.

- CARPENTER, A.B., and OGLESBY, T.W., 1976, A model for the formation of luminescently zoned calcite cements and its implications: Geol. Soc. Am. Abstracts with Programs, v. 8, p. 469-470.
- CHAFETZ, H.S., 1972, Surface diagenesis of limestone: Jour. Sed. Petrology, v. 42, p. 325-329.
- CHOQUETTE, P.W., 1971, Late ferroan dolomite cement, Mississippian carbonates, Illinois Basin, U.S.A.: in Bricker, O.P., ed., Carbonate Cements: Baltimore, John Hopkins Univ. Press, p. 339-346.
- CHOQUETTE, P.W., and JAMES, N.P., 1987, Diagenesis #12. Diagenesis in limestones - 3. The deep burial environment: Geoscience Canada, v. 14, p. 3-35.
- CHOQUETTE, P.W., and PRAY, L.C., 1970, Geological nomenclature and classification of porosity in sedimentary carbonates: Am. Assoc. Petroleum Geologists Bull., v. 54, p. 207-250.
- COCKBAIN, A.E., 1984, Stromatoporoids from the Devonian reef complexes, Canning Basin, Western Australia: Geological Survey of Western Australia Bull. No. 129, 108p.
- COLEMAN, P.J., 1951, *Atrypa* in Western Australia: Jour. Palaeontology, v. 25, p. 677-690.
- COOPER, R.W., HALL, W.D.M., and STYLES, G.R., 1984, The Devonian stratigraphy of the Central Pillara Range: in Purcell, P.G., ed., The Canning Basin, W.A.: Proc. Geological Soc. Aust./Petroleum Exploration Soc. Aust. Symposium Perth, p. 229-234.
- COPPER, P., 1986, Frasnian/Famennian mass extinction and cold-water oceans: Geology, v. 14, p. 835-839.
- CRAIG, H., 1957, Isotopic standards for carbon and oxygen and correction factors for mass-spectrometric analysis of carbon dioxide: Geochim. Cosmochim. Acta, v. 12, p. 133-149.
- CURTIS, R., EVANS, G., KINSMAN, D.J.J., and SHEARMAN, D.J., 1963, Association of dolomite and anhydrite in the Recent sediments of the Persian Gulf: Nature, v. 197, p. 679-680.
- DE RAAF, J.F.M., READING, H.G., and WALKER, R.G., 1965, Cyclic sedimentation in the Lower Westphalian of North Devon, England: Sedimentology, v. 4, p. 1-52.
- DENNIS, K., and MILES, R.S., 1979, Eubrachythoracid arthrodires with tubular rostral plates from Gogo, Western Australia: Linnean Soc. Zool.-Jour., v. 67, p. 297-328.
- DENNIS-BRYAN, K., and MILES, R.S., 1983, Further eubrachythoracid arthrodires from Gogo, Western Australia: Linnean Soc. Zool. Jour., v. 77, p. 145-173.
- DERRICK, G.M., and PLAYFORD, P.E., 1973, 1:250,000 Geological series-Explanatory notes, Lennard River, Western Australia, Canberra, Aust. Government Pub. Service.

- DICKSON, J.A.D., 1966, Carbonate identification and genesis as revealed by staining: *Jour. Sed. Petrology*, v. 36, p. 491-505.
- DICKSON, J.A.D., 1983, Graphical modelling of crystal aggregates and its relevance to cement diagnosis: *Phil. Trans. Royal Soc. Lond.*, v. A 309, p. 465-502.
- DOROBEK, S.L., 1987, Petrography, geochemistry, and origin of burial diagenetic facies, Siluro-Devonian Helderberg Group (carbonate rocks), central Appalachians: *Am. Assoc. Petroleum Geologists Bull.*, v. 71, p. 492-514.
- DRUCE, E.C., 1976, Conodont biostratigraphy of the Upper Devonian reef complexes of the Canning Basin, Western Australia: *Aust. Bur. Mineral Resources Bull. No. 158*, 303p.
- DRUCE, E.C., and RADKE, B.M., 1979, The geology of the Fairfield Group, Canning Basin, Western Australia: *Aust. Bur. Mineral Resources Bull. No. 200*, 62p.
- DUNHAM, J.B., and OLSON, E.R., 1980, Shallow subsurface dolomitization of subtidally deposited carbonate sediments in the Hanson Creek Formation (Ordovician-Silurian) of central Nevada: *in* Zenger, D.H., Dunham, J.B., and Ethington, R.L., eds., *Concepts and Models of Dolomitization*: Soc. Econ. Paleontologists Mineralogists Spec. Pub. No. 28, p. 259-297.
- DUNHAM, R.J., 1962, Classification of carbonate rocks according to depositional texture: *in* Ham, W.E., ed., *Classification of Carbonate Rocks*: Am. Assoc. Petroleum Geologists Memoir No. 1, p. 108-121.
- DUNHAM, R.J., 1969, Early vadose silt in Townsend mound (reef), New Mexico: *in* Friedman, G.M., ed., *Depositional Environments in Carbonate Rocks*: Soc. Econ. Paleontologists Mineralogists Spec. Pub. No. 14, p. 139-181.
- DUPONT, E., 1881, Sur l'origine des calcaires devoniens de la Belgique: *Academie Royale de Belgique Bull.*, Ser. 3, v. 2, p. 264-280.
- EMBLETON, B.J.J., 1984, Australia's global setting: continental palaeomagnetism: *in* Veevers, J.J., ed., *Phanerozoic earth history of Australia*: Oxford Geological Science Series No. 2, Oxford, Clarendon Press, p. 11-16.
- EMBRY, A.F., and KLOVAN, J.E., 1971, A Late Devonian reef tract on northeastern Banks Island, N.W.T.: *Bull. Canadian Petroleum Geology*, v. 19, p. 730-781.
- ETMINAN, H., LAMBERT, I.B., BUCHHORN, I., CHAKU, S., and MURPHY, G.C., 1984, Research into diagenetic and mineralising processes, Lennard Shelf Reef Complexes, W.A.: *in* Purcell, P.G., ed., *The Canning Basin*: Perth, Proc. Geol. Soc. Aust./Petroleum Exploration Soc. Aust. Symposium, p. 447-453.
- EVAMY, B.D., 1963, The application of chemical staining technique to a study of dedolomitization: *Sedimentology*, v. 2, p. 164-170.
- EVAMY, B.D., 1967, Dedolomitization and the development of rhombohedral pores in limestones: *Jour. Sed. Petrology*, v. 37, p. 1204-1215.
- FAIRCHILD, I.J., 1980, Stages in a Precambrian dolomitization, Scotland: cementing versus replacement textures: *Sedimentology*, v. 27, p. 631-650.

- FAIRCHILD, I.A., 1983, Chemical controls on cathodoluminescence of natural dolomites and calcites: new data and review : *Sedimentology*, v. 30, p. 579-583.
- FANNING, K.A., BYRNE, R.H., BRELAND, J.A., BETZER, P.R., MOORE, W.S., and ELSINGER, R.J., 1981, Geothermal springs of the West Florida continental shelf: evidence for dolomitization and radionuclide enrichment: *Earth Planet. Sci. Lett.*, v. 52, p. 345-354.
- FISCHER, A.G., 1964, The Lofer cyclothems of the Alpine Triassic: *in* Merriam, D.F., *ed.*, *Symp. Cyclic Sedimentation: Kansas Geological Survey Bull. No. 169*, p. 107-149.
- FLUGEL, E., 1982, *Microfacies Analysis of Limestones: Berlin Heidelberg, Springer-Verlag*, 633p.
- FOLK, R.L., 1965, Some aspects of recrystallization in ancient limestones: *in* Pray, L.C., and Murray, R.C., *eds.*, *Dolomitization and Limestone diagenesis: Soc. Econ Paleontologists Mineralogists Spec. Publ. No. 13*, p. 14-48.
- FOLKMAN, Y., 1969, Diagenetic dedolomitization in the Albian-Cenomanian Yagur dolomite on Mount Carmel (N. Israel): *Jour. Sed. Petrology*, v. 39, p. 380-385.
- FORMAN, D.J., and WALES, D.W., 1981, Geological evolution of the Canning Basin, Western Australia: *Aust. Bur. Mineral Resources Bull. No. 210*, 91p.
- FRANK, J.R., 1981, Dedolomitization in the Taum Sauk Limestone (Upper Cambrian), southeast Missouri: *Jour. Sed. Petrology*, v. 51, p. 7-18.
- FRANK, J.R., CARPENTER, A.B., and OGLESBY, T.W., 1982, Cathodoluminescence and composition of calcite cement in the Taum Sauk Limestone (Upper Cambrian), southeast Missouri: *Jour. Sed. Petrology*, v. 52, p. 631-638.
- FREEMAN-LYNDE, R.P., WHITLEY, K.F., and LOHMANN, K.C., 1986, Deep-marine origin of equant spar cements in the Bahama Escarpment limestones: *Jour. Sed. Petrology*, v. 56, p. 799-811.
- FRIEDMAN, I., and O'NEILL, J.R., 1977, Compilation of stable isotope fractionation factors of geochemical interest: U.S. Geological Survey Prof. Paper No. 440K, 12p.
- FURSICH, F.T., 1973, *Thalassinoides* and the origin of nodular limestone in the Corallian Beds (Upper Jurassic) of southern England: *Neues Jahbr. Geol. Palaontol., Monatsh.*, v. 1973, p. 136-156.
- GARRISON, R.E., and FISCHER, A.G., 1969, Deep-water limestones and radiolarites of the Alpine Jurassic: *in* Friedman, G.M., *ed.*, *Depositional Environments in carbonate rocks: Soc. Econ. Paleontologists Mineralogists Spec. Publ. No. 14*, p. 20-56.
- GEBELEIN, C.D., and HOFFMAN, P., 1973, Algal origin of dolomite laminations in stromatolitic limestone: *Jour. Sed. Petrology*, v. 43, p. 603-613.

- GELLATLY, D.C., SOFOULIS, J., DERRICK, G.M., and MORGAN, C.M., 1968, The older Precambrian geology of the Lennard River 1:250,000 sheet area SE 51/8, Western Australia: Aust. Bur. Mineral Resources Record No. 1968/126.
- GINSBURG, R.N., 1971, Landward movement of carbonate mud: new model for regressive cycles in carbonates (abstract): *Am. Assoc. Petroleum Geologists*, v. 55, p. 340.
- GINSBURG, R.N., and JAMES, N.P., 1976, Submarine botryoidal aragonite in Holocene reef limestones, Belize: *Geology*, v. 4, p. 431-436.
- GIVEN, R.K., and LOHMANN, K.C., 1985, Derivation of the original isotopic composition of Permian marine cements: *Jour. Sed. Petrology*, v. 55, p. 430-439.
- GIVEN, R.K., and WILKINSON, B.H., 1985, Kinetic control of morphology, composition, and mineralogy of abiogenic sedimentary carbonates: *Jour. Sed. Petrology*, v. 55, p. 109-119.
- GLENISTER, B.F., 1958, Upper Devonian ammonoids from the Manticoceras Zone, Fitzroy Basin, Western Australia: *Jour. Paleontology*, v. 32, p. 58-96.
- GOEDE, A., GREEN, D.C., and HARMON, R.S., 1982, Isotopic composition of precipitation, cave drips and actively forming speleothems at three Tasmanian cave sites: *Helictite*, v. 20, p. 17-28.
- GONZALEZ, L.A., and LOHMANN, K.C., 1985, Carbon and oxygen isotopic composition of Holocene reefal carbonates: *Geology*, v. 13, p. 811-814.
- GOODWIN, P.W., and ANDERSON, E.J., 1980, Punctuated aggradational cycles: a general hypothesis of stratigraphic accumulation (abstract): *Proc. Geol. Soc. America*, v. 12, p. 435.
- GRAHAM, D.W., BENDER, M.L., WILLIAMS, D.F., and KEIGHWIN, L.D., 1981, Strontium to calcium ratio in Cenozoic planktonic foraminifera: *Geochim. Cosmochim. Acta*, v. 46, p. 1281-1292.
- GREGG, J.M., 1985, Regional epigenetic dolomitization in the Bonnetterre dolomite (Cambrian), southeastern Missouri: *Geology*, v. 13, p. 503-506.
- GREGG, J.M., and SIBLEY, D.F., 1984, Epigenetic dolomitization and the origin of xenotopic dolomite texture: *Jour. Sed. Petrology*, v. 54, p. 908-931.
- GREY, K., 1978, Devonian atrypid brachiopods from the reef complexes of the Canning basin: *Western Aust. Geological Survey Rept. No. 5*, 70p.
- GROVER, G., and READ, J.F., 1978, Fenestral and associated vadose diagenetic fabrics of tidal flat carbonates, Middle Ordovician New Market Limestone, southwestern Virginia: *Jour. Sed. Petrology*, v. 48, p. 453-474.
- GROVER, G., and READ, J.F., 1983, Paleoaquifer and deep burial related cements defined by regional cathodoluminescence patterns, Middle Ordovician carbonates, Virginia: *Am. Assoc. Petroleum Geologists Bull.*, v. 67, p. 1275-1303.
- GUPPY, D.J., LINDNER, A.W., RATTIGAN, J.H., and CASEY, J.N., 1958, The geology of the Fitzroy Basin, Western Australia: *Aust. Bur. Mineral Resources Bull. No. 36*, 116p.

- HALL, W.D.M., 1984, The stratigraphic and structural development of the Givetian-Frasnian reef complex, Limestone Billy Hills, Western Pillara Range, W.A.: *in* Purcell, P.G., *ed.*, The Canning Basin, W.A.: Proc. Geological Soc. Aust./Petroleum Exploration Soc. Australia Symposium Perth, p. 215-222.
- HALLEY, R.B., and SCHOLLE, P.A., 1985, Radial fibrous calcite as early-burial, open-system cement: isotopic evidence from Permian of China (abst.): Am. Assoc. Petroleum Geologists Bull., v. 69, p. 261.
- HARDIE, L.A., 1987, Dolomitization: A critical view of some current views: Jour. Sed. Petrology, v. 57, p. 166-183.
- HATHAWAY, J.C., and DEGENS, E.T., 1969, Methane-derived marine carbonates of Pleistocene age: Science, v. 165, p. 690-692.
- HECKEL, P.H., 1972, Possible inorganic origin for stromatactis in calcilutite mounds in the Tully Limestone, Devonian of New York: Jour. Sed. Petrology, v. 42, p. 7-18.
- HENNESSY, J., and KNAUTH, L.P., 1985, Isotopic variations in dolomite concretions from the Monterey Formation, California: Jour. Sed. Petrology, v. 55, p. 120-130.
- HILL, D., and JELL, J.S., 1970, Devonian corals from the Canning basin, Western Australia: Western Aust. Geological Survey Bull. No. 121, 158p.
- HUBBARD, D.K., BURKE, R.B., and GILL, I.P., 1986, Styles of reef accretion along a steep, shelf-edge reef, St. Croix, U.S. Virgin Islands: Jour. Sed. Petrology, v. 56, p. 848-861.
- HUGHES, M.W., and ALLISON, G.B., 1984, Duterium and Oxygen 18 in Australian Rainfall: Commonwealth Scientific Industrial Research Organization Australia, Division of Soils Technical Pap. No. 46, 13p.
- HURLEY, N.F., 1986, Geology of the Oscar Range Devonian reef complex, Canning Basin, Western Australia (Unpubl. Ph.D. dissertation): Michigan, U.S.A., University of Michigan, 269p.
- HURLEY, N.F., and VAN DER VOO, R., 1987, Paleomagnetism of Upper Devonian reefal limestones, Canning Basin, Western Australia: Geol. Soc. America Bull., v. 98, p. 138-146.
- ILLING, L.V., WELLS, A.J., and TAYLOR, J.C.M., 1965, Penecontemporary dolomite in the Persian Gulf: *in* Pray, L.C., and Murray, R.C., *eds.*, Dolomitization and limestone diagenesis - a symposium: Soc. Econ. Paleontologists Mineralogists Spec. Publ. No. 13, p. 89-111.
- IRWIN, H., CURTIS, C., and COLEMAN, M., 1977, Isotopic evidence for source of diagenetic carbonates formed during burial of organic-rich sediments: Nature, v. 269, p. 209-213.
- JACOBSON, R.L., and USDOWSKI, H.E., 1976, Partitioning of strontium between calcite, dolomite and liquids: Contrib. Mineral. Petrology, v. 59, p. 171-185.
- JAMES, N.P., and CHOQUETTE, P.W., 1983, Diagenesis #6. limestones- the sea floor diagenetic environment: Geoscience Canada, v. 10, p. 162-179.

- JAMES, N.P., and CHOQUETTE, P.W., 1984, Diagenesis #9- the meteoric diagenetic environment: *Geoscience Canada*, v. 11, p. 161-194.
- JAMES, N.P., and GINSBURG, R.N., 1979, The seaward margin of Belize Barrier and Atoll Reefs: *International Assoc. Sedimentologists Spec. Publ. No. 3*, 191p.
- JAMES, N.P., GINSBURG, R.N., MARSZALEK, D.S., and CHOQUETTE, P.W., 1976, Facies and fabric specificity of early subsea cements in shallow Belize (British Honduras) reefs: *Jour. Sed. Petrology*, v. 46, p. 523-544.
- JAMES, N.P., and GRAVESTOCK, D.I., 1986, Lower Cambrian carbonate shelf and shelf margin buildups, South Australia: 12th International Sedimentological Congress, Australia, Abstracts, p. 154.
- JAMES, N.P., and KLAPPA, C.F., 1983, Petrogenesis of early Cambrian reef limestones, Labrador, Canada: *Jour. Sed. Petrology*, v. 53, p. 1097-1119.
- JENKYN, H.C., 1974, Origin of red nodular limestones (Ammonitico Rosso, Knollenkalke) in the Mediterranean Jurassic: a diagenetic model: *in* Hsu, K.J., and Jenkyn, H.C., eds., *Pelagic sediments: on land and under the sea*: *Int. Assoc. Sedimentologists Spec. Publ. No. 1*, p. 249-272.
- JOHNSON, J.G., KLAPPER, G., and SANDBERG, C.A., 1985, Devonian eustatic fluctuations in Euramerica: *Geological Soc. Am. Bull.*, v. 96, p. 567-587.
- JONES, B., OLDERSHAW, A.E., and NARBONNE, G.M., 1979, Nature and origin of rubbly limestone in the Upper Silurian Read Bay Formation of Arctic Canada: *Sedimentary Geol.*, v. 24, p. 227-252.
- JULIA, R., 1983, Travertines: *in* Scholle, P.A., Bebout, D.G., and Moore, C.H., eds., *Carbonate Depositional Environments*: *Am. Assoc. Petroleum Geologists Memoir No. 33*, p. 64-72.
- JUTSON, J.T., 1934, *The Physiography of Western Australia*: Geological Survey Western Australia Bull. no. 95.
- KATZ, A., and MATHEWS, A., 1977, The dolomitization of CaCO₃: an experimental study at 252-295°C: *Geochim. Cosmochim. Acta*, v. 41, p. 297-308.
- KENDALL, A.C., 1977, Fascicular-optic calcite: a replacement of bundled acicular carbonate cements: *Jour. Sed. Petrology*, v. 47, p. 1056-1062.
- KENDALL, A.C., 1985, Radial fibrous calcite: A reappraisal: *in* Schneidermann, N., and Harris, P.M., eds., *Carbonate Cements*: *Soc. Econ. Paleontologists Mineralogists Spec. Publ. No. 36*, p. 59-77.
- KENDALL, A.C., and TUCKER, M.E., 1973, Radial fibrous calcite: a replacement after acicular carbonate: *Sedimentology*, v. 20, p. 365-389.
- KENNEDY, W.J., and GARRISON, R.E., 1975, Morphology and genesis of nodular chalks and hardgrounds in the Upper Cretaceous of southern England: *Sedimentology*, v. 22, p. 311-386.
- KERANS, C., 1985, Petrology of Devonian and Carboniferous carbonates of the Canning and Bonaparte Basins: *Western Australian Mining and Petroleum Research Institute: Report No. 12,302p*.

- KERANS, C., HURLEY, N.F., and PLAYFORD, P.E., 1986, Marine diagenesis in Devonian reef complexes of the Canning Basin Western Australia: *in* Schroeder, J.H., and Purser, B.H., eds., Reef Diagenesis: Heidelberg, Springer-Verlag.
- KUKAL, Z., 1971, Open-space structures in the Devonian limestones of the Barrandian (Central Bohemia): *Casopis pro Mineralogii a Geologii*, v. 16, p. 345-362.
- LAND, L.S., 1973, Contemporaneous dolomitization of Middle Pleistocene reefs by meteoric water, North Jamaica: *Bull. Marine Science*, v. 23, p. 64-96.
- LAND, L.S., 1980, The isotopic and trace element geochemistry of dolomite: the state of the art: *in* Zenger, D.H., Dunham, J.B., and Ethington, R.L., eds., Concepts and Models of Dolomitization: Soc. Econ. Paleontologists Mineralogists Spec. Pub. No. 28, p. 87-110.
- LAND, L.S., 1985, The origin of massive dolomite: *Jour. Geol. Education*, v. 33, p. 112-125.
- LAND, L.S., and HOOPS, G.K., 1973, Sodium in carbonate sediments and rocks: a possible index to salinity of diagenetic solutions: *Jour. Sed. Petrology*, v. 43, p. 614-617.
- LAND, L.S., and MOORE, C.H., 1980, Lithification, micritization and syndepositional diagenesis of biolithites on the Jamaican island slope: *Jour. Sed. Petrology*, v. 50, p. 357-370.
- LAND, L.S., and PREZBINDOWSKI, D.R., 1981, The origin and evolution of saline formation water, Lower Cretaceous carbonates, south-central Texas, U.S.A.: *Jour. Hydrology*, v. 54, p. 51-74.
- LECOMPTE, M., 1937, Contribution a la connaissance des recifs du Devonian de l'Ardenne; Sur la presence de structures conservees dans des efflorescences cristallines du type "Stromatactis": *Musee Royal d'Historie Naturelle de Belgique Bull.*, v. 13, p. 1-14.
- LEES, A., 1964, The structure and origin of the Waulsortian (Lower Carboniferous) reefs of west-central Eire: *Trans. Royal Soc. London Philosophical*, v. B247, p. 483-531.
- LEES, A., HALLET, V., and HIBO, D., 1985, Facies variation in Waulsortian buildups, Part 1; A model from Belgium: *Geological Jour.*, v. 20, p. 133-158.
- LEES, A., and MILLER, J., 1985, Facies variation in Waulsortian buildups, Part 2; Mid-Dinantian buildups from Europe and North America: *Geological Jour.*, v. 20, p. 159-180.
- LOGAN, B.W., 1984, Pressure responses (deformation) in carbonate sediments and rocks: Analysis and application, Canning Basin: *in* Purcell, P.G., ed., The Canning Basin, W.A.: *Proc. Geological Soc. Australia/Petroleum Exploration Soc. Australia Symposium Perth*, p. 235-252.
- LOGAN, B.W., and SEMENIUK, V., 1976, Dynamic metamorphism; processes and products in the Devonian carbonate rocks, Canning Basin, Western Australia: *Geol. Soc. Australia Spec. Pub. No. 6*, 138p.

- LOHMANN, K.C., and MEYERS, W.J., 1977, Microdolomite inclusions in cloudy prismatic calcites: a proposed criterion for former high-magnesium calcites: *Jour. Sed. Petrology*, v. 47, p. 1078-1088.
- LONG, J.A., 1987, Late Devonian fishes from the Gogo Formation, Western Australia - new discoveries: *Search*, v. 18, p. 203-205.
- LONGMAN, M.W., 1981, A process approach to recognizing facies of reef complexes: *in* Toomey, D.F., *ed.*, *European Fossil Reef Models: Soc. Econ. Paleontologists Mineralogists Spec. Pub. No. 30*, p. 9-40.
- LORENS, R.B., 1981, Sr, Cd, Mn, and Co distribution coefficients in calcite as a function of calcite precipitation rate: *Geochim. Cosmochim. Acta*, v. 45, p. 553-561.
- LOWENSTAM, H.A., 1950, Niagran reefs of the Great Lakes area: *Jour. Geology*, v. 58, p. 430-487.
- LOWENSTEIN, T.K., 1987, Evaporite depositional fabrics in the deeply buried Jurassic Buckner Formation, Alabama: *Jour. Sed. Petrology*, v. 57, p. 108-116.
- LUCIA, F.J., 1972, Recognition of evaporite-carbonate shoreline sedimentation: *in* Rigby, K.J., and Hamblin, K., *eds.*, *Recognition of Ancient Sedimentary Environments: Soc. Econ. Paleontologists Mineralogists Spec. Publ. No. 16*, p. 160-192.
- MACHEL, H-G., 1985, Cathodoluminescence in calcite and dolomite and its chemical interpretation: *Geoscience Canada*, v. 12, p. 139-147.
- MACHEL, H-G, and MOUNTJOY, E.W., 1986, Chemistry and environments of dolomitization- A reappraisal: *Earth-Science Reviews*, v. 23, p. 175-222.
- MACINTYRE, I.G., 1977, Distribution of submarine cements in a modern Caribbean fringing reef, Galeta Point, Panama: *Jour. Sed. Petrology*, v. 47, p. 503-516.
- MACINTYRE, I.G., 1985, Submarine cements - the peloidal question: *in* Schneidermann, N., and Harris, P.M., *eds.*, *Carbonate cements: Soc. Econ. Paleontologists Mineralogists Spec. Publ. No. 36*, p. 109-116.
- MACUMBER, P.G., 1970, Lunette initiation in the Kerang district: *Mining Geol. Jour. Victoria*, v. 6, p. 16-18.
- MARLAND, G., 1975, The stability of $\text{CaCO}_3 \cdot 6\text{H}_2\text{O}$ (ikaite): *Geochim. Cosmochim. Acta*, v. 39, p. 83-91.
- MARSHALL, J.F., 1983, Submarine cementation in a high-energy platform reef: One Tree Reef, southern Great Barrier Reef: *Jour. Sed. Petrology*, v. 53, p. 1133-1149.
- MARSHALL, J.F., 1986, Regional distribution of submarine cements within an epicontinental reef system: central Great Barrier Reef, Australia: *in* Schroeder, J.H., and Purser, B.H., *eds.*, *Reef Diagenesis: Berlin Heidelberg, Springer-Verlag*, p. 8-26.
- MATHUR, A.C., 1975, A deeper water mud mound facies in the Alps: *Jour. Sed. Petrology*, v. 45, p. 787-793.

- MATSUMOTO, R., and MATSUHISA, Y., 1985, Chemistry, carbon and oxygen isotope ratios, and origin of deep-sea carbonates at sites 438, 439, and 584: Inner slope of the Japan Trench: Deep Sea Drilling Project, Initial Rep., v. 87, p. 669-678.
- MATTES, B.W., and MOUNTJOY, E.W., 1980, Burial dolomitization of the Upper Devonian Miette buildup, Jasper National Park, Alberta: *in* Zenger, D.H., Dunham, J.B., and Ethington, R.L., eds., Concepts and Models of Dolomitization: Soc. Econ. Paleontologists Mineralogists Spec. Pub. No. 28, p. 259-297.
- MATTHEWS, A., and KATZ, A., 1977, Oxygen isotope fractionation during the dolomitization of calcium carbonate: *Geochim. Cosmochim. Acta*, v. 41, p. 1431-1438.
- McCROSSAN, R.G., 1958, Sedimentary "Boudinage" structures in the Upper Devonian Ireton Formation of Alberta: *Jour. Sed. Petrology*, v. 28, p. 316-320.
- McKENZIE, J., 1981, Holocene dolomitization of calcium carbonate sediments from the coastal sabkhas of Abu Dhabi, U.A.E.: a stable isotope study: *Jour. Geology*, v. 89, p. 185-198.
- McKENZIE, J.A., HSU, K.J., and SCHNEIDER, J.F., 1980, Movement of subsurface waters under the sabkha, Abu Dhabi, UAE, and its relation to evaporative dolomite genesis: *in* Zenger, D.H., Dunham, J.B., and Ethington, R.L., eds., Concepts and Models of Dolomitization: Soc. Econ. Paleontologists Mineralogists Spec. Publ. No. 28, p. 11-30.
- MEYERS, W.J., 1974, Carbonate cement stratigraphy of the Lake Valley Formation (Mississippian), Sacramento Mountains, New Mexico: *Jour. Sed. Petrology*, v. 44, p. 837-861.
- MEYERS, W.J., 1978, Carbonate cements: Their regional distribution and interpretation in Mississippian limestones of southwestern New Mexico: *Sedimentology*, v. 25, p. 371-400.
- MEYERS, W.J., and LOHMANN, K.C., 1985, Isotope geochemistry of regionally extensive calcite cement zones and marine components in Mississippian limestones, New Mexico: *in* Schneidermann, N., and Harris, P.M., eds., Carbonate Cements: Soc. Econ. Paleontologists Mineralogists Spec. Pub. No. 12, p. 223-239.
- MIDDLETON, M.F., 1984, Seismic geohistory analysis: a case history from the Canning Basin, Western Australia: *Geophysics*, v. 49, p. 333-343.
- MIRSAL, I.A., and ZANKL, H., 1985, Some phenomenological aspects of carbonate geochemistry. The control effect of transition metals: *Geologische Rundschau*, v. 74, p. 367-377.
- MONTY, Cl., 1973, Les nodules de manganese sont des stromatolithes oceaniques: *Acad. Sci. C.R., Ser. D.*, v. 276, p. 3285-3288.
- MOOK, W.G., and GROOTES, P.M., 1973, The measuring procedure for high-precision mass-spectrometric analysis of isotopic abundance ratios, especially referring to carbon, oxygen and nitrogen: *Jour. Mass Spectrometry Ion Physics*, v. 12, p. 273-298.

- MOORE, C.H., 1985, Upper Jurassic subsurface cements: a case history: *in* N. Schneidermann and P.M. Harris, *eds.*, Carbonate Cements: Soc. Econ. Paleontologists Mineralogists Spec. Pub. No. 36, p. 291-308.
- MORROW, D.W., 1982, Diagenesis 2 Dolomite- Part 2. Dolomitization models and ancient dolostones: *Geoscience Canada*, v. 9, p. 95-107.
- MORROW, D.W., 1986, The sea-level rise staircase on continental margins and the origin of upward-shoaling carbonate sequences: *Bull. Canadian Petroleum Geology*, v. 34, p. 284-285.
- MULLINS, H., and LYNTS, G.W., 1977, Origin of the northwestern Bahama Platform: a review and reinterpretation: *Geological Soc. America Bull.*, v. 88, p. 1447-1461.
- MULLINS, H., and NEUMANN, A.C., 1979, Deep carbonate bank margin structure and sedimentation in the northern Bahamas: *in* Doyle, L.J., and Pilkey, D.H., *eds.*, *Geology of continental slopes*: Soc. Econ. Paleontologists Mineralogists Spec. Publ. No. 27, p. 165-192.
- MULLINS, H.T., NEUMANN, A.C., WILBER, R.J., and BOARDMAN, M.R., 1980, Nodular carbonate sediment on Bahamian slopes: possible precursors to nodular limestones: *Jour. Sed. Petrology*, v. 50, p. 117-131.
- NAZAROV, B.B., COCKBAIN, A.E., and PLAYFORD, P.E., 1982, Late Devonian radiolaria from the Gogo Formation, Canning Basin, Western Australia: *Alcheringa*, v. 6, p. 161-173.
- NELSON, C.S., and LAWRENCE, M.F., 1984, Methane-derived high-Mg calcite submarine cement in Holocene nodules from the Fraser Delta, British Columbia, Canada: *Sedimentology*, v. 31, p. 645-654.
- NEUMANN, A.C., KOFOED, J.W., and KELLER, G.H., 1977, Lithoherms in the Straits of Florida: *Geology*, v. 5, p. 4-10.
- NICHOLS, R.A., 1966, Petrology of irregular nodular beds, Lower Carboniferous, Anglesey, North Wales: *Geol. Magazine*, v. 103, p. 477-486.
- NICOLL, R.S., 1984, Conodont studies in the Canning basin- A review and update: *in* Purcell, P.G., *ed.*, *The Canning Basin, W.A.: Proc. Geological Soc. Aust./Petroleum Exploration Soc. Aust. Symposium Perth*, p. 439-443.
- NOBEL, J.P., and HOWELLS, K.D.M., 1974, Early lithification of the nodular limestones in the Silurian of New Brunswick: *Sedimentology*, v.21, p. 597-609.
- OLDERSHAW, A.E., and SCOFFIN, T.D., 1967, The source of ferroan and non-ferroan calcite cements in the Halkin and Wenlock limestones: *Geological Jour.*, v. 5, p. 309-321.
- OPDYKE, B.N., WILKINSON, B.H., LOHMANN, K.C., and GIVEN, K.R., 1986, Primary magnesium, stable isotopic, and trace elemental composition of Late Devonian marine calcite neptunian dike cement from Canning Basin, Australia (abstr.): *Am. Assoc. Petroleum Geologists Bull.*, v. 70, p. 628.
- PEDONE, V.A., *in prep*, Ph.D. dissertation: New York, SUNY at Stony Brook.
- PETERSEN, M.S., 1975, Upper Devonian (Famennian) ammonoids from the Canning basin, Western Australia: *Paleontology Soc. Mem.*, v. 8, 55p.

- PIERRE, C., ORTLIEB L., and PERSON, A., 1984, Supratidal evaporitic dolomite at Ojo De Liebre Lagoon: mineralogical and isotopic arguments for primary crystallization: *Jour. Sed. Petrology*, v. 54, p. 1049-1061.
- PIERSON, M.S., 1981, The control of cathodoluminescence in dolomite by iron and manganese: *Sedimentology*, v. 28, p. 601-610.
- PISCIOTTO, K.A., and MAHONEY, J.J., 1981, Isotopic survey of diagenetic carbonates, Deep Sea Drilling Project leg 63: Deep Sea Drilling Project Initial Repts., v. 63, p. 595-609.
- PLAYFORD, G., 1976, Plant microfossils from the Upper Devonian and Lower Carboniferous of the Canning basin, Western Australia: *Palaeontographica*, v. 158, pt. B, p. 1-71.
- PLAYFORD, P.E., 1969, Devonian carbonate complexes of Alberta and Western Australia: A comparative study: Geological Survey of Western Australia Report No. 1, 43p.
- PLAYFORD, P.E., 1976, Devonian reef complexes of the Canning basin, Western Australia: 25th International Geological Congress Excursion Guide 38A: 39p.
- PLAYFORD, P.E., 1980, Devonian "Great Barrier Reef" of Canning Basin, Western Australia: *Am. Assoc. Petroleum Geologists Bull.*, v. 64, p. 814-840.
- PLAYFORD, P.E., 1981, Devonian reef complexes of the Canning basin, Western Australia: Geological Society of Australia fifth Australian Geological Convention, Field Excursion Guidebook 64p.
- PLAYFORD, P.E., 1984, Platform-margin and marginal-slope relationships in Devonian reef complexes of the Canning Basin: *in* Purcell, P.G., *ed.*, The Canning Basin, W.A.: Perth, Proc. Geol. Soc. Australia/ Petroleum Exploration Soc. Australia Symposium, p. 189-214.
- PLAYFORD, P.E., and COCKBAIN, A.E., 1969, Algal stromatolites: Deep water forms in the Devonian of Western Australia: *Science*, v. 165, p.1008-1010.
- PLAYFORD, P.E., COCKBAIN, A.E., DRUCE, E.C., and WRAY, J.L., 1976, Devonian stromatolites from the Canning Basin, Western Australia: *in* Walter, M.R., *ed.*, *Stromatolites: Developments in Sedimentology* No. 20, Amsterdam, Elsevier, p. 543-564.
- PLAYFORD, P.E., HURLEY, N.F., KERANS, C., and MIDDLETON, M.F., (*in press*), Reefal platform development, Devonian of the Canning Basin, Western Australia: *in* Crevello, P.D., Sarg, J.F., Wilson, J.L., and Read, J.F., *eds.*, *Controls on Carbonate Platform and Basin Development: Soc. Econ. Paleontologists Mineralogists Spec. Publ.*
- PLAYFORD, P.E., and LOWRY, D.C., 1966, Devonian reef complexes of the Canning Basin, Western Australia: Geological Survey of Western Australia Bull. No. 118, 150p.
- PLAYFORD, P.E., McLAREN, D.J., ORTH, C.J., GILMORE, J.S., and GOODFELLOW, W.D., 1984, Iridium anomaly in the Upper Devonian of the Canning Basin, Western Australia: *Science*, v. 226, p. 437-439.

- POPP, B.N., ANDERSON, T.F., and SANDBERG, P.A., 1986, Textural, elemental, and isotopic variations among constituents in Middle Devonian limestones, North America: *Jour. Sed. Petrology*, v. 56, p. 715-727.
- PRATT, B.R., 1982, Stromatolitic framework of carbonate mud-mounds: *Jour. Sed. Petrology*, v. 52, p. 1203-1227.
- PRATT, B.R., 1984, *Epiphyton* and *Renalcis*- Diagenetic microfossils from calcification of coccoid blue-green algae: *Jour. Sed. Petrology*, v. 54, p. 948-971.
- PRATT, B.R., 1986, Sponge-constructed stromatolitic mud mounds, Silurian of Gaspé, Quebec- Discussion: *Jour. Sed. Petrology*, v. 56, p. 459-460.
- PRATT, B.R., and JAMES, N.P., 1986, The St George Group (Lower Ordovician) of western Newfoundland: tidal flat island model for carbonate sedimentation in shallow epeiric seas: *Sedimentology*, v. 33, p. 313-343.
- PURCELL, P.G., 1984, The Canning Basin, W.A. - An introduction: *in* Purcell, P.G., *ed.*, The Canning Basin, W.A.: *Proc. Geological Soc. Aust./Petroleum Exploration Soc. Aust. Symposium Perth*, p. 3-19.
- RADKE, B.M., and MATHIS, R.L., 1980, On the formation and occurrence of saddle dolomite: *Jour. Sed. Petrology*, v. 50, p. 1149-1168.
- RATTIGAN, J.H., and VEEVERS, J.J., 1961, Devonian: *in* Veevers, J.J., and Wells, A.T., *The Geology of the Canning Basin, Western Australia*: *Aust. Bur. Mineral Resources Bull. No. 60*, p. 22-61.
- READ, J.F., 1973a, Carbonate cycles, Pillara Formation (Devonian), Canning Basin, Western Australia: *Bull. Can. Petroleum Geologists*, v. 21, p. 38-51.
- READ, J.F., 1973b, Paleo-environments and paleogeography, Pillara Formation (Devonian), Western Australia: *Bull. Can. Petroleum Geologists*, v. 21, p. 344-394.
- READ, J.F., GROTZINGER, J.P., BOVA, J.A., KOERSCHNER, W.F., 1986, Models for generation of carbonate cycles: *Geology*, v. 14, p. 107-110.
- REECKMANN, S.A., and GILL, E.D., 1981, Rates of vadose diagenesis in Quaternary dune and shallow marine calcarenites, Warrnambool, Victoria, Australia: *Sed. Geology*, v. 30, p. 157-172.
- REID, R.P., 1987, Nonskeletal peloidal precipitates in Upper Triassic reefs, Yukon Territory (Canada): *Jour. Sed. Petrology*, v. 57, p. 893-900.
- RICKEN, W., 1986, Diagenetic bedding: a model for marl-limestone alternations: *Lecture Notes Earth Science No. 6*, Berlin, Springer-Verlag, 210p.
- RIGBY, J.K., 1986, Late Devonian sponges of Western Australia: *Geological Survey of Western Australia Report No. 18*, 59p.
- ROBERTS, H.H., and WHELAN, T., 1975, Methane-derived carbonate cements in barrier and beach sands of a subtropical delta complex: *Geochim. Cosmochim. Acta*, v. 39, p. 1085-1089.
- ROBINSON, P., 1980, Determination of calcium, magnesium, manganese, strontium, sodium and iron in the carbonate fraction of limestones and dolomites: *Chemical Geology*, v. 28, p. 135-146.

- ROGERS, J.P., 1971, Tidal sedimentation and its bearing on reservoir and trap in Permian Phosphoria strata, Cottonwood Creek Field, Big Horn Basin, Wyoming: *Mtn. Geol.*, v. 8, p. 71-80.
- ROLFE, W.D.I., 1966, Phyllocarid fauna of European aspect from the Devonian of Western Australia: *Nature*, v. 209, p. 192.
- ROSS, J.P., 1961, Ordovician, Silurian, and Devonian bryozoa of Australia: *Aust. Bureau Mineral Resources Bull. No. 50*, 172p.
- ROSS, R.J., JAANUSSON, V., and FRIEDMAN, I., 1975, Lithology and origin of Middle Ordovician calcareous mud mound at Meiklejohn Peak, southern Nevada: *U.S. Geological Survey Prof. Paper No. 871*, 48p.
- SALLER, A.H., 1984, Petrologic and geochemical constraints on the origin of subsurface dolomite, Enewetak Atoll: an example of dolomitization by normal seawater: *Geology*, v. 12, p. 217-220.
- SALLER, A.H., 1986, Radial calcite in Lower Miocene strata, subsurface Enewetak Atoll: *Jour. Sed. Petrology*, v. 56, p. 743-762.
- SANDBERG, P.A., 1975, New interpretations of Great Salt Lake ooids and non-skeletal carbonate mineralogy: *Sedimentology*, v. 22, p. 497-537.
- SANDBERG, P.A., 1983, An oscillating trend in Phanerozoic non-skeletal carbonate mineralogy: *Nature*, v. 305, p. 19-22.
- SANDBERG, P.A., 1985, Aragonite cements and their occurrence in ancient limestones: *in* Schneidermann, N., and Harris, P.M., *eds.*, Carbonate Cements: *Soc. Econ. Paleontologists Mineralogists Spec. Publ. No. 36*, p. 33-57.
- SCHLAGER, W., 1974, Preservation of cephalopod skeletons and carbonate dissolution on ancient Tethyan sea floors: *in* Hsu, K.J., and Jenkyns, H.C., *eds.*, Pelagic Sediments: on Land and under the Sea: *Spec. Publ. International Assoc. Sed. No. 1*, p. 49-70.
- SCHOLLE, P.A., and HALLEY, R.B., 1985, Burial diagenesis: out of sight, out of mind: *in* Schneidermann, N., and Harris, P.M., *eds.*, Carbonate Cements: *Soc. Econ. Paleontologists Mineralogists Spec. Publ. No. 36*, p. 309-334.
- SCHWARZACHER, W., 1961, Petrology and structure of some Lower Carboniferous reefs in northwestern Ireland: *Am. Assoc. Petroleum Geologists Bull.*, v. 45, p. 1481-1503.
- SELLEY, R.C., 1970, Studies of sequence in sediments using a simple mathematical device: *Jour. Geol. Soc. London*, v. 125, p. 557-581.
- SHARMA, T., and CLAYTON, R.N., 1965, Measurement of O18/O16 ratios of total oxygen of carbonates: *Geochim. Cosmochim. Acta*, v. 29, p. 1347-1353.
- SHEARMAN, D.J., 1966, Origin of marine evaporites by diagenesis: *Trans. Inst. Min. Metall.*, v. 75, p. 208-215.
- SHEPPARD, S.M.F., and SCHWARZ, H.P., 1970, Fractionation of carbon and oxygen isotopes and magnesium between metamorphic calcite and dolomite: *Contrib. Mineral. Petrology*, v. 26, p. 161-198.
- SHINN, E.A., 1968a, Practical significance of birdseye structures in carbonate rocks: *Jour. Sed. Petrology*, v. 38, p. 215-223.

- SHINN, E.A., 1968b, Burrowing in Recent lime sediments of Florida and the Bahamas: *Jour. Paleontology*, v. 42, p. 879-894.
- SHINN, E.A., 1983a, Birdseyes, fenestrae, shrinkage pores, and loferites: a reevaluation: *Jour. Sed. Petrology*, v. 53, p. 619-628.
- SHINN, E.A., 1983b, Tidal flat environment: *in* Scholle, P.A., Bebout, D.G., and Moore, C.H., *eds.*, Carbonate Depositional Environments: Am. Assoc. Petroleum Geologists Memoir No. 33, p. 172-210.
- SHINN, E.A., and ROBBIN, D.M., 1983, Mechanical and chemical compaction in fine-grained shallow-water limestones: *Jour. Sed. Petrology*, v. 53, p. 595-618.
- SIBLEY, D.F., 1980, Climatic control of dolomitization, Seroe Domi Formation (Pliocene), Bonaire, N.A.: *in* Zenger, D.H., Dunham, J.B., and Ethington, R.L., *eds.*, Concepts and Models of Dolomitization: Soc. Econ. Paleontologists Mineralogists Spec. Pub. No. 28, p. 247-258.
- SIPPEL, R.F., and GLOVER, E.D., 1965, Structures in carbonate rocks made visible by luminescent petrography: *Science*, v. 150, p. 1283-1287.
- SOLOMON, S.T., and WALKDEN, G.M., 1985, The application of cathodoluminescence to interpreting the diagenesis of an ancient calcrete profile: *Sedimentology*, v. 32, p. 877-896.
- STEPHENS, G.G., and CROCKER, R.L., 1946, Composition and genesis of lunettes: *Trans. Roy. Soc. South. Aust.*, v. 70, p. 302-313.
- TAYLOR, H.P., 1978, Oxygen and Hydrogen isotope studies of granitic rocks: *Earth Planetary Science Letters*, v. 38, p. 177-210.
- TEICHERT, C., 1939, Nautiloid cephalopods from the Devonian of Western Australia: *Royal. Soc. Western Australia Jour.*, v. 25, p. 103-121.
- TEICHERT, C., 1941, Upper Devonian goniatite succession of Western Australia: *Am. Jour. Science*, v. 239, p. 148-153.
- TEICHERT, C., 1943, The Devonian of Western Australia, a preliminary review: *Am. Jour. Science*, v. 241, p. 69-94, 167-184.
- TEICHERT, C., 1947, Stratigraphy of Western Australia: *Am. Assoc. Petroleum Geologists Bull.*, v. 31, p. 1-70.
- TEICHERT, C., 1949, Stratigraphy and palaeontology of the Devonian portion of the Kimberley Division, Western Australia: *Aust. Bur. Mineral Resources Report No. 2*, 55p.
- TEXTORIS, C., and CAROZZI, A.V., 1964, Petrography and evolution of Niagaran (Silurian) reefs, Indiana: *Am. Assoc. Petroleum Geologists Bull.*, v. 48, p. 397-426.
- THOMAS, G.A., 1957, Lower Carboniferous deposits in the Fitzroy Basin, Western Australia: *Aust. Jour. Science*, v. 19, p. 160-161.
- TOWNER, R.R., and GIBSON, D.L., 1983, Geology of the onshore Canning Basin, Western Australia: *Aust. Bur. Mineral Resources Bull. No. 215*, 51p.
- TSIEN, H.H., 1985, Origin of Stromatactis - a replacement of colonial microbial concretions: *in* Toomey, D.F., and Nitecki, M.H., *eds.*, Paleogeology: Berlin Heidelberg, Springer-Verlag, p. 274-289.

- TUCKER, M.E., 1983, Diagenesis, geochemistry, and origin of a Precambrian dolomite: the Beck Spring Dolomite of eastern California: *Jour. Sed. Petrology*, v. 53, p. 1097-1119.
- VEEVERS, J.J., 1959, Devonian brachiopods from the Fitzroy Basin, Western Australia: Australian Bureau Mineral Resources Bull. No. 45, 173p.
- VEIZER, J., 1983, Chemical diagenesis of carbonates: theory and application of trace element technique: *in* Arthur, M.A., Anderson, T.F., Kaplan, I.R., Veizer, J., and Land, L.S., eds., *Stable Isotopes in Sedimentary Geology: Soc. Econ Paleontologists Mineralogists Short Course No. 10*, p. 3,1-3,100.
- VEIZER, J., FRITZ, P., and JONES, B., 1986, Geochemistry of brachiopods: oxygen and carbon isotopic records of Paleozoic oceans: *Geochim. Cosmochim. Acta*, v. 50, p. 1679-1696.
- VEIZER, J., and HOEFS, J., 1976, The nature of O^{18}/O^{16} and C^{13}/C^{12} secular trends in sedimentary carbonate rocks: *Geochim. Cosmochim. Acta*, v. 40, p. 1387-1395.
- VEIZER, J., LEMIEUX, J., JONES, B., GIBLING, M.R., and SAVELLE, J., 1978, Paleosalinity and dolomitization of a Lower Paleozoic carbonate sequence, Somerset and Prince of Wales islands, Arctic Canada: *Canadian Jour. Earth Sci.*, v. 15, p. 1448-1461.
- VIDETICH, P.E., 1985, Electron microprobe study of Mg distribution in Recent Mg-calcites and recrystallized equivalents from the Pleistocene and Tertiary: *Jour. Sed. Petrology*, v. 55, p. 421-429.
- WALKDEN, G.M., and BERRY, J.R., 1984, Syntaxial overgrowths in muddy crinoidal limestones: cathodoluminescence sheds new light on an old problem: *Sedimentology*, v. 31, p. 251-267.
- WALLACE, M.W., 1987, The role of internal erosion and sedimentation in the formation of stromatactis mudstones and associated lithologies: *Jour. Sed. Petrology*, v. 57, p. 695-700.
- WANLESS, H.R., 1979, Limestone response to stress: pressure solution and dolomitization: *Jour. Sed. Petrology*, v. 49, p. 437-462.
- WAPET (WEST AUSTRALIAN PETROLEUM PTY LTD), 1971, Crossland Nos. 1, 2, & 3, well completion report: Aust. Bur. Mineral Resources file No. 72/975.
- WAPET (WEST AUSTRALIAN PETROLEUM PTY LTD), 1972, Barbwire No. 1, well completion report: Aust. Bur. Mineral Resources file No. 72/2001.
- WARD, W.B., *in prep*, Ph.D. dissertation: New York, SUNY at Stony Brook.
- WARD, W.C., and HALLEY, R.B., 1985, Dolomitization in a mixing zone of near-seawater composition, Late Pleistocene, Northeastern Yucatan peninsula: *Jour. Sed. Petrology*, v. 55, p. 407-420.
- WARREN, J.K., and KENDALL, C.G.ST.C., 1985, Comparison of sequences formed in marine sabkha (subaerial) and salina (subaqueous) settings- modern and ancient: *Am. Assoc. Petroleum Geologists Bull.*, v. 69, p. 1013-1023.

- WEBER, J.N., 1964, Trace element composition of dolostones and dolomites and its bearing on the dolomite problem: *Geochim. Cosmochim. Acta*, v. 28, p. 1817-1868.
- WELLS, A., 1962, Primary dolomitization in Persian Gulf: *Nature*, v. 194, p. 274-275.
- WEST, I.M., BRANDON, A., and SMITH, M., 1968, A tidal flat evaporitic facies in the Visean of Ireland: *Jour. Sed. Petrology*, v. 38, p. 1079-1093.
- WHALLEY, W.B., MARSHALL, J.R., and SMITH, B.J., 1982, Origin of desert loess from some experimental observations: *Nature*, v. 300, p. 433-435.
- WIEDENMAYER, F., 1978, Modern sponge bioherms of the Great Bahama Bank: *Ecologiae Geol. Helvetica*, v. 71, p. 699-744.
- WIGLEY, T.M., and PLUMMER, L.N., 1976, Mixing of carbonate waters: *Geochim. Cosmochim. Acta*, v. 40, p. 989-995.
- WILKINSON, B.H., 1979, Biomineralization, paleoceanography, and the evolution of calcareous marine organisms: *Geology*, v. 7, p. 425-427.
- WILKINSON, B.H., 1982, Cyclic cratonic carbonates and phanerozoic calcite seas: *Jour. Geological Education*, v. 30, p. 189-203.
- WILKINSON, B.H., and GIVEN, R.K., 1986, Secular variation in abiogenic marine carbonates; constraints on Phanerozoic atmospheric carbon dioxide contents and oceanic Mg/Ca ratios: *Jour. Geology*, v. 94, p. 321-333.
- WILSON, J.L., 1974, Characteristics of carbonate-platform margins: *Am. Assoc. Petroleum Geologists*, v. 58, p. 810-824.
- WILSON, J.L., 1975, *Carbonate Facies in Geologic History*: New York, Springer-Verlag, 471p.
- WONG, P.K., and OLDERSHAW, A.E., 1980, Causes of cyclicity in reef interior sediments, Kaybob reef, Alberta: *Can. Soc. Petroleum Geologists Bull.*, v. 28, p. 411-424.
- WRAY, J.L., 1967, Upper Devonian calcareous algae from the Canning basin, Western Australia: *Colorado School of Mines Prof. Contr. No. 3*, 76p.

APPENDIX A

SAMPLE CATALOGUE

All specimens listed can be located in the Museum Collection at the Department of Geology, University of Tasmania.

Sample Catalogue, Geikie Gorge Area

Grid references from the Fitzroy Crossing 1:100 000 topographic map sheet and shown on the geological map of the Geikie Gorge area (enclosed)

UTGD no.	Sample code	Field no.	Lithology	Stratigraphy	Location description	Grid reference (100m)
70242	R, PT	79698A	Neptunian dyke filling	Pillara Limestone	West Copley Valley	80019N 7818E
70243	R, CA	84-22	Peloidal grainstone	Pillara Limestone	West Copley Valley	80016N 7818E
70244	R, CA	84-77	Neptunian dyke filling	Pillara Limestone	West Copley Valley	80021N 7810E
70245	R, PT	84-82	Peloidal grainstone	Napier Formation	West Copley Valley	80011N 7804E
70246	R, CA	84-101	Neptunian dyke filling	Napier Formation	West Copley Valley	80009N 7810E
70247	R, PT, CA	84-128	Peloid grainstone	Napier Formation	West Copley Valley	80015N 7812E
70248	R, PT	84-133	Deep-water stromatolite	Napier Formation	West Copley Valley	80017N 7812E
70249	R, PT	84-156	Fenestral stromatolite	Pillara Limestone	West Copley Valley	80011N 7811E
70250	R, PT	84-167A	Deep-water stromatolite	Napier Formation	West Copley Valley	80011N 7810E
70251	R, CA	84-167	Lithoclast breccia	Napier Formation	West Copley Valley	80011N 7810E
70252	R, PT, CA	84-206	Framestone	Pillara Limestone	West Copley Valley	80014N 7823E
70253	R, CA	84-207	Framestone	Pillara Limestone	West Copley Valley	80014N 7823E
70254	R, PT, CA	84-227	Neptunian dyke filling	Pillara Limestone	West Copley Valley	80017N 7822E
70255	R, CA	84-233	Fibrous marine cement	Pillara Limestone	West Copley Valley	80017N 7822E
70256	R, PT	84-242	Neptunian dyke filling	Pillara Limestone	West Copley Valley	80021N 7815E
70257	R, PT, CA	84-255	Zebra limestone	Napier Formation	West Copley Valley	80027N 7814E
70258	R, CA	84-269	Peloid grainstone	Napier Formation	West Copley Valley	80024N 7808E
70259	R, PT	84-326A	Zebra limestone	Pillara Limestone	West Copley Valley	80002N 7807E
70260	R, PT	84-326B	Stromatactis mudstone	Pillara Limestone	West Copley Valley	80002N 7807E
70261	R, PT	84-326C	Deep water stromatolite	Pillara Limestone	West Copley Valley	80002N 7807E
70262	R, PT	84-326D	Deep water stromatolite	Pillara Limestone	West Copley Valley	80002N 7807E
70263	R, PT	84-341	Ooid grainstone	Napier Formation	West Copley Valley	80001N 7812E
70264	R, CA	84-371	Stromatactis	Napier Formation	West Copley Valley	80003N 7807E
70265	R, PT	84-451	Neptunian dyke	Pillara Limestone	West Copley Valley	80027N 7808E
70266	R, CA	84-463	Headress sponge	Napier Formation	West Copley Valley	80003N 7805E
70267	R, CA	84-465	Stromatactis	Napier formation	West Copley Valley	80002N 7807E
70268	R, PT	84-L	Wackestone	Sadler Limestone	Emanuel Range	Loc. #3, Playford, 1981
70269	R, CA	84-X	Renalcis Framestone	Pillara Limestone	West Copley Valley	80015N 7824E
70270	R, PT, CA	85-28Z	Renalcis framestone	Pillara Limestone	Northern Geikie Gorge	80047N 7913E
70271	PT	85-28A	Onkoid rudstone	Pillara Limestone	Northern Geikie Gorge	80047N 7913E
70272	R	85-33	Amphipora floatstone	Pillara Limestone	Northern Geikie Gorge	80059N 7928E
70273	R, CA	85-33A	Intraclast Grainstone	Pillara Limestone	Northern Geikie Gorge	80059N 7928E
70274	R, CA	85-33C	Intraclast Grainstone	Pillara Limestone	Northern Geikie Gorge	80059N 7928E
70275	CA	85-33D	Intraclast Grainstone	Pillara Limestone	Northern Geikie Gorge	80059N 7928E
70276	R, CA	85-36	Dolomite	Pillara Limestone	Northern Geikie Gorge	80062N 7925E
70277	R, CA	85-36A1	Dedolomite	Pillara Limestone	Northern Geikie Gorge	80062N 7925E
70278	R, CA	85-36B	Dolomite & dedolomite	Pillara Limestone	Northern Geikie Gorge	80062N 7925E
70279	R, CA	85-36D1	Amphipora rudstone	Pillara Limestone	Northern Geikie Gorge	80062N 7925E
70280	R, PT, CA	85-36D3	Stachyodes rudstone	Pillara Limestone	Northern Geikie Gorge	80062N 7925E
70281	R, PT, CA	85-36E	Dolomite & dedolomite	Pillara Limestone	Northern Geikie Gorge	80062N 7925E
70282	R, CA	85-37A	Dedolomite	Pillara Limestone	Northern Geikie Gorge	80056N 7926E
70283	CA	85-37	Mudstone & vert fenest	Pillara Limestone	Northern Geikie Gorge	80056N 7926E
70284	R, PT, CA	85-53A	Lime mudstone	Pillara Limestone	Northern Geikie Gorge	80041N 7910E
70285	R, CA	85-53B	Dolomite & dedolomite	Pillara Limestone	Northern Geikie Gorge	80041N 7910E
70286	R, CA	85-53D	Dolomite	Pillara Limestone	Northern Geikie Gorge	80041N 7910E
70287	R, CA	85-53Z	Dedolomite	Pillara Limestone	Northern Geikie Gorge	80041N 7910E
70288	R, CA	85-53	Dedolomite	Pillara Limestone	Northern Geikie Gorge	80041N 7910E
70289	R, CA	85-58	Dolomite	Pillara Limestone	Northern Geikie Gorge	80047N 7921E
70290	R, CA	85-111B	Peloidal grainstone	Napier Formation	Central Geikie Gorge	79997N 7883E
70291	R, PT	85-111D	Sphaerocodium frame	Pillara Limestone	Central Geikie Gorge	79997N 7883E
70292	R, PT	85-112L	Renalcis framestone	Pillara Limestone	Northern Geikie Gorge	80032N 7904E
70293	R, PT, CA	85-112A	Lithoclast breccia	Napier Formation	Northern Geikie Gorge	80032N 7904E
70294	PT	85-112I	Framestone	Pillara Limestone	Northern Geikie Gorge	80032N 7904E
70295	R, PT, CA	85-112TB	Dolomite and dedolomite	Pillara Limestone	Northern Geikie Gorge	80032N 7904E
70296	R, CA	85-112TA	Dedolomite	Pillara Limestone	Northern Geikie Gorge	80032N 7904E
70297	R, PT, CA	85-112TC	Fenestral grainstone	Pillara Limestone	Northern Geikie Gorge	80032N 7904E
70298	R, CA	85-112U	Dolomite	Pillara Limestone	Northern Geikie Gorge	80032N 7904E
70299	R, PT	85-244	Ooid grainstone	Napier Formation	North Copley Valley	80087N 7867E
70300	R, PT	85-267	Pisoid rudstone	Pillara Limestone	South Copley Valley	79980N 7822E
70301	R, PT	85-280	Ooid grainstone	Pillara Limestone	S.W. Copley Valley	79953N 7805E
70302	R, CA	85-280A	Deep water stromatolite	Napier Formation	S.W. Copley Valley	79953N 7805E
70303	R, CA	85-305	Dedolomite	Pillara Limestone	West Copley Valley	80090N 7771E
70304	R, PT	85-324	Sponge-Renalcis	Napier Formation	Geikie Range	80036N 7944E
70305	R, CA	85-330	Recrystallized limestone	Napier Formation	W. of Fossil Downs Station	79924N 7879E
70306	R, PT, CA	85-342	Lithoclast breccia	Napier Formation	West Copley Valley	80015N 7827E
70307	R, CA	85-343	Lithoclast breccia	Napier Formation	West Copley Valley	80019N 7830E
70308	R, PT, CA	85-344	Lithoclast breccia	Napier Formation	West Copley Valley	80025N 7828E
70309	R, PT	85-344A	Skeletal wackestone	Napier Formation	West Copley Valley	80025N 7828E
70310	R, CA	85-345	Lithoclast breccia	Napier Formation	West Copley Valley	80018N 7825E
70311	R, CA	85-ca	Speleothem	Pillara Limestone	Cascade Cave	80056N 7926E
70312	R, CA	85-cor1	Poikilitic calcite cement	Pillara Limestone	West Copley Valley	80018N 7822E
70313	R, CA	85-cor2	Poikilitic calcite cement	Pillara Limestone	West Copley Valley	80018N 7822E
70314	R, PT, CA	85-cru1	Dendritic cave crust	Pillara Limestone	West Copley Valley	80025N 7810E
70315	R, CA	85-cru2	Dendritic cave crust	Pillara Limestone	West Copley Valley	80013N 7815E
70316	R, CA	85-ONK	Onkoid	Pillara Limestone	Northern Geikie Gorge	80073N 7935E
70317	R, PT, CA	85-spo	Sponge floatstone	Napier Formation	West Copley Valley	80045N 7831E
70318	R, PT	85-sta	Stromatactis mudstone	Napier Formation	West Copley Valley	80045N 7831E
70371	CA	85-36BZ	Granistone	Pillara Limestone	Northern Geikie Gorge	80062N 7925E

Sample Catalogue, Barbwire Terrace

UTGD no.	Sample code	Field no.	Lithology	Stratigraphy	Well name and depth	Latitude	Longitude
70319	R, PT, CA	E1-985.11	Regional dolomite	Nullara Limestone	Eremophila #1, 385.11 m	19 46' 49 98"S	125 12' 12.71"E
70320	CA	E1-492.78	Supratidal dolomite	Nullara Limestone	Eremophila #1, 492.78 m	"	"
70321	R, PT	E1-513.13	Supratidal dolomite	Nullara Limestone	Eremophila #1, 513.13 m	"	"
70322	R, PT	E1-550.57	Supratidal dolomite	Nullara Limestone	Eremophila #1, 550.57 m	"	"
70323	CA	E1-732.87	Supratidal dolomite	Pillara Limestone	Eremophila #1, 732.87 m	"	"
70324	CA	E1-733.20	Supratidal dolomite	Pillara Limestone	Eremophila #1, 733.20 m	"	"
70325	R, CA	E1-790.87	Supratidal dolomite	Pillara Limestone	Eremophila #1, 790.87 m	"	"
70326	PT	E1-864.90	Supratidal dolomite	Pillara Limestone	Eremophila #1, 864.90 m	"	"
70327	R, PT, CA	E1-880.65	Supratidal dolomite	Pillara Limestone	Eremophila #1, 880.65 m	"	"
70328	CA	E1-926.74	Supratidal dolomite	Pillara Limestone	Eremophila #1, 926.74 m	"	"
70329	CA	E1-927.92	Supratidal dolomite	Pillara Limestone	Eremophila #1, 927.92 m	"	"
70330	R, PT	E1-1220.40	Laminated limestone	Pillara Limestone	Eremophila #1, 1220.4? m	"	"
70331	CA	D1A-390.85	Regional dolomite	Nullara Limestone	Dampiera #1A, 390.85 m	19 49' 06" S	125 16' 06" E
70332	PT	D1A-493.94	Fanestral dolomite	Nullara Limestone	Dampiera #1A, 493.94 m	"	"
70333	CA	D1A-551.09	Regional dolomite	Nullara Limestone	Dampiera #1A, 551.09 m	"	"
70334	CA	D1A-600.90	Regional dolomite	Nullara Limestone	Dampiera #1A, 600.90 m	"	"
70335	R, PT	D1A-886.60	Regional dolomite	Pillara Limestone	Dampiera #1A, 886.60 m	"	"
70336	R, PT	D1A-1082.10	Dolomitized rudstone	Pillara Limestone	Dampiera #1A, 1082.10 m	"	"
70337	R, PT	D1A-1145.30	Marl	Pillara Limestone	Dampiera #1A, 1145.30 m	"	"
70338	AP	D1A-1169.20	Marl	Pillara Limestone	Dampiera #1A, 1169.20 m	"	"
70339	AP	D1A-1169.90	Marl	Pillara Limestone	Dampiera #1A, 1169.90 m	"	"
70340	AP	D1A-1170.00	Marl	Pillara Limestone	Dampiera #1A, 1170.00 m	"	"
70341	AP	D1A-1174.85	Marl	Pillara Limestone	Dampiera #1A, 1174.85 m	"	"
70342	PT, CA	CS1-1088.80	Regional dolomite	Nullara Limestone	Cassia #1, 1088.80 m	19 44' 09.7" S	125 30' 54" E
70343	PT, CA	CS1-1169.22	Regional dolomite	Nullara Limestone	Cassia #1, 1169.22 m	"	"
70344	PT	CS1-1234.00	Dolomitized wackestone	Nullara Limestone	Cassia #1, 1234.00 m	"	"
70345	PT, CA	CS1-1303.10	Regional dolomite	Nullara Limestone	Cassia #1, 1303.10 m	"	"
70346	PT, CA	CS1-1447.42	Regional dolomite	Nullara Limestone	Cassia #1, 1447.42 m	"	"
70347	CA	CS1-1533.00	Regional dolomite	Nullara Limestone	Cassia #1, 1533.00 m	"	"
70348	R	CS1-1538.00	Saddle dolomite	Nullara Limestone	Cassia #1, 1538.00 m	"	"
70349	R, PT	B1-253.00	Regional dolomite	Pillara Limestone	Boab #1, 253.00 m	19 34' 42" S	125 08' 45" E
70350	CA	B1-258.00	Regional dolomite	Pillara Limestone	Boab #1, 258.00 m	"	"
70351	CA	B1-259.00	Regional dolomite	Pillara Limestone	Boab #1, 259.00 m	"	"
70352	R, PT, CA	B1-311.00	Regional dolomite	Pillara Limestone	Boab #1, 311.00 m	"	"
70353	R, PT	B1-356.45	Lithoclast breccia	Pillara Limestone	Boab #1, 356.45 m	"	"
70354	AP	B1-367.00	Lithoclast breccia	Pillara Limestone	Boab #1, 367.00 m	"	"
70355	R, PT	B1-367.40	Lithoclast breccia	Pillara Limestone	Boab #1, 367.40 m	"	"
70356	R, PT	B1-387.31	Marl	Pillara Limestone	Boab #1, 387.31 m	"	"
70357	AP	B1-395.30	Brachiopod marl	Pillara Limestone	Boab #1, 395.30 m	"	"
70358	PT, CA	B1-412.53	Regional dolomite	Pillara Limestone	Boab #1, 412.53 m	"	"
70359	R, PT, CA	B1-422.32	Regional dolomite	Pillara Limestone	Boab #1, 422.32 m	"	"
70360	R, PT, CA	B1-434.50	Regional dolomite	Pillara Limestone	Boab #1, 434.50 m	"	"
70361	CA	B1-440.62	Regional dolomite	Pillara Limestone	Boab #1, 440.62 m	"	"
70362	PT, CA	H1-379.01	Regional dolomite	Nullara Limestone	Halgania #1, 379.01 m	19 41' 28" S	125 23' 44" E
70363	PT, CA	H1-472.52	Regional dolomite	Nullara Limestone	Halgania #1, 472.52 m	"	"
70364	CA	H1-485.40	Regional dolomite	Nullara Limestone	Halgania #1, 485.40 m	"	"
70365	CA	C1-203.00	Regional dolomite	Pillara Limestone	Caladenia #1, 203.00 m	19 40' 46" S	125 06' 26" E
70366	PT, CA	C1-267.20	Regional dolomite	Pillara Limestone	Caladenia #1, 267.20 m	"	"
70367	PT, CA	A1-688.00	Regional dolomite	Pillara Limestone	Abutilon #1, 688.00 m	19 27' 18" S	125 07' 00" E
70368	PT, CA	A1-617.13	Regional dolomite	Pillara Limestone	Abutilon #1, 617.13 m	"	"
70369	CA	AR1-210	Regional dolomite	Pillara Limestone?	Anstida #1A, 210.00 m	19 53' 55" S	125 19' 36" E
70370	CA	AR1-508.50	Regional dolomite	Pillara Limestone?	Anstida #1A, 508.50 m	"	"

Sample codes

R = Hand Specimen
PT = Polished Thin Section
CA = Chemical Analysis
AP = Acetate Peel

APPENDIX B

ANALYTICAL DATA

UTGD no.	Field no.	O18 (PDB)	C13 (PDB)	Sr (ppm)	Na (ppm)	Mn (ppm)	Fe (Mol%)	Ca (Mol%)	IR (Wt%)
REPLACEMENT DOLOMITE									
70281	85-36E-2	-2.90	1.20	120	77	679	0.26	61.49	0.00
70285	85-53B-2	-2.49	1.86	127	93	485	0.15	59.41	0.00
70295	85-112TB-2	-2.57	1.67	140	82	717	0.20	60.30	0.00
70278	85-36B-2	-3.08	1.61	114	104	215	0.24	61.33	1.42
70289	85-58	-2.95	2.30	151	48	155	0.15	57.65	0.00
70298	85-112U	-2.48	1.51	172	47	198	0.10	56.55	0.00
70276	85-36	-2.62	1.56	136	88	156	0.85	56.32	0.00
70317	85-spo D	-5.71	0.44						
DEDOLOMITE									
70277	85-36A1	-7.52	-0.91						
70281	85-36E-1	-9.07	-6.00						
70278	85-36B-1	-7.97	-1.42						
70282	85-37A	-8.64	-1.26						
70288	85-53	-8.67	0.33						
70285	85-53B-1	-9.60	-3.09						
70295	85-112TB-1	-8.46	-7.88						
70296	85-112T A	-8.87	-5.62						
70303	85-305	-8.81	-3.53						
70287	85-53-z	-9.06	-6.59						
RECRYSTALLIZED CALCITE									
70302	85-280A-2	-7.47	-0.64						
70305	85-330	-6.57	-0.20						
70302	85-280A-1	-7.37	-0.85						
SPELEOTHEM CALCITE									
70311	85-ca	-6.91	-3.61						
70311	85-ca	-7.71	-4.00						

UTGD no.	Field no.	O18 (PDB)	C13 (PDB)
DENDRITIC CAVE CRUSTS			
70314	85-cru1	-0.34	0.62
70315	85-cru2	0.17	-2.12
70315	85-cru2	-0.68	7.05
NON-LUMINESCENT CALCITE CEMENT			
70283	85-37	-5.07	1.58
70280	85-36D3	-6.30	1.13
70275	85-33D	-4.89	1.68
70270	85-28Z	-6.54	2.23
70316	85-ONK	-5.44	1.78
70274	85-33C	-3.49	3.24
70284	85-53A	-4.65	3.17
70273	85-33A	-5.77	2.37
70279	85-36D1	-6.65	1.40
70371	85-36BZ	-6.40	1.13
70301	85-280	-4.63	2.67
70307	85-343	-4.85	2.22
BRIGHT CALCITE CEMENT			
70243	84-22	-9.82	1.73
70297	85-112TC	-10.47	1.28
DULL CALCITE CEMENT			
70308	85-344	-9.48	0.87
70317	85-spo 1	-10.15	-0.36
70317	85-spo 2	-14.22	1.60
70246	84-101	-12.86	2.04
70269	84-X	-10.76	1.73
70290	85-111B	-10.10	1.29

UTGD no.	Field no.	O18 (PDB)	C13 (PDB)
LATE DULL CALCITE CEMENT			
70286	85-53D	-12.91	-2.89
70313	85-cor 2	-11.64	2.63
70312	85-cor 1	-16.32	-8.69
70293	85-112A	-11.04	-3.27
FIBROUS MARINE CALCITE CEMENTS			
70255	84-233B	-5.54	2.66
70255	84-233C	-6.42	2.12
70255	84-233A	-5.12	3.30
70254	84-227A	-5.18	1.67
70254	84-227B	-5.44	1.50
70254	84-227C	-5.27	1.53
70254	84-227D	-5.16	1.70
70257	84-255	-4.60	3.82
70252	84-206	-5.64	2.56
70253	84-207	-5.10	3.21
70244	84-77A	-4.79	2.41
70244	84-77B	-4.92	2.36
70264	84-371	-5.22	1.53
70267	84-465	-6.42	0.86
70258	84-269A	-5.42	2.06
70258	84-269B	-4.80	2.26
70266	84-463	-4.69	1.31
70247	84-128	-4.59	2.15
70251	84-167	-6.00	2.11
70310	85-345	-5.66	2.35
70308	85-344	-4.98	2.07
70306	85-342	-6.03	2.30

Analytical Data, Gelkie Gorge Area

UTGD no.	Well Name	Depth (m)	O18 (PDB)	C13 (PDB)	Sr (ppm)	Na (ppm)	Mn (ppm)	Fe (Mol%)	Ca (Mol%)	IR (Wt%)
REGIONAL DOLOMITE TYPE, REPLACEMENT DOLOMITE										
70359	Boab	422.32	-2.83	-0.16	72	200	358	1.30	51.21	15.65
70358	Boab	412.53	-4.12	-0.75	63	94	532	1.90	50.94	11.16
70352	Boab	311.00	-4.72	3.82	33	276	430	1.01	50.55	0.11
70351	Boab	259.00	-1.93	2.11	98	414	382	0.24	50.79	3.30
70360	Boab	434.50	-3.25	1.18	77	597	260	0.82	50.65	34.70
70350	Boab	258.00	-1.94	1.70	98	508	441	0.21	51.14	3.10
70361	Boab	440.62	-3.42	1.93	93	50	210	0.51	50.87	13.42
70369	Aristida	210.00			88	351	287	0.51	50.40	19.26
70370	Aristida	508.50	-2.17	0.45	79	220	233	0.40	50.06	7.90
70366	Caladenia	267.20	-3.23	1.71	47	237	261	0.40	50.73	0.00
70366	Caladenia	267.20	-2.96	1.59	50	252	229	0.38	50.73	13.57
70365	Caladenia	203.00	-2.73	1.59	73	1591	234	0.49	50.06	31.27
70331	Dampiera	390.85	-3.08	1.36	95	398	558	1.11	50.51	11.60
70333	Dampiera	551.09	-3.08	1.24	93	164	373	0.63	51.47	21.17
70334	Dampiera	600.90	-2.36	0.40	83	321	307	0.62	50.34	20.56
70363	Halgania	472.52	-3.78	1.48	77	170	178	0.26	50.23	0.97
70368	Abutilon	617.13	-2.57	0.94	81	314	256	0.42	51.50	0.47
70362	Halgania	379.01	-6.16	1.59						
70346	Cassia	1447.42	-7.72	2.11						
70342	Cassia	1088.80	-9.22	2.06						
70343	Cassia	1169.22	-7.23	2.04						
70319	Eremophila	385.11	-1.69	0.46						
REGIONAL DOLOMITE, CLOUDY DOLOMITE CEMENT										
70362	Halgania	379.01	-6.75	1.40	67	25	734	0.74	51.19	0.00
70351	Boab	259.00	-2.95	1.77						
70346	Cassia	1447.42	-7.19	2.00						
70347	Cassia	1533.00	-9.01	1.68						
70343	Cassia	1169.22	-6.87	2.13						
70345	Cassia	1303.50	-8.97	0.10						

Analytical Data, Barbwire Terrace

Appendix B

Analytical Data, Barbwire Terrace

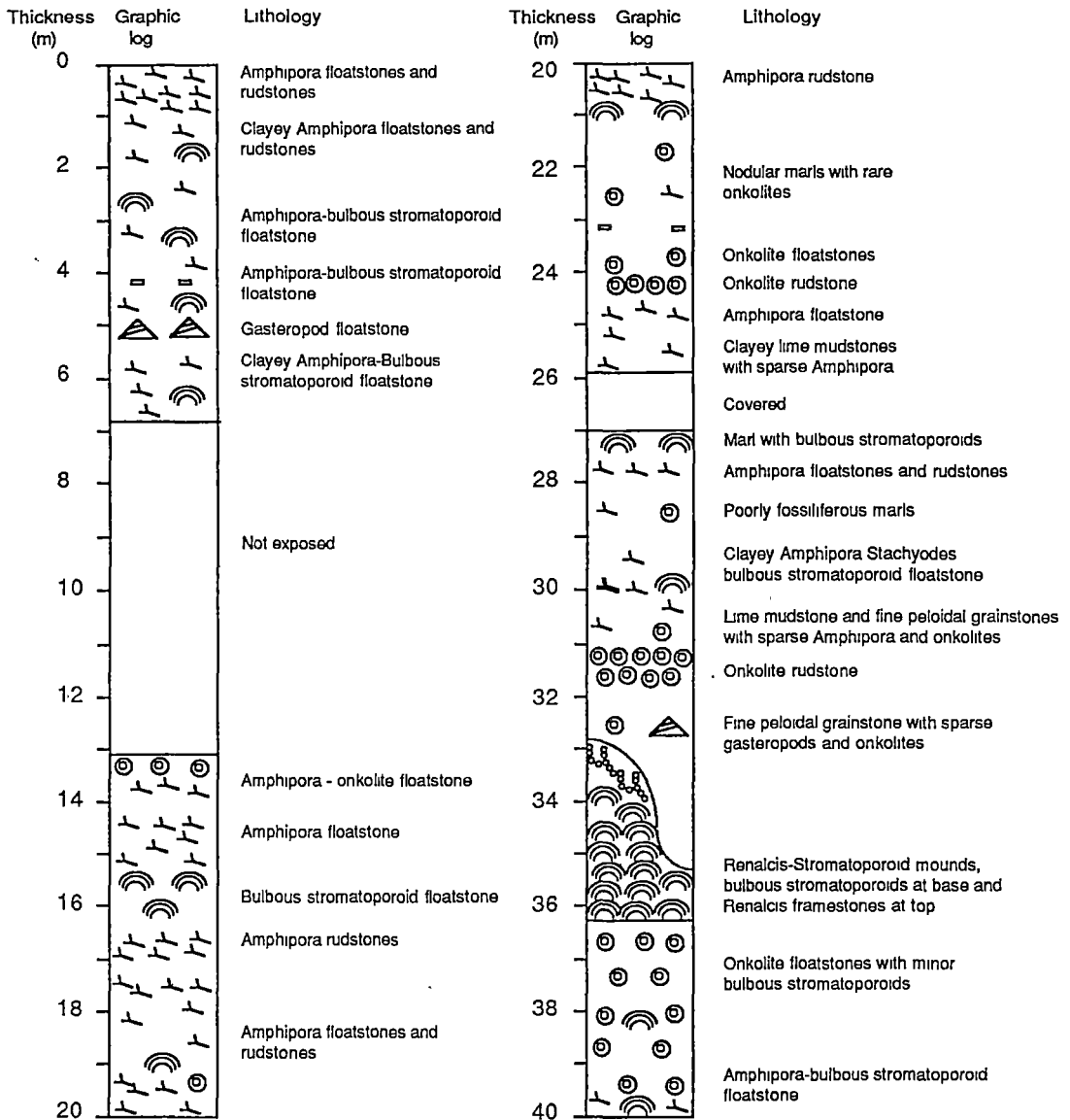
UTGD no.	Well Name	Depth (m)	O18 (PDB)	C13 (PDB)	Sr (ppm)	Na (ppm)	Mn (ppm)	Fe (Mol%)	Ca (Mol%)	IR (Wt%)
REGIONAL DOLOMITE, LIMPID DOLOMITE CEMENT										
70358	Boab	412.53	-4.59	-1.16						
70360	Boab	434.50	-7.07	-1.79						
70361	Boab	440.62	-7.34	-1.69						
SYNSEDIMENTARY SUPRATIDAL DOLOMITE										
70328	Eremophila	926.74	0.08	1.69	376	1456	374	2.14	54.45	41.70
70324	Eremophila	733.20	-1.10	0.16	225	860	538	0.52	55.31	42.80
70323	Eremophila	732.87	-1.94	0.41	385	1261	778	1.97	49.73	48.60
70325	Eremophila	790.87	-1.04	0.57	169	848	543	1.60	48.06	43.50
70327	Eremophila	880.65	-0.44	1.67	381	1398	580	3.96	53.57	52.20
70328	Eremophila	926.74	-0.38	1.52	761	1183	366	1.99	53.83	39.10
70329	Eremophila	927.92	-1.12	1.44	386	1095	336	2.05	52.00	35.80
70320	Eremophila	492.78	-0.42	1.37						
POIKILITIC DULL LUMINESCENT CALCITE CEMENTS										
70343	Cassia	1169.22	-18.04	-3.81						
70364	Halgania	485.40	-17.32	-2.70						
70367	Abutilon	688.00	-16.91	-4.40						
70368	Abutilon	617.13	-13.62	-4.97						
70366	Caladenia	267.20	-11.80	-6.45						
EQUANT CALCITE CEMENTS										
70319	Eremophila	385.11	-12.52	-4.31						
70352	Boab	311.00	-11.84	-4.60						
70350	Boab	258.00	-7.30	-5.60						
70351	Boab	259.00	-8.43	-6.22						

APPENDIX C

STRATIGRAPHIC SECTIONS IN THE STROMATOPOROID UNIT OF THE PILLARA LIMESTONE

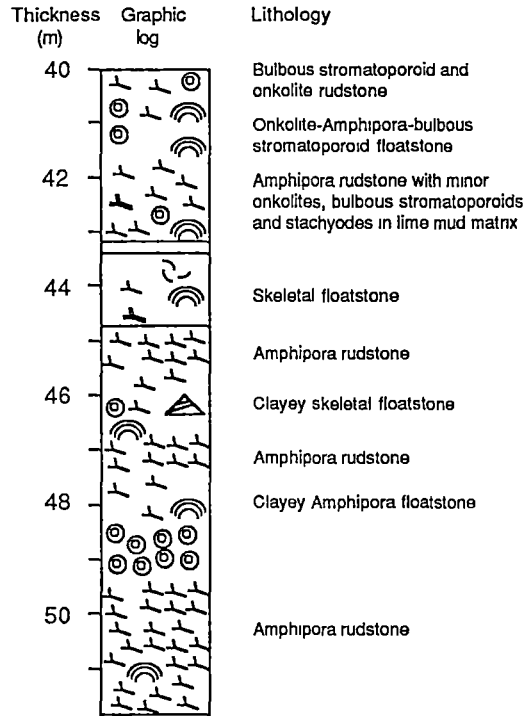
Section 1, Stromatoporoid unit, Northern Geikie Gorge

Locality shown on geological map of the Geikie Gorge Area (enclosure)



- | | | | |
|--|-------------------------|--|--------------------------------------|
| | Renalcis | | Gasteropods |
| | Stachyodes | | Oncolites |
| | Amphipora | | Tentaculitoids |
| | Bulbous stromatoporoids | | Brachiopods |
| | Thamnoporids | | Nautiloids |
| | Bryozoans | | Undifferentiated skeletal components |
| | Fenestrae | | Placoderm fish plates |
| | Crinoids | | |

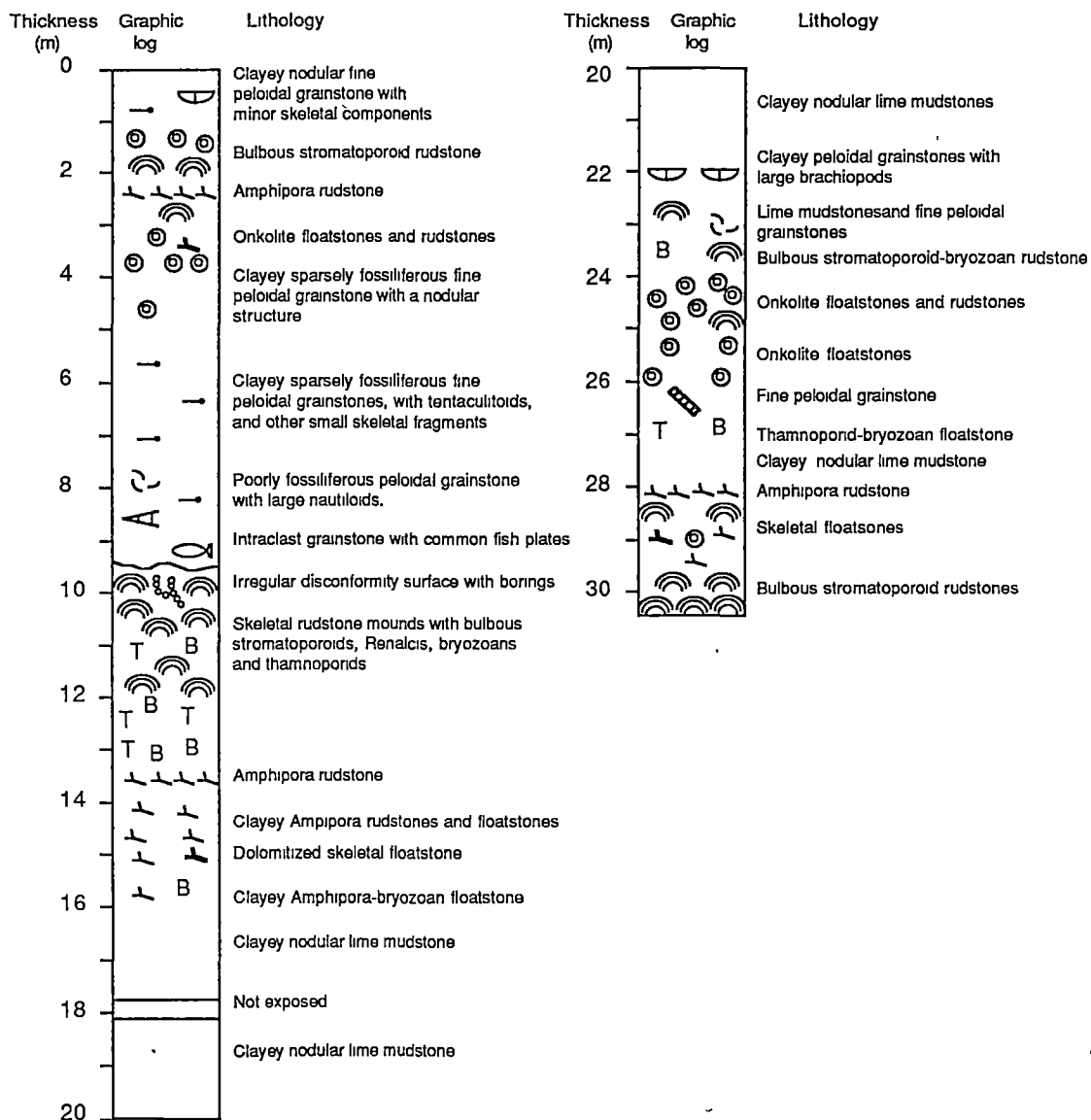
Section 1, Stromatoporoid unit, Northern Geikie Gorge (cont)



- | | | | |
|--|-------------------------|--|--------------------------------------|
| | Renalcis | | Gasteropods |
| | Stachyodes | | Oncoids |
| | Amphipora | | Tentaculitoids |
| | Bulbous stromatoporoids | | Brachiopods |
| | Thamnoporids | | Nautiloids |
| | Bryozoans | | Undifferentiated skeletal components |
| | Fenestrae | | Placoderm fish plates |
| | Crinoids | | |

Section 2, Stromatoporoid unit, Northern Geikie Gorge

Locality shown on geological map of the Geikie Gorge Area (enclosure)



- | | | | |
|--|-------------------------|--|--------------------------------------|
| | Renalcis | | Gasteropods |
| | Stachyodes | | Oncoids |
| | Amphipora | | Tentaculitoids |
| | Bulbous stromatoporoids | | Brachiopods |
| | Thamnopords | | Nautiloids |
| | Bryozoans | | Undifferentiated skeletal components |
| | Fenestrae | | Placoderm fish plates |
| | Crinoids | | |